THE UNIVERSITY OF HULL

SELF ORGANISATION IN BRAIDED SYSTEMS: DEM ANALYSIS OF THE RIVER FESHIE, SCOTLAND

being a Thesis submitted for the Degree of Doctor of Philosophy

by

Joseph Anthony Langham BSc (Hons)

February,2004

PAGE NUMBERING AS ORIGINAL

Abstract

A series of high quality Digital Elevation Models (DEMs) of a braided river system, the River Feshie, Scotland, are used to show that channel morphology and sediment flux are scale invariant and thus not dominated by a specific length scale. This is interpreted as more evidence that braided river systems are self-organised with large magnitude events possible as part of the functioning of the system and not necessarily the result of large external inputs.

The approaches adopted for identifying self-organisation in braided river systems identified scale invariant structures in channel morphology and the flux of sediment moving through the system. Both approaches required the acquisition of high quality, high resolution DEMs. Ground survey was considered the most accurate and precise technique for acquiring individual survey points. Remote survey and in particular digital photogrammetry were preferred for the survey of large areas of the braided system. Acquisition and post processing of DEMs using digital photogrammetry was carried out and the results tested against a GPS derived 'true surface' to determine the magnitude and structure of error. It was found that the post processing procedures adopted reduced both the Mean Error and Standard Deviation of Error significantly.

The scaling characteristics of the static morphology were assessed using a Fast Fourier Transform deconstruction of a morphometric designed to show downstream fluctuations in elevation. The dominant waveforms showed a poor correlation with morphological forms such as pools and riffles and were shown to be scale invariant using a linear regression model. Sediment movement quantified by differencing DEMs demonstrated that sediment flux over a 2-year period was also predominantly scale invariant. These results add to a small amount of evidence that examine scaling and self-organisation at the system level.

Acknowledgements

Many thanks to the taxpayers who made this research possible through a Natural Environmental Research Council studentship. (GT 04/99/FS/103). Thanks to the Glen Feshie estate for allowing access to the fieldwork site.

I would like to offer special thanks to my supervisors Barbara Rumsby, James Brasington and Graham Ferrier. Without their guidance and support the project would never have succeeded. Brendan Murphy deserves special thanks because he provided me with field expertise and assistance throughout the project. Thanks also to the Department of Geography for providing me with facilities and support.

Thanks to my family and friends for their support, encouragement and interest throughout the PhD. Special thanks go to Amanda who has preserved a measure of my sanity during the final years of my thesis. In addition, Rob and Mel deserve a special mention as last minute field recruits.

Table of contents

CHAPTER 1. INTRODUCTION

Abstract

This chapter introduces the important themes of the thesis. Initially scaling and self-organisation in braided rivers is explained with reference to recent research (**1.1.0**) and four research themes are outlined. The structure of the thesis is outlined in **1.2.0.**

1.1.0 Scaling and self-organisation in braided rivers.

This thesis focuses on the scaling properties of braided river systems by analysing the static and dynamic scaling properties of a braided section of the River Feshie Scotland, using multiscale DEMs acquired over a two-year time interval. This research follows on from other studies that have attempted to analyse the static and dynamic structure of braided river form. In particular the fractal approaches employed by Sapozhnikov and Foufoula-Georgiou (1996, 1997, 1998) have demonstrated that the planimetric structure of channel inundation of braided rivers is statistically identical over a range of scales from laboratory models through to the largest braided river systems ($10^0 - 10^4$) and as changes occur over time.

The recent focus on scaling characteristics within geomorphology has not occurred in a theoretical void. The identification of fractals by Mandlebrot (1963) lead to numerous studies that have identified fractal structures in nature (Burrough, 1984) and geomorphologists have attempted to employ fractal theory to measure and quantify landforms (Evans and McLean, 1995). One of the most profound implications of a fractal landform or landscape is that the fractal is indicative of a set of processes shaping the landform over a number of scales. In contrast, a scale specific (non fractal) landscape can be interpreted as being dominated by a specific set of processes at each scale. The importance of the fractal has been further increased since the publication by Bak *et al.* (1987), of a paper that introduced the concept of Self Organised Criticality (SOC). SOC suggests that fractal structures and 1/f noise (scale invariant dynamic system behaviour) are indicative of systems that can exhibit wide-ranging, non-linear fluctuations in their behaviour whilst at statistical equilibrium. The computational modeling approaches adopted by Bak *et al.* (1987) demonstrate that systems exhibiting SOC can be achieved using a minimal number of modeling rules suggesting that detailed knowledge of the interaction of numerous small scale processes is not required when a system is self organised critical. Instead, simplified rules that lump a number of processes under a single term can be used to identify the fundamental emergent properties of the system. The implications of scaling characteristics, SOC and simplified modeling approaches to the study of braided river systems has become a major discussion point in recent influential river science publications (Paola, 2001; Paola and Foufoula-Georgiou, 2001; Ashmore, 2001). However, studies that have directly addressed scaling with methodologies designed to measure morphology or sediment dynamics over a range of scales are few and have focused on laboratory not field approaches. Without such studies progress in identifying the fundamental processes (or rules) that govern braided river behaviour will not be possible because many of the existing techniques for determining sediment transport (e.g. direct sampling) and channel morphology (e.g. planimetric mapping and cross sections) fail to measure change at a high resolution over a long enough period or large enough spatial extent, a prerequisite for determining scaling characteristics. Developments in survey methods and computer power are integral to undertaking this task.

The 1990s have produced some important technological developments that improve field scale measurement of topography, these include advances in ground survey techniques, such as surveying GPS and automated tacheometric equipment, and remote sensing techniques such as digital photogrammetry and LiDAR. These new technologies allow the construction of high accuracy, high resolution Digital Elevation Models (DEMs) offering considerable potential for improving our knowledge of river channel morphometry and process at a variety of scales. In particular, because these data are 3 dimensional and spatially extensive, this means system scale morphological changes can be identified in X,Y and Z allowing the calculation of morphological change - a surrogate for sediment movement.

With these new opportunities also come new challenges. The opportunity of gathering large amounts of data very rapidly often means that data quality is overlooked (Lane, 1999). If this occurs then the significance of further analysis is undermined, therefore it is important that the structure and magnitude of error associated with each data source is carefully defined. Understanding the principles behind the survey acquisition method, allows the definition of theoretical error and provides a basis for understanding the error incorporated into surveys. This information, combined with empirical estimates of error calculated using independent check data, can ensure that the survey design meets the required quality level.

Whist improved data acquisition techniques offer potential for addressing scaling issues care is required in the application of such data. Within a braided river there are numerous measurable attributes which could be used to define scaling characteristics, many of which would be inappropriate for determining self-organisation. Reference to existing geomorphological theory provides a good starting point for developing meaningful measurements of system form (morphometrics). Theory on bedload movement and relationships between form and process (the morphological method) relates well to self-organised critical theory, which was developed using models of granular movement (Bak *et al.*, 1987).

Sediment dynamics is one area of river science that can benefit directly from improvements in field data. High quality DEMs enable use of the morphological method (Neill, 1969; McLean and Church, 1999[2]) to infer sedimentary movement from elevation measurements. Although initially this concept was used only at the broadest scales to calculate sediment budgets based on limited cross sectional data (McLean and Church, 1999[2]) more recent studies have shown that sedimentary movement can be more accurately determined using high quality DEMs (Brasington et al., 2000; Westaway, 2001). In particular the highly unpredictable nature of sediment movement and its large spatial and temporal variability suggests that the morphological method applied using high quality data could improve understanding of the scaling characteristics of channel form and sediment dynamics by more closely defining the magnitude and frequency of sediment movement.

This thesis aims to more closely define these scaling relationships by assessing the static and dynamic morphological characteristics present in a braided reach of the River Feshie in Scotland. In order to structure this research four research themes have been identified. These are briefly described below and expanded upon at the end of **Chapter 2.**

Research Theme 1: Acquisition, correction and testing of high quality morphological data.

This research theme centres on the acquisition of data designed to determine the scaling characteristics of the study system (introduced in **Chapter 4**).

Research Theme 2. Static scaling properties

This research theme aims to identify downstream patterns in channel form indicative of the passage of sediment slugs or waves, the scaling characteristics of these waves provides evidence about the self organised properties of the system.

Research Theme 3: Dynamic scaling properties

A second obvious approach to the problem of system scale organisational behaviour is dynamic scaling. The flux of sediment through a river channel can be measured by differencing of DEMs, a technique that gives spatially distributed information about scour and fill. The volume and pattern of these changes is direct evidence of how the river system organises itself.

Research theme 4: The self organised properties of braided rivers

The final theme is broader. It aims to take the specific findings of the previous themes and put them in the context of systems level theories, in particular SOC, and geomorphological theories and models.

1.2.0 Thesis structure

In order to structure these research themes the relevant geomorphological and theoretical arguments will be clarified **(Chapter 2).** The suitability of various data acquisition methods will then be considered **(Chapter 3).** The most suitable of these are then incorporated into a data acquisition and processing strategy **(Chapter 4).** The quality of the resultant DEMs is defined in **Chapter 5** together with the robustness of specific derived morphometrics. The DEM quality results demonstrate that the data are of sufficient accuracy and precision to be used to define periodicities in static morphology **(Chapter 6). Chapter 7** addresses smaller spatial scales that allow the differencing of DEMs to analyse the scaling characteristics of actual sediment movement.

The geomorphological context behind the research questions is introduced in detail in **Chapter 2,** a literature review explaining the fundamental research and assumptions upon which this thesis are founded. The systems level approach and the development of SOC are explained. The chapter goes on to highlight the weaknesses of traditional methods of measuring sediment movement and conceptualising sediment dynamics. The small number of studies that have adopted systems level analysis or addressed specific scaling relationships are examined to analyse what progress has been made in this area. Finally, the four specific research themes are re-statated and explained in more detail.

It is the type and quality of morphological data that can now be acquired that allows investigation of scaling at the system level. **Chapter 3** introduces these data acquisition techniques. The basic principles behind developments in ground survey techniques such as GPS and automated EDM are outlined with both theoretical and practical point acquisition errors reviewed. The basic principles behind remote sensing techniques such as digital photogrammetry and LiDAR are also explained. Data quality for remote sensing techniques is also described. The chapter finishes by giving an assessment of the overall strengths and weaknesses of each acquisition technique by discussing data quality and also spatio- temporal resolution considerations.

Chapter 4 uses the information of the previous chapters to design a data acquisition and processing strategy that is appropriate for addressing the research themes. The fieldsite is introduced and its suitability for addressing the research aims assessed. The data acquisition strategy is described along with a full description of each data set. The photogrammetric DEM is given special attention because post-processing procedures have been shown to significantly improve data quality (Westaway, 2001). The post processing stages developed for use with the photogrammetric data used in this thesis are described together with the methodological issues raised.

Chapter 5 assesses the quality of the complete DEMs. The quality of a high resolution GPS derived DEM (Brasington *et al.*, 2000) is emphasised and its suitability as a true surface against which to test photogrammetrically derived DEMs established. Improvements to the quality of the photogrammetrically derived DEM resulting from the post processing procedures are demonstrated. The second half of the chapter aims to establish if the DEMs are of sufficient quality to be used to predict specific derived morphometrics. In particular Level Of Detection (LOD) thresholds are found for each DEM to indicate their suitability for deriving sedimentary movement and a comparative approach is adopted to show differences in Mean Bed Level (MBL) between a high resolution GPS derived surface ('true surface') and the photogrammetric DEM of the same area.

Chapter 6 analyses the static morphology of the system. This is based on the rationale that the process of self-organisation will imprint onto the morphology of the braided river system. Downstream fluctuations in MBL are deconstructed using the Fast Fourier Transform. The dominant waveforms are compared to traditionally identified forms of organisation (confluence-diffluence and pool riffle) to attempt to identify a correspondence. The magnitude frequency data are then tested against a power law model to determine if they are scale specific or scale invariant.

Chapter 7 is concerned with the dynamic scaling characteristics of the system. DEMs of a reduced reach are differenced giving a DEM of change. The patterns of sedimentary change are described qualitatively and then with two morphometrics. The first determines the cross sectional change in volume downstream and shows high magnitude low frequency fluctuations. The second is a measure of lateral activity and is dominated by high frequency waveforms. The downstream changes are shown to exhibit a high level of scale invariance.

Chapter 8 concludes the thesis by describing the significant findings of the research and emphasising new questions raised by the approaches adopted.

CHAPTER 2. LITERATURE REVIEW:

SELF-ORGANISATION IN UNCONSTRAINED RIVERS

Abstract

In this chapter the theoretical background to the thesis is discussed and the research themes outlined. The research paradigm, a systems level approach, is justified in **2.2** and a specific systems level theory, Self Organised Criticality (SOC), is explained. **Sections 2.3-2.7** discuss what evidence there is that suggests braided river systems are SOC. Initially the extent of the 'system' for investigation is defined **(2.3)**. Then evidence of sediment dynamics is considered **(2.4)** specifically addressing studies that have directly measured bedload movement, flume based studies and the longer timescales considered by palaeo geomorphologists. **Section 2.5** discusses again the extent of the system in view of concepts introduced in **Section 2.4,** which provide some of the most compelling evidence that braided rivers could be SOC. The static and dynamic scaling properties of braided river morphology are discussed in **Section 2.6**. Finally, approaches for synthetically modeling braided rivers are compared with similar approaches used for defining the characteristics of SOC systems **(2.7).**

2.1.0 Introduction

Recent research focusing on braided rivers has incorporated a number of non-traditional approaches to the problem of understanding form and process. In particular the fractal approaches employed by Sapozhnikov and Foufoula-Georgiou (1996, 1997) and the synthetic cellular modeling used by Murray and Paola (1993, 1997) have stimulated debate about the theoretical approaches used within river science (Paola, 2001). Integral to these unconventional approaches is the systems level of investigation because the system organises itself and produces a set of dynamics called emergent properties. Unlike other contemporary forms of investigation (e.g. Lane, 1997), the systems level does not attempt to define the interaction of processes and individual elements in the system, instead the system is considered a black box in which complex interactions occur and from which specific properties are emergent. One set of emergent properties that have been shown to be applicable for complex systems is SOC (Bak, 1996). SOC has been suggested as a well-founded systems level approach that could be applicable to the study of river channels and braided river systems (Paola and Foufoula-Georgiou, 2001). As a theory it directly addresses issues of scale and process/ form interactions and is therefore applicable to other areas of geomorphology. As such, if it can be demonstrated that river systems exhibit SOC behaviour then this will have profound implications for approaches to modeling and management.

Determining whether river systems are SOC or otherwise is a substantial challenge. There are theoretical issues about how the theory should be applied, what scale of system should be considered and how this should be bounded. Current knowledge of sediment flux and channel morphology suggests that SOC behaviour is possible but the data fall short of the temporally and spatially extensive evidence needed for definitive proof. The fractal approaches employed by Sapozhnikov and Foufoula-Georgiou (1996, 1997) have made some progress by demonstrating some of the scaling characteristics of braided river morphology but they fail to address the scaling properties of the more important process, sediment flux.

2.2.0. A systems level approach

At the core of investigations of scale independence and self-organisation is a focus on a systems level that is concerned with defining the emergent properties of the system. Bak (1996) makes the distinction between reductionist physics and systems level physics very clear. Physics has been reductionist from its inception: attempting to break down complex structures into simple units that can be closely defined deterministically. The success of this approach has been substantial, determining the behaviour of many systems through a focus on individual parts: atoms, electrons and molecules for instance. Nevertheless, the limitations of this approach are found when attempting to understand systems with many degrees of freedom and thus large variability. Here, knowledge of each individual element is not enough to predict the behaviour of the system. Systems that behave in this way are often termed complex systems (Bak, 1996).

Contemporary river science has followed the philosophical lead of physics by adopting reductionism as its primary method of investigation. As opposed to dealing with the behaviour of entire river systems or morphologically specific systems within a river network, the rivers morphology and processes have typically been broken down into separate elements. Many studies of braided, gravel-bed rivers, have dealt with a number of these elements but within a very spatially limited section of river such as confluences (Ashmore *et al.*, 1992), with the aim of determining interactions between them. Other studies have been concerned with determining the specific role played by one element of the system, elements such as grain size (Rice and Church, 1998) and bed roughness (Hassan and Reid, 1990). Like physics this reductionist approach has produced progress in describing processes, for instance the mechanisms behind sediment movement have been well considered (Gomez and Church, 1989). However also in physics the limitations of reductionism have also been encountered because although many of the mechanisms behind sediment entrainment have been identified, the spatial and temporal patterns of sediment movement are still poorly understood and thus channel changes are poorly predicted. It is an understanding of this spatially extensive organization that a systems scale approach can begin to achieve.

The potential impact of a systems level approach to our understanding of river form and dynamics is far reaching. By adopting a systems level approach a large body of theory from non-linear dynamics becomes applicable to river science. These theories, including entropy, dissipative systems approach and SOC, have been developed outside of geomorphology and are well founded. The challenge presented by these theories is how to apply them to fluvial systems in a meaningful way so that empirical data has value in relation to the concepts within each theory. In short: if the right metric is not available then the value of these approaches will be very limited because they will be inapplicable and untestable. The data processing and methodological aspects of this thesis (**Chapters 3-5**) concern themselves specifically with developing high quality data. Before these practical aspects can be tackled the most pressing concern is the theoretical application of systems level theories.

Entropy is one systems level concept that has been applied to fluvial geomorphology in an attempt to show how the system organises itself to maximise entropy (energy dissipation) (Leopold and Langbein, 1962; Brebner and Wilson, 1967). This approach has had some success, for instance Yang (1971) explained the formation of pools and riffles and sediment movement using energy dissipation principles and Fiorentino and Claps (1993) showed an entropy based morphological analysis of river basin networks. The use of entropy to explain river system organisation is based on the concept that the laws governing behaviour in the river system are analogous to those governing entropy in a thermodynamic situation. Heat in the thermodynamic system is potential energy in the river system and temperature in the thermodynamic system is elevation in the stream system (Davy and Davies, 1979). The system optimises itself so that the potential energy available does the least amount of work within the constraints imposed by the system. The system organises itself into a configuration that dissipates energy and therefore maximises entropy.

The use of entropy to explain the operation of river systems is very compelling. It reflects a common theme in systems level approaches that some common factor is dictating system organisation. In river systems the channel is shaped by particular flows and processes but the operation of the system and its statistical configuration is controlled by a separate factor. However there are specific reasons why the concept of entropy is inappropriately applied to river systems (Davy and Davies, 1979). The analogy adopted between the river system and the thermodynamic has been shown to be inapplicable because the thermodynamic system requires that the system is isolated and all processes irreversible. These factors are important because only an isolated system with continually increasing entropy can evolve to a state of equilibrium where entropy is maximised relative to the constraints put on a system (Davy and Davies, 1979). These reasons are not applicable to river drainage basins, when applied in the most general terms, because the drainage basin will tend to reduce elevation and maximise entropy, however a braided river system is an open system with throughputs of material and energy, entropy will not continually increase as the system organises itself but will change according to sediment and water flux.

SOC is an alternative systems level theory that has potential for explaining how river systems behave. Like entropy, SOC does not attempt to address the small-scale interactions of form and process instead it offers an explanation for emergent system scale behaviour.

2.2.1 Introducing Self Organised Criticality

Self Organised Criticality (SOC) is the first general theory of complex systems that has a solid mathematical basis. Developed originally as an explanation for the well documented phenomenon of 1/f noise (fluctuations in signal over all scales corresponding to a power law) (Bak *et al.*, 1987), SOC has since been applied to a number of disparate subjects, complex systems ranging from earthquakes through to economics. SOC ties together the previously unexplained phenomenon of 1/f noise and fractals by adopting simple modeling approaches based on the principle of universality.

Complexity theory and the self organised critical explanation for 1/f noise should not be mistaken for chaos. Chaotic systems are simple dynamical systems compared to complex systems, which have numerous degrees of freedom (a large number of interacting elements or units). Like complex systems chaotic systems exhibit emergent properties but these show a white noise spectrum not the power law spectrum of complex systems. Systems that exhibit chaotic behaviour cannot produce spatial fractals. Chaos has been linked to fractals because chaotic behaviour has been modeled using 'strange attractors' (abstract mathematical objects) which have fractal properties (Bak, 1996). However, the theoretical basis and historical development of chaos theory and SOC are separate. In the same year that Gleick (1987) was publishing the work *Chaos*, an explanation of the well developed chaos theory, Bak *et al.*

(1987) were publishing the first explanation of 1/f noise based on SOC. 1/f noise is the term used to describe the low frequency power spectra of systems that display power law behaviour $f^{-\beta}$ over vastly different scales (Bak, 1996). The signal can alternatively be seen as a superimposition of signals of all frequencies and therefore containing features at all scales. The power of the frequency component is inversely proportional to the frequency f. SOC assumes that this signal is uniquely characteristic of complex systems (Bak and Chen, 1993).

Fractals are another phenomenon that have been linked to SOC. First conceptualized by Mandlebrot (1963) fractals are geometric forms with structures at all scales of magnification. These scale invariant structures have been found in a range of natural features most notably Norwegian fjords (Mandlebrot, 1963) and river drainage basins (Rinaldo *et al.*, 1996). Fractals exhibit exactly the same signal as 1/f noise, implying that the systems that created the fractal are self organized. The scale invariance of 1/f noise and fractals is an important phenomenon because it implies that the set of dominant processes that created the signal were working in the same way at all scales. This has profound consequences for the way in which the system dynamics are modeled.

The modeling approaches used to define SOC are key to understanding its significance. The underlying philosophy behind the modeling is the principle of universality (Bak, 1996). This means constructing the simplest possible model of a system but still representing the crucial dynamics of that system. This is in contrast to mechanistic modeling that attempts to model every part or element of the system and in so doing determining the relations between them.

The canonical example of SOC and one that represents this modeling principle is the sand pile model of Bak *et al.* (1991). This is a computer model, which drops theoretical grains of sand onto a flat surface developing a sand pile. A toppling rule is used to allow grains of sand to shift from one square to another when they reach a critical value. The toppling to adjacent squares can cause these to exceed their critical limit and also topple. The resultant toppling over 1 or more squares is termed avalanching. The initial state of the model is stability because no squares exceed their thresholds. The second state is one where some instability is achieved but this follows no statistical rules. Finally the mature sand pile has potential avalanches of all sizes. When the mature model is used to simulate a large number of avalanches (10^6) the magnitude of avalanches is the logarithm of the size of the avalanche (**Figure 2.1**). At this point the sand pile reaches a self-organized critical state. Bak *et al.* (1987) tested the robustness of the critical state by changing parameters in the model such as the critical value for toppling, the size of each toppling event and the size of the grains of sand. Despite all these adaptations each model reached a critical state demonstrating the robustness of SOC within the model.

The sand pile model contains all the important characteristics of a SOC system. It is an open system; energy, in the form of sand grains with potential energy (initially) and kinetic energy (upon toppling) are externally introduced. It has many spatial degrees of freedom because there are many grains of sand. A crucial part of the sediment dynamics is that they are non- linear (the magnitude and frequency of avalanches cannot be described by a linear model) (Paola, Foufoula-Georgiou, 2001). Contingency is similarly important in SOC. The addition of a single grain of sand to the sand pile model in a critical state could cause an avalanche involving the entire pile, this is a major catastrophic event sparked by the addition of a single grain (Bak, 1996). Yet this is only possible because the preconditions of the pile were contingent on very minor details. If these minor details had been different then the resultant avalanche might have been of a different size or occurred at a different point in time. Because the critical state arises through contingency this makes avalanche prediction difficult. Prediction is reliant on a perfect knowledge of the position of every grain of sand together with its toppling threshold. Clearly this is possible with a computer program because these things can be calculated foreach iteration, but in a real world complex system such high quality high resolution monitoring is not possible. The dynamics of the sand pile are such that perfect knowledge of each sand grain for the entire system is required to predict specific avalanche events. Perfect knowledge of part of the system is of no predictive value. In short, study of the individual grains gives no information about the emergent property. The sand pile must be viewed as a single functioning unit (Bak, 1996).

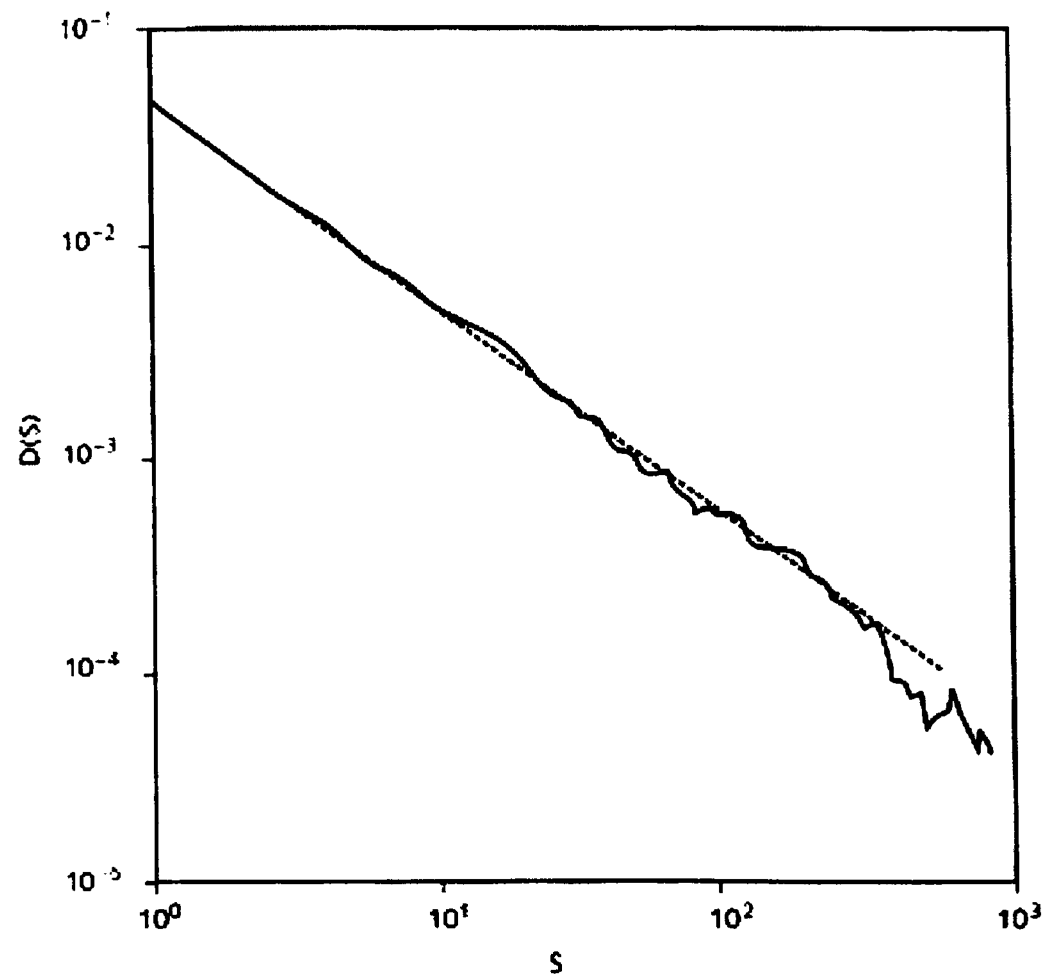

Figure 2.1 Taken from Bak (1996). S= the number of avalanches, D(S)=avalanche magnitude. The distribution is a power law with exponent 1.1. Longer simulations on bigger systems extended the range of the power law.

The reductionist position is undermined by these arguments. A reductionist approach to the sand pile would measure a small section of the pile, in a real world system it would do this imperfectly and for a limited length of time. Yet to begin to understand the dynamics of the system the entire pile would need to be measured perfectly from its initiation.

Laboratory experiments that have attempted to construct SOC systems have had mixed results. Experiments that have used sand piles show that SOC systems can be constructed but only for smaller sand piles. Held (1990) produced a SOC sand pile on a 1.5 in diameter plate. For larger plate sizes (3 in) SOC was replaced by avalanches with finite-size scaling caused by relaxational oscillations (fluctuations occurring at specific length scales) (Held, 1990). SOC has been produced more successfully using rice piles. Frette (1996) recorded the size of energy dissipation events of rice piles and found that rice with large aspect ratios became SOC whereas less elongated grains did not. This result was interpreted as being caused by the different relaxation mechanisms of the rice, with the elongated rice sliding and the less elongated rice bouncing down the rice pile or flowing like a fluid. These results show that SOC is not a universal phenomenon, insensitive to the details of the system even in the archetypal granular system. This means that care is needed when determining the type of self-organization operating in any system.

The experimentation and application of SOC extend far beyond that of Bak *et al.* (1991) computational sand pile. The sand pile model is concerned with morphology and movement of material so geomorphology is an obvious area for investigating the existence of SOC. Furthermore many geomorphological systems have proved very hard to model using traditional reductionist approaches because of their large variability and apparent stochasticism, for instance bedload movement in rivers is poorly defined by bedload equations (McLean *et al.*, 1999[1]). Geomorphological investigations addressing SOC have focused around landslides (Noever, 1993), landscape development (Rigon *et al.*, 1994) and drainage basin structure (Rinaldo *et al.*, 1996). Of these, the hydrological example is the most relevant. The branching structure of drainage basins has been shown to follow a simple power law since Horton (1945). The relationship was based on the drainage area and a system of channel ordering. Rinaldo *et al.* (1996) took this analysis one step further and modeled the fundamental dynamics of the system, basing their computational model, like Bak's (1987), on the principal of universality. They showed that the computational channel networks optimised to a state that maximised entropy (maximised energy inefficiency) and these networks compared well with real drainage basin networks. Rinaldo *et al.* (1996) conclude that the surface of the earth has organised itself into a structure optimised to dissipate energy and SOC could be the by-product of the optimisation process.

Braided river systems have also been shown to exhibit some scaling properties that suggest that they could be self organized critical. In particular the work of Sapozhnikov and Foufoula-Georgiou (1996, 1997) has highlighted the scaling properties of braided river morphology. This, along with existing knowledge of sediment dynamics and channel change has highlighted SOC as an area of potential progress to be further investigated (Paola and Foufoula-Georgiou, 2001).

2.3.0 Investigating SOC in braided river systems

The above section has described the basic principles behind 1/f noise and SOC. The most important research developing SOC has been cited showing that SOC, although relatively new, is an accepted part of mainstream physics that has also been applied to a range of environmental systems and natural phenomenon. The next two sections **(2.3 and 2.4)** consider if river systems could be SOC systems. Initially the extent of the 'system' under investigation is defined. In context of this, existing geomorphological knowledge about river systems is used to assess if the characteristics of the system are conducive to SOC. Specific examples of fractal structures and self similarity (and self affinity) in channel form are described along with attempts at cellular modeling of braided river systems.

2.3.1 Defining the system extent

This study is primarily concerned with the structure and organization of 'braided river systems' so before any lengthy comparisons between SOC systems and braided river systems can begin the latter need to be more closely defined and contextualised. These definitions will be questioned in the latter stages of this discussion as arguments concerning the scale of enquiry are considered.

A braided river system is a 'section' or 'part' of the entire basin scale sediment erosional transportational and depositional system. Typically the braided section is in the transportational or depositional part of this larger system at a point where lateral constraints on channel movement imposed by valley walls are removed. The river braiding itself is characterised by lateral instability coupled with multiple channels and complex assemblages of bars. This thesis is mainly concerned with just this braided section and treats it as a separate system in its own right. There is a clear morphological basis for making this distinction although it can be contested on the grounds that conditions downstream and more significantly upstream can have a major impact on the braided system itself. There is also the important aspect of the drainage basin, of which the braided system is a part. This could have an impact on the operation of the system and fundamentally effect the organisation of morphology and sediment movement within the system. Horton (1945) showed that river segments conform to power law scaling and this demonstrates that river drainage basin systems are organised according to a fractal structure. This means that a small section of the drainage basin morphology will be statistically identical to a larger section if it is re-scaled. Recent modeling work by Rinaldo *et al.*, (1996) has shown that this fractal form could be indicative of a system dominated by scale invariant processes Rinaldo *et al*, (1996) will be discussed in more detail below along with further consideration of fractal form and scale invariant processes). If a braided river system is then designated within this system then its signal will be superimposed onto the signal of the larger river network. The resultant signal, the product of two signals operating at different scales, might be difficult to disentangle. This argument over system definition is important and is continued at length later in the chapter.

Many studies that have looked at river channels at the system scale have shown ways of defining and quantifying river channel systems. Methods of defining channel pattern are predominantly the result of attempts to develop methods to quantify braiding intensity with the fundamental aim of finding out what parameters are important in determining channel pattern. For example Leopold and Wolman (1957) used a semi-quantitative classification of alluvial channel systems consisting of straight, braided and meandering. This system is fundamentally limited by its use of two different criteria to define channel types. Sinuosity is defined as the ratio of thalweg length to valley length and is used to measure meandering channels. Degree of braiding is defined by channel multiplicity. There is no attempt to identify a measure that shows how a meandering channel can increase in instability until it becomes a braided channel. No consideration is given to the exact definition of single to braided channels.

The problem of defining extent of braiding was tackled more thoroughly by Brice (1964) who introduced the concept of the braiding index. This gives a fully quantitative approach to defining braiding intensity (**Equation 2.1**).

$$\text{Braiding index} = \frac{2\ (\text{Sum of lengths of island and (or) bars in a reach}}{\text{Length of reach measured midway between banks}} \qquad \textbf{Equation 2.1}$$

Brice (1964) distinguished between bars (transient index) islands (stabilized index) and both (total index). The stabilized index refers to vegetated islands usually not inundated at bankfull discharge and Brice (1964) claims this makes it nearly constant with changing discharge. There are clear problems with Brice's index. The stabilized index is useless on systems that have no vegetation (such as proglacial systems) and vegetation extent and distribution is governed by the amount and distribution of erosion (more specifically cut bank erosion) verses vegetation colonization rates. The validity of the stabilized index is further compromised by the subjectivity of the transient verses stabilized index. The transient index Brice (1964) admitted was stage dependent making the classification more indicative of stage than morphological characteristics of the channel system.

Rust (1978) tried to tackle the problem of stage dependence as part of an attempt to define braiding intensity using a braiding parameter. The perimeter of the braid is defined as the mid line of the channels surrounding each bar or island whether or not these channels have water in them. The braid length is then defined as the distance between the extremities of the braid. The second part of the braiding parameter is a measure of meander wavelength. The braiding parameter is then expressed as the number of braids per mean meander wavelength. Rust (1978) considered the successes of the parameter to be the reduced variability with stage until the point when bars start becoming flooded.

Rust's braiding parameter ultimately suffers from the same problems as Brice's Index. The braid length is dependent on identification of channels that surround bars but this is open to considerable interpretation and definition problems particularly because an uninundated channel can still be classified as a channel. Close observation of the upper braided section of the river Feshie shows that channels are not always well defined, channels differ in size, shape and definition. Similarly the concept of bars is questionable given the complex assemblages of sediment and distributions of slope (discussed in length below). Similar problems of definition surround the meander wavelength. In short, Rust (1978) gave no details about how he identifies and measures these features. There is little appreciation of the subjectivity of the measures.

Rust (1978) identified the problem of feature size and makes an attempt to classify these by ordering channels and bars according to size. This allowed the braiding parameter to be expressed in terms of first second or other recognizable order of bar and channel. Again, this system suffers from all the problems of definition and subjectivity associated with the full braiding parameter. Despite the subjectivity of this approach it is successful in broad terms, at quantifying degree of braiding and this becomes clear when multi-channel and single-channel diagrams are given their braiding parameter. This works because the morphological differences are obvious features, easily identified subjectively, however the resultant insensitivity negates much of the significance of the parameter and this makes it less useful for comparative purposes because it just demonstrates that a braided channel is braided. It does little to reveal the underlying characteristics of braided river topography.

The approaches described above are reliant at least in part on channel inundation this gives rise to a debate about what is the appropriate stage in which to measures these indices. Schumm (1968) classified channels at bankfull stage and defined braided channels as 'single-channel bedload rivers, which at low water have islands of sediment or relatively permanent vegetated islands'. In contrast Rust (1978) and other authors (Miall, 1977) studied braided systems at low flow and defined them as multi-channelled. The issue is further complicated because the concept of bankfull stage is not applicable to many braided river systems, which inundate relic channels in flood and have no clear banktop. The difference of opinion over applicable stage highlights the inadequacies of using stage as a means of delimiting the system to be studied and suggests that a more easily defined method for measuring the character of a system is needed.

Howard *et al.* (1970) used multivariate analysis to cross correlate parameters in an attempt to find the variables most important to braiding. To do this specific morphological elements of braided rivers were defined. These are; segments (anabranches), nodes (where segments branch or join) and islands (enclosed by segments). Howard also draws upon relationships developed as part of a topological theory of networks (Berge 1962, Kansky (1963). The parameters derived by Howard *et al.* (1970) demonstrate the value of division of the reach into sub reaches allowing within river as well as between river analysis. The scale free parameters allow simple analysis of scale dependence. Many of the results support other findings for example the number of stream channels increases with gradient (Leopold and Wolman, 1957) and braided channels are less sinuous than single thread streams (Wolman *et al.*, 1964).

2.3.2. Defining the active elements in a braided river system

A braided river system has all the characteristics that are important in SOC systems. It is an open system and has external sources of energy because geological uplift gives the bedrock potential energy. The bedrock is weathered to create sediment, which enters the fluvial system analogous to sand being added to the sand pile. A note of caution is needed at this point: the sand pile game adds grains of sand at a steady state to the system, landslides and colluvial slopes that dominate sediment input in the initial stages of upland catchments are not steady state systems and there is evidence that these might also conform to SOC principles (Noever, 1993). The water that drives the fluvial system has no analogy in the sand pile game but represents a second source of potential and kinetic energy entering the top of the system. Finally, a braided river system, like SOC systems, has many degrees of freedom.

If we accept that water and sediment are the primary agents at work in braided river systems then it can be assumed that the movement of sediment and the configuration of sediment (channel and braidplain morphology) could be indicative of SOC by exhibiting 1/f noise and fractal structures respectively. Within river science few studies have set about looking specifically for evidence at this scale, a majority of contemporary studies have adopted a more reductionist approach. Most system scale analysis that has taken place in the discipline (Howard *et al.*, 1970 for instance) has pre-dated theories on complexity and SOC although there are a few notable exceptions (Sapozhnikov and Foufoula-Georgiou, 1996, 1997)

2.4.0 Self organisation in river science

Evidence of system scale organisation can be found in river geomorphology studies that do not directly address the underlying system dynamics. Examples of this evidence can be drawn from direct measurement of bed load transport, experimentation using flumes and morphologically derived measures of sediment movement. Larger magnitude events have primarily been studied using palaeo geomorphological techniques interpreting the causes of morphologically durable episodes. These studies have never been analysed using a SOC theoretical framework yet such an interpretation could have profound implications for our understanding of river network and braided system dynamics. A systematic analysis of all of river science's theories and studies in relation to SOC is not presented here, instead the more salient points are considered.

2.4.1 Sediment dynamics

Sediment movement in river channels has received a large amount of attention and is often considered a key geomorphic process (Church and Hassan, 2001). Most of the studies address sediment movement with the aim of determining the mechanisms of sediment movement (Andrews and Parker, 1987) or quantifying amounts of sediment moving through a system (McLean *et al.*, 1999[1]). The underlying objective of these approaches is to understand the processes at work in the river by more closely defining the functional relations between highly non-uniform flow and sediment transport. Although many different approaches have been used a common thread that runs through all these investigations is the spatial and temporal variability of sediment movement, a variability that makes sediment entrainment and transport difficult to measure and predict. The high spatial and temporal variability shown by bedload has been attributed to a number of factors. At the smallest scale the entrainment of single particles varies due to turbulent eddying (Komar, 1988), at larger scales then microbedforms and bed armouring (Andrews and Parker, 1987; Sutherland, 1987). Bedload movement in braided river channels in particular is thought to be highly non-uniform and characterised by random short-term fluctuations resulting from rapid local channel changes (Ashmore, 1988, 1991, Described in detail below).

The spatial and temporal variability of bedload movement has been highlighted by studies that directly measured bedload movement (Hamamori, 1962; Helley and Smith, 1971; Hubbell 1964). Some of the most temporally comprehensive measurements have been made by in situ bedload traps such as that used on Turkey Brook, UK (Reid *et al.,* 1985) or Virginia Creek, USA (Tacconi and Billi, 1987). These techniques negate many of the negative sampling effects of portable samplers to show that bedload on a single channel gravel bed river exhibits regular pulsing behaviour. Laboratory and field measurements by other researchers shows similar results with bedload transport rates fluctuating from zero to four times the average (Hubbell, 1987) and the distribution of rates generally corresponds to the probability distribution described by Hamamori (1962) **Figure 2.2**. McLean and Tassone (1987) found similar results using repeat Arnhem samples of the Fraser river, with individual measurements reaching as much as 6 times the mean transport rate and the distribution highly skewed with 70% of samples smaller than the mean. Whilst some of this variability can be attributed to the inefficiency of bedload sampling devices (McLean *et al.*, 1999[1]) the apparent stochastic nature of bedload movement is the primary cause (Wilcock and McArdell, 1993).

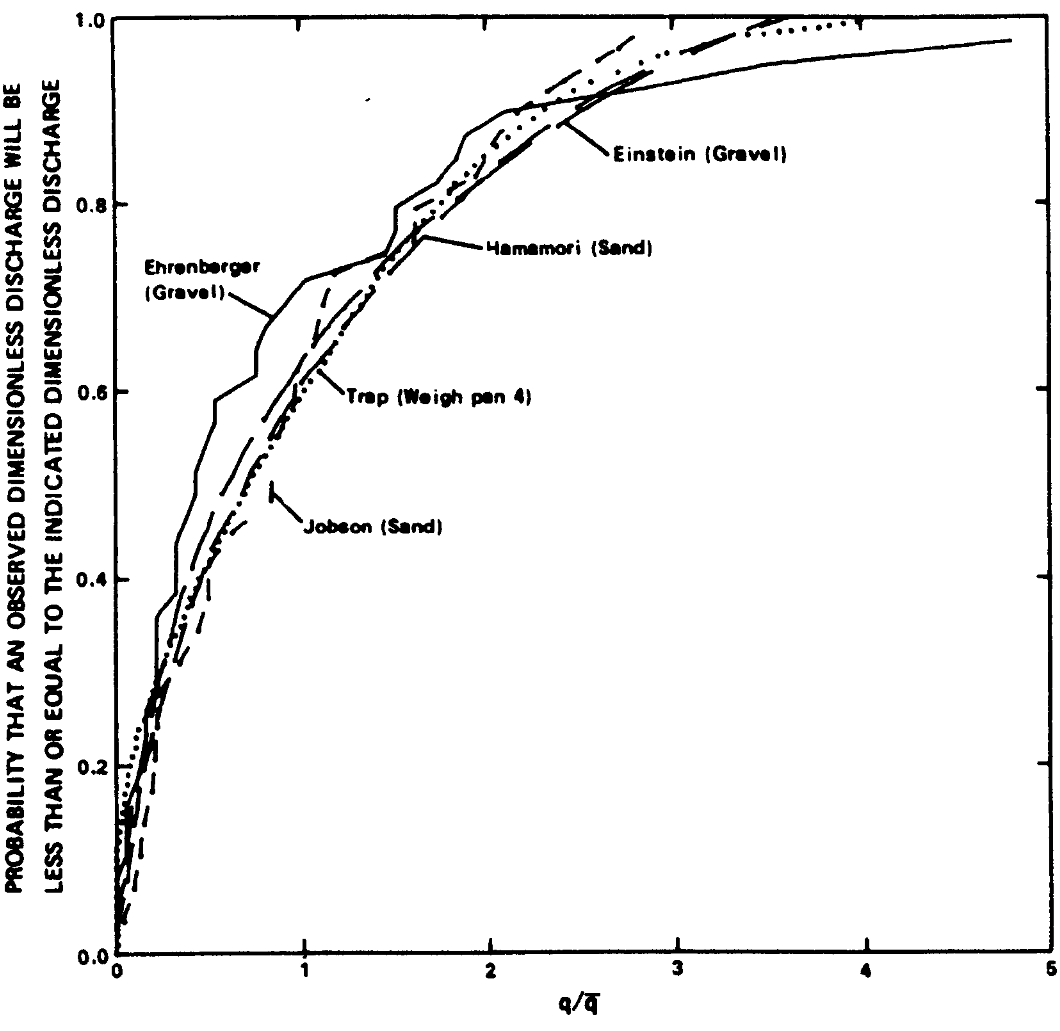

Figure 2.2 Probability distribution function with laboratory and field data for comparison. Taken from Hubbell *et al.*, 1985

The morphological method is an alternative method of studying bedload sediment dynamics that has been used to show the spatial and temporal variability of sediment movement over a range of scales. The morphological method is also termed the inverse method because it takes advantage of the necessary relation between sediment transport and channel morphology

(Ashmore and Church, 1998). The main advantage of the morphological method is that it is a way of showing the patterns and quantity of bedload movement without relying on relations between flow intensity and sediment movement.

The morphological method uses changes in sediment storage along the river channel to determine sediment movement. A number of methods have been determined including a step length method applicable to meandering rivers where erosion is assumed to be predominantly from the outside of meander bends and deposition on the next point bar downstream. An alternative method, the sediment budget, is required for a river channel where erosion and deposition is less discretely distributed (Ashmore and Church, 1998). The sediment budget works by subdividing the rivers into a number of adjacent cells. The output from the upstream cell is equal to the input for the downstream cell and this makes a sediment balance calculation for each possible (McLean *et al.*, 1999[2]). One of the most important concerns with the sediment budget approach is defining cell size. If the cells are too small then active sediment will pass through an entire cell without being measured producing an inaccurate measurement of sediment flux. Making cells too large reduces the resolution of sediment flux measurements. A full explanation of the theoretical issues surrounding the morphological method and its application can be found in Ashmore and Church (1998) and in **Chapter** 7 of this thesis. This section will concern itself with the sediment dynamics that have been identified through use of the morphological method.

Application of the morphological method has been particularly effective in single thread streams where bank retreat rates have been combined with assumptions of sediment movement distances (step lengths) to calculate sediment movement rates (Neill, 1971,1987). This technique is viable because each step length was assumed equivalent to one half of the meander wavelength and this was combined with bank retreat rates or meander sweep rates to calculate sediment volumes. The morphological method has also been used to determine sediment flux for single channels over longer timescales and larger spatial scales. Ham and Church (2000) identified a morphologically significant flood with a return period of 5 years as the dominant controls on sediment movement in the Chilliwack River, Canada. At a larger scale again the morphological method was used on the Fraser River, Canada by McLean and Church (1999[2]) in a study that used cross sectional data and aerial photographs to calculate long term sediment budgets. This study, like those of Neill (1971) and Ham and Church (2000), relied upon discrete sites of persistent erosion and deposition operational over the timescales applicable for the study. This illustrates a fundamental problem of the morphological method, the temporal frequency between surveys is often large and so many of the smaller sediment movement events are missed. The temporal frequency of survey effectively dictates the minimum scale of sediment movement event. In the case of McLean and Church (1999[2]) the sites of erosion and deposition were operating over a period of years and changed over decades as the main channel re-aligned. These loci of instability were tracked down the main channel over decades. The range of scales of sediment movement event were limited by the sampling scale and frequency.

Braided river systems are morphologically more complex environments than single thread systems. This makes the morphological method more applicable than direct measurement but also makes accurate results dependent on high quality data. Goff and Ashmore (1994) used seven cross sections spread over 60m to calculate bed load transport rates for the proglacial Sunwapta River, Canada. The data shows a link between discharge and bed load transport rate but this is accompanied by significant scatter as bedload activity fluctuates widely during peak discharges. Time averaged measurements of bedload movement show significant spatial and temporal variation associated with the evolution of bars (**Figure 2. 3**).

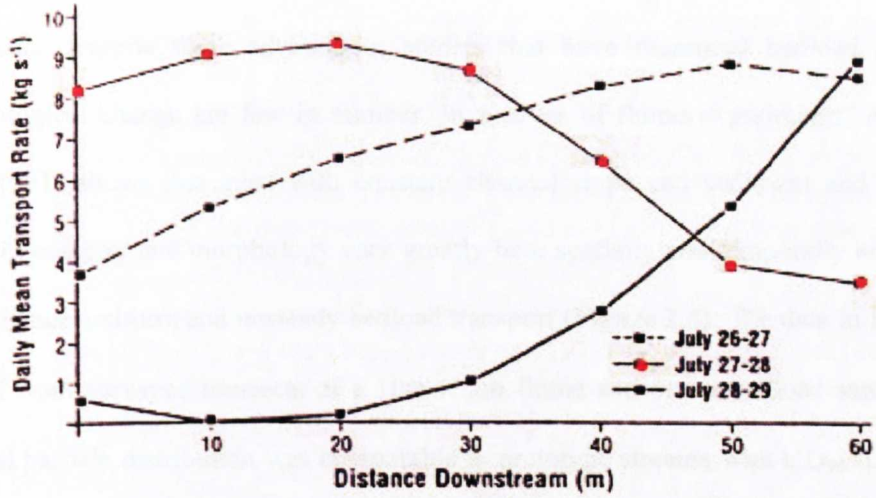

Figure 2.3. Taken from Goff and Ashmore, 1994. Spatial and temporal variation in bed material transport rate associated with bar evolution, Sunwapta River, 1990. The downstream fluctuations in sediment transport rate were linked to the evolution of bars. As sediment was eroded from specific sites then sediment transport increased downstream until deposition occurred.

Like attempts at applying the morphological method to a single channel, studies of braided rivers have produced limited information about the specific sediment dynamics of braided rivers because the cross sectional data on which they are based place severe limitations on the spatial extent or downstream resolution. This ensures that sediment dynamics can only be investigated over very limited spatial and temporal extents. Nevertheless, if the existence of SOC behaviour is to be properly considered then the sediment and morphological dynamics of the system need to be considered over an extensive range of scales. Although the field evidence of sediment dynamics outlined above shows many of the properties that could be indicative of SOC (non-linearity, apparent stocasticism) this is far from convincing. Flume research is one environment in which high quality data collection has been possible allowing quantification of sediment flux over a range of scales.

2.4.2 Experimental sediment dynamics

Flume research offers an environment in which many of the variables associated with river channels can be controlled and measurements of morphological change and bedload movement can be made at regular intervals. Braided channel morphology is ideal to study in the flume environment because it is the result of running flow through a channel with unconsolidated bed and banks. Despite these advantages, studies that have measured bedload movement and morphological change are few in number. In a series of flume experiments, Ashmore (1982, 1988, 1991) shows that even with constant channel slope and sediment and flow discharge channel geometry and morphology vary greatly both spatially and temporally and this is linked to highly non-uniform and unsteady bedload transport **(Figure 2.4).** The data in **Figure 2.4** were derived from surveyed transects of a 10m × 2m flume and direct bedload sampling. The bed material particle distribution was comparable to prototype streams with a D_{50}=1.16mm and bed material along with some of the water was recirculated. Each of the 10 runs lasted for 60 hours during which 80 transects and 240 bedload measurement were taken. **Figure 2.4** is indicative of the morphological and dynamic complexity of the braided system. All three measured variables fluctuate greatly over time. In some cases the fluctuations correlate (frequency of unit bars and bed material mobility), however in others bed load pulses are out of phase with changes in bed form. These measurements take advantage of the experimental approach to take measurements of a rapidly evolving system every hour for up to 60 hours per run. The duration and frequency of these measurements surpasses anything possible in larger scale natural channels even those of a rapidly evolving proglacial system such as that studied by Lane (1995,1997). However the morphological measurements in the flume are still based on cross sectional data which, even when closely spaced, is of limited value in determining spatial patterns of erosion and deposition in a channel configuration as complex and dispersed as a braided system. Attempts at acquiring fully three dimensional data of braided systems in flumes have been limited. Stojic (1998) used photogrammetric techniques to derive DEMs over 19 epochs, the focus of the publication is photogrammetric acquisition of data and as such the derived sediment fluctuations are poorly described. Data acquisition techniques are described in more detail in **Chapter 3.**

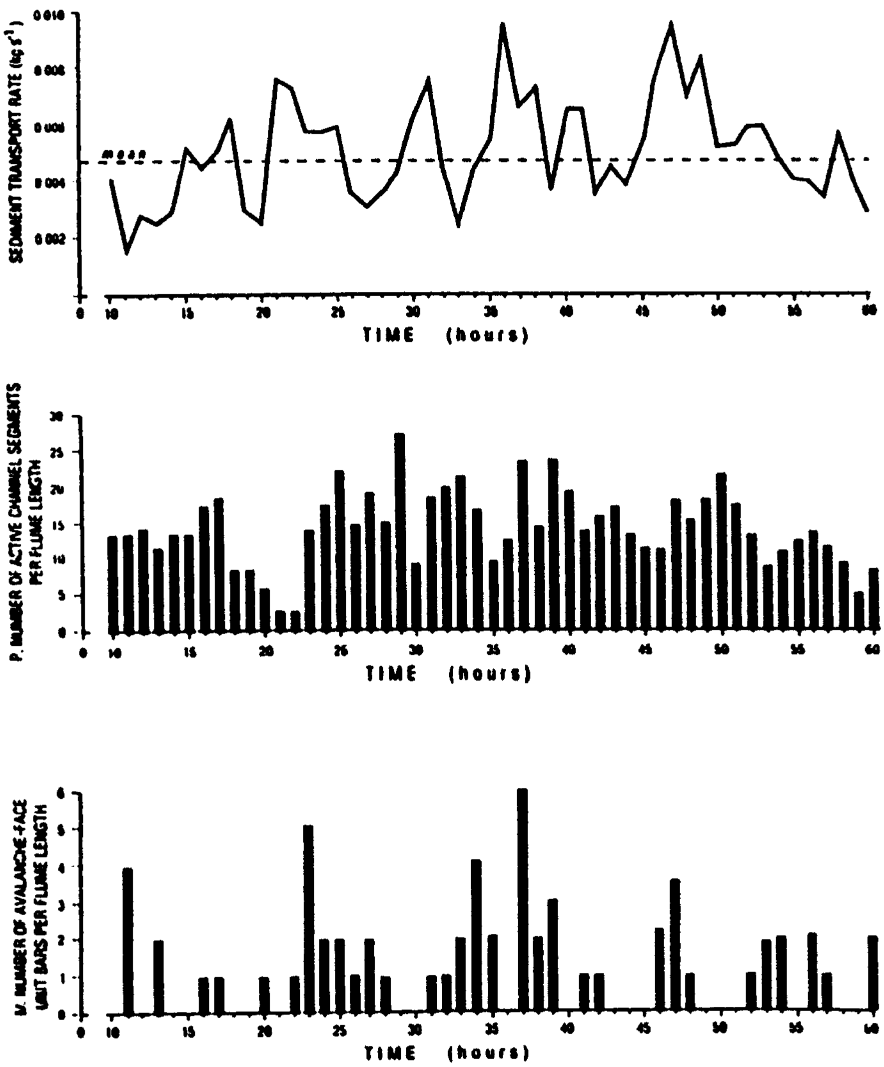

Figure 2.4 Taken from Ashmore (1991). Time series of bedload and morphological parameters from run 10.

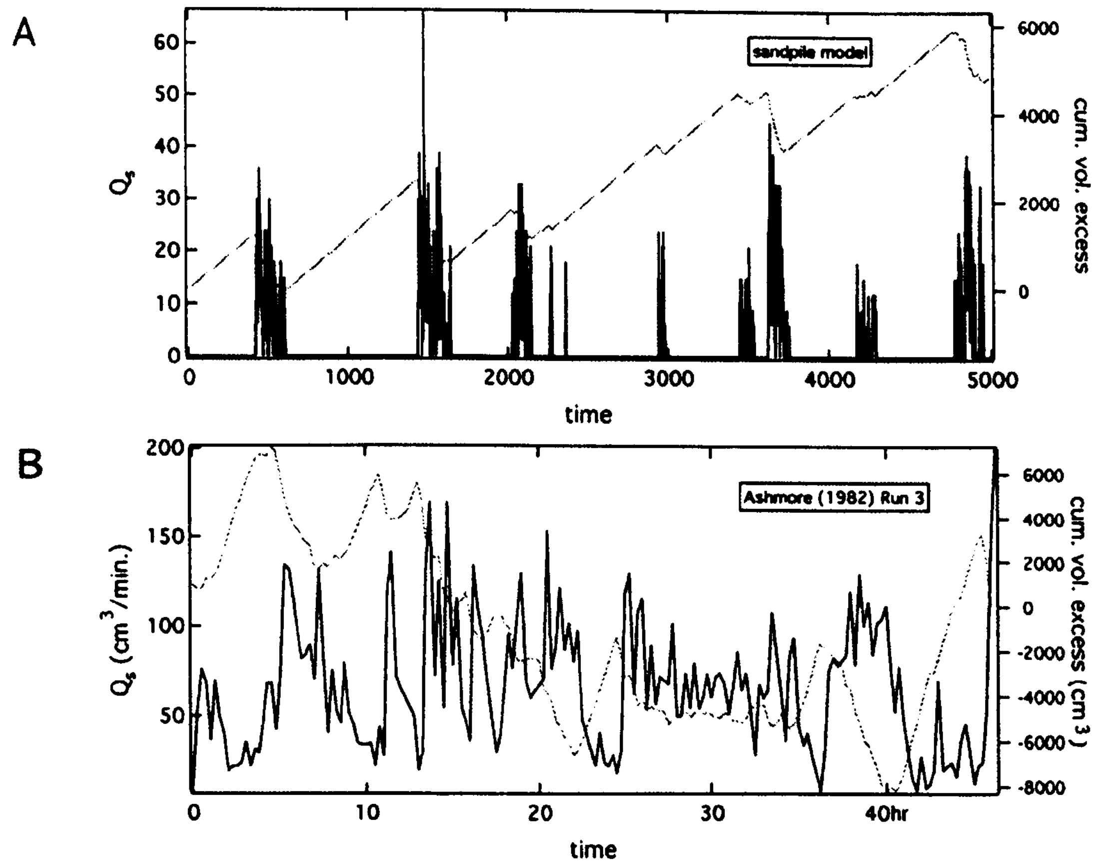

Figure 2.5 Taken from Paola and Foufoula-Georgiou (2001). Sequences of sediment output (black) from (A) the original Bak *et al.*, (1987) sand pile model with steady sediment supply and (B) an experimental braided river (Ashmore, 1985). The grey lines in the background show cumulative excess mass (cumulative input-output) in each system.

The flume results of Ashmore (1985) have been directly compared with the sand pile model of Bak (1987) by Paola and Foufoula-Georgiou (2001) **(Figure 2.5)**. The range of fluctuations of sediment output and storage from both models are large despite the steady state sediment input into both systems although the braided model shows a lower level of intermittency. An important difference between the systems is that the braided river has two material types in transport, sediment and water. Although these are closely coupled they operate at different time scales and the interaction between the two has not yet been well defined.

2.4.3 Sediment slugs

Along with flume attempts at defining sediment dynamics over a range of scales, geomorphological theory has addressed this through discussion of sediment slugs. Sediment slugs or waves have been studied as specific examples of the large variability of sediment transport rates (Nicholas *et al.*, 1995). In particular sediment slugs have been reported over a large range of scales. Attempts have been made to explain this large variability in transport by defining the dominant controls on slugs of varying sizes. Nicholas *et al.* (1995) attempt this by firstly making a distinction between endoslugs (generated wholly within channel) and exoslugs (generated from external sediment sources). They state that there appears to be a gradual change in the relative importance of extrinsic factors as slug magnitude increases. Three scales of slug are also defined, macroslug (minor channel change), megaslug (major channel change) and superslug (major valley floor adjustment). Macroslugs can be caused by fluctuations in sediment transport and storage caused by the inherent behaviour of the braided river system (this could also be termed self organisation). The development and migration of marked bar complexes has been interpreted as the result of spatial variations in hydraulics leading to different entrainment and transport conditions (Davoren and Mosely 1986; Laronne and Duncan, 1992; Goff and Ashmore, 1994). Slugs that are bigger than the macroscale are considered by Nicholas *et al.* (1995) almost exclusively the result of non-fluvial supply events, the results of landslips and major hydrologic events that are episodic or stochastic in nature.

The distinction between endoslugs and exoslugs is an important one in the context of this thesis. Endoslugs, generated as a result of the operation of the braided river system, best represent self organisation of that system. When other sediment is input from outside (exoslugs) the braided system must re-organize but it is unclear how this would occur. Wathen and Hoey (1998) studied the dispersion of a slug of coarse sediment delivered to the Allt Dubhaig, Scotland, and found that it was moved downstream as a discrete wave without significant dispersion, but what was unclear from their study was what the underlying organization of the river channel was without the influence of the exoslug. What was the structure and magnitude of sediment flux in the reach without the external sediment input. The study by Wathen and Hoey (1998) demontrates how the study of sediment slugs leads to a focus on the impact of specific events. These are easily explained and are manageable fieldwork tasks, but neglect of sediment flux that is the result of self organisation of the braided or channel system itself.

The division of sediment slugs into categories by Nicholas *et al.* (1995) was done to make assertions about the dominant processes for each category. The breaking down of the wider system into sub-systems in this way could be construed as running counter to the principle of a systems level approach because assumptions are made about the dominant process acting within each subsystem. This re- introduces the debate in **Section 2.3.1** concerning the extent of the system that should be under investigation.

Similar divisions according to magnitude can also be found in palaeo geomorphological investigations of fluvial landscapes. High magnitude events are often separated from the operation of the rest of the system and treated as specific episodes in the river channels history. This inevitably results in special explanations for specific episodes of aggradation or degradation (climate, sediment supply) (Macklin and Lewin, 1993). Any application of SOC theory to river channel development has to question this on the grounds that many large magnitude events occur as an integral part of the operation of the system. The frequency of an event with a given magnitude will be dependent on the power law function.

3.4.4 Large magnitude perturbations

Larger magnitude less frequent events (termed megaslug or superslug by Nicholas *et al.* (1995) often leave durable morphological signatures on the fluvial landscape in the form of river terraces, abandoned channels and sediment stratigraphy. Palaeo-geomorphological techniques have been developed specifically to interpret and explain these residual landforms to put them in the context of contemporary processes and external forcing controls such as climatic change and glacial retreat. An example of this is Passmore and Macklin's (2000) description and analysis of late Holocene channel and floodplain development at Lambley on the South Tyne, UK, a study that specifically relates channel changes and lateral instability to a sediment slug. Analysis of the river over a 135-year period using historic maps and APs shows that the wandering planform had been present throughout although localised instability and braiding had propagated downstream. Lithofacies and palaeochannel analysis showed that channel fills were diagnostic of floodplain construction by laterally mobile, low sinuosity and frequently divided channels. Sub reaches had experienced alternating periods of channel stability and instability over late Holocene timescales. The fluctuations in channel instability are interpreted as manifestations of the spatial and temporal variability in processes of fluvial sediment transfer (Schumm, 1973). The localised braiding is attributed to coarse sediment supply. Alternatively, patterns of channel adjustment are interpreted as reflecting the translation of bed sediment 'slugs' (Nicholas *et al.*, 1995) or waves (Macklin and Lewin, 1989) introduced from upstream reaches and erosion of valley side bluffs. Incision in the South Tyne basin in general and at Lambley coincide. The incision of channel beds is attributed to high magnitude floods large enough to disrupt channel bed armour and narrowing and deepening the active valley floor and in so doing increasing channel gradient. The event or series of events promoted further incision by confining subsequent flood flows and decoupling the channel from its floodplain.

If SOC theory is applied to the evidence of channel and floodplain changes on the South Tyne then a slightly different interpretation is possible to that of Passmore and Macklin (2000). Maps and APs from the last 135 years show a wandering channel consistent with low magnitude, high frequency sediment movements. Larger sediment movements cause increased lateral instability and morphological changes as they pass downstream. The lateral instability could be conceived as the interaction of channel geometry and the sediment slug crossing a threshold. The smaller wave structures operating in the system were not sufficient to cross the threshold to generate lateral instability. Incision is the morphological manifestation of very high magnitude infrequent fluctuations in the system occurring at the lowest point in a sediment cycle. Sediment supply is low, a threshold is crossed and incision results. These morphologically striking features do not necessarily represent a change in the fundamental dynamics governing the system but could be the result of fluctuations crossing internal geomorphic thresholds. The concept of internal and external thresholds was emphasised by Schumm (1977,1979) who recognised the effect of geomorphic thresholds on river channel pattern. The threshold is also a common concept in engineering where particle entrainment occurs at a specific flow velocity when upward lift and drag forces exceed gravitational and bed packing effects. Leopold and Wolman (1957) indicate thresholds for gradient and discharge over which rivers tend to be braided. Schumm and Khan (1972) showed that river channels changed from straight to meandering to braided as slope, stream power and sediment transport increased.

A special explanation that is often cited as instrumental in causing big disruptive events in river systems is the operation of extrinsic factors, especially climatic and land use changes (Macklin and Lewin 1993). Passmore and Macklin (2000) suggest that the large amount of incision could be the result of increased magnitude and frequency of flooding associated with the latter stages of the Medieval Warm Period and the Little Ice Age (Rumsby and Macklin 1996). Similar correlations have been found between Holocene climatic changes and patterns of channel and floodplain development in other areas of Northern England (Macklin and Lewin, 1993; Passmore *et al.*, 1993; Howard *et al.*, 1998). More detailed analysis has shown that upland British catchments have experienced periods of enhanced and reduced activity in response to the changing magnitude and frequency of climatically driven flood episodes (Harvey, 1991; Passmore *et al.*, 1993; Rumsby and Macklin, 1994).

There can be little doubt that climate is an external forcing variable changing the behaviour of river systems by changing the magnitude and frequency of flood events. Within a SOC framework climatic change is akin to changes in magnitude and frequency of inputs into the system. If the river system is compared analogously to Bak's (1996) computational sand pile then the climatic change represents increased input or larger grains of sand. During tests of the robustness of the sand pile SOC system Bak (1996) found that such changes resulted in a period of re-organisation followed by the re- establishment of SOC. If a river system is also SOC then a similar response should be expected provided that the system can adapt more rapidly than climatic changes (assuming that climate constantly changes).

If river systems are SOC then this has important implications for palaeo-geomorphological interpretations of large magnitude events and sedimentary episodes. It suggests that large magnitude events with durable morphological signatures should not necessarily be interpreted as the result of climatic or land use changes but could occur infrequently as a result of contingency and the behaviour of the SOC system. A similar confusion was identified by Passmore and Macklin (2000) who highlight the difficulty of disentangling the effects of climate from other intrinsic factors, on Holocene morphology and determining the controlling mechanisms of the underlying fluvial system. Clearly if the system can be assumed to be SOC over palaeo-geomorphological timescales (>1000 years) then measurements of frequent small magnitude events could be used to estimate the occurrence of high magnitude low frequency events (**Figure 2.6**). If this interpolation of magnitude and frequency could be relied upon it could be used in interpretations of floodplain development and challenge the importance of climate as the driving force behind major sedimentary and channel change episodes.

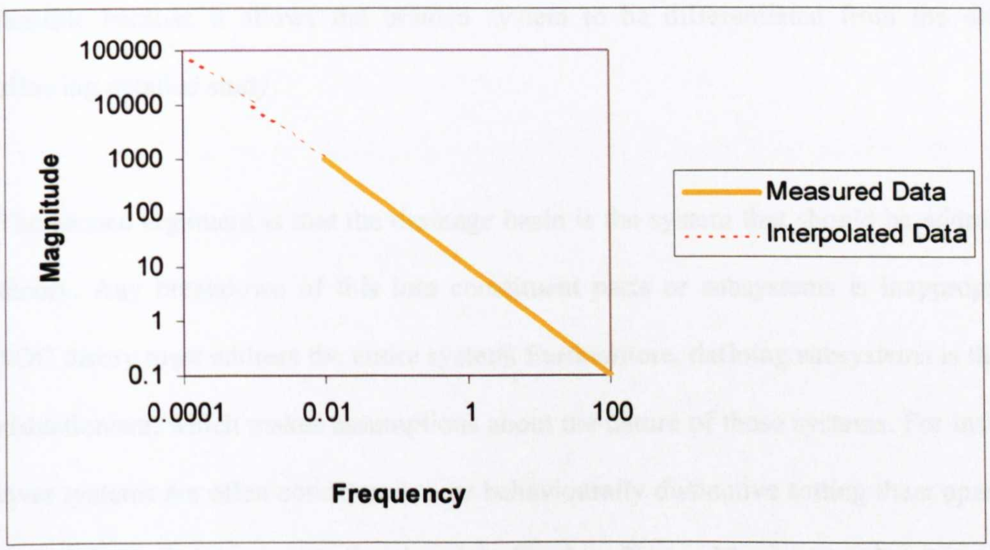

Figure 2.6. A power law well defined by measured data could be interpolated to estimate the frequency of high magnitude sediment movement events in much the same way as flow magnitude frequency data is interpolated to predict the occurrence of flood events.

2.5.0 Extent of enquiry

The discussion about the scale and origin of sediment slugs clearly raises questions about the range of scales that SOC theory could be applied to in fluvial systems. In particular the clear distinctions made between macroslugs, dominated by channel processes and megaslugs, dominated by external sediment inputs (Nicholas *et al.*, 1995) suggest that a single overriding theory is inappropriate. This is re-enforced by the palaeo-geomorphological analysis of the same phenomenon that explains major discontinuities in channel form through correlation with climatic changes.

There are two possible lines of argument concerning this. The first is that these studies are very useful in defining different systems within the drainage basin and external controls on those systems. In this way the hillslope is distinct from the river channel, the constrained river channel different from the unconstrained braided system. Climate works independently as an external influence affecting some of the fundamental controls on morphology and sediment dynamics. This argument is partially mechanistic because it seeks to break down the larger drainage basin system into a more manageable set of systems. It fundamentally assumes that these systems are distinctive and behave according to different sets of rules. Finally, this argument is practically feasible because it allows the braided system to be differentiated from the drainage basin allowing detailed study.

The second argument is that the drainage basin is the system that should be addressed by SOC theory. Any breakdown of this into constituent parts or subsystems is inappropriate because SOC theory must address the entire system. Furthermore, defining subsystems is the first step in reductionism, which makes assumptions about the nature of those systems. For instance braided river systems are often considered to be behaviourally distinctive setting them apart from single thread channels whereas studies that describe the effects of large megaslugs suggest that these cause lateral instability and channel braiding (Church 1983, Passmore and Macklin, 2000). This means that it is unclear if braided systems are actually behaviourally distinctive, in terms of the relationship between magnitude and frequency of events or whether their lateral instability is the result of higher net sediment throughput or a larger range of sediment fluctuations.

These arguments are illustrated by **Figure 2.7**. Graph A illustrates the first argument. This represents a number of subsystems that each operate within the drainage basin. At the largest spatial and temporal scales is the channel network itself, which has infrequent high magnitude processes. These overlap with the sediment fluctuations of the braided river, which overlap with the highest frequency lowest magnitude hillslope processes. The hillslopes are fed by rock wall weathering which is the landscape equivalent of rice being dropped onto the top of the rice pile. All the relationships shown are power law scaling relationships. This is not necessarily correct because a SOC system could exist surrounded by other systems that are not SOC. There is however some evidence that drainage basins (Rinaldo *et al.*, 1996), hillslopes (Noever, 1993) and braided rivers (Sapozhnikov and Foufoula-Georgiou, 1996 1997) could all be SOC. The extent of the power law relationships for each subsystem is another issue raised by this graph. The power law exponents for the three sub-systems have been arbitrarily chosen for **Figure 6.2 (A)**. They are all different to illustrate that the processes operating within each subsystem are different.

Graph B illustrates the second argument. The inverse power law relationship is indicative of 1/f noise and a signal that the system is SOC. Because the power law relationship is over a number of orders of magnitude this shows that the same processes are controlling sediment dynamics/storage over all scales. The system is termed scale invariant. The graphs (A and B) illustrate a number of questions that are fundamental to the adaptation of SOC to fluvial systems: If a subsystem is inaccurately defined how will this affect the magnitude frequency signal? Over how many orders of magnitude does a power law relationship need to extend to be considered as evidence of SOC? These are theoretical questions which are relevant to this thesis but are best addressed using experimental and computational approaches such as those employed by Bak *et al.* (1987) and Bak and Chen (1991).

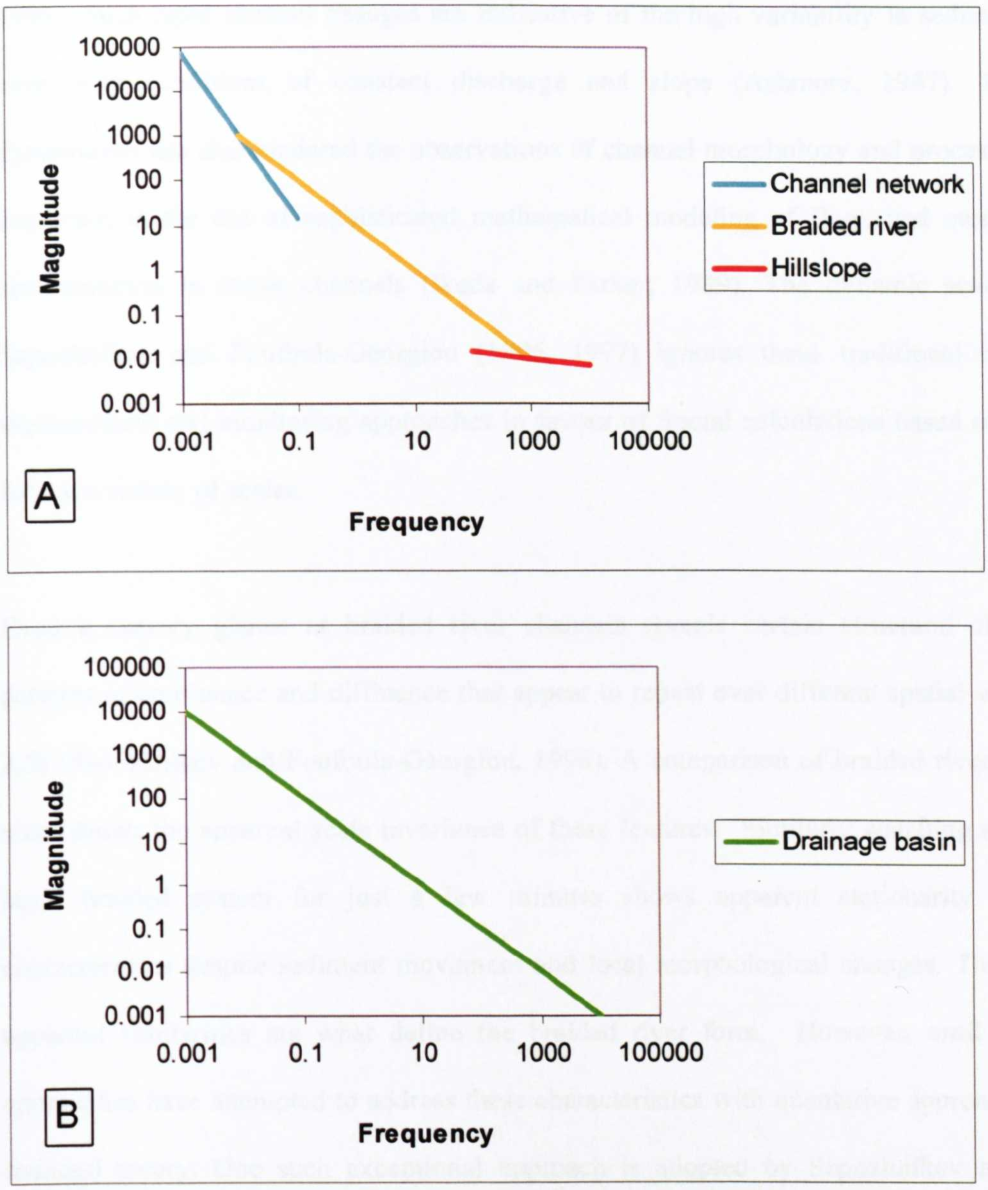

Figure 2.7 Theoretical models considering magnitude frequency relations within a drainage basin.

2.6.0 SOC in braided river systems

A number of studies have adopted the former of these arguments to investigate the scaling properties and self organisation of braided rivers (Nykanen *et al.*, 1998 Sapozhnikov and Foufoula-Georgiou, 1996, 1997). These studies follow a string of more conventional studies that have also regarded braided rivers as morphologically and functionally different from other river channels (Ashmore, 1991). Braided rivers have proved difficult to describe using conventional methods such as hydraulic geometry (Leopold and Maddock, 1953) mainly because braided channels are not stable but change rapidly through lateral instability and avulsion (Ashmore, 1991). Such rapid channel changes are indicative of the high variability in sediment transport even with conditions of constant discharge and slope (Ashmore, 1987). This channel dynamicism has also hindered the observations of channel morphology and process that proved important in the use of sophisticated mathematical modeling of flow, bed morphology and sedimentation in stable channels (Ikeda and Parker, 1989). The dynamic scaling work of Sapozhnikov and Foufoula-Georgiou (1996, 1997) ignores these traditional river channel measurement and monitoring approaches in favour of fractal calculations based on planimetric data at a variety of scales.

Even a cursory glance at braided river channels reveals certain structural characteristics, patterns of confluence and diffluence that appear to repeat over different spatial scales (**Figure 2.8**) (Sapozhnikov and Foufoula-Georgiou, 1996). A comparison of braided rivers of different sizes shows the apparent scale invariance of these features. Similarly watching a single small scale braided system for just a few minutes shows apparent stationarity of structural characteristics despite sediment movement and local morphological changes. These and other apparent similarities are what define the braided river form. However, until recently few approaches have attempted to address these characteristics with quantative approaches and well founded theory. One such exceptional approach is adopted by Sapozhnikov and Foufoula-Georgiou (1996, 1997) who developed a fractal scaling analysis to consider self-similarity (or affinity) and dynamic scaling within and between braided river channels.

Sapozhnikov and Foufoula-Georgiou (1996) used a method developed for studying the self-affinity of objects with any topology (Sapozhnikov and Foufoula-Georgiou, 1995) to show that three braided rivers exhibit anisotropic scaling characteristics (self affinity). The method developed was based on Sierpinsky carpet, a template that is used to demonstrate that the number of changes for a given *object* scales with the size of the observed region and the carpet size (explained in more detail in **Chapter 7**). The *object* used by Sapozhnikov and Foufoula-Georgiou, 1996, 1997) was the inundated area of braided rivers. It was found that a small section of any one of the rivers is statistically identical to a larger section of the same river provided that it is stretched differently along its downstream and cross stream axis **(Figure 2.9)**. The relative amount of stretch between downstream axis and cross stream axis is characterised by two fractal exponents v_X and v_y which can then be used to compose the scaling anisotropy (vx/vy) and the fractal dimension (D= vy-vx+1)/vy. A second finding of Sapozhnikov and Foufoula-Georgiou (1996) is that the fractal exponents of the three rivers studied were very similar (vx = 0.72-0.74 and vy = 0.51-0.52) despite their different scales (0.5km –15km in braid plain width), slopes (7×10^{-3} –8×10^{-5}) and types of bed material (gravel to sand). This implies that stretching each river by λ in the downstream direction and $\lambda^{vy/vx}$ in the cross stream direction will produce images that are statistically similar.

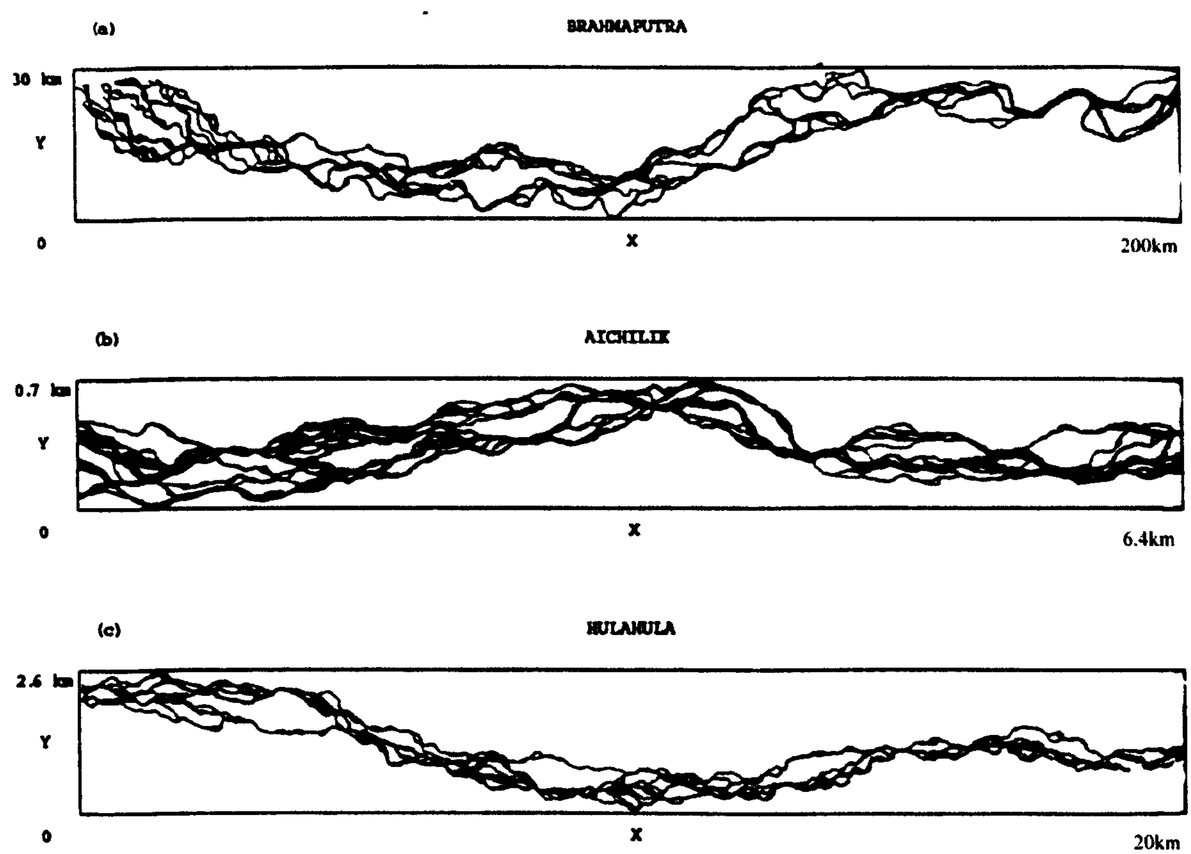

Figure 2.8. Digitised images of (a) the Brahmaputra River (Bangladesh), (b) the Aichilik River (Alaska) and (c) the Hulahula River (Alaska). Taken from Sapozhnikov and Foufoula-Georgiou (1996)

A follow up paper by Sapozhnikov and Foufoula-Georgiou (1997) determined that braided rivers also scale dynamically. Using a braided river created in a flume, sequences of photographs were analysed using the same fractal scaling analysis techniques to show temporal changes in the experimental braided river. This enabled the rates of evolution to be established for different reach sizes and a dynamic exponent to be estimated (z). The dynamic exponent (z) allows time to be re-scaled so that objects (braided reaches) of different sizes evolve identically (in the statistical sense). Sapozhnikov and Foufoula-Georgiou (1997) explain this analogously by considering movies of each section of river. When projected onto a wall side by side it is intuitive for the smaller scale section to evolve more rapidly than the larger scale section. The dynamic exponent allows one of the movies to be temporally re-scaled (played at a different speed) so that both braided river systems evolve at the same speed. The derived value of z was 0.5, this was interpreted as a relatively weak dependence of the rate of evolution on the spatial scale of the system.

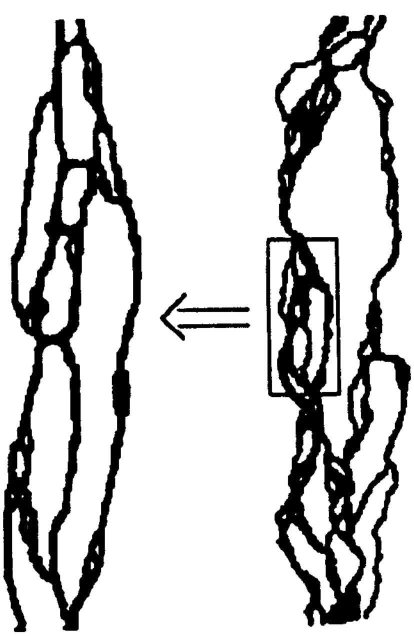

Figure 2.9. Taken from Paola and Foufoula-Georgiou (2001). A small section of inundated braided river channel resembles a larger section,

There are two specific criticisms that are immediately apparent with these studies. Both use planimetric data and this means it is actually the extent of inundation that is used to define the fractal dimensions. However, the extent of inundation of braided rivers changes with discharge so this implies that the fractal dimension might also change. Neither of the Sapozhnikov and Foufoula-Georgiou studies addresses this issue because the 1996 study uses single images from three different rivers without consideration of discharge and the 1997 study is a flume experiment with constant discharge. A second criticism made by opponents of fractal scaling is that the method used for defining the fractal dimension is such that a fractal dimension can be found for any object and this renders the fractal dimension of braided rivers meaningless. This is an incorrect criticism based on poor knowledge of fractals and how they are defined. In the case of Sapozhnikov and Foufoula-Georgiou (1996, 1997) fractal scaling work, the method used for defining fractal dimension was carefully developed Sapozhnikov and Foufoula-Georgiou (1995) and the power law scaling relationships closely describe the data in both papers.

These criticisms are addressed more directly by a third paper (Nykanen *et al.*, 1998), which defines the spatial scaling of river patterns by defining the extent of inundation using Synthetic Aperture Radar imagery. This paper used several reaches of the Tanana River (Alaska) to show that self-affine spatial scaling was present under different flow rates with Vx (0.70-0.77) and Vy (0.47-0.50) varying little with discharge and in line with previously reported exponents (Vx 0.72-0.74 and Vy 0.51-0.52) (Sapozhnikov and Foufoula-Georgiou, 1996). The second criticism is addressed by a key finding of the paper, that channel reaches that have topographic controls imposed (such as mountains) or are prevented from fully developing their floodplains do not exhibit self affine spatial scaling. This is augmented by the observation that braided rivers that have a main channel several tens of times bigger than other braidplain channels were not found to be self affine. This apparent lack of scaling is mainly due to the small number of channel sizes, which limited the definition of a scaling relationship. These key findings show that Sapozhnikov and Foufoula-Georgiou's (1995) method is a good indictor of spatial scaling and it is carefully applied so that only well established power law scaling relationships are taken as evidence of self affine scaling.

The three papers described above are seminal (Sapozhnikov and Foufoula-Georgiou, 1996 1997, Nykanen *et al.*, 1998). They show spatial and temporal scale invariance in a number of braided rivers suggesting that these are SOC systems. These changes are not dependent on discharge but are dependent on unconstrained channel braiding, suggesting that it is the braiding itself that is the morphological manifestation of SOC. Furthermore, the scale invariances could be taken as an indication of a set of universal physical mechanisms responsible for braiding over a range of scales (Nykanen *et al.*, 1998). Although the scaling analysis itself does not provide insight into what these universal physical mechanisms are, the suggestion that the system could be SOC increases the validity of a range of simplified modeling approaches of the type employed by Bak (1991). One such modeling approach is the simple cellular model developed by Murray and Paola (1993, 1997, discussed below). If braided rivers are assumed to be scale invariant then this also increases the validity of experimental research using scaled down physical models.

The work of Sapozhnikov and Foufoula-Georgiou (1996, 1997) is by no means conclusive evidence that braided rivers are SOC. The studies fail to measure all geometric dimensions of change, they are planimetric and as such they only measure the scaling and (in the 1997 paper) flux of flow inundation, a measure that is closely linked to flow flux. The other important material flux relevant for determining the SOC characteristics of braided river is sediment flux. This is not considered at all by the analysis. The two fluxes are clearly related, with flow flux driving sediment flux, which in turn changes channel morphology effecting the extent of inundation. However, a large change in the pattern of flow can be attributed to relatively small amounts of morphological change (small sediment flux) at a key point in the system. This is traditionally termed avulsion, a key mechanism of channel change in braided river systems (Ashmore, 1993)

One method of producing more conclusive evidence of SOC is to use three-dimensional measurements of topography. This could lead to studies of *dynamic multiscaling* (Sapozhnikov and Foufoula-Georgiou (1997), where scaling is defined in three spatial dimensions (X,Y and Z) and over time. This could be achieved by developing the Siepinsky carpet (two dimensional) into a Sierpinsky Cube (three dimensional) for use on high quality DEMs. Alternatively the principles of the morphological method could be used to quantify patterns of sediment flux. Only with such high quality measurement of sediment dynamics can SOC in braided river systems be tested.

The Sapozhnikov and Foufoula-Georgiou papers (1996, 1997) raise an important question about the most appropriate method of measuring scale invariance. This is potentially a broad question because a SOC system with many different elements could show scale invariance in a number of key morphologies and processes that represent the dominant dynamics of the system whilst scale dependence in others that are peripheral. This could be the case with braided rivers given a number of elements (grain size, flow regime, vegetation) that might not be directly related to the operation of the system itself. If this is applicable then certain measured processes or morphologies could be scale dependent because they are not primarily controlled by SOC. Ashmore (2001) uses a collation of data about confluence and diffluence spacing to show that these are scale specific and can be related to discharge. However, this does not necessarily mean that the primary controls on SOC are not scale invariant. In fact, because the confluence and diffluence data were mainly collected at low flow, a morphologically insignificant discharge that is sometimes an order of magnitude smaller than competent flows, the significance of the scale dependence can be doubted. The lack of competence and activity at low flow suggest that the river is not organising itself and therefore any measurement based on flow distribution at low flow would not necessarily display scale invariance. In this case it is the low flow element of the flow regime that does not conform to scale invariance.

This focus on dominant processes is an approach that comes from SOC and the modeling approaches employed by Bak *et al* (1991). It was the simple but effective modeling of sand piles that initially defined SOC by producing 1/f noise. Similar synthetic modeling approaches for defining the emergent properties of braided rivers have been limited to a few attempts (Murray and Paola, 1993, 1997) but these have shown sufficient success in offering explanations for braiding to stimulate discussion over modeling approaches (Paola, 2001)

2.7.0 Computational modeling of braided river systems

The established approach for modeling fluvial systems is a form of reductionism based primarily on classical mechanics. The aim of such modeling is to employ approximated forms of the fundamental governing equations to model river flow and in some cases sediment dynamics. This traditional modeling approach attempts to retain as many aspects of the governing equations as possible (Paola, 2001). This is fundamentally at odds with the modeling approach suggested by Bak (1991, 1996) for modeling 1/f noise and determining the emergent properties of SOC systems. Bak's (1991, 1996) modeling, based on the principle of universality aimed to model the crucial dynamics of a system with the minimum number of expressions.

In braided river research a similar modeling approach has been suggested by Paola (2001), it is termed synthesism. The aim of synthesism is to use representations of the crucial lower level dynamics to construct a higher level model. Examples of this approach include Howard *et al,* (1970) and Rachocki (1982), both attempt to simply represent the geometry of multi-channel networks. Synthesist modeling approaches are in stark contrast with more traditional reductionist approaches, which start with governing equations such as the shallow water equations (Lane, 1995; McArdell and Faeh, 2001). Traditional, reductionist stream flow models are based on the principles of computational fluid dynamics although computational limitations require vertical integration of the fundamental flow equations and the use of a drag law to model the interactions between the channel boundary and flow. The aim is to represent the fluid flow and boundary interactions as accurately as possible by incorporating terms for turbulence and input velocities (Lane, 1995).

The biggest success of the synthesist modeling approach in the study of braided rivers is Murray and Paola's (1994, 1997) cellular model. This model is actually a hybrid of synthetic and reductionist approaches. It uses highly simplified representations of flow and sediment movement. The model is a variation of a cellular automata model used in dynamical systems research. The model uses a series of rules to represent the fundamental dynamics of the system **(Figure 2.10)**

The model reproduces braided channel patterns that capture some of the dynamical aspects of real braided river systems. The braided pattern evolves, by erosion in narrowing sections and deposition at flow expansion, into dynamic equilibrium. Despite steady state inputs into the model, sediment output at the downstream end have broadband spectra (Paola, 2001) similar to those found experimentally by Ashmore (1991).

The importance of the Murray and Paola (1993, 1997) model lies not only with its new approach to the problem of modeling a braided river system but mainly with what we can learn from its simulation of the emergent properties of the system. Paola (2000) focuses specifically on this point. The flow formulation in the Murray and Paola (1993, 1997) model is simplistic but the end result is fully developed two dimensional braiding. Flow concentration and expansion are modeled with a rule that lets an upstream cell pass flow to three downstream cells depending on the relative elevations of those cells. Crucially the sediment transport law that is attached to flow must be non-linear to generate braiding. If a linear law is substituted instead then sediment flux matches water flux and channel topography becomes static. The non-linear law means that sediment flux 'over-reacts' to increases in flow and this means channel topography cannot be optimised (Paola, 2001). Non-linearity is a key component of both Murray and Paola's (1993, 1997) model and SOC systems.

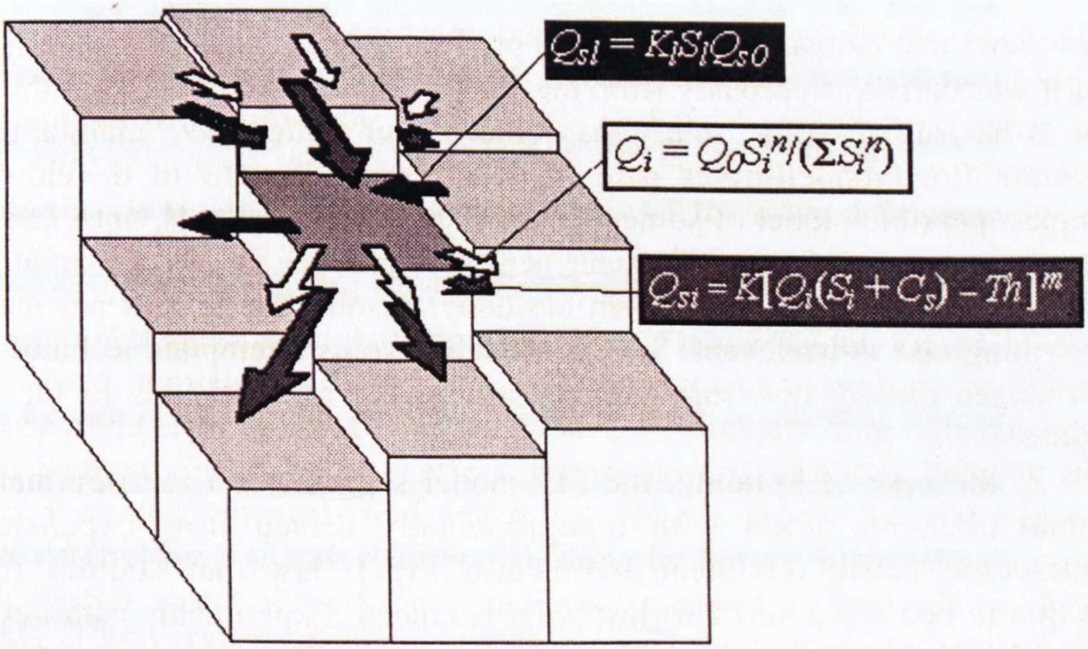

Figure 2.10. Water and sediment routing in the Murray-Paola (1994) braid model. A given cell receives and distributes water from its neighbouring cells. Water fluxes (white arrows and box) to each of the three adjoining downstream cells Q_i, are determined by the slopes to those cells, S_i, according to a power law, where Q_o is the discharge coming from the target cell. Only positive slopes receive water. If all slopes to the three downstream cells are negative, the water is allocated analogously, with more water flowing where the slopes are least negative. A normal-flow approximation suggests a value of 0.5 for the exponent n. Direct sediment flux Q_{si}, is determined by the stream power index, or $Q_i S_i$ (grey arrows and box) modified by adding a constant (C_s) equal to three times the average slope, to allow sediment transport on locally flat or uphill areas. K is constant, Th is a sediment-transport threshold and m is an exponent that must be greater than 1 to produce braiding. A reasonable value is 2.5. Lateral sediment transport Q_{sl}, (black arrows and box) is based on standard expressions for gravitationally induced component of sediment transport on transverse slopes. K_l is a constant and Q_{so} is the direct sediment transport in the target cell. Taken from Paola (2001).

Paola (2001) considers synthesism and reductionism to be the two main 'end-member' models of river behaviour that will ideally converge into a 'standard model'. This model will have a structure capable of resolving channels within a cell network and as such should be applicable to the range of channel planforms from meandering to braided. If such modeling advances are to be achieved then two specific areas need to be addressed experimentally and through field studies.

The first and most important, concerns the nature of the organisation of the braided river system itself. There is some evidence to suggest that braided river systems could be SOC. With data that is designed to directly address SOC this idea can be better tested and the fundamental organisational properties of braided river systems can be established as criteria upon which to base computational models. Both fractality of topography and power law scaling could change the conceptualisation of models at a fundamental level. Once again the issue of scale of enquiry is important here. If a single computational model applicable to all channel planforms is to be realised then the scale of enquiry that field studies and theory should be addressing is larger than the braided system alone. It should be concerned with establishing the sediment dynamics and organisational properties of all types of planform and maybe not differentiating systems on the basis of planform.

The second area that needs to be addressed by laboratory and fieldwork is the shortage of data that describes sediment movement over a range of spatial and temporal scales. A good knowledge of the magnitude and frequency relations of sediment movement will not only help determine the organisational properties of the system but are important for model calibration and validation. Without such evidence the rapid advances of computational models will be hindered by a lack of sophisticated morphometrics.

2.8.0 Conclusion and research themes

The discussion in this chapter has explained the importance of a systems level approach to understanding of river geomorphology. In particular it has described the theory of SOC and the role this could have in improving understanding of channel change and sediment dynamics.

Four specific themes warrant re-iteration here:

1) Scale of enquiry: The scale at which systems level approaches should be applied is contentious. Breaking the drainage basin system down into subsystems such as confined channel systems and braided channel systems makes some big assumptions about the functioning of those systems yet this is important for practical reasons. In river science this distinction is emphasised by the continuum of channel form between a single thread channel and a multiple channelled braided system. Evidence of large magnitude sediment pulses moving down through channels shows that these increase channel multiplicity suggesting that a braided system cannot (and should not) be set aside as an independent system.

2) Bedload sediment movement has been quantified using a variety of methods and over a variety of scales. The unpredictable spatial and temporal flux is a feature that is prominent at all scales suggesting that river channels could be SOC systems; however to test SOC data needs to be high quality and measure sediment movement over a large range of spatial and temporal scales.

3) The fractal scaling properties of braided rivers have been tested by applying a fractal analysis technique to the submerged areas of a braided river (Sapozhnikov and Foufoula-Georgiou 1996 1997; Nykanen *et al* 1998). These show that braided channels scale anisotropically both statically and dynamically. This planimetric analysis is encouraging but it fails to test scaling in all three dimensions and the scaling properties of sediment flux.

4) Computational modeling of river channels and in particular braided river systems has made rapid progress recently. The adoption of synthetic modeling techniques has produced new understanding of channel braiding. However, these improvements need to be matched by spatially extensive studies of actual river channels so that new

synthetic approaches can be better directed and validated using appropriate morphometrics.

There are numerous ways in which the self organisation and scaling characteristics discussed above can be investigated. The work of Sapozhnikov and Foufoula-Georgiou (1996, 1997) takes a two dimensional, planimetric approach to identifying scaling characteristics whilst others have made simple observations about channel size and relations (Rust, 1978; Howard *et al.*, 1970). However, this thesis is not concerned with the scaling characteristics of braided rivers *per se* but with how scaling is indicative of self-organisation. The focus is on dynamic scaling and how the spatial and temporal pattern of sediment movement fits with existing theories of self organisation such as SOC. The techniques available with which to quantify dynamic scaling at a variety of scales are very few. Direct measurement of bedload (e.g. Helley Smith sampling) is a technique restricted to a few sampling sites and poorly defines sediment movement over an entire braided river system. The morphological method offers greater potential particularly with recent advances in remote and ground survey techniques (discussed in length in **Chapter 3**). The development of digital photogrammetric techniques allow the acquisition of a large number of elevation points over spatially extensive systems and with resolutions suitable for DEM construction (discussed in **Chapter 3**). High quality DEMs allow the potential of the morphological method to be better realised. Static DEMs can be analysed in more sophisticated ways than transects and differencing DEMs shows spatial patterns of sediment movement. This thesis aims to take advantage of these advances in data quality to demonstrate the scaling characteristics of a braided river system and then interpret these indicators in relation to the theory of SOC.

2.8.1 Research theme 1: Acquisition, correction and testing of high quality morphological data.

The first research theme centres on the acquisition of data designed to determine the scaling characteristics of the study system (introduced in **Chapter 4**). The discussion above has shown that morphological form could be indicative of the self-organisation dominant in the system and so the acquisition of high quality morphological data, in the form of DEMs, is important.

There are a number of theoretical and practical issues surrounding the acquisition of DEMs. Ground survey and remote survey have specific advantages as regards spatio-temporal resolution and the propagation of error but these have not been discussed in the context of scaling and SOC. The magnitude and structure of error is particularly important because it defines for what applications data can be used . The improved DEMs with well defined errors can then be used to address the second research theme.

There are some specific questions that will be addressed: What techniques for acquiring morphological data are most appropriate for addressing the multi-scale, spatially extensive data required for scaling analysis at the system scale? And what magnitude and structure of error is incorporated into DEMs using ground and remote survey techniques and how does this effect the application of those DEMs to problems of scaling and self organisation.

2.8.2 Research theme 2. Static scaling properties

Improved data acquisition techniques allow more sophisticated analysis of the morphology and dynamics of river channels. In particular the three dimensional scaling properties of river channel morphology can be investigated. The passage of slugs of sediment through the river channel system inevitably have an impact on the shape of the channel. If slugs of different magnitudes and frequencies are passing through the system then these will also cause changes in form and, provided topographic measurements are of sufficient quality, then these changes will be identifiable. The second research theme aims to identify downstream patterns in channel form indicative of the passage of sediment slugs or waves, the scaling characteristics of these waves provides evidence about the self organised properties of the system.

The specific questions that will be addressed are: How can patterns in morphology, indicative of self organisation be reliably identified? And what scaling characteristics are emergent from analysis at the system scale?

2.8.3 Research theme 3: Dynamic scaling properties

A second obvious approach to the problem of system scale organisational behaviour is dynamic scaling. The flux of sediment through a river channel can be measured by differencing of DEMs, a technique that gives spatially distributed information about scour and fill. The volume and pattern of these changes is direct evidence of how the river system organises itself.

The third research theme aims to identify the dynamic scaling properties of the field site by answering the following questions: Does sediment movement occur according to specific length scales or is it scale invariant? And how do the dynamic scaling characteristics compare to the static scaling characteristics?

2.8.4 Research theme 4: The self organised properties of braided rivers

The final theme is broader. It aims to take the specific findings of the previous themes and put them in the context of systems level theories, in particular SOC, and geomorphological theories and models. The final theme considers what the static and dynamic scaling properties of the river system show about the organisational properties of the system.

The following question will be addressed: Do the static and dynamic scaling characteristics determined in this thesis support the idea that braided river systems are self organised critical?

CHAPTER 3. MORPHOLOGICAL DATA ACQUISITION

Abstract

It is clear from discussion in **Chapters 1** and **2**, that high quality data over a spatially extensive area and covering a range of spatial scales is necessary for addressing issues of spatial scaling and self-organization. Morphological data are one type of data that can incorporate the range of scales necessary. Static self organization (research theme 2) and sediment dynamics (research theme 3) can both be inferred from morphological data provided that data quality can be demonstrated. Acquisition of such high quality data is a major challenge. In the last 30 years topographic data acquisition has advanced rapidly with improved ground survey technologies and the advent of digital remote sensing systems. These have been matched by improved data handling and storage facilities due to advances in computing hardware and software. Many of these advances have only recently come under close scrutiny by river scientists interested in assessing error in the data acquisition and DEM construction techniques (Desmet, 1997; Lane, 2001). This is partly a result of the highly quantitative geomorphological aims of research topics addressing issues such as those described in **Chapter 2**. Such topics require a good understanding of the types of error introduced by each survey method. In particular errors are not always transparent in many automated softcopy (digital) photogrammetric systems and this means the fundamental limitations of the photogrammetric method could easily be overlooked by inexperienced users (Lane, 2001). Initially error terminology is defined (**Section 3.2**). Secondly, sources of error in terrain measurement for fluvial geomorphology are introduced (**Section 3.3**). Data acquisition method is one of the most important of these and is discussed in detail with an initial focus on ground survey techniques (**Section 3.4**) and then remote sensing techniques (**Section 3.5**). The implications of the data acquisition techniques on data distribution and density (**Section 3.6**) and terrain characteristics are discussed (**Section 3.7**). Finally, issues surrounding spatio- temporal resolution are addressed (**Section 3.8**).

3.1.0 Introduction

Surveying of river channel topography has traditionally been based on ground survey techniques. Repeat survey of monumented cross sections has been one of the most enduring data acquisition methods of the discipline, providing key data in important developments such as hydraulic geometry (Leopold *et al.,* 1957) and adopted as a standard for river monitoring (Ashmore *et al.,* 1992 Ferguson and Ashworth, 1992; McLean and Church, 1999[2]). The same techniques are currently used for river management applications (the lower Fraser River, British Columbia for instance) although advances in remote sensing techniques have recently started impacting on river management strategies such as the management of the Waimakariri River in New Zealand (Westaway, 2001). Advances in technology, in particular the GPS and robotized total station have made high resolution ground survey, suitable for DEM construction, possible at the mesoscale. The increase in usage of remote sensing techniques is due in part to the availability of sophisticated instrumentation such as Compact Airborne Spectrographic Imager (CASI) and Light Detection And Ranging (LiDAR), but mainly as a result of improved computational software and hardware. Improved quality of data acquisition and processing techniques offer considerable advances on the largely qualitative approaches of photographic interpretation more traditionally adopted (Westaway, 2001).

3.2.0 Types of error encountered in terrain survey

Measurement of any physical quantity is unlikely to be exactly equal to the true amount. The sorts of uncertainties associated with measurements of terrain surfaces have been well defined first by surveyors and then photogrammetrists. These errors fall into three categories; random, systematic and gross (Butler *et al,* 1998; Cooper and Cross, 1988; Cooper, 1998).

Random error is inherent in any data set. Random errors are experimental uncertainties that can be revealed by repeating measurements (Taylor, 1997). If systematic error is removed then random error will be normally distributed around the true value. The distribution of random error is important as it gives a measure of precision (Cooper and Cross, 1988; Wise,1998).

Systematic error involves regular or repeated error throughout a set of measurements. Systematic error is conventionally termed accuracy by photogrammetrists. These errors occur as a result of inexact functional models, improperly calibrated equipment (Cooper, 1998) and user error. As a result they are theoretically avoidable unlike random error. Also unlike random error, repeated measurements with the same instrument will not reduce or reveal the error because every measurement will include the same systematic error. As a result, systematic error is potentially more significant. However it is often assumed to be negligible because it is difficult to quantify. A clear example of this is Root Mean Square Error (RMSE) (**Equation 2.1**) which became established as the standard for assessing error in photogrammetric work despite its inability to detect systematic error.

$$RMSE = \sqrt{\frac{\sum_{i=1}^{n}(p_i - s_i)^2}{n}}$$ **Equation 2.1**

Where p_i = photogrammetrically acquired elevation and s_i= survey acquired elevation.

RMSE is one method for defining the standard deviation of measurements and it is useful for characterizing the reliability of measurements (Taylor, 1997). However, RMSE has a tendency to understate the uncertainty especially when the number of measurements is small. Recently researchers have questioned this use of RMSE as a method of determining the reliability of DEM surfaces and as a result changed to using an alternative method, Standard deviation of Error (SDE) for determining precision (**Equation 2.2**) and Mean Error (ME) for determining accuracy (Lane, 2000)

$$SDE = \sqrt{\frac{\sum_{i=1}^{n}((p_i - s_i) - \overline{((p_i - s_i))})^2}{n}} = \sqrt{\frac{\sum_{i=1}^{n}(p_i - s_i)^2}{n} - \overline{(p_i - s_i)}^2} \qquad \textbf{Equation 2.2}$$

The term gross error is commonly used to refer to survey blunders. In photogrammetric research these are the result of intermittent failings in the functional model used or incorrect procedures. Gross error is often considered to be due to human error with manual photogrammetric measurements. However automated photogrammetric techniques show similar gross errors (Nagao *et al.*, 1988; Chandler, 1999) resulting from failings in the pixel matching process (see **Section 5.5**). The term reliability is used in the context of gross error, reliability ibeing considered in terms of internal and external reliability. Internal reliability relates to the magnitude of individual blunders that can be identified. The lower the internal reliability the higher the threshold for distinguishing gross error from topographic variability. External reliability relates to the effect of an undetected blunder on information computed from a measurement (Cooper and Cross, 1988). High internal reliability necessarily results in high external reliability.

3.2.1 Determination of error in DEMs

Error in regularly gridded DEMs is usually assigned a single value (Ez) in just one direction (elevation). This is theoretically incorrect because the error value represents two types of error: Systematic error due to datum shifts in XY and/or Z; and a random distribution of error values around E_Z. Errors calculated between data sets occur in all three dimensions hence error should ideally be presented as a three dimensional vector (Westaway, 2001). However given that gridded data works on fixed X,Y arrays the scope for defining a three-dimensional vector is reduced. The smallest planimetric error that can be defined is equivalent to the grid cell size, but in practice this is usually ignored with analysis of Z co-ordinates only. The DEM data presented in this project are primarily regularly gridded data and therefore all errors are dealt with in this way by focusing on Ez.

3.3 Sources of error

The section above defined the error terminology used in this thesis and went on to describe three types of error. Just as important as knowing what sorts of error are possible is knowing the likely sources of those errors. Clearly error can be introduced from a variety of sources during the process of acquiring elevation data and building DEMs.

Desmet (1997) outlines 4 closely interrelated factors that need to be considered when assessing error in DEMs: 1) the data acquisition method; 2) spatial density and distribution of points; 3) the interpolation method used and (4) the characteristics of the terrain being modeled. Broadly speaking these factors are a relevant conceptualisation of the sources of error, however the following discussion of data acquisition methods highlights the dependence of spatial density and distribution of points on the method of data acquisition. This is particularly true in river science where technological improvements in survey methods have dramatically altered the distribution of data points collected, from cross sectional profiles with low downstream resolution to high resolution regularly gridded DEMs. Desmet (1997) also fails to consider time as a dimension in which error can occur. Time and temporal resolution is an integral part of river science studies of dynamism and as such represents another potential source of error. Spatio-temporal resolution is discussed in considerable detail at the end of this section.

3.4 Ground survey in river science

Ground survey is used here to describe methods that directly measure the land surface with equipment that is based on the land surface. Most often this involves direct contact with a surveying pole or staff, but trigonometric based survey approaches using ground based equipment are similarly included.

Ground survey is a foundation for morphological data collection and as such it has produced much of the quantitative evidence on which fluvial geomorphological theory is based. Leopold, Wolman and Miller (1964) illustrate this point with ground survey data used to define specific morphological units (riffles, bars and pools) and width depth relationships. The work of Wolman and Miller (1964) is one example of the work carried out by researchers at the United States Geological Society (USGS) during the quantative revolution of geomorphology in the 1950s and 1960s. The qualitative approaches pioneered by W.M. Davis were challenged as research was focused on measuring landforms and processes.

This thesis draws a clear distinction between monumented cross sections and high-resolution data collection techniques, which although not gridded, can still be used for the construction of DEMs. Monumented cross-sections involve the survey of a large number of points along transects with fixed ends, aligned perpendicular to the channel or direction of flow. The downstream resolution of this approach is typically very large. Transects on the Waimakariri are positioned over two active widths apart, approximately 800m (Hicks *et al.,* 1999) and at 50m to 120m apart on the Fraser River where channel width is up to 500m (McLean and Church, 1999[2]). Given the complex topography and characteristic length scales associated with braided river morphology the construction of a DEM using such coarse data is of little use apart from at the largest scales of analysis, for calculating crude sediment budgets (McLean and Church, 1999[2]). Furthermore a good appreciation of the rates and types of channel changes is necessary to implement a suitable survey design. If channel changes are too rapid then channel cross sections fail to remain orthogonal to the direction of flow (Coldwell, 1957; Lewin, 1990) and in extreme cases avulsion can leave cross sections completely dry.

High resolution data sets have a downstream resolution similar to that of the cross stream resolution and this means the resolution of data sets is described as a point density, for instance Lane *et al.*, (1995) used data with point densities between 1.0 and 7.4 points per m^2 and Brasington *et al.*, (2000) used data with point densities between 0.69 and 1.10 points per m^2. The consistent downstream and cross-stream resolution makes high resolution data sets suitable for DEM construction. The high downstream resolution means that morphological variability is well accounted for and this means that cross-stream transects need not be monumented. This increases the flexibility of the technique allowing better representation of complex topography. As in monumented cross sections a good knowledge of the dynamism of the survey site is needed to choose suitable survey areas and apply a suitable survey design. Although DEM data are not dependent on direction of flow in relation to cross sections there is still the need for the main channel to stay within the survey area and for sufficient activity to take place to make the large expenditure of resources worthwhile.

3.4.1 Ground survey techniques

A range of techniques and technologies have been used as the basis for recording topographic information. The most basic approaches have been reliant on leveling and planimetric mapping, the Electromagnetic Distance Measurer (EDM) and total station have greatly improved accuracy and efficiency. Most recently equipment that uses the Global Positioning System (GPS) has been used.

Surveying and re-surveying of monumented cross sections and planimetric mapping of transect ends and other specific features such as bank tops have long been achievable through the use of leveling equipment and plane table mapping. As such, the methods involved have been well documented, with both theoretical (Bannister, 1998) and field based data quality assessments available. Lane (1998) illustrates leveling accuracy by showing that the elevation determination possible is ±0.01m. Over a 100m distance this equates to a 1m uncertainty. This estimate is in line with reported accuracies of Werritty and Ferguson (1980) who describe the survey of 5 cross sections between 250-280m long from a single station and this gives a working accuracy of 1m.

Rapid advances in survey accuracy can be attributed to the adoption of EDM and total stations. The EDM works by generating an electromagnetic wave that is refracted off a retro prism and is received back by the source EDM. The distance between the EDM and the prism is calculated by halving the time elapsed between the moment of transmission and moment of reception, multiplied by the speed of light. Improvements in the accuracy of individual measurements are augmented by a reduction in the number of instrument relocations needed, electronic logging of measurements and automated correction for earth curvature. As with leveling and optical methods EDM and total station have been applied to enough surveying projects for theoretical and working accuracies to be well established (Bannister, 1998; Lane, 1998). EDM distance accuracies published by the equipment manufacturers are very good, ±0.005m +5ppm for the Geodimeter 400series (Barker *et al.,* 1998) and ±0.003m +3ppm for the Topcon GTS4B (Topcon 1991). The working accuracies recommended by Bannister (1998) stress the influence of atmospheric refraction on measurements. Bannister (1998) suggests that 95% of points measured with EDM should be below 500m and any measurement over 1500m could result in atmospheric refraction of up to 0.5m.

Subtle refinements of EDM/total station equipment have brought improvements such as automatic prism tracking and remote control of EDM point collection. These improve the ease and efficiency of the ground survey process without altering the fundamental accuracy of measurements.

Despite these improvements in accuracy and efficiency a majority of studies have still relied on the same basic technique of resurveying of monumented cross sections although there are some notable exceptions where high-resolution data have been collected over limited extents. For instance Lane *et al.* (1995) augmented photogrammetrically derived data with high resolution EDM acquired data to generate a DEM of the submerged sections of the Haut Glacier d'Arolla in the Pennine Alps, Switzerland and Brasington *et al.*(2000) used high resolution EDM measurements to survey areas of the River Feshie not accessible to GPS survey.

Rapid acquisition of a large number of high accuracy and high precision points through ground survey has been further aided by the development of surveying equipment that uses the Global Positioning System (GPS). The application of the GPS to surveying problems is relatively recent and the fundamental principles quite different from the tachometric techniques described above. The GPS has two advantages over traditional tachometric approaches. It does not require line of sight and errors do not propagate substantially with distance.

The GPS is a means of acquiring a three- dimensional position using measurements from earth orbiting satellites. Comprehensive reviews of the development and application of GPS technology can be found in Hoffman and Wellenhof *et al.*, (1997) and Van Sickle (1996). This review of the GPS will attempt to highlight the underlying principles behind the system along with theoretical issues about data quality.

The GPS was originally developed and designed for a variety of military uses by the United States (US) from the 1970s to the 1990s. A key characteristic of the GPS is that it is a passive system allowing a limitless number of receivers to monitor the carrier waves. This has lead to development of receivers for civilian use for navigation and surveying purposes. The removal of the p-code in 1999 has been a significant step forward for non- specialist users.

The principle underlying the GPS is that of trilateration. A ground based receiver calculates the distance to a number of satellites using two carrier frequencies, L1(1575.42MHz) and L2

(1227.60MHz) that are broadcast by each GPS satellite. If distances can be calculated to enough satellites (theoretically three but in practice at least four) then the ground receiver can be located to within millimeter accuracy (post removal of p-code, see below) (Van Sickle, 1996).

There are three basic codes used in GPS to transmit information. The navigation code carries much of the basic information needed for GPS to function on both carrier waves (L1 and L2). Information is included on the satellite's ephemeris (needed to fix WGS1984 co-ordinates) atmospheric correction, anti-spoofing, almanac and satellite health. The C/A (coarse acquisition) code and P (precise code) carry the raw data from which GPS receivers derive their time and distance measurements. The C/A code uses the L1 frequency to transfer the Standard Positioning Service (SPS) used to provide a minimum level of positioning capability (+- 100m). This is intentionally degraded using Selective Availability (SA) to reduce the absolute accuracy of civilian receivers. The P-code uses both frequencies (L1 and L2) to transfer the Precise Positioning Service (PPS) that allows millimetre precision when sampled for sufficiently long periods (Van Sickle, 1996). Until 1999 the p-code was encrypted making it ineffective for non military users. Both SA and the P code were originally introduced into the GPS system to intentionally reduce the accuracy of the system for all non-US military users. The P-code encryption was removed in 1999 because it had become ineffective due to the development of the phase shift method for accurately determining location (see below).

To calculate location the GPS is reliant on calculating its range from a number of satellites. This is accomplished to within a few meters using a method called pseudoranging. This precision is improved upon using phase shift measurements, which allow millimeter precision.

There are fundamental reasons why these more complex methods are needed instead of simpler electromagnetic solutions to define distance used by EDMs. The EDM system only needs one clock (more correctly termed oscillator) because the electromagnetic wave emitted by the device is reflected by the prism and received by the same device. To calculate the distance to the prism the device halves the time elapsed between emission and reception. In contrast the GPS uses the pseudoranging approach, which monitors the carrier waves generated by atomic clocks in GPS satellites and compares them against its own quartz clock. The distance from satellite to receiver is then calculated by multiplying the time taken with the speed of signal (i.e. speed of light). This solution is problematic because it is reliant on perfect synchronisation between the two clocks (satellite and receiver), which is not possible hence, the pseudoranging method only results in an estimation of distance (that when calculated from 4 or more satellites) gives positional information accurate to at least 30m. Theoretically, pseudoranging is accurate to approximately 1% of the chipping rate (related to oscillator frequency), which equates to 3 meters for the C/A code and 0.3m for the P code. The cessation of P code encryption means that the p-code can now be used for the pseudoranging approach, significantly improving the accuracy of the pseudoranging method.

The phase shift method of ranging is used together with pseudoranging in surveying applications of GPS (**Figure 3.1**). The method uses the carrier phase measurements themselves instead of the C/A and p codes. This means that the user is immune from the C/A code degradation, SA and p-code encryption. Phase shift estimates the fractional part of the phase cycle to within 1% of the carrier cycle equating to 0.19m for L1 and 0.24m for L2. The phase shift measurements do not reveal the integer number of wavelengths between the transmitter and receiver. These are calculated by relating linear combinations of range equations between multiple receivers and multiple satellites, termed single, double and triple differencing by Van Sickle (1996).

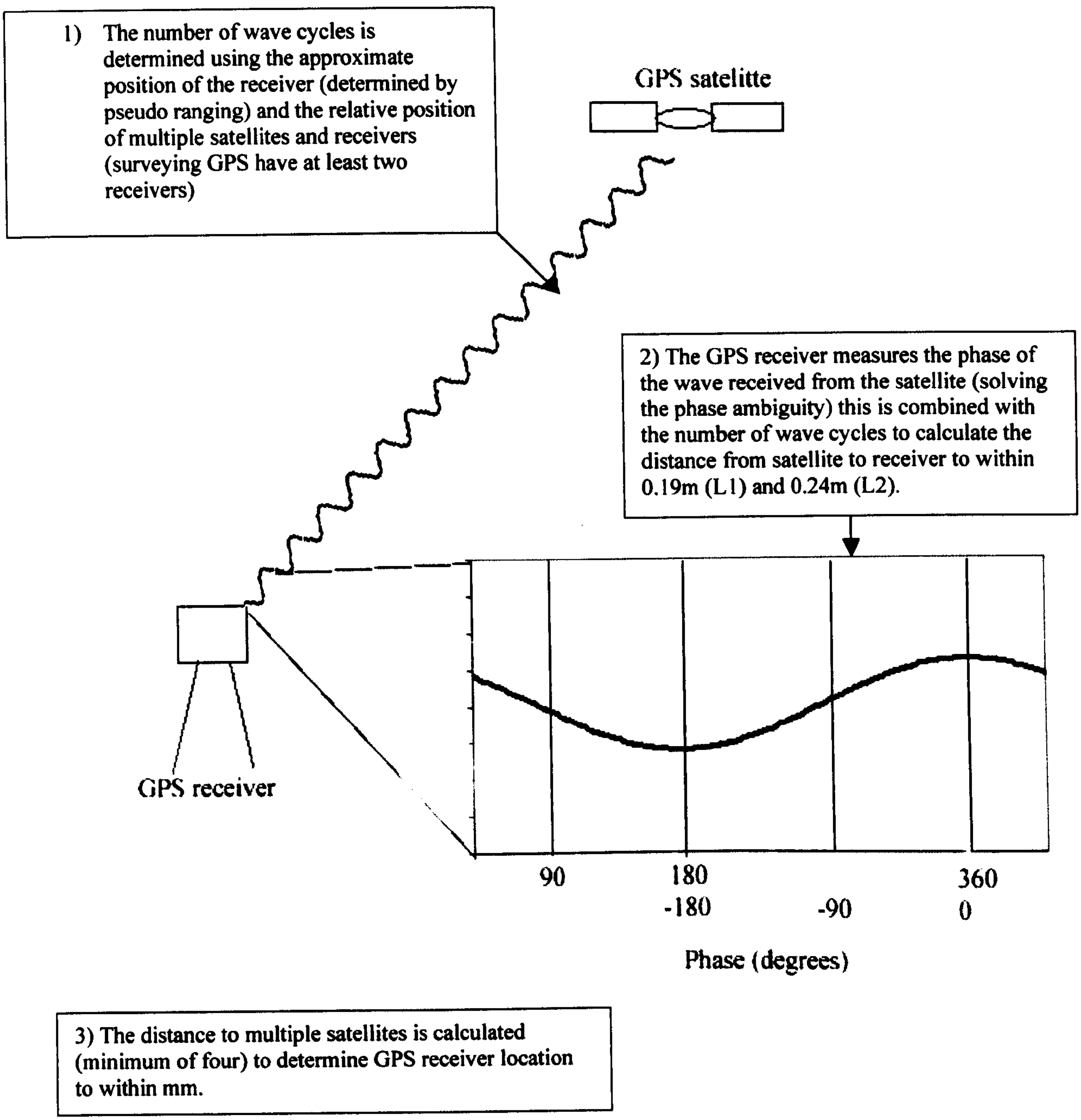

Figure 2.1 The phase shift method of determining GPS receiver location

Different methods have been developed for using GPS surveying equipment in the field. Static applications involve the setting up of two or more receivers over stationary points for periods in excess of 30 minutes, this allows a very accurate assessment of relative position between the receivers and is applicable for determining base line lengths and setting out control points and bench marks.

However a majority of users of surveying GPS equipment are interested in taking a large number of points in short time periods. This is possible using two or more receivers when one unit is set up statically over a known point (base unit) and a second unit is moved to unknown points (rover). This system is capable of determining a large number of points very rapidly with very little loss of point quality. Observations collected by both base station and rover are used to calculate the vector between the units. This vector is then applied to the known point of the base station. This rapid point acquisition process is often termed kinematic (also, stop and go) and is made possible by an initialisation period before the survey begins. The initialisation is necessary for both instruments to solve the phase ambiguity (see **Figure 2.1**) and provided the receivers remained locked onto a sufficient number of satellites, then points can be collected very rapidly.

The real positional data of survey points are calculated either by post processing of the base station and rover data or in real time using the Real Time Kinematic (RTK) function available in some GPS surveying equipment. RTK works by using a radio link between the receivers to allow telemetry of the data and online processing. RTK is advantageous because it allows the operator to keep track of the quality of data being produced, particularly if the study design includes a network of known checkpoints.

Considering the theoretical accuracies associated with the GPS method, uptake for geomorphological uses has been limited. Brasington *et al*,. (2000) suggest confusion regarding the methods and reliability have hindered usage. Studies that have used and analysed the effectiveness of the GPS are limited within geomorphology (Fix and Burt, 1995; Twigg, 1998; Brasington, 2000). These studies have reported the following considerations. GPS point quality compares adequately with tachometric survey. This comparison is not entirely appropriate given that error is introduced in different ways between the systems. Tachometric survey predominantly introduces error with increasing measurement distances. These errors are augmented by additional errors such as frequency drift and atmospheric refraction in field use producing discrepancies of up to 0.5m over 1.5km (Bannister, 1998) In comparison uncertainty is introduced in GPS measurements from less spatially dependent factors. Errors for individual receivers (in order of magnitude) are caused by 1) satellite clock bias 2) ionospheric effect, 3) receiver clock error, 4) orbital bias and 5) tropospheric effects. With kinematic or RTK surveying system further uncertainty is introduced by the difference in location between base station and rover receivers, the base line effect. For a majority of surveying applications the base line effect is very minor, with manufacturers (Leica) suggesting that the effect is negligible with baselines below 15km. The scales associated with geomorphological survey are typically below 15km making the error a-spatial.

Compared with the total station or EDM, the GPS is considered a very efficient method for point acquisition (Brasington, 2000). Only a single operator is required to conduct a GPS based survey. This is not possible for all but the most sophisticated of EDM equipment (radio controlled with automated prism tracking). GPS point acquisition rates by a single operator are reported as over 2000 points per 8 hour fieldwork day including periods of downtime (Brasington, 2000). This compares very favourably to point acquisition speeds collected using total station of 240 points per hour (Lane *et al.*, 1994; Keim *et al.*, 1999). The GPS also allows several rovers to be slaved to one base station improving the point acquisition speed possible with a team of operators (Brasington, 2000).

Unlike traditional ground survey methods direct line of sight is not required between rover and base station for GPS survey, with the RTK method limited by VHF radio contact (line of sight uninterrupted by major topographic features) and the kinematic method only by the 15km base line restriction. However, obstructions affect the GPS in other ways, by limiting the amount of sky visible. In practical terms this means the more sky that is unobstructed by hill slopes, trees or buildings then the more satellites are available for the receiver to trilaterate its position. The GPS is reliant on the configuration of satellites overhead. Ideally these should be evenly spaced and not close to the horizon (increased atmospheric effects). The configuration of satellites is termed Geometrical Dilution of Precision (GDOP). When GDOP increases then the accuracy and precision of co-ordinates calculated by the receiver declines. When this effect exceeds a user defined threshold then the rover ceases to take measurements. Downtime differs depending on the number of satellites available overhead but even with obstructions caused by mountainous topography such as those described by Brasington (2000) downtime was limited to 1 to 2 hours per day.

3.4.2 Attributes and limitations of ground survey

Aside from the specific accuracies and limitations attributable to surveying equipment and techniques there are generic attributes and limitations applicable to using ground survey techniques for the measurement and monitoring of dynamic river environments.

First, there are issues with the sampling strategy associated with ground survey. Bearing in mind that there are an infinite number of scales that morphology can be sampled on, then a relevant sampling scale needs to be determined, in relation to the study objectives but also dependent on spatio-temporal resolution (discussed below). Even once this sampling decision has been made it by no means guarantees how it will be interpreted in the field. Ground survey results are reliant on the decisions made by the ground survey team, who must decide on the scale of feature that is significant enough to warrant specific attention.

In practice differing point resolution and distribution is an inevitable characteristic of ground survey data. There have been no attempts, either theoretical or empirical, to define it's importance in changing characteristics of the resultant DEM. The nearest approximations are studies that assess the effect of differing grid resolutions (Brasington, 1998). Studies that have obtained high resolution topographic information of river channels using ground survey have relied on changing point resolution to better represent areas of high topographic variability, yet without having a grasp on the implications of either point resolution or changing point resolution on DEM quality. Brasington *et al.*, (2000) monitored a reach of the River Feshie for two years using ground survey techniques. The sampling strategy for the study adopted a quasi-systematic method in which bars and bank tops were surveyed in tightly spaced transects, breaks of slope were given particular attention. However, survey point distribution diagrams show inconsistencies in the spacing of transects and more worryingly inconsistencies in survey point density and distribution between exposed bars and submerged channels. These spatial inconsistencies are represented well by differences in the moving average point densities (3m radius) that show variations between 0.001 and 4.5 points per square metre. The disparity in point density is a direct result of the sampling strategy implemented in the study, which aimed to sample areas of high topographic change more finely. An assumption made by the study was that this sampling strategy improved the quality of DEMs given the limited resources available for each survey but this assumption was not tested.

Given that one of the key aims of studies using high resolution topographic data is to determine morphological change by re-survey, this highlights specific issues concerning the comparability of DEMs with differing point densities. Changes in topographic form often mean a substantial change in surface variability between surveys. When for instance a flat bar top becomes incised with small channels, this means the point resolution would be increased in the second survey to account for the dissected terrain. Brasington *et al.*, (2000) intentionally implemented a higher resolution survey for their second survey (in 1999) after identifying significant channel change.

A second limitation of ground survey is that of grain scale roughness which has an important effect on the magnitude and nature of errors, particularly in relation to survey pole diameter (Lindsay *et al*, 2002). Although many studies give consideration to point density and distribution the effects of errors associated with grain scale roughness are rarely considered. Two theoretical reasons exist that suggest error can be introduced to ground survey at the grain scale; First, survey poles tend to slip into the cavities between grains, particularly when surveying submerged topography. Points acquired on rough surfaces (relative to pole diameter) will yield lower elevation readings compared to points acquired on smooth surfaces (Lindsay *et al.*, 2002). Similarly increasing pole diameter means the pole sits higher on the surveyed surface and this effect will be more pronounced on rough surfaces. Repeat surveys rarely occupy the same survey points as the original survey, mainly because in river environments and particularly submerged areas, this is not possible (although the GPS stake out mode makes this more feasible). This causes a second error associated with horizontal displacement of survey points, which produces 'apparent ' differences between surfaces (Lindsay *et al.*, 2002)

Lindsay *et al.*, (2002) investigated these two types of error using theoretical and empirical error models. The theoretical modeling indicated that elevation measurements for realistic relative pole diameters (2-3cm) produced significant biases and this represented a reach scale positive bias away from the 'true' mean measured if the pole diameter was zero. One result of this effect would be apparent volumes of scour and fill caused by independent survey of the same surface, the magnitude of this effect being dictated by the pole diameter. A survey simulation using high resolution (0.003m) DEM data and a range of pole diameter sizes was conducted to attempt to establish the magnitude of this effect. The average error associated with mean scour and mean fill depths was between $0.55D_{50}$ and $0.56D_{50}$ and a negative relation between pole diameter and scour and fill was defined. Larger pole diameters resulted in increased error. Field experiments were conducted to confirm laboratory results and also to define the impact of survey pole slippage, which was not included in the survey simulation. These tests also found a negative trend in mean scour and fill of $0.23D_{50}$ and $0.28D_{50}$. Linear regression for both simulation and field data showed a significant negative relation between pole diameter and error in mean total change. The pole diameter model explained 30% of the variation in mean total error.

There are a number of implications from these results: 1) survey pole diameter should not change between surveys; 2) measures of scour and fill are positively biased when survey points are imprecisely re-occupied; 3) changes in the surficial texture between surveys result in increased uncertainty, with smooth to rough surfaces producing a negative mean bed level bias.

The third consideration is that survey frequency needs to be commensurate with the rate of morphological change. The rapid morphological changes associated with many braided river systems mean that a large amount of change can occur between surveys and this change may be too great in magnitude for some study objectives such as the application of the morphological method. The theoretical implications of this are mentioned in a number of studies (Brasington *et al.*, 2000; Lane, 1998), however very little evidence has systematically been collected to show its effect. Lindsay *et al.*, (2002) provide the only systematic analysis of this issue. Eleven photogrammetrically derived DEMs of a 1:36 Froude scaled braided river model were used to show the effects of temporal resolution. The DEMs are described in Stojic *et al.*(1998). The eleven DEMs were evenly distributed over the 100 minute duration of the experiment giving a high temporal resolution. The temporal resolution was artificially coarsened by selectively removing DEMs. The cumulative scour/fill volumes changed significantly as a result of the temporal coarsening with the 10 minute survey interval showing 420% greater scour and fill volumes than the 100 minute interval. The significant difference was attributed to large amounts of compensating scour and fill. Nearly 65% of the channel area experienced at least one compensating event over the 100 minute period.

Lindsay *et al.* (2002) has implications for field studies, it highlights the importance of study design, the initial assessment of a fieldwork site coupled with a knowledge of survey limitations. In particular an appreciation of the rate and types of morphological change is important. This can be achieved by analysis of photographs of the fieldwork site (preferably APs) to identify long term rates of change and a pilot study to better gauge sub-annual sediment dynamics.

Finally, ground survey techniques are a very labour intensive form of data acquisition in comparison with remotely sensed data. Careful consideration needs to be given to all elements of survey design before committing to ground survey. In particular spatio-temporal resolution and point acquisition rates highlight the need for realistic expectations as regards ground survey accuracy in representing topographic surfaces.

3.5.0 Remote sensing techniques

This review of data acquisition and quality through remote sensing is largely based upon a comprehensive review by Westaway (2001). Because of the recent publication of this thesis, this review will draw out only the more important points from his discussion whilst including additional information from sources not investigated by Westaway and recently published sources.

The term remote sensing is used here to refer to any non contact method of determining landform surface properties. The exception being optical tachometric survey of points from two (or more) known benchmarks to determine location, this is considered ground survey.

3.5.1. Historical development

The potential of aircraft-mounted cameras for rapidly acquiring large amounts of accurate information on terrain was first identified in the First World War (Smith, 1941). In a short space of time these techniques were being used for non-military purposes for the mapping of terrain and to supplement geomorphological field investigations. Initially data were used qualitatively for defining relative bank heights and symmetries and the presence of islands (Smith, 1943). However the quantitative potential of high quality imagery had been recognised with early attempts at using stereoscopic measurements (Shaw, 1953).

The use of aerial photographs in fluvial geomorphology had developed considerably by the 1960s although within fluvial geomorphology usage was typically qualitative (Sundborg, 1956; Crickmay, 1960; Wolman, 1967). Progress in photographic quality due to advanced lens calibration and film quality produced improvements in the quantitative reliability of the photogrammetric process although the complexity of the process ensured that uptake was limited to only a few applications by river scientists, including derivation of Manning's n roughness coefficient by the United States Geological Survey (reported in Lohman and Robinove, 1964) and power spectrum analysis of river meanders (Speight 1965). Other quantitative approaches employed aerial photographs to estimate wave conditions (Putnam 1947) and analysis of sequential photographs to calculate river surface flow velocities (Linton, 1952; Oros, 1952). Channel classification was a particular focus in the 1960s and 1970s, with aerial photographs predominantly used to define channel planforms (Howard *et al.*, 1970).

Planimetric use of aerial photographs in contemporary fluvial geomorphology is still very common at a range of scales. At the smallest scale possible (with typical 1:3000 scale photographs) qualitative assessments of bedforms have been conducted. At the channel scale aerial photographs have been used to aid interpretation of flow processes (Westaway, 2001). Similarly at the reach scale aerial photographs have been widely used to define and classify fluvial form (Schumm, 1989) and to explore scaling properties associated with braiding rivers at a range of scales (Sapoznicov and Foufoula-Georgiou, 1996). Perhaps the most comprehensive contemporary use of aerial imagery has been to show channel planform change. Using a time series of aerial photographs the channel changes can be identified. Initial attempts at this were predominantly qualitative, channel boundaries were extensively based on the interpretation of the researcher (Fahnstock and Bradley, 1973; Werritty and Ferguson, 1980; Kondolf and Swanson, 1993; Warburton *et al.*, 1993). Recent increases of computer power and Geographical Information Systems (GIS) software coupled with a recent interest in process at the reach scale has lead to more sophisticated automated techniques for identifying channel boundaries and water depths (Gurnell *et al*, 1994; Bryant and Gilvear; 1999; Winterbottom, 2000).

The aerial photogrammetric techniques discussed above address a number of the problems associated with ground survey. Aerial imagery captures a large amount of reflectance data in a very short space of time and this significantly reduces the role of spatio-temporal resolution factors. However techniques for extracting basic information from aerial photographs are fundamentally constrained by their two dimensional nature. This causes two problems, First, extent of inundation is extensively used to define channel boundaries, this is problematic because stage differs considerably in natural river systems. This is a particular problem for studies based on rivers that have an active bedload and are unconstrained. These are typically braided with low channel relief and discharge is often flashy increasing the possible range of inundated terrain between high and low flows. Second, river channel morphology has an important vertical dimension, but non-stereoscopic use of aerial photographs is fundamentally planimetric analysis and fails to adequately represent these differences.

3.5.2 Multispectral sensors

Recent advances in airborne multispectral sensors have made them a viable alternative for acquiring planimetric information on river channels (Gilvear *et al.*, 1999). Multispectral sensors record the radiation reflected from the earth's surface in a number of bands. For instance the Daedalus 1260 scanner collects data in 12 bands covering 0.38μm to 14.00μm (Lyon *et al.*, 1992) and CASI has up to 288 user defined bands between 0.4μm and 0.9μm at 1.8-nm spectral intervals (Lillesand and Kiefer, 1994). This means radiation beyond that of the human eye can be detected allowing better differentiation of surfaces. Applications of airborne multispectral imagery include the quantification of planform change and channel bathymetry on the rivers Tay and Tummel, Scotland using Airborne Thematic Mapper (Winterbottom,1995; Bryant and Gilvear, 1999), the evaluation of bottom sediment types and water depth using Daedalus 1260 (Lyon *et al.*, 1992) and the mapping of water depth on small chalk streams in southern England using CASI (Acornley *et al.*, 1995). Whilst these examples are very encouraging the primary problem with airborne multispectral imagery is acquiring it. Planimetric approaches using APs are more reliable in the UK because there are more planes with survey cameras commercially available. The original plan for this thesis was to analyze water depth at the fieldsite using multispectral data. This was not forthcoming.

Satellite mounted multispectral sensors have also had limited uses although the coarse spatial resolution (>10m) makes these applicable only for larger river systems (Diakite, 1986; Salo *et al.*, 1986).

3.5.3 Photogrammetry

Photogrammetry is a method for extracting three dimensional terrain data using aerial photographs. This retains the advantages of basic image analysis because spatio-temporal resolution constraints are largely overcome but it also produces fully three dimensional data, which addresses planimetric limitations. Like planimetric approaches, photogrammetry can also be used retrospectively using archive aerial photographs, provided the photographs are of sufficient quality, calibration certificates are available and most critically sufficient ground control can be identified (Chandler and Cooper, 1988; Chandler and Cooper, 1989; Chandler and Clark, 1992; Brunsden and Chandler, 1996). The photogrammetric approach uses high quality photographs that contain large amounts of explanatory information including reflectance data, this aids in error identification and interpretation of results (Lane *et al.*,1993).

Photogrammetric techniques have been applied to fluvial geomorphology in two main areas; to 1) measure the erosion rates of specific river banks, 2) to measure channel form and monitor channel change. The measurement of bank erosion will not be discussed here but reviews can be found in Westaway (2001) and Lawler (1993). The application of photogrammetry to measure channel form and channel change has occurred at every scale of investigation common to river science and thus has involved a range of photographic scales from aerial or terrestrial camera setups. Similarly temporal resolution of data is very varied depending on the study objectives and the rate of change in the channel being studied.

Micro scale photogrammetric studies predominantly fall into two categories. First are studies that employ photogrammetry to produce DEMs of flume topography. Stojic *et al.* (1998) produced close range DEMs of a braided river (scaled 1:20) to study sediment transport. Chandler *et al.* (2001) used similar techniques to gather topographic information on a gravel and sand surface, and Smart and Brasington (2001) for a basin being actively eroded by rainfall. Second, there are studies that employ close range digital photogrammetry to study actual river surfaces such as channels and bars. Butler *et al.* (1998) used a gantry mounted calibrated camera to produce DEMs of the gravel bedded River Affric, Scotland. Butler (2001) was instrumental in the development of dual media photogrammetry by developing techniques for acquiring high quality subaqueous DEMs. This is an important development for the acquisition of river channel elevation values because, even at low flow, water obscures areas of the river channel. This was later modified by Westaway (2001) for determining bed elevations through clear water at the channel scale (see **Section 4.5.9** for discussion of problems of subaqueous data capture).

Early photogrammetric work at the channel scale is dominated by that of Lane (1994, 1995, 1996,1998). These papers establish a number of the more important questions to be addressed as regards acquisition, limitations and usage of high quality topographic information. Lane used analytical and subsequently digital terrestrial photogrammetry to monitor a 50m section of a rapidly evolving proglacial stream, at the Haut Glacier d'Arolla, Switzerland. Lane *et al.* (1995) combined photogrammetric techniques with tachometric survey of subaqueous zones to model topography and channel changes. The modeling work that evolved from this demonstrates many of the uses of high quality topographic information. Channel changes were accurately quantified over a temporal scale fine enough to relate to discharge and sediment supply variations, channel changes could be visualised and described the spatial structure of process (Lane *et al.* 1995, 1996). The DEMs also provided a set of boundary conditions suitable for process based flow modeling (Lane and Richards, 1998; Bradbrook, 2000). Terrestrial photogrammetry has been used more recently by Chandler and Ashmore (2001) and Stojic (2001) to produce DEMs of the Sunwapta River, Canada. Unlike Lane this work involved the use of an uncalibrated camera which introduces an extra problem into the photogrammetric process but makes the photogrammetric method accessible to those without specialist calibrated equipment.

Initial uses of photogrammetry at the reach-scale employed analogue photogrammetric techniques to measure river channel morphology. These studies are restricted by the very limited speed of point acquisition possible using manual photogrammetric techniques. The data points acquired are typically incorporated into contour plots of river morphology. Examples of this include measurements of channel position and floodplain geometry (Lewin and Manton, 1975; Lewin and Hughes, 1976; Lewin and Weir, 1977). Dixon *et al.* (1998) used similar techniques but larger resolution aerial photographs (1:5000) to establish bank lines on the upper River Severn, Wales. Ham and Church (2000) mapped channel boundaries on the Chilliwack River between 1952 and 1991. When coupled with bank height measurements this was sufficient for a sediment budget to be calculated. Sherstone (1983) used the full three-dimensional potential of photogrammetric methods to calculate the volume of a newly created channel on the Muskawa River, Canada

Automated digital photogrammetric techniques have fundamentally changed data collected at the reach scale. Softcopy photogrammetry automates the point acquisition process allowing the collection of a large number of points in a very short time and permitting the collection of high resolution DEMs. Lapointe *et al.* (1998) recorded the impact of a large flood event on a 34km long (approximately 250m wide) reach of the Ha! Ha! River, Quebec, using DEMs constructed from 30000 to 40000 data points acquired using computer assisted photogrammetry.

The first use of softcopy photogrammetry using a fully automated pixel matching algorithm at the reach scale was applied by Shankar (1997) who generated a DEM of the North Ashburton River, New Zealand, with a grid cell size of 1.6m over a 500m × 150m reach. The most significant study using digital photogrammetry at the reach scale was by Westaway (2000). Westaway produced DEMs of braided reaches on two New Zealand rivers. These were derived using digital photogrammetric software and a range of photographic scales (1:3000 – 1:5000). The implications of Westaway's work are numerous and are discussed in greater length in **Chapter 4**. The accuracy and extent (2400m × 800m) of the DEMs were sufficient to allow patterns of erosion and deposition to be established and sediment budgets to be calculated. The subaqueous areas of the DEMs were derived using two methods. A clear water method based on correction of light refracted off the river bed and a turbid water case based on the application of an empirical relationship between water depth and pixel DN values.

3.5.4. The basic principles of softcopy photogrammetry

Lengthy explanations of the photogrammetric method exist elsewhere (Lane et al., 1993; Wolf and Dewitt, 2000) however a basic explanation is provided here to enable comprehension of the photogrammetric processing model described in **Chapter 4** and decisions taken regarding photographic specifications.

The photogrammetric method attempts to define the geometric relationship between the three-dimensional object (object space), a two dimensional image of the object (image space) and the camera lens. This relationship is best illustrated using a straight line that passes through the object space A, through the perspective centre of the camera lens (O) and is projected onto the image space (a) **(Figure 3.2)**

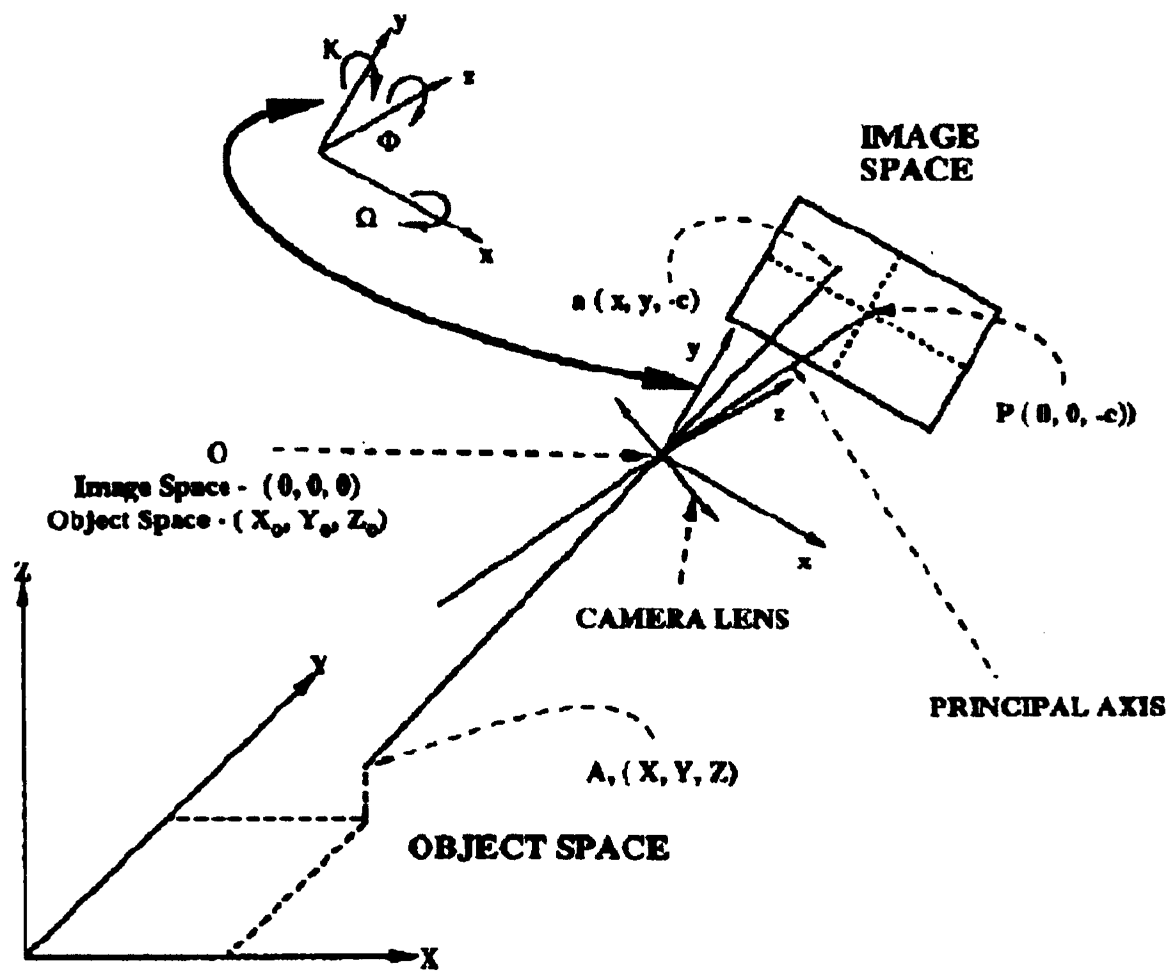

Figure 3.2 The relationship between object space, the camera lens and image space (Taken from Westaway, 2000) Attributed to Lane (1993) but it does not appear in the reference list.

This relationship can be described mathematically using **Equation 3.1** (Ghosh, 1988):

$$\begin{bmatrix} x \\ y \\ -c \end{bmatrix} = kM \begin{bmatrix} X - X0 \\ Y - Y0 \\ Z - Z0 \end{bmatrix}$$

Equation 3.1

Where (x,y) are the co-ordinates of point a in the image space, (c) is the focal length of the camera, (X, Y, Z) are the co-ordinates of point A in the object space, (X_0,Y_0,Z_0) are the co-ordinates of the perspective centre of the camera lens in the object space, k is a scale factor and M is the rotation matrix in **Equation 3.2**

$$\begin{matrix} m_{11} & m_{12} & m_{13} \\ m_{21} & m_{22} & m_{23} \\ m_{31} & m_{32} & m_{33} \end{matrix}$$

Equation 3.2

Where $m_{11}...m_{33}$ are functions of the camera orientation, ω, φ and κ (**Figure 3.2**)

The elements matrix M, scale factor and X_0,Y_0,Z_0, can be considered the external orientation parameters of the camera (Ghosh 1988). When expanded the location of every point on the image can be described by two equations (also the collinearity equations). These are shown in **Equations 3.3 and 3.4**

$$x = \frac{-c\left[m_{11}(X - X_0) + m_{12}(Y - Y_0) + m_{13}(Z - Z_0)\right]}{\left[m_{31}(X - X_0) + m_{32}(Y - Y_0) + m_{33}(Z - Z_0)\right]}$$

Equation 3.3

$$y = \frac{-c\left[m_{21}(X - X_0) + m_{22}(Y - Y_0) + m_{23}(Z - Z_0)\right]}{\left[m_{31}(X - X_0) + m_{32}(Y - Y_0) + m_{33}(Z - Z_0)\right]}$$

Equation 3.4

Assuming that the camera external orientation parameters are also known, these equations are sufficient to calculate the unique position (X,Y,Z) of points in the object space when combined with the co-ordinates of the same point on two overlapping images. The camera's external orientation can be calculated using a bundle adjustment, a simultaneous least squares solution of the collinearity equations using Ground Control Points (GCPs, also termed Photograph Control Points, PCPs, in Westaway, 2001) with known object space co-ordinates and identifiable on the imagery.

Lens distortion can cause significant errors in the functioning of the photogrammetric triangulation by changing the relationship between the object space and the image space. This can be corrected using standardized laboratory lens calibration techniques that calculate well established lens distortion parameters. These parameters can then be added to the collinearity equations (Wolf, 1978).

The final element in the photogrammetric process is to calculate the co-ordinates (X,Y,Z) of points in the object space. This can be carried out manually using traditional photogrammetric techniques and equipment. Alternatively the point collection process can be carried out automatically using digital photogrammetric techniques. Digital photogrammetry allows the user to acquire large numbers of points very rapidly through the use of automated stereomatching and image processing algorithms. These allow the generation of high resolution DEMs with quantifiable precision using commercially available packages such as ERDAS Imagine OrthoMAX and VirtuoZo (Chandler, 1999). This software is designed to be accessible to a wide market and as such can be run on inexpensive UNIX workstations

3.5.5 Photogrammetric controls on surface quality

Although a surface created by digital photogrammetric techniques is fundamentally controlled by the same factors as traditional photogrammetry there are a number of extra factors relating specifically to DEM collection that effect surface quality (Lane, 2000). The traditional controls on photogrammetric data quality will be dealt with first: these are camera calibration, base to distance ratio and ground control.

Camera calibration is carried out periodically for all metric survey cameras. Copies of the calibration certificates provide some of the measurements required by digital photogrammetric software to determine the internal orientations of the camera. The internal orientations of the camera are defined through a number of parameters each defined in microns. The most important of these are the focal length, the principle point of autocollimation, radial distortion and fiducial positions. In digital photogrammetry these measurements are required by the software to enable the block triangulation process (see below)

Base to distance ratio refers to the resolution of the aerial photographs. This is dictated by the camera lens and the flying height of the aerial platform. Photographic image scale is the first control on data precision although with digital photogrammetry the transfer of the hardcopy to digital format is also an important control. This is best achieved by scanning the diapositives (Chandler, 1999) because the printing process introduces new forms of error associated with ink spreading and distortion of print paper. The scanning procedure is another way error can be introduced therefore high resolution photogrammetric scanners (8 to 24 microns) are necessary to ensure that image distortion and systematic error does not occur (Smith, 1997). Scanning resolution is the second control on theoretical photogrammetric precision because the precision of topographic measurements (PT) has a one to one correspondence with the pixel dimensions of the imagery used

(Lane, 2001) and this is composed of photographic scale and scanning resolution. The pixel dimensions (in metres) on the ground is referred to as the object space pixel resolution and is calculated using **Equation 3.5.**

$$\delta Y = s \times (\delta x / 1000000) = p_T \qquad \textbf{Equation 3.5}$$

Where the photograph scale is 1:s and δ x is the scanning resolution

used (in microns), p_T refers to the approximate area covered by each pixel on the ground. The same figure is also the theoretical vertical precision and this makes it possible to predict the maximum precision with which elevation measurements can be made before the photogrammetric analysis takes place (Shearer 1990). The theoretical vertical precision is really a theoretical value for the Standard Deviation of Error (SDE). A stated SDE is equivalent to one standard deviation. When applied to a theoretical range of values 68% of values will lie within ±1 standard deviation, 95% within ± 2 standard deviations.

There are a number of uncertainties associated specifically with the final automated stages of the digital photogrammetric process. These have received relatively little attention and are poorly quantified, however Lane (2000) has made some progress. The automated stereo matching process uses a numerical algorithm to match corresponding points on each image. As a result an important step in extracting elevation data (and controlling data quality) is removed from a human operator and the quality of the final DEM is reliant on the nature of the extraction algorithm and the DEM collection parameters (Smith *et al.*, 1997; Butler *et al.*, 1998; Gooch *et al.*, 1999).

3.5.6 Softcopy photogrammetric surface quality for geomorphologists

The introduction of softcopy photogrammetric methods has increased the availability and applicability of photogrammetric approaches for geomorphologists. Lane (2000) outlines the fundamental problems with this; first, non- trained photogrammetrists may not fully understand the photogrammetric principles behind DEM generation. This can lead to basic errors throughout the photogrammetric process, including use of inadequate photographic and scanning equipment, lack of appreciation of camera calibration and lack of awareness of bundle adjustment parameters. Cooper (1998) similarly stresses the need for knowledge of basic photogrammetric parameters.

Secondly, the increase in data point acquisition by digital photogrammetric techniques removes an important control on data quality. Traditional techniques requires a stereomark to be placed over a point of interest, this allows a high degree of control over where points are placed and removes much of the potential for mismatching of points. In contrast digital systems use area based point matching algorithms which significantly increases the chances of point mis-matching (known as blunders, see below).

Thirdly, collection of check data that is sufficient for testing of DEMs is problematic. DEMs can cover large spatial areas of complex terrain and collection of data of a sufficient quantity and quality becomes an important issue. Lane (2000) identifies a number of specific issues. One is coarse check data with respect to the photogrammetric grid cell size. This is relevant primarily for microscale studies such as Butler (1998) where millions of photogrammetrically derived pixels are checked using just a few check points. This problem was solved using a laser profiler to generate a larger number of check points but this led to other problems of datum definition and coarse photogrammetric resolution with respect to check data. In gravel bed river environments large topographic variability over small scales caused by large clasts and microscale bedforms leads to a problem about where to site the survey pole. For instance if the DEM grid cell size is over 50% of the median grain size then the variance contained in the check data cannot be detected photogrammetrically. This results in an increase in the Root Mean Square Error that is considerably larger than that estimated from the scale of imagery (Westaway *et al.,* 2000). Insufficient check points are a particular problem for DEMs that cover large spatial scales, Lane *et al.* (2000) showed that whilst variables used for geomorphological research were sensitive to changes in DEM parameters, accuracy statistics based on check points were not. The 860 points used in the study represented only a very small sample of the points derived through photogrammetric processes. This is problematic for geomorphological applications of photogrammetry because the fine tuning of DEM parameters cannot be achieved by assessing accuracy statistics based on check point data. The final issue is the quality of check point data. The errors associated with ground survey have been assessed above. Given that DEMs can be generated for areas in excess of 1000m the error introduced to measurements by optical surveying devices could be significant.

3.5.7 Airborne Laser Scanners (ALS)

ALS is alternative method of acquiring high quality topographic data using remote sensing techniques. There are a number of commercial systems available including LiDAR and Airborne Laser Terrain Mapper (ALTM). These all use the same basic principles for deriving elevation values. A laser pulse is emitted from a range finder device mounted on the underside of the aircraft. This is reflected off the target and received back by the range finder which uses the return time to calculate the relative distance of the plane and the target (Hansen and Jonas, 2000). The exact location of the plane is monitored by real time kinematic GPS and the orientation and attitude of the plane are continually monitored by an onboard Inertial Reference System (IRS). Post processing software is used to combine the exact position of the range finder with the laser return times to calculate the X,Y,Z coordinates of the target (Hansen and Jonas, 2000).

There are some advantages and disadvantages of using ALS compared with digital photogrammetry. ALS is an efficient method of acquiring large quantities of high quality topographic data. The post processing is fully automated and data can usually be delivered within weeks of the flying date. In contrast digital photogrammetry is semi automated with a number of intermediate steps required (bundle adjustment) before acquiring the final DEM. ALS has a typical vertical precision of ±0.1-0.15m and a ground resolution of as high as 0.5m. The precision and resolution achieved using digital photogrammetry is dependent on the photograph scale and scanning resolution, this makes it a more versatile technique. More advanced ALS systems can be configured to record the return period of a number of laser pulses allowing the determination of multiple layers within the landscape, for instance vegetation elevation and water depth (Ritchie, 1996). In contrast photogrammetry cannot directly determine vegetation elevation or water depth but orthophotographs are a by product of the photogrammetric process and these can be used for similar purposes. The spectral reflectance information in the orthophotographs can be used to determine water depth (Westaway, 2001) and there is significant potential for identifying vegetation types and surface texture information such as grain size.

Given some of the advantages of ALS, applications in river science have been few. The most important applications have been to acquire topography for numerical modeling (French, 2001; Charlton *et al.*, 2001; Schmidt, 2001) and to assess three dimensional channel change (Finnegan *et al.*, 2001;Kesarwani, 2001; Westaway, 2001). The limited take up is probably due to the practical aspects of acquiring ALS data. Few survey planes are equipped with ALS sensors and as a result it is expensive to acquire. In comparison the photogrammetric method is reliant on good quality photographs and these can be obtained using survey planes fitted with metric cameras or in some cases oblique terrestrial photographs.

3.6.0 Data distribution and density

The distribution and density of survey points is a source of error that is intrinsically linked to data acquisition method. The fundamental implications together with the attributes of ground survey versus remote survey are discussed below.

Terrain surfaces are a continuous phenomenon and as such any measurement using a finite number of points necessarily has a finite data resolution. As the number of measured points increases, the resolution also increases, the difference between the real X, Y value and the measured X and Y value tends to zero. Traditional methods of data collection (terrestrial survey and manual photogrammetry) predominantly involve manual point collection, either in the field or using a photogrammetric workstation. This means sampling strategy is very constrained by the principles of spatio-temporal resolution but it also means the sampling strategy can be adapted to focus on more important terrain features such as breaks of slope (Li, 1992,1994; Lane *et al.*, 1994; Gong *et al.*, 2000). In contrast the data produced by digital remote sensing systems have a very high resolution of points, produced through automated stereomatching with the photogrammetric method. So large increases in resolution only marginally increase expense (Huang, 2000). Unlike manual methods the density of sampling is not dictated by specific features although the overall increase in point resolution suggests these features are suitably detected without varying point acquisition spatially.

3.6.1 Interpolation method

The interpolation method used to create a continuous surface from point elevation measurements is a source of error for DEMs produced using photogrammetric and ground survey methods. Unlike data acquisition method and point density, this area of research has been relatively neglected and as a result the propagation of error caused by different interpolation algorithms is unknown. (Desmet, 1997). Given that the point matching process in digital photogrammetry is never 100% successful a true raster DEM is not produced. The grid cells that do not include a matched point need to be interpolated, the numbers of grid cells requiring interpolation increases as the number of grid cells with matched points declines. Many digital photogrammetric systems (such as Erdas Orthomax) automatically interpolate between matched points using a bi-linear interpolation method (Delauney triangulation). Uncritical use of such a system is likely to lead to acceptance of this interpolation method without consideration of other interpolation methods. Carter and Shankar (1997) outline some of the characteristics of a good interpolation method, it should be suitable for handling large sets of gridded data and honour the data sampled as closely as possible. Kriging is an alternative to Delauney triangulation although Desmet (1997) showed that for gridded data this produced topographic artifacts negatively affected the quality of the DEM surface. The optimal interpolation method suitable for any given terrain is likely to depend on the exact nature of that terrain, computational time available and to what use the resultant DEM is likely to be put.

3.7.0 Terrain characteristics

The characteristics of the terrain itself are an important factor on the effectiveness of data acquisition, point distribution and interpolation techniques. The generic issue as regards terrain characteristics is the suitability of data density and distribution relative to the terrain and study goals. There are also some more specific issues surrounding terrain characteristics. Firstly, there are issues surrounding remote sensing techniques. A survey camera is a passive system that records reflectance to generate an image and as such is affected by shadows and reflectance distortion caused by atmospheric affects and change of medium (refraction at the water air interface). These can cause low point densities (Brown and Arbogast, 1999), or refracted point matches (Butler, 2001) and point mismatching (blunders) (Derose *et al.*, 1998; Lane *et al.*, 2000). Shadow effects have a more pronounced effect on point quality when the sun is low in the sky relative to relief. Ground survey methods are not affected by shadows and only optical survey equipment is affected by atmospheric distortion. However, ground survey is affected by the differential roughness of terrain surfaces (Lindsay *et al.*, 2002) and inconsistencies in point densities resulting from the failure of equipment operators to consistently survey morphological features.

3.8.0 Spatio-temporal resolution considerations

Spatio-temporal resolution principles apply to all survey techniques and are a key control on survey design and study objectives. There is a play off between the extent of survey, resolution and frequency of survey. This means that given limited time and resources careful consideration needs to be given to each of these factors in order to optimise the value of data collected in relation to the study objectives. For example a study of micro bedforms will necessarily require a finer spatial resolution of points than one of macro reach morphology, however, it may not require as large a spatial extent for the survey. Similarly if the study aims to assess landform changes then micro bedform evolution is typically more rapid than that of macro reach morphology and so the temporal resolution of survey is also a factor.

These factors are most apparent with ground survey techniques, which, despite improvements in technology, are very labour intensive in the field. Remote sensing approaches are less affected by spatio temporal resolution in the field. Westaway (2001) suggests remote sensing techniques break down the relationship between the three spatio-temporal controlling factors by pointing out: 1) the sizeable spatial extent of remotely sensed data reduces spatial constraints. 2) sample density is theoretically limited only by the spatial resolution of data collected and 3) temporal sampling frequency is potentially much better than with terrestrial methods. It is clear that these points are valid interpretations that demonstrate the substantial improvement that remotely sensed data represents over ground survey approaches. However remotely sensed data does not mean a complete redundancy of spatio-temporal factors and so compromise remains an important part of study design but for different reasons.

If the same principles of finite resources adopted for ground survey are applied to remote sensing then it is clear that remote sensing is ultimately constrained by the same spatio-temporal controlling factors. First, data acquisition is both temporally and spatially constrained. Financial considerations apply to the collection of remotely sensed data as they do to collection of ground survey data, limiting the extent of survey and temporal resolution of survey. More influential are probably the limited conditions in which airborne sensors can be used. Data collection is temporally constrained by the frequency of suitable overhead weather and light conditions. Sensors mounted on an aerial platform can only collect data of a suitable quality when the sun is high in the sky, at high latitudes this can be just a few hours per day during the summer months. They are similarly reliant on good overhead weather conditions, which are not always forthcoming in the mountainous areas where many fluvial geomorphological studies are based. Spatial resolution is similarly constrained by the minimum flying height of aircraft and sensor characteristics. Furthermore remotely sensed data often requires some ground truthing or calibration measurements particularly where study objectives require small, quantifiable errors.

Secondly, data storage and processing requirements mean that spatio-temporal resolution factors are just as relevant as with ground survey. Rapid increases in computer power and storage capacity mean that very large data sets can now be processed and this is improving with constant hardware and software development. This means that remotely sensed data sets are substantially larger than anything that could be practically conceived using ground survey approaches and there is little doubt that they offer significant advances in data volume. Because remote sensing data are handled digitally then high-resolution data can be processed with only small increases in time and cost. However ultimately data volumes are still constrained by storage and processing capabilities. In particular increasing resolution vastly increases data volume with a doubling of resolution increasing data volume by four times.

Many remote sensing data sources require significant post processing to obtain data in the correct format. DEM generation through photogrammetry involves a number of labour intensive processing and validation stages (Westaway, 2001). In practical terms this means that increasing resolution, spatial or temporal frequency increases the amount of post processing required in the computer laboratory.

Conclusions 3.9.0.

This chapter has discussed the theoretical and practical aspects of topographic data acquisition with the aim of determining the strengths and weaknesses of the available methods.

Technological improvements have greatly improved the effectiveness of ground survey techniques for acquiring high quality topographic data. In particular the surveying GPS effectively negates the large errors associated with acquiring survey points over 500m, whilst also increasing point acquisition rates.

Remote sensing methods have also improved substantially over the last few decades. This is partly due to improvements in sensors (CASI and LiDAR) but mainly as a result of hardware and software improvements. In particular softcopy (digital) photogrammetry has been successfully used to acquire DEMs of braided rivers at a variety of scales (Stojic, 1998; Westaway, 2001).

There are different fundamental qualities that can be associated with the ground survey and remote survey methods of acquiring DEMs. High resolution ground survey produces a very high quality surface but data collection is highly constrained by spatio-temporal consideration. Digital photogrammetry produces a lower quality surface subject to a number of unavoidable types of error (blunders and systematic error) but it is reliant on APs which can be collected very efficiently and therefore are not as constrained by spatio-temporal considerations.

Good survey design can make use of these qualities to ensure that survey method is tailored to research objectives. Objectives that require data over large spatial extents can use photogrammetric techniques and augment these with the higher quality ground survey of more limited areas.

Used in combination these survey methods are suitable for addressing the research themes outlined in **Chapter 2**. Remote survey techniques such as digital photogrammetry partially break down spatio- temporal restrictions allowing three dimensional survey of entire braided river systems at high resolutions. Ground survey techniques offer a higher accuracy survey method with which to quantify errors in the photogrammetric model and to conduct high accuracy, small scale studies on sub-systems.

CHAPTER 4. STUDY DESIGN AND METHODOLOGY

Abstract

This chapter describes the project design and methodology used to address the research themes outlined in **Chapter 2**. An important focus for the chapter is the application of different types of data collection techniques to cover the large spatial extent and high resolutions required by the research themes, employing the strengths of both ground and remote survey. The study design (**Section 4.2.**) introduces the fieldsite, the River Feshie Scotland, describes the important morphological and flow characteristics and presents a rationale detailing why the River Feshie is a suitable fieldsite. The study design then describes the data sets collected, relating each back to specific research themes. **Section 4.3** describes the generic design considerations when acquiring DEMs using ground survey and remote survey. The specific methodology used for the construction of DEMs from Ground Survey data is defined in **Section 4.4**. The methodology for acquiring and post processing DEMs through digital photogrammetry is considered at length in **Section 4.5**. This analysis includes photogrammetric block triangulation results, explanation of a post processing model and description of the issues surrounding each error correction process.

4.1.0 Introduction

To effectively address the research themes presented in **chapter 2** the study design and methodology must take into account a number of important issues about how to quantitatively represent braided river systems. The study design must incorporate ways of measuring the entire system (to address the system scale) but to do so at a high enough resolution and accuracy to allow a range of scales to be investigated. A further fundamental concept introduced in the literature review is the link between sediment dynamics, scaling characteristics and self-organization. The survey design must include a method for determining sediment movement (research theme 3) or inferring links between self-organization and sediment movement (research theme 2). The discussion of direct sampling techniques (e.g. Helley Smith) in the literature review shows that these methods would not be effective at measuring sediment movement at different scales over a spatially extensive system. The morphological method shows more promise particularly when combined with the ground and remote survey techniques described in **Chapter 3**. Remote survey and in particular digital photogrammetry offers the capacity to collect three-dimensional data over a large area, at the system scale, whilst maintaining a resolution and theoretical accuracy sufficient for analysis at a range of scales. Improvements in ground survey techniques offer the potential to closely define error in the photogrammetrically derived model but also to produce high accuracy DEMs of limited subsystems with which to define sediment movement and self organization at smaller scales.

Data acquisition considerations as well as geomorphological considerations were important when choosing the field site. The field site had to have mature, well developed braiding so that the system had morphology and a morphological dynamism imposed by the operation of the system and indicative of the self-organization working within the system.

4.2.0 Study design

The previous chapter highlighted the importance of a number of different factors that determine the quality of morphological representations. These are interlinked. Survey method affects point density, distribution and precision; similarly topography affects the scale, efficiency and effectiveness of survey methods. Given the significance of these issues it is important that they are carried over into any considerations of study design. This means the quality of data acquired is intrinsically linked with geomorphological considerations when designing the study. Two of the most important decisions concerning study design are the choice of study site and the choice of data sets that are collected. Both these choices need to consider not only the geomorphological qualities in relation to the study aims but also data quality issues.

4.2.1 Introduction to the study site

For this research a reach of the River Feshie in Scotland was chosen. The River Feshie is one of the most morphologically active upland rivers in the country with a number of unconstrained multi-channel sections. As such it has received much attention from researchers interested in braided river dynamics in the last 25 years (Werritty and Ferguson, 1980; Ferguson and Werritty,1983; Ferguson and Ashworth, 1992; Brasington *et al.*, 2000; Rumsby *et al.*, 2000). The river drains the southwestern margin of the Cairngorm Mountains, Scotland, flowing northwards to a confluence with the Spey close to Loch Inch (**Figure 4.1**). A majority of the drainage basin is underlain by Moinian schists and lies at between 700 - 1000m in height (Ferguson and Werritty, 1983).

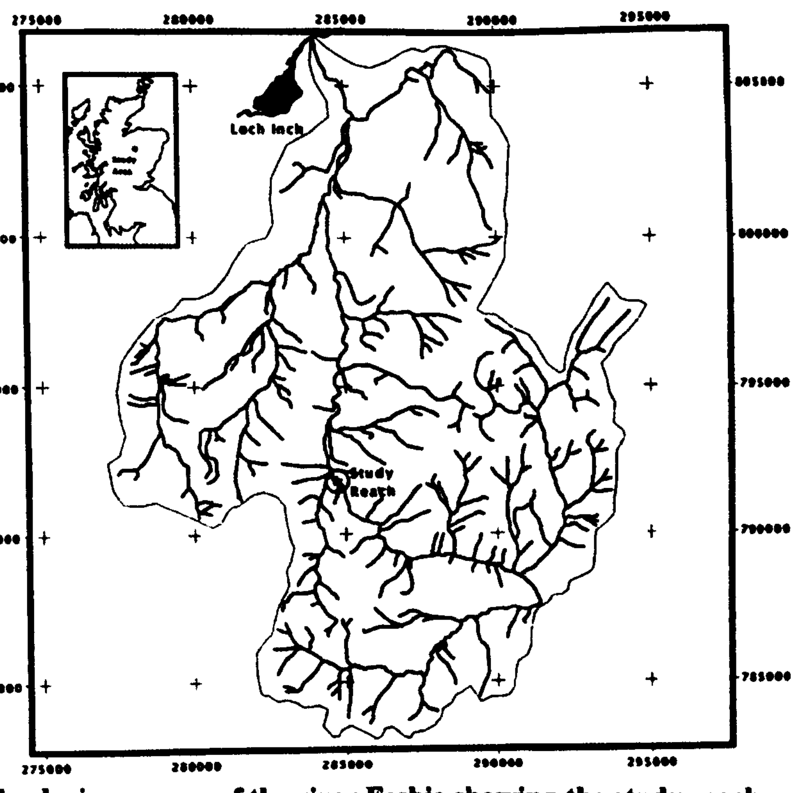

Figure 4.1. The drainage area of the river Feshie showing the study reach.

There are predominantly three zones where braiding occurs on the Feshie. This study focuses on the uppermost of these, an area where the river channel escapes the constraints of steeply sloping hillslopes and talus cones for a distance of approximately 3000m, enough for lateral instability to develop (**Figure 4.2**). The channel slope at this point is approximately 1% and this coupled with the flashy hydrologic regime leads to extensive reworking of the non-cohesive valley floor sediments.

4.2.2 Floodplain morphology

Prior to the Feshie's emergence into the first braided section it is well constrained by steep valley walls although some meandering and limited historical channel division is evident (Brazier, 1989; Rumsby *et al.,* 2000). The channel is well coupled to active debris cones and Holocene colluvial fans both adding unsorted angular inorganic material into the channel (**Figure 4.3**). This material is loosely packed and thus easily entrained. The close proximity of these sediment sources to the main channel's emergence from constraint suggests these could be an important control on the quantity and type of sediment input into the upstream end of the braided section. The debris cones are also an input source of tree trunks into the system.

As the floodplain widens there is evidence of increasing lateral instability and channel switching (**Figure 4.3**). Some constraint is re-imposed downstream by a late glacial alluvial fan made by a steep left bank tributary. This alluvial fan is not an absolute constraint in the way that steep valley walls are and this is emphasised by the semicircular scour of historical channels and the contemporary active zone is multi channeled.

Figure 4.2. The uppermost of the River Feshie's three braided sections. The foreground is upstream and the adjoining channel is from a late glacial alluvial fan.

Figure 4.3. The river emerges from valley wall constraints (upper right) and develops lateral instability although still constrained by a Holocene alluvial fan (centre right). Flow direction is from right to left.

Below the influence of the alluvial fan evidence of lateral instability and channel division increases further with larger quantities of exposed sediments (**Figure 4.4**). Observations of palaeochannels indicate that the river has been morphologically active for distances of up to 150m to the left and right of its present day location (Werritty and Ferguson, 1980). The morphology and dynamism of the active zone is well described in qualitative geomorphological terms by Ferguson and Werritty (1983). The morphological features described include mid-channel bars, lateral bars and overbank bars, all features associated with braided or multi-channel rivers. At the downstream end of this section the channel is again constrained initially by high Holocene terraces and later steep valley walls.

Figure 4.4. Increasing lateral instability downstream of the Holocene alluvial fan. Flow is from right to left.

The geomorphological significance of this site has been shown by several generations of research (Ferguson and Werritty, 1983; Brasington *et al.*, 2000; Rumsby, 2000) showing that it is suitable for investigations of multi-channel behavior and morphological dynamics. Uniquely for a river in the UK the length of lateral instability at the site is over 2.5km suggesting that many of the organizational properties that could be present in braided rivers will be well developed. The fieldwork site is less dynamic than other braided river systems (such as proglacial systems), the extent of vegetation on the flood plain is indicative of this.

4.2.3 Flow Regime

No contemporary flow record was available for the fieldwork site during the study however, a flow record has been maintained 14km downstream at Feshiebridge since January 1993, and this shows that the Feshie has a highly variable flow regime. The drainage area at Feshiebridge is 235km^2 approximately three times larger than the drainage area for the fieldwork site (80km^2). However a gauge maintained by St Andrews University in the late 1970's at the lower end of the fieldwork site shows the upper catchment has flows similar in character to Feshiebridge. The University of St Andrews gauge was used in conjunction with current metering of flows up to 20m^{3}s $^{-1}$ to establish a well defined rating curve used to extrapolate flood discharges. Mean flow was measured at 3m^{3}s^{-1} to 4m^{3}s^{-1} with a minimum of below 1m^{3}s^{-1}. Values recorded in the field in 1998 and 1999 during low flow periods (as determined by the Feshiebridge gauge) did not exceed 2m^3 s^{-1}. A new gauge is now in place at the same location as the old St Andrew's gauge as part of a NERC CHASM project.

The flashy flood regime found at Feshiebridge is well replicated by the St Andrews gauge. Ferguson and Werritty calculated the channel capacity close to the gauge as between 20 and 30m^{3}s^{-1}, capacities that were exceeded 51 times and 16 respectively in the first three years of gauging. This is inconsistent with the usual assumption that overbank flooding (flooding where the channel capacity is exceeded) occurs once per year and implies either that the years gauged were unusually eventful or that the channel was unadapted for such a large number of high flows. Given that channel capacity in braided rivers is hard to define it suggests theories on bankful discharge, on which annual exceedence are based, are inappropriate. Ferguson and Werritty (1983) attribute flood events to prolonged frontal rainfall in autumn and winter and diurnal snowmelt events in the spring with convective storms in the summer on one occasion causing a flood over $100m^3s^{-1}$ in under 2hrs and over in one day (Ferguson and Werritty,1980, do not state the date of this flood)

4.2.4 Fieldsite rationale

The fieldsite chosen is suitable for investigating the research themes outlined in **Chapter 2** because historically the channel has always been braided going back to the first map of the fieldsite (1749-1751),(Werritty and Ferguson, 1980) and contemporary braiding at the site is well developed. This means that the organizational behavior of the system is well developed. The computational experiments by Bak and Chen (1991) and the rice pile experiment by Christensen *et al.* (1991) show that self-organized critical systems must be well developed for them to exhibit scale invariant behavior. The fieldsite is a suitable scale to allow remote survey and ground survey techniques to be effectively used. A smaller system would require smaller scale aerial photography to maintain the resolution and accuracy of the derived DEMs in comparison to the channel and morphological scale. A larger system would have added logistical and locational difficulties, it would have meant using a braided system not in the UK, adding complexity to the timing of the aerial survey and the collection of ground survey data. The rate of morphological change at the fieldsite is suitable for annual re-survey (Ferguson and Werritty, 1983). More rapid changes such as those measured by Lane (1995) on the proglacial braided system developing from the Haute Glacier d'Arolla, Switzerland, would require frequent, daily survey not commensurate to aerial survey. Less active systems would not change enough over the course of the study to produce evidence of dynamic scaling characteristics.

A different approach to addressing the research themes would be an experimental approach, this would have given control over all of the main variables allowing the collection of high quality data addressing each research theme. There are however scientific as well as practical reasons why this was not possible. A braided river created in a flume would take a substantial amount of time to develop self-organization to the degree where scaling characteristics could be identified. The two dimensional, planimetric scaling identified by Sapozhnikov and Foufoula-Georgiou (1997) took eight days to stabilize. The measurement of the experimental braided river surface would have been problematic because this would have required the application of close range digital photogrammetric techniques using a non-metric camera. At the advent of this study such techniques had not been successfully applied to flume surfaces. The final practical consideration was the availability of a flume of appropriate proportions. At the start of this study a suitable flume for investigating braided river dynamics was not available at the University of Hull.

4.2.5 Data acquisition

In order to investigate the research themes described in **Chapter 2** a number of different data sets were collected between 2000 and 2002. These were augmented by data collected in 1998 and 1999, prior to the research in this thesis. In order to properly address the research themes high accuracy, high resolution DEM data were required over a large extent to allow analysis at the system scale. However, this would not be effective unless the quality of the DEMs could be established. Higher quality data was needed to establish the quality of the system scale DEM.

At the start of the project in 1999 there were a number of options available for acquiring the quality and extent of data necessary. Ground survey of the fieldwork site was one option. In 1998 and 1999 high accuracy, high resolution DEMs had been collected on a small experimental reach (160m× 60m, later published in Brasington, 2000). This proved that ground survey was logistically possible and that very good quality DEMs of a limited area could be produced. Ground survey was aided by the extremely low base flows that typically occurred during the summer, which meant survey was unlikely to be interrupted for long periods of time by rainfall. Hydrograph analysis also showed that summer flood events are rare, this provided some assurance that morphologically significant events were not likely to occur during a survey. The hydrograph also showed that flows large enough to produce bedload movement were very likely over the autumn, winter and spring, causing the morphological changes necessary to investigate the dynamic properties of sediment movement.

Data acquisition using remote survey was an option. Although the River Feshie is bounded by steep valley hillslopes above and below the fieldsite the valley widens at the braided section. APs taken in 1988 showed that the hillslopes were wide enough apart to allow access by an aerial survey plane. However, like most active gravel bed rivers the location is not ideal for aerial survey because the mountainous area has a high annual rainfall and high cloud cover particularly in the crucial summer months when the survey is attempted. The low base flows during the summer would also improve the effectiveness of aerial survey because only a very small area of topography was submerged.

The data collection aspect of the project was designed to address the research themes (**Chapter 2**) but also to take into account the qualities of the survey methods described in **Chapter 3**. Digital photogrammetry was chosen as the most appropriate method of acquiring a DEM of the entire system, this was reliant on the acquisition of APs with suitable coverage and scale but also a network of Ground Control Points (GCPs) (**Table 4.1, Figure 4.5**). An extensive amount of check data was also required with which to independently establish the quality of the complete DEM. A high resolution ground survey DEM of a limited extent was also collected (Experimental Reach 1) to allow a more in depth assessment of photogrammetric DEM quality (**Table 4.2, Figure 4.5**). The system scale photogrammetric DEM is a key data set for addressing the second research theme because it provides high quality data over a large spatial extent. The application of this data set to determine static scaling characteristics is considered in **Chapter 6**. The DEM quality assessments acquired using Experimental Reach 1 are integral for defining spatial patterns of error that could affect detection of the actual spatial scaling characteristics of the system.

Research Theme 3 considers the dynamic element of the system. This was originally to be addressed by photogrammetrically acquiring full system scale DEMs of the fieldsite annually. However, this plan was amended because APs of the site were only forthcoming at the end of the first year of the project (2000). A smaller area of the system was GPS surveyed in 2002 with a medium point resolution to enable the calculation of a DEM of difference (Experimental Reach 2)

Date	Data set	Survey method	Description	Extent (m)	Number of survey points	Point Resolution
1998	Survey Control Network	Total station and GPS (Geotronics)	A survey control network of Bench Marks (BMs), established and surveyed with both GPS and Total station to define a local co-ordinate system. Check points were established for checking GPS setup and determining GPS accuracy	Approximately 200m × 200m	7 BM's 18 Check points	--------------
1998	Experimental Reach 1 1998	Predominantly GPS (Geotronics), some use of total station	A high accuracy, high-resolution survey of a small reach at the upper end of the fieldwork site.	Approximately 160m × 60m	9246 survey points	0.64 pts/m^2 (3m radius moving window)
1999	Experimental Reach 1 1999	Predominantly GPS (Geotronics) some use of total station	Re-survey of the 1998 reach with increased point resolution and better representation of deep water areas	Approximately 160m × 60m	14741 survey points	0.98 pts/m^2 (3m radius moving window)
2000	Experimental Reach 1 2000	Predominantly GPS (Geotronics and Leica) some use of total station	Re-survey of 1998 and 1999 reach with an extension upstream to measure active bank erosion	Approximately 285m× 60m	29686 survey points	0.84 pts/m^2 (3m radius moving window)
2002	Experimental Reach 2 2002	GPS (Leica)	An extensive ground survey of an active section of channel at a lower resolution than Experimental reach 1	Approximately 680m × 175m	21209 survey points	0.15 pts/m^2 (5m radius moving window)

Table 4.1 Data used in the construction of DEMs acquired through ground survey

Date	Data set	Survey method	Description	Extent (m)	Number of survey points	Point Resolution
2000	Water depth 2000	GPS (Leica)	Survey points with associated depth measurements and bed surface classification	Approximately 100m × 60m	80 survey points	--------------
2000	Aerial Photographs 2000	Aerial Photography taken with a Zeiss LMK Aerial Survey Camera	Near vertical colour aerial photographs (1:4000) acquired in August 2000 and scanned at 14 microns	Approximately 3000m×1500m	Approximately 801000000 pixels	0.056m= Object- space pixel resolution
2000-2001	Ground Control Points (GCPs) and check data set 1	Total station and GPS (Leica)	A spatially extensive collection of survey points recognizable on the Y2000 photographs, for use as GCP and check point data	Approximately 3000m×1500m	189 survey points	---------------
2001	Check data set 2	GPS (Leica)	A large number of survey points focused on the area of exposed sediments.	3000m × 500m	7515 survey points	0.02 pts/m^2 (15m radius moving window)
2002	Full Photogrammetric DEM	Photogrammetry	The complete DEM of the upper braided section based on photogrammetric techniques and the above data sets.	3011m×1036m	12485679 derived points	0.5m grid resolution

Table 4.2 Data for the construction of photogrammetrically derived DEM

Figure 4.5 DEM models and survey data used in the project. The key shows elevations in metres

The ground survey data collected in 1998 and 1999 prior to the start of this thesis was aimed at addressing issues of data quality and defining the qualities of DEMs acquired using ground survey and in particular surveying GPS. These established that sediment movement could be identified using the morphological method over a limited, meso scale reach (Brasington *et al.*, 2000). The area surveyed (named Experimental Reach 1 in **Table 4.1** and **Figure 4.5**) was approximately 160m × 60m and was chosen because it was a well constrained reach at the upstream end of the braided system at the point where channel instability begins. The reach incorporated a straight channel section, a diffluence and a medial bar incised with chute structures. The reach was surveyed using surveying GPS and EDM with an average point resolution of 0.64pts/m^2 in 1998 increased to an average of 0.98 pts/m^2 in 1999.

The geomorphological significance of Experimental Reach 1 is limited by its spatial extent. In particular it provides a very small snapshot of channel change and sediment movement over a system that has exhibited significant morphological changes above and below the reach. In order to account for these changes and develop ideas on the system scale, data over a much larger extent was needed. The data sets shown in **Table 4.2** were collected to address this scale. These are composed of GCPs, check points and aerial photographs that were used in the construction of the photogrammetric DEM. The procedure used in the construction of the DEM is given below (**Section 4.3.5**). The system scale survey covered a 2.5km length of the system. The survey extended upstream of Experimental Reach 1 to a point where the river was a single channel but unconstrained by valley hillslopes. It covered the development of braiding in the reach and the extended far enough downstream to a point where the active system was narrowing before convergence into a single channel at the downstream end of the braided section. The photogrammetric survey was reliant on the acquisition of good quality APs covering a suitable extent and at a suitable scale. The APs were acquired on the 11th August 2000 by the Cambridge Aerial Survey unit using a Zeiss LMK aerial survey camera. Nine photographs covering the fieldsite were acquired at a scale of approximately 1:4000 scale in two flying lines. The Flight was funded by NERC. In the original project design multispectral imagery as well as APs were to be collected by the NERC Aerial Survey Facility (ASF) however technical problems meant the NERC plane was unable to acquire the data and it was contracted out to the Cambridge Aerial Survey unit. Also in the original project design was a flight in 2001. This was not possible due to adverse flying conditions. The photographs were scanned using a photogrammetric quality scanner at 14 microns giving an object space pixel resolution of 0.056m (see **Equation 3.5**). The object space pixel resolution is also equal to the theoretical precision. A theoretical precision of 0.056m is a satisfactory theoretical error within the context of the study and it ensures that computer file sizes are not excessively large, increasing processing time.

Photogrammetric DEM acquisition was also reliant on the acquisition of GCPs necessary for the photogrammetric process. 189 GCPs were acquired after the flight in 2000 using ground survey (GPS and EDM) of features identifiable on both the APs and in the field. Although the APs and the GCPs represent the minimum requirement for acquiring DEMs of the system the project themes required the DEM to be of high quality. To achieve this a number of further data sets were collected. Subaqueous survey points (80 survey points) together with water depth measurements were collected to facilitate the development of a depth classifier for better defining subaqueous topography. A larger less extensive set of check points (7515 points) was collected to allow for the development of post processing correction procedures and to closely define the quality of the finished DEM.

Experimental Reach 1 was repeat surveyed in 2000 using ground survey techniques (**Table 4.1**). The primary aim of this survey was to provide a very high quality surface with which to compare the photogrammetric DEM. The survey extended Experimental Reach 1 upstream by 155m (285 × 60m) to incorporate a confluence. The average point resolution was dropped from 0.98 pt /m^2 in

1999 to 0.84pts/m^2 to allow for this extension. The 2000 Experimental Reach 1 survey incorporated all the morphological features expected of a braided river. The upstream end of the reach was a confluence followed by a straight section of channel with a pool and then a diffluence. The channel boundaries included a range of different angles including vertical cutbanks and gently sloping sections. There were a variety of water depths including a deep pool (>2m) and shallow steep riffles. These features meant that the reach was a suitable section of river against which to test the photogrammetric DEM, to better clarify the strengths and weaknesses of the photogrammetric method when used for defining complex topography.

The final data set collected, Experimental Reach 2 (**Table 4.1**) is a GPS derived medium resolution data set. These data enable an assessment of sediment dynamics over an extended reach. It was collected because the aerial photographs needed for further photogrammetric work were unlikely to be taken. Although the spatial extent of this data set is much more limited than a photogrammetric DEM the accuracy is superior thereby reducing the Level Of Detection (LOD discussed in **Chapter 4**) of any differencing model.

4.3.0 Acquiring DEMs using ground survey and digital photogrammetry

Chapter 2 has explained the rational for acquiring high quality topographic data. The first sections of this chapter have defined error and reviewed techniques for the collection of high quality topographic data. The last section used these considerations to explain how a study site was chosen and what data sets should be collected. This section of **Chapter 4** describes the practical aspects of DEM acquisition using ground survey and digital photogrammetry.

A distinction is made here between the methods for DEM extraction and the quality of the finished DEMs which will be dealt with in **Chapter 5**. This distinction is in part imposed retrospectively because data quality is an issue that is relevant throughout the data collection and DEM construction processes. However it is necessary to make clear the difference between a DEM development method, which in digital photogrammetry is an experimental and iterative process, and that of defining the quality of a finished DEM product in relation to important geomorphological variables.

4.3.1 Background to method development

There are a number of issues that need to be considered when developing a method for producing a DEM. The ideal sequence is based around considerations of 1) the final application of the model because this is critical for defining 2) the necessary quality of the DEM, which in turn defines 3) the exact specifications of the ground survey or photogrammetry and the extent of the post processing procedures required. In practical terms defining the specifications of ground survey and photogrammetry is harder than this sequence implies. For instance at the outset of this project no studies had dealt with DEM quality with a specific focus on scaling issues and morphological change. The morphological method for determining sediment movement had been theoretically well defined (Ashmore and Church, 1988) but knowledge of the effects of grid resolutions and accuracy and precision of individual points on resultant budgets was untested. Similarly the effects of data quality on morphometric approaches were even less well understood. At the advent then not enough information was available to closely define necessary data quality. Instead data quality was estimated based on theoretical considerations. Just as little was known about digital photogrammetry as a data acquisition tool, the theoretical accuracy and precision of the method were understood and could be calculated but the practical applications of the method to braided river systems was untried and therefore the photogrammetric specifications to achieve a given data quality also needed to be estimated.

Because necessary and achievable data quality were estimated in this study this meant the above sequence is not a true representation of the experimental rationale. The ground survey tailored the resolution of point acquisition to meet the estimated requirements of the DEM. This was based on the known data quality characteristics of ground survey DEMs defined by the 1998 and 1999 surveys. The photogrammetric survey was based on a rational defined by the following sequence:

1) Estimation of necessary data quality for final application
2) Estimation of achievable data quality using varying scales of AP and photogrammetric approaches
3) Basic error assessment throughout the photogrammetric processing and post processing to ensure that error does not significantly exceed estimated necessary data quality.
4) Comprehensive assessment of data quality of final DEM including the assessment of significant geomorphological variables.

The sequence above is the inevitable result of having both a final application and data acquisition method that are theoretically sound but practically untested

Since the start of this study in 1999 a number of publications have produced evidence to aid understanding of data quality for DEM building (Brasington *et al.*, 2000) and the practical application of photogrammetry to geomorphology (Lane, 2000[1]) and river channels (Lane, 2000[2], Westaway, 2000[1]). These studies, along with the results from this thesis, mean that future studies can tailor data acquisition specifications more closely to data quality needs.

4.4.0 Method for DEM construction using ground survey techniques.

One of the fundamental advantages of ground survey over photogrammetric techniques is that DEM construction using the data acquired in the field is a very quick process. Although collection of ground survey data in the field is a very labour intensive task the survey points can be directly downloaded from the survey equipment or from a storage card. In the case of GPS without the RTK function some post processing is needed. The manufacturers of surveying equipment provide suitable software for this. The 2000 survey used a Leica GPS without a RTK function and so post processing was necessary. The survey point data were exported from the survey equipment as .ascii format files.

The data files were imported into Arcview GIS for DEM construction. The DEMs were constructed using the Triangular Interpolation Network (TIN) method, which is interpolation using Delauney triangulation, a method that exactly intersects with all the data values. Other interpolation methods were considered but research shows these to be less effective for terrain that includes sharp breaks in slope (Desmet, 1997). A further conversion of the TINs to grids was carried out so that the large number of raster tools available in Arcview could be used for further analysis. The incorporation of artifacts into the model during this conversion is minimal provided that the grid cell size is small relative to the TIN facet area (Brasington *et al.*, 2000).

4.5.0 Method for DEM extraction using digital photogrammetric survey.

Figure 4.6 shows the method used to extract and correct the final photogrammetric DEM. The method is split into 4 stages. The first stage is concerned with extraction of the DEM using the photogrammetric software, Orthomax. This includes an initial error assessment and feedback loop for unsatisfactory error. Once satisfactory error has been achieved the DEM is post processed in stage two.

Stage two involves orthorectification of the images used in the production of the DEM. The fully rectified images are then used to separate wet and dry areas of the DEM so that they can be dealt with separately. The dry areas were re-interpolated using the TIN interpolation method to make the DEM directly comparable with the DEM acquired through ground survey. The wet areas of the DEM were replaced by elevation data based on empirically determined water depth information and a water surface interpolated from dry waters edge elevations. These new submerged elevations were required because the digital photogrammetric process is poor at determining submerged elevations (Westaway, 2001). Finally the wet and dry areas of the DEM were merged.

Stage three is concerned with the mosaicking of the individual DEMs. Although each of the individually produced DEMs falls within specific statistical error tolerances some systematic errors still exist within the surfaces. In order for the DEMs to mosaic together without distinctive breaks of slope in overlap regions the systematic errors needed to be removed and the DEMs mosaicked using a feathering function. The systematic errors of the DEMs were identified by fitting linear trend lines to the error residuals calculated from the GCPs not used in the photogrammetric process. The trend lines were used to define correction surfaces, which were applied to the DEMs in Arcview before the DEMs were mosaicked in Erdas Imagine.

Stage 4 is the final post processing stage, applied to the mosaicked DEM of the whole braided river system. When the DEM was compared to independent check data it was found that many of the error residuals were larger than the required data quality. A correction surface was developed to reduce the error residuals of the DEM. The correction surface was defined using >3500 ground survey point error residuals (half of Check data set 2) and was smoothed in Arcview using a 5m ×5m moving window filter.

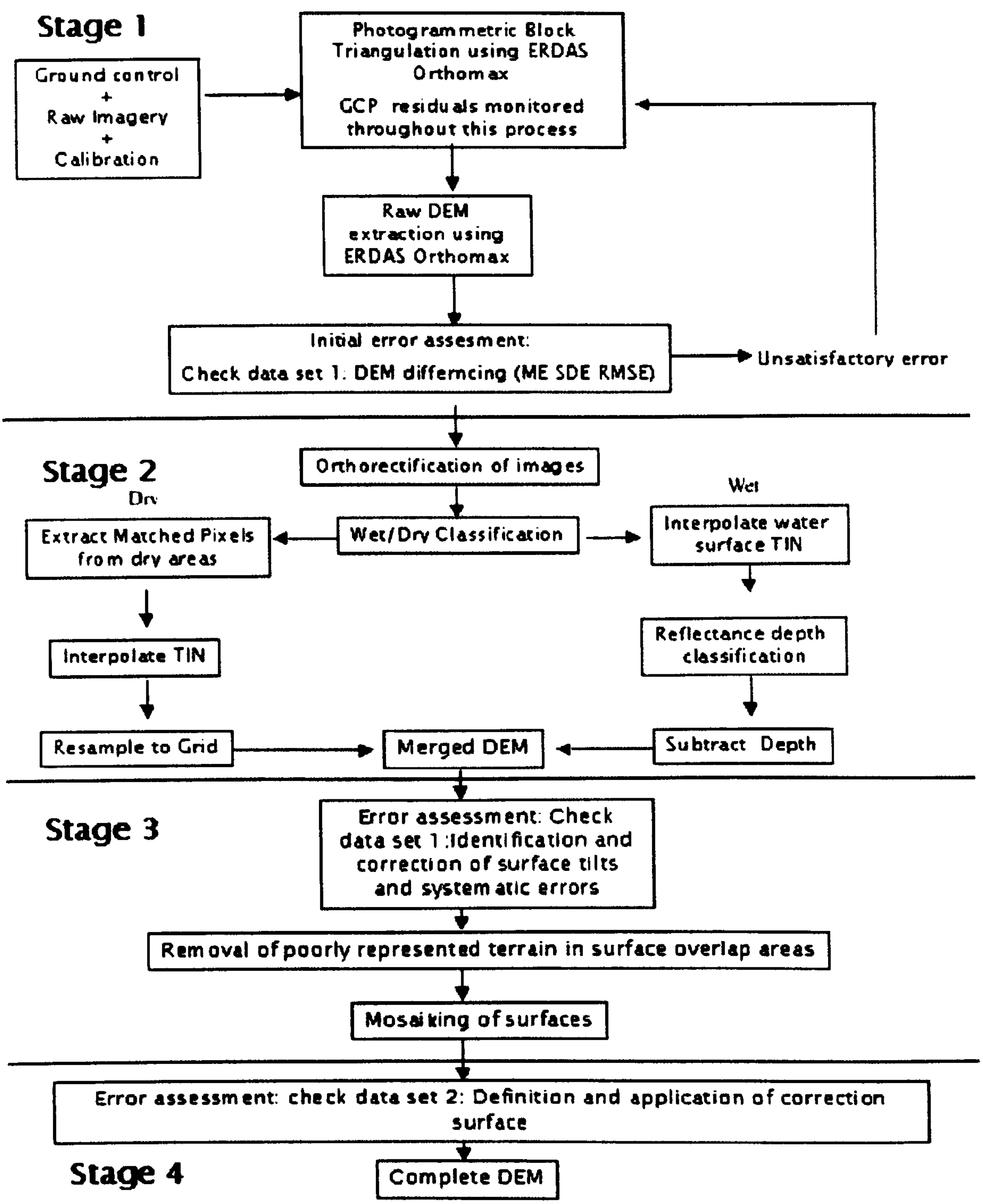

Figure 4.6 Model for the extraction and post processing of a high quality DEM using digital photogrammetry.

4.5.1 Stage 1 Photogrammetric specifications and processing

The photogrammetric processing for this study was done using the Orthomax module of Erdas Imagine (version 8.3). This is a popular piece of software within the UK academic community because it was inexpensive to purchase through the CHEST (Combined Higher Education Software Team) licensing agreement. The software was installed on a number of UNIX machines predominantly Sun Workstations.

Many of the stages involved in digital photogrammetry are the same as those in conventional photogrammetry (discussed in **Chapter 3**) therefore this discussion of methods will be far from exhaustive. Instead it will attempt to describe the process of DEM generation using digital photogrammetric software, highlight any specific issues and present the results of each stage of photogrammetric processing.

4.5.2 Input data

As with other modeling procedures the quality of the result is dependent on the quality of data used in the modeling process. Digital photogrammetry like conventional photogrammetry is very dependent on the quality of photographs and GCPs. The theoretical considerations involved in the determination of data specifications along with the quality of derived data have been dealt with in **Chapter 3**. In summary: The photographs were acquired at a scale of approximately 1:4000 and the diapositives were scanned at 14 microns giving an object space pixel dimension of 0.056m. 189 GCPs were collected after the photographs using recognizable features on the floodplain, predominantly vegetation.

4.5.3 Block triangulation

The principles of block triangulation are described above in **Chapter 3**. Block triangulation is a key process in both conventional and digital photogrammetry, it aims to establish the three dimensional position and orientation of the camera at the time each photograph was exposed. Camera position is derived through defining the position of GCPs (with known three dimensional position in object space) on the image-space co-ordinates (two dimensions). The digital process is very similar to that of conventional photogrammetry consisting of interior and exterior orientations. The interior orientation attempts to model the interior geometry of the camera. Lens calibration information inputted by the user along with image space information on the fiducial marks is combined with GCP information in both object and image spaces to tie the fiducial marks on the original photograph (diapositive) to the digital imagery.

A single camera was used in this study, an AF/ZEISS LMK. The Cambridge Aerial Photography Unit supplied a copy of the lens calibration certificate. The photographs were imported into Orthomax in the .tif file format and were automatically sequentially numbered (Erdas, 1995). The GCP data were entered as a .txt file format.

Positioning of the fiducial marks on screen to determine the interior orientation of the images was carried out in Orthomax. Several facilities exist to aid this process including magnification and automated estimates of position. The estimates were all examined and repositioned if necessary to ensure correct positioning.

The exterior orientation phase of the block aims to fit the photogrammetric block to a horizontal datum described by the GCPs by rotating and transforming it (Dixon *et al.*, 1998). This involves identifying GCPs on two or more photographs thereby defining their image space position. This information can then be used to perform a simultaneous least-squares bundle adjustment to define the camera's position and orientation.

In Orthomax the image-space positions of the GCPs are derived using the Ground Point Measurement Tool, which allows the location of GCPs to be identified on the photographs. The block triangulation is then carried out iteratively using the least squares bundle adjustment until a convergence value is reached. Both the number of iterations (up to 20) and the convergence value can be user defined (Erdas, 1995). The quality of the bundle adjustment is measured using three statistics. These statistics aim to measure the closeness of the bundle adjustment to the theoretical condition of collinearity by giving measures of object to image geometry. The internally generated statistics are: 1) The standard deviation of unit weight, a statistic that represents the overall quality of the bundle adjustment by showing the conformance of the bundle adjustment to specified parameters (Erdas, 1995). This parameter should be as close to unity as possible. 2) The standard deviation of the residuals associated with the exposure station (the location of the camera at the time of exposure) coupled with 3) the standard deviation of the residuals associated with the GCP positions represent the deviation from the theoretical collinearity equations.

The block statistics generated in this study can be seen in **Table 3.3**. These compare favorably with those produced by similar photogrammetric studies in particular Westaway (2001). However there are a number of important differences in the way photogrammetric blocks were formed by Westaway and how they were formed in this study. The most obvious difference is that Westaway formed large blocks including all photographs for each photogrammetric model he produced. In contrast this study triangulated a separate block for each pair of photographs. The reason for this important difference is explained by the GCPs (in Westaway Photo Control Points) available. Westaway used 45 (1999) and 55 (2000) high quality GCPs on the Waimakariri, spread in a regular grid over the surface of the braided river. These were constructed from marker boards with the central marker board of each GCP leveled. This study used 189 poor quality GCPs spread over a smaller area. The GCPs were of a poorer quality because no GCP markers were in position at the time of the flight. The GCPs were defined afterwards by ground survey of the features that could be identified on both the ground and the APs. There are two disadvantages of this method. First the GCPs could not be evenly spread but instead were dependent on the distribution of suitable features. Second, the features used for the GCPs tended to be changes in vegetation, a less precise method for defining a location in X, Y and Z than the GCP marker board system used by Westaway (2000). The large quantity of GCPs collected reflects their individual quality and it was predicted that a large number would be removed during the block triangulation stage. The quality of the GCPs also meant block convergence with acceptable residuals was more difficult to achieve. It was found that the block triangulation process was more successful when just two photographs were used per block triangulation. Similarly large quantities of GCPs were removed during the triangulation to aid in the reduction of residuals. Westaway (2001) found tie points an effective method of reducing residuals. Tie points use features identifiable on both photographs to tie the images together. No XYZ location (object space) is needed for tie points and so they become more effective when few GCPs are available. In this thesis no tie points were used because the large amount of GCPs was sufficient.

			MEAN GCP RESIDUAL MEAN ERROR (m)			MEAN GCP RESIDUAL STANDARD DEVIATION (m)		
Photogrammetric Block Number	**Number of GCPs**	**Standard Deviation of Unit Weight**	**X**	**Y**	**Z**	**X**	**Y**	**Z**
-1	13	1.08	0.05	0.04	0.02	0.06	0.04	0.03
0	9	1.13	0.01	0.00	0.00	0.05	0.10	0.05
1	14	1.02	0.01	0.03	0.00	0.06	0.05	0.03
2	20	0.99	0.07	0.06	0.03	0.09	0.08	0.04
3	11	1.01	0.00	0.01	0.00	0.08	0.07	0.04
4	17	1.35	0.00	0.01	0.00	0.04	0.05	0.02
5	19	0.92	-0.01	0.02	0.01	0.09	0.06	0.03
6	20	1.10	-0.02	0.00	0.00	0.13	0.15	0.04

Table 4.3. Results from the block triangulation process

4.5.4 DEM collection

Following the derivation of a successful bundle adjustment and block triangulation DEMs were generated using the 'DEM Tool' in Orthomax.

Orthomax uses an area based algorithm (Vision Algorithm) to identify corresponding points on two overlapping images using contrast and brightness. The process for identifying corresponding points uses a hierarchical approach that performs correlations at increasingly higher resolutions. This approach is necessary to take into account large changes in elevation and prevents false fixes. Subsequent increased resolution iterations are constrained by the previous coarser resolution iterations which are used to generate orthorectified images above and below the predicted elevations (Erdas, 1995). The entire DEM collection process can be guided via 12 DEM collection parameters (Appendix 1). Experiments altering these parameters have shown improvements in surface quality and matching precision (Pyle, 1997; Gooch and Chandler, 1999; Lane *et al.*, 2000[1]). The default DEM collection parameters were used for all DEMs generated in this study because the experimental work by Gooch and Chandler (1999) and Lane (2000[1]) is unclear how the parameters should be optimized to achieve best results for the braided topography that characterizes the study site.

4.5.5 Stage 2 Individual DEM processing

Each DEM output from the digital photogrammetric process was assessed for error using GCPs not used in the block triangulation process. Each photogrammetric block was altered, DEMs re-acquired and re-assessed for error. This process was continued until block alterations failed to show improvements in the error statistics.

Examination of the DEMs showed that submerged topography was very poorly defined by the digital photogrammetric process. This observation was supported by the work of Butler (2001) and Westaway (2000) which showed that the area based pixel matching algorithm used in Orthomax during the DEM collection process matched very few pixels in submerged areas and those that were matched measured the waters surface or a refracted channel bed. This weakness of the digital photogrammetric method resulted in reduced overall quality statistics for the resultant DEMs and produced a systematic positive increase in the elevation of submerged topography (Westaway, 2000). In order to overcome this problem the submerged area of channel in each DEM needed to be separated from the dry areas of the DEM so that each could be processed separately.

4.5.6 Orthorectification and classification of images

Before separate processing for wet and dry areas could commence these areas needed to be defined. This was achieved using a supervised classification of orthorectified images. The images were orthorectified using the Ortho Tool module in Erdas Imagine Orthomax. This allows one of the sources images, used to create a DEM to be orthorectified according to that DEM. This method for the production of a fully rectified image is the most precise method available because the location of each AP pixel is changed according to its elevation as defined by the DEM. The alternative method is georeferencing, which uses known points (usually GCPs) to stretch the AP in two dimensions. Georeferencing was considered sufficient by Westaway (2001) because of the small vertical relief associated with braided river morphology. However, orthophotographs demonstrate one clear advantage of digital photogrammetry over other data acquisition techniques such as ALS or ground survey.

The orthorectified images were classified in order to differentiate wet and dry areas using a supervised classification developed in Erdas Imagine. The classification was developed by sampling the Digital Number (DN) values of submerged areas using training areas and then applying the classification to the orthorectified imagery. The results of this process were problematic for two reasons:

Some vegetation types had a spectral signature so similar to that of submerged zones that many of the DN values were identical. Only a more sophisticated classification algorithm capable of analyzing the distribution of DN values over a given area or taking into account spatial context could offer an automated solution to this problem. Such an algorithm was considered too time consuming to be developed. For the purposes of this study the supervised classification was heavily manually edited to exclude vegetation.

Aside from interference from vegetation, classification of fully wet and fully dry cells was not problematic. Difficulties arose at the channel edges because grid cells spanned both wet and dry areas, an inevitable result of using raster data. However defining waters edge was particularly problematic in this case because the coarse grain size and shallow channel depths meant large clasts had submerged bases and upper sections exposed above the water surface (**Figure 4.7**). When such an area is classified the extent of the submerged zone is very dependent on the exact make up of the training areas used in the classification.

Fundamentally there is a clear distinction between the DN values of wet and dry areas (**Figure 4.8**). However any DN values that fall in the grey area of **Figure 4.8** could be interpreted as either wet or dry. It is the classification of these values that alter the extent of the water classification. This is illustrated by **Figure 4.9**, which shows variations in extent of inundation according to DN threshold values. This is a point of concern initially for the modeling process because the classification is a key element in the submerged zone processing but also a geomorphological concern because extent of inundation has been used as a metric in a number of influential studies (Sapozhnikov and Foufoula-Georgiou, 1996). **Figure 4.10** shows the final submerged zone classification.

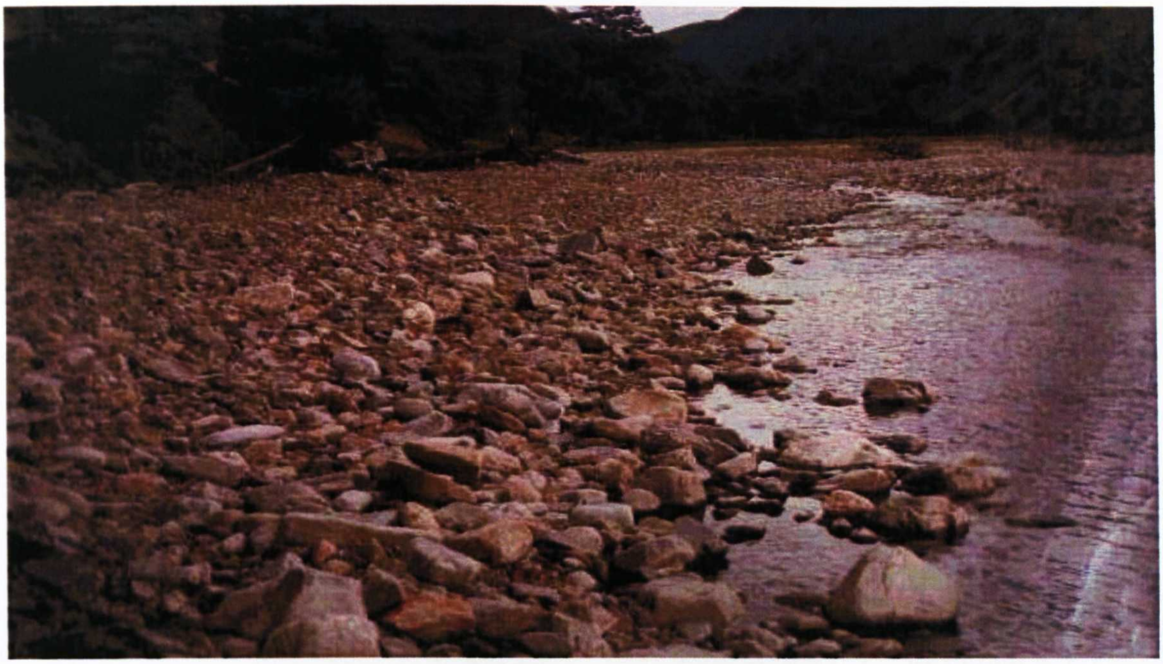

Figure 4.7 Looking upstream at Experimental Reach 1. The large clasts are light in colour when compared to the water. An orthophotograph with a pixel size of 0.5m will be ineffective at defining waters edge.

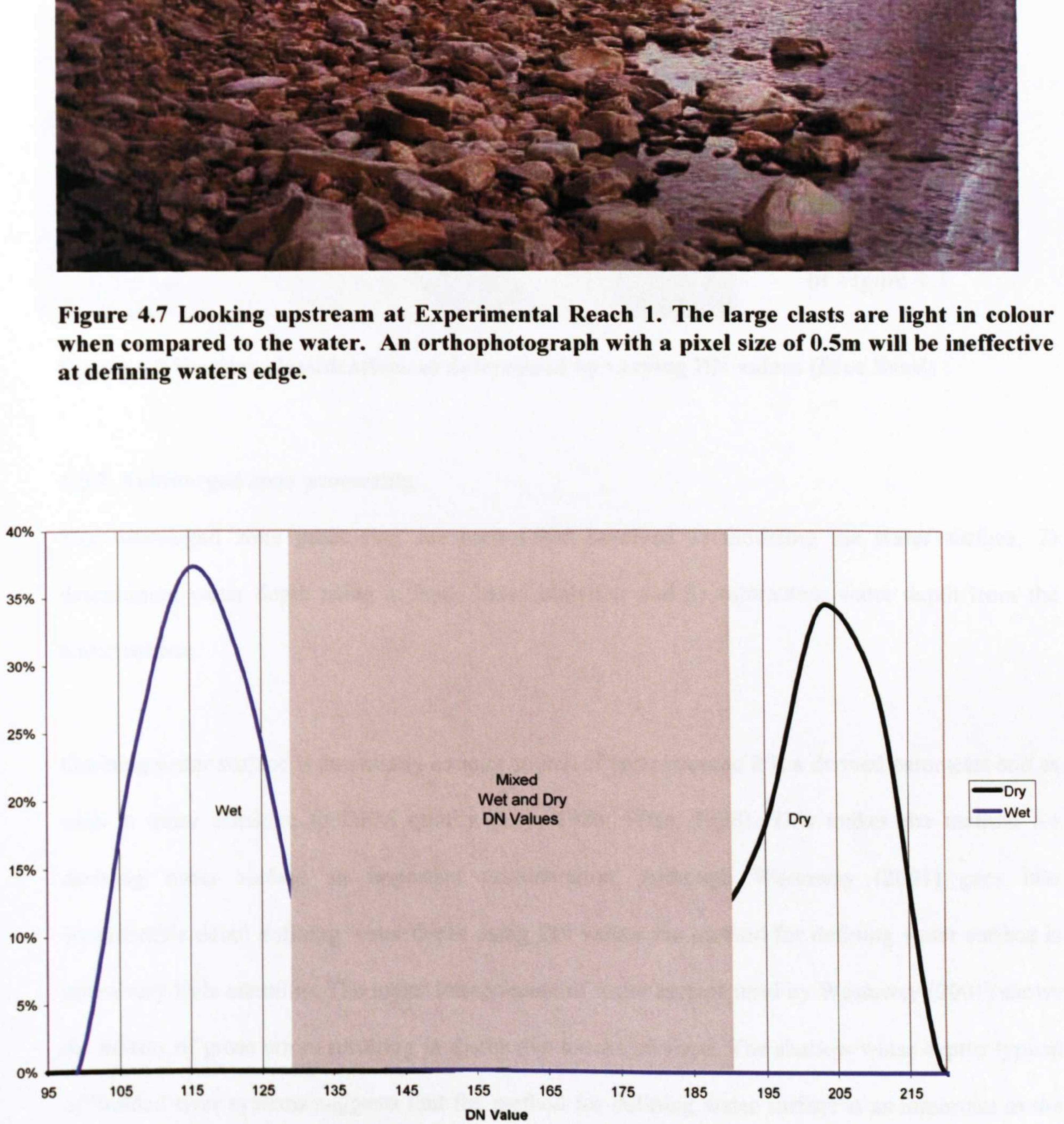

Figure 4.8 Distribution of DN values for submerged and dry areas (blue band)

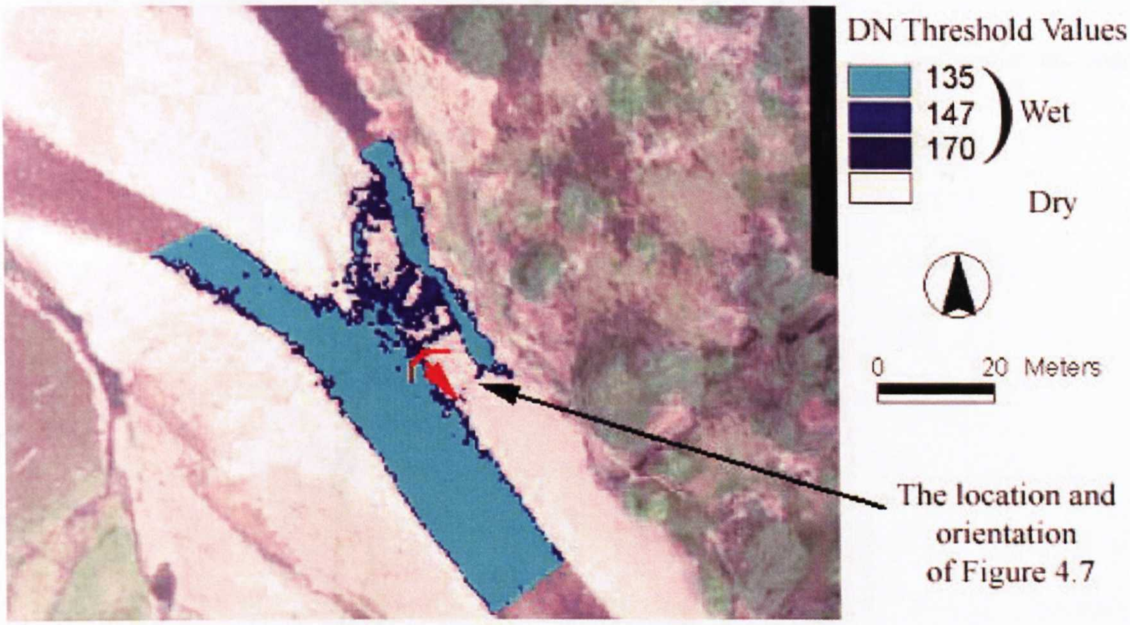

Figure 4.9 Wet/dry classifications as determined by varying DN values (Blue Band)

4.5.7. Submerged zone processing

The submerged zone processing for each DEM involved 1) modeling the water surface, 2) determining water depth using a depth based classifier and 3) subtracting water depth from the water surface.

Defining water surface is potentially a major source of error because it is a derived parameter and as such is more sensitive to DEM quality (Ley, 1986; Wise, 1998). This makes the method for deriving water surface an important consideration. Although Westaway (2001) goes into considerable detail defining water depth using DN values the method for defining water surface is given very little attention. The linear interpolation of water surface used by Westaway (2001) shows the effects of gross errors resulting in distinctive breaks of slope. The shallow water depths typical of braided river systems suggests that the method for defining water surface is as important as the method for defining water depth. The research in this thesis puts a greater emphasis on the method used for defining water surface.

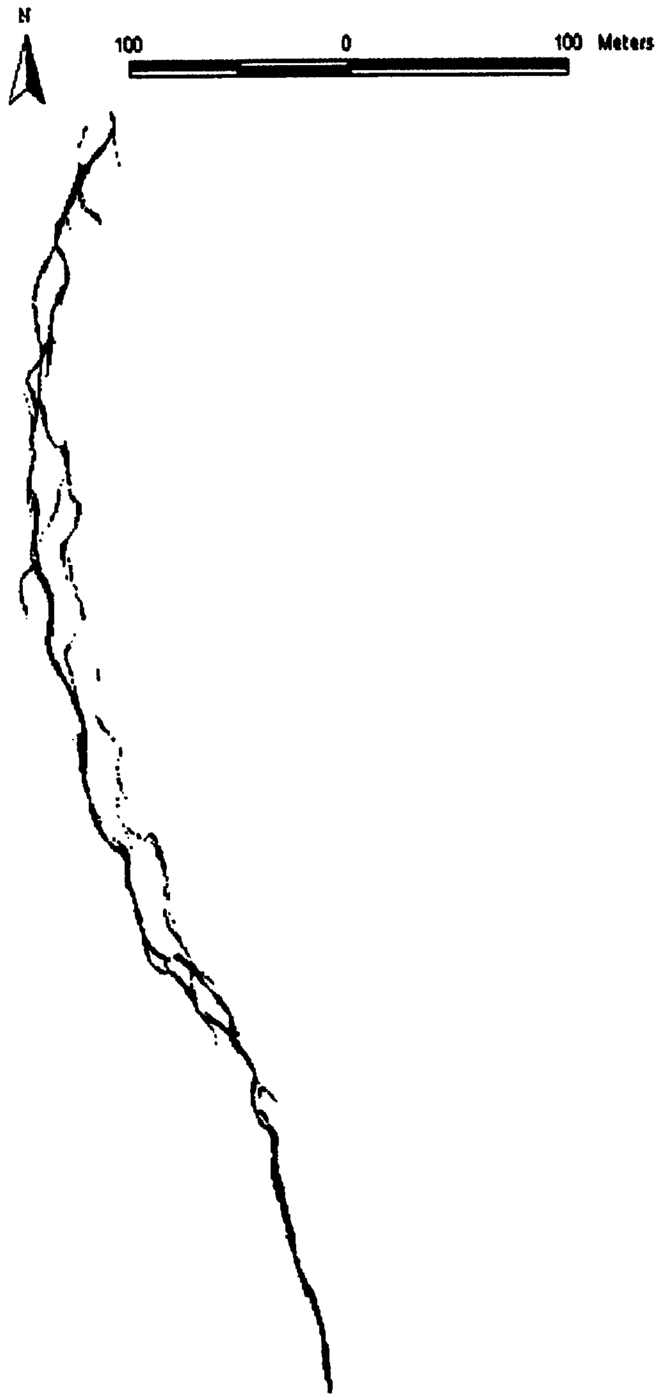

Figure 4.10 The final submerged zone classification

An edge detection algorithm in ERDAS Imagine was used to convert the submerged zone classification to show waters' edge. The edge data were imported into Arcview GIS where they were multiplied by the photogrammetric DEM to attribute each water's edge cell with an elevation. It is here that the importance of **Figures 4.7 – 4.9** can be seen. If the submerged classification varies due to the effects described in **Section 5.5** then this will inevitably result in changes in edge elevation values affecting a large section of the water surface model. **Figure 4.7** illustrates this point but also raises the issue of what surface is being seen (stereo-matched) by the digital photogrammetry. With surfaces like braided river topography there is considerable surface roughness caused by large clasts and vegetation. It is unclear whether the digital pixel matching process is most effective at matching the shadow areas between clasts and vegetation (lower elevations) or the tops of clasts and vegetation (higher elevations). Lane (2000[1]) posed this question without reaching a substantive conclusion and it is likely that an extremely high resolution, high accuracy data set is needed to satisfactorily answer it. **Figure 4.7** shows that the upper surface of large clasts are substantially above that of the water surface. If these raised surfaces are successfully stereo-matched and included in the waters edge elevation file then these extreme values will influence a large number of cells in the water surface elevation map. Neither of these water's edge/elevation issues are quantitatively assessed here because data of sufficient resolution were not available. However interpolation of water surface from the unfiltered water's edge elevations gives a poor water surface model (**Figure 4.11a**) that contains exceptionally steep water surface slopes as a result of large localized variability in downstream waters edge elevations. The problem is also heightened by the TIN interpolation method used. The TIN method was chosen because it was the most successful at interpolating cross-stream values. If the surface in **Figure 4.11a** were to be used without modification then it is clear that the resultant submerged topography would not be dominated by water depth but by water surface artifacts.

The solution to this problem adopted in this study was an area based filter of water edge elevations (5m×5m) that replaces the cell value with the minimum value in the filter area. This approach is useful because it negates the effects of high elevation values and this has the effect of reducing angular shapes in the interpolated water surface model. There are however a number of assumptions and systematic errors associated with this approach. It is assumed that the lowest value is not based on a stereo-match substantially below the water surface. This is not considered a likely occurrence because the dark colour of the water at the time the APs were collected inhibited digital pixel matching below the surface. This assumption was manually checked for a few lengths of channel boundary. It is also assumed that the minimum value (for any given filter area) is not substantially above the water's surface. In order to increase the likelihood of this second assumption being correct the filter area can be increased but this increases the significance of a third effect, the substitution of a correct (at water level) downstream value, upstream. This third effect represents a systematic error introduced by the approach. This effect is magnified by large water surface slopes, such as those present in some riffles, and increasing filter size. There is a trade off between filter size (increased smoothing) and accurately representing steeply sloping areas of the DEM. Preliminary experimentation with filter sizes using Experimental Reach 1 showed that a 5m filter was appropriate because it filtered out extreme values whilst not excessively distorting the values of steeply sloping areas. This was adopted for the Full Photogrammetric DEM. The water surface model based on filtered data is greatly improved visually, reducing the spatial extent and magnitude of steeply sloping sections (**Figure 4.11**).

4.5.8 Determining water depth using a depth based classifier

The second element of submerged zone processing is determination of water depth. This problem has previously been tackled by Westaway (2001) who developed a solution that related water depth to water colour on digital photographs. Quality assessments of depth estimates compared to measured depth showed that Mean Errors (ME) were all below 0.0015m and Standard Deviation of

Error (SDE) below 0.2m. These results are encouraging given the water depth ranged from 0m to 1.5m. Other attempts at producing water depth maps from remotely sensed pixel colour include Winterbottom and Gilvear (1997) and Gilvear *et al.* (1998).

Given these results, a similar approach to that used by Westaway (2001) was adopted in this study. The first key stage in this approach was to determine a relationship between water depth and water colour. The data used to develop this relationship consisted of ground survey data collected using GPS receivers along with measured water depths and the orthorectified digital colour imagery used for the water classification. Testing of water depth with DN values in 3 bands showed that the blue band was the most effective. **Figure 4.12** shows the relationship defined.

The trend line shown on **Figure 4.12** is a power function. This was accepted as the relationship for transforming DN values to water depths. This power function transformation was not chosen due to theoretical reasons but because it better represents deeper areas of the channel for which only a few measurements were possible. The power function poorly represents depths in excess of 0.80m, **Figure 4.13** shows that less than 2 percent of the system is deeper than 0.8m. The comparison of water depths in **Figure 4.13** shows that the water depth in the experimental reach shows some differences when compared to the rest of the system. In particular there is less shallow water (0.1-0.3m) but more values between 0.4 and 0.7m.

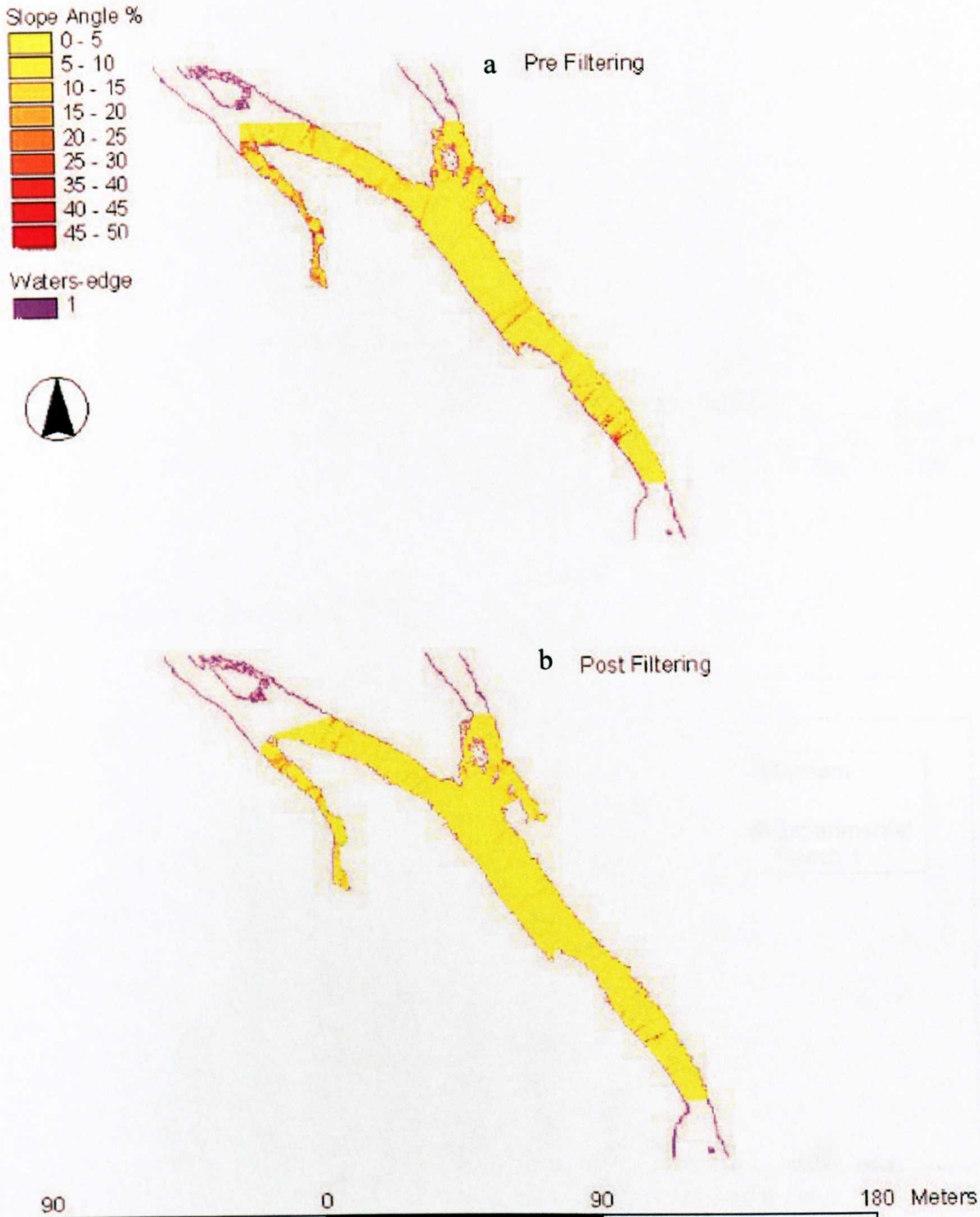

Figure 4.11. Water surface slope angle. Before filtering the water surface includes more high angle surfaces.

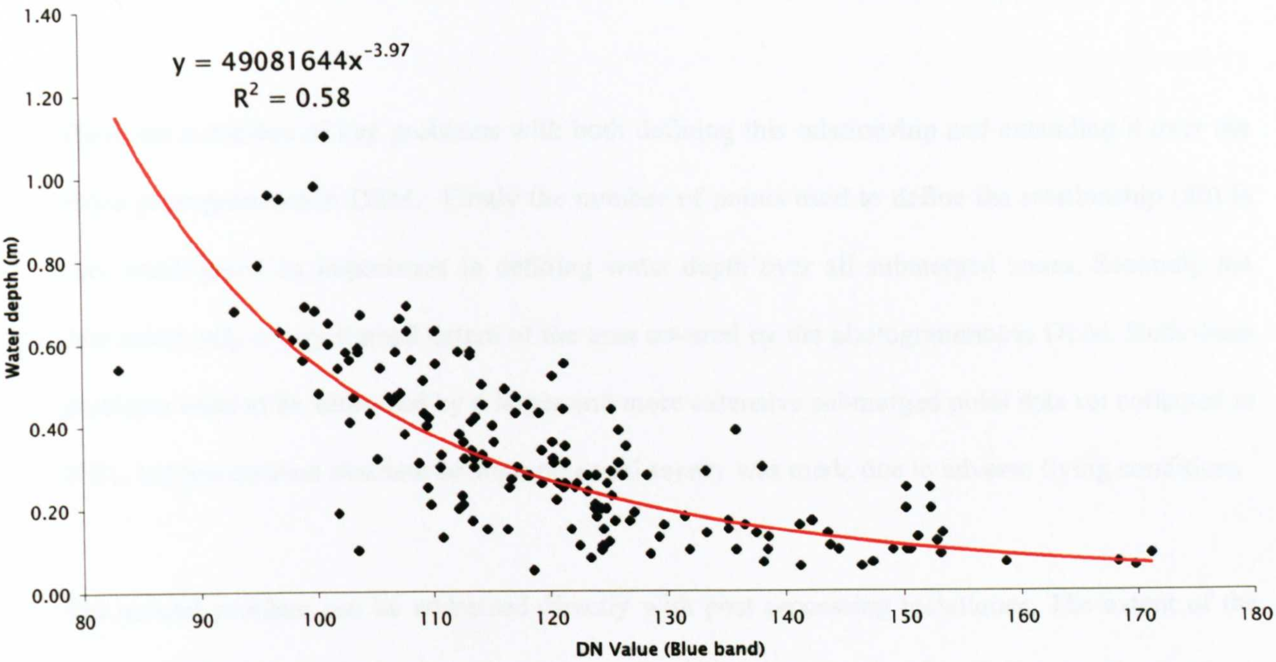

Figure 4.12. DN values and water depth

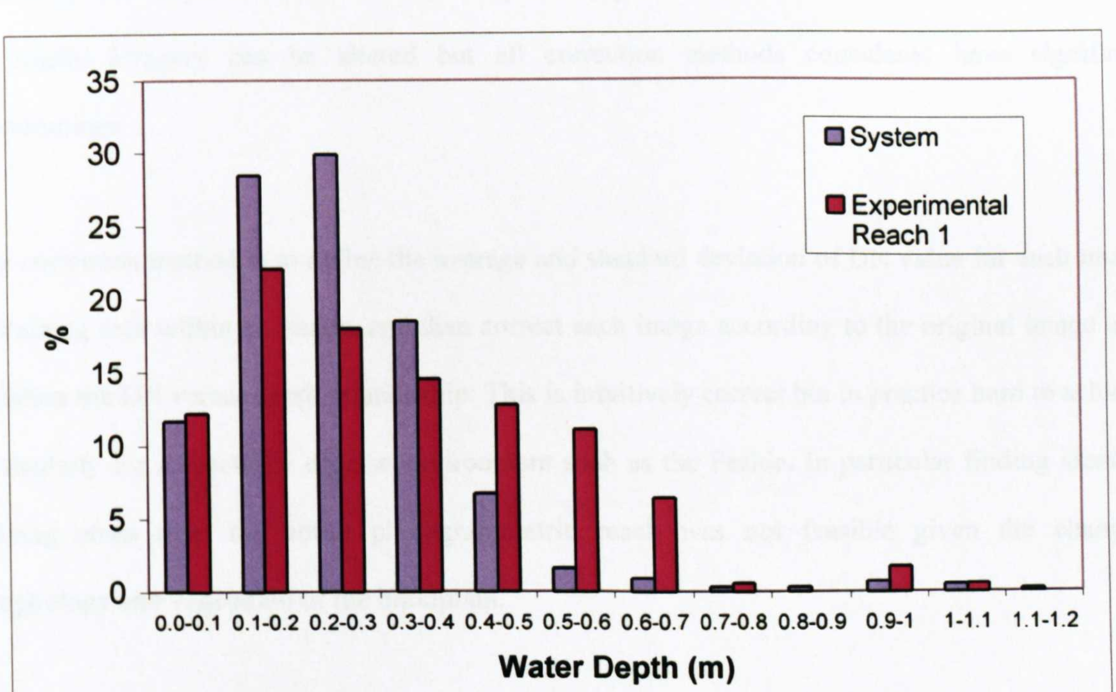

Figure 4.13. Distribution of water depth measurements taken over the entire system (2001) and over the Experimental Reach 1 (2000).

There are a number of key problems with both defining this relationship and extending it over the entire photogrammetric DEM. Firstly the number of points used to define the relationship (80) is very small given its importance in defining water depth over all submerged zones. Secondly the data cover only a very limited extent of the area covered by the photogrammetric DEM. Both these problems were to be addressed by a larger and more extensive submerged point data set collected in 2001, but this became obsolete because no aerial survey was made due to adverse flying conditions

The second problem can be addressed directly with post processing techniques. The extent of the water depth data is limited to just two photographs which is adequate when defining water depth on just those photographs. However photographs of upstream and downstream sections are exposed differently resulting in different DN values representing water of the same depth. To correct for this the digital imagery can be altered but all correction methods considered have significant shortcomings.

One correction method is to define the average and standard deviation of DN value for each image, or training area within an image, and then correct each image according to the original image used to define the DN versus depth relationship. This is intuitively correct but in practice hard to achieve, particularly for a spectrally diverse environment such as the Feshie. In particular finding identical training areas over the entire photogrammetric reach was not feasible given the changing morphology and vegetation of the braidplain.

An alternative solution is to use the 60% overlap area between photographs to sequentially adjust the next image up and downstream. At first glance this also appears to be a good solution because the training area is effectively the overlap region. Differencing of the overlap regions reveals the shortcomings of this method (**Figure 4.14**), highlighting systematic differences between images. The overlap region is viewed from a slightly different angle by each photograph because the camera position is different and this produces differences in DN values. The result is that DN values are dependent on the position of the surface relative to the camera as well as real differences in DN values related to photograph exposure. When this effect is propagated over a number of photographs away from the original, the DN corrections become dominated by error resulting from within photograph trends in DN.

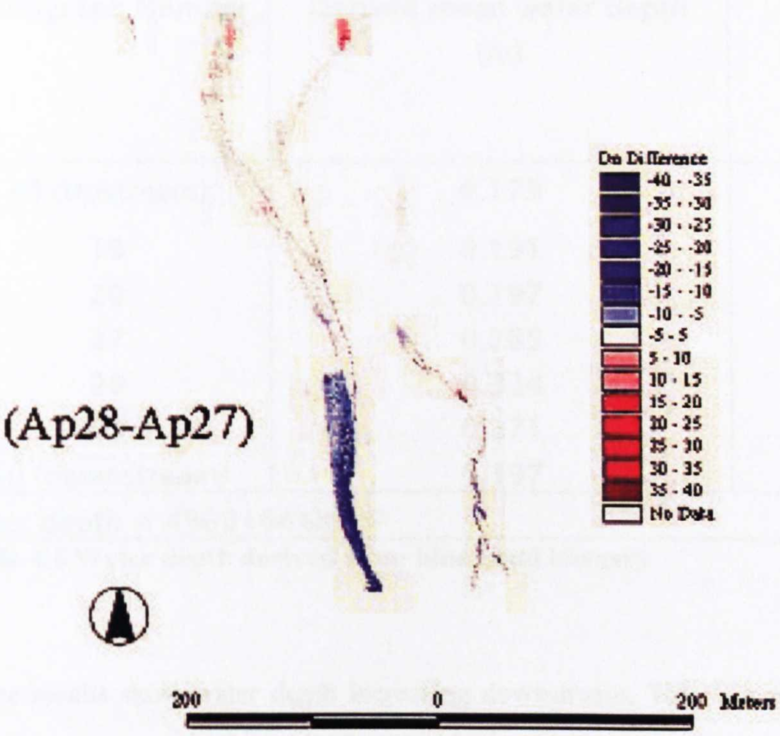

Figure 4.14 DN differences between APs in the overlap zone. AP28 has consistently lower values than AP 27 at the southerly (upstream) end of the overlap and higher values at the northerly end of the overlap. The difference between the two photographs changes systematically from south to north.

Empirical correction of these within photograph trends has proved just as problematic because the braidplain itself changes in character downstream. This complicates the modeling of DN values within photographs because it is impossible to tell which changes in DN are related to downstream morphological and ecological changes and which are apparent changes due to angle of incidence.

Due to the shortcomings of these correction procedures they were not adopted in this study. Instead water depths were derived using the relationship defined in **Figure 4.12.** The mean water depths are shown in **Table 4.4**

Photograph Number	Derived mean water depth (m)	Derived water depth attributable to within photograph trend (m)
18 (Upstream)	0.179	0.008
19	0.191	0.009
20	0.197	0.009
27	0.285	0.014
28	0.334	0.016
29	0.371	0.022
30 (downstream)	0.397	0.017

Water depth = $49081644X^{-3.97}$

Table 4.4 Water depth derived from blue band imagery

These results show water depth increasing downstream. This is a worrying result because lateral instability also increases downstream and intuitively this implies that water depth should decrease as topographic variability also decreases. Measured water depth data collected in 2001 **(Table 4.5)** shows that water depth does not increase downstream. Although the measured water depth data were collected one year after the APs from which the derived water depths were acquired, channel changes over the period are unlikely to have had a significant impact on the statistical distribution of water depths. The magnitude of the errors associated with the derived water depths over the system is indicated by the fourth column in **Table 4.5.** Water depths are underestimated by almost 0.1m in the channel covered by AP 18 but they are overestimated by 0.1m in the channel covered by APs 28 and 29. This systematic change in water depth is the result of changes in atmospheric conditions during the flight or AP exposure resulting in lower DN values, resulting in increased derived water depth values.

	Water depth (m)		
Photograph Number	**Measured (2001)**	**Derived (2000)**	**ME Difference (Derived-Meas)**
18 (Upstream)	0.274	0.179	-0.095
19	0.270	0.191	-0.079
20	0.246	0.197	-0.049
27	0.233	0.285	0.052
28	0.232	0.334	0.102
29	0.268	0.371	0.103
30 (Downstream)	0.308	0.397	0.089

Table 4.5 Measured water depth (2001) compared to derived water depth (2000) for the areas covered by APs 18 to 30.

The third column in **Table 4.4** shows the water depth attributable to trends in DN values within each photograph. Modeled using the DN values of submerged zones fitted with downstream linear trend lines, these figures show that only a very small depth is attributable to downstream changes in DN within any one photograph. The angle of incidence problem (described above) is still relevant to these data and could be canceling out many of the real changes in depth within each photograph.

No attempt was made to correct the water depth measurements because there were insufficient reliable data on which to base a correction relationship. The relationship shown in **Figure 4.12** was used to derive water depths without further correction procedures. The errors shown in **Table 4.5.** were considered tolerable because of the small amount of submerged topography within the system.

4.5.9 Dry zone processing

Dry zone processing was considered necessary to establish more control over the DEM produced by Orthomax and to make the photogrammetric DEM directly comparable with a GPS derived DEMs.

4.5.10 Extraction and filtering of stereo matched cells

DEM generation in Orthomax produces two raster files, one containing elevation data (*.elev)* and the other showing which cells were stereo-matched (**Chapter 3. Section 3.8**) and the quality of those stereo matches (*.stat*). The *.elev* is the product of a bilinear interpolation of matched points to generate elevation values for unmatched cells. This interpolated DEM product is unsatisfactory because it inhibits data quality filtering and application of alternative interpolation algorithms. In this study the .stat files were used to strip out the interpolated data leaving just the stereo matched data.

4.5.11 Re-interpolation using TIN

The filtered elevation data were then re-interpolated using a Triangular Irregular Network (TIN) and this surface was then converted to the more versatile raster format. The choice of interpolation method was primarily dictated by the format of previous data sets. The GPS derived DEMs (Years 1998, 1999 and 2000) for the experimental reach had all been interpolated using a TIN so for the photogrammetrically derived data set to be directly comparable it would also have to be interpolated using a TIN.

Before further processing the dry zone and submerged zone were merged.

4.5.12 Stage 3 DEM Mosaiking

At the completion of Stage 2 the processing for each individual DEM is complete. However for the photogrammetric DEM to be of significant geomorphological use and to fit in with the aims of this project the individual DEMs needed to be mosaicked.

The mosaicking process was done using the mosaic function in ERDAS Imagine. Initial experiments in mosaicking photogrammetrically derived surfaces showed two problems with this simple process: 1) noticeable join lines between surfaces in the form of steps in elevation, 2) poor surface representation on one of the DEMs significantly reducing the quality of the mosaicked surface.

4.5.13 Analysis and correction of elevation steps

An example of one of the elevation steps associated with mosaicking is given in **Figure 4. 14**. The elevation steps are due to systematic inaccuracy in the surface elevation on one or both DEM surfaces. This is fundamentally a result of inaccuracy in the photogrammetric triangulation process (including inaccuracies in the data used within that process), which is responsible for determining the relations of ground control points with both images and thus determining the elevation of stereo-matched pixels.

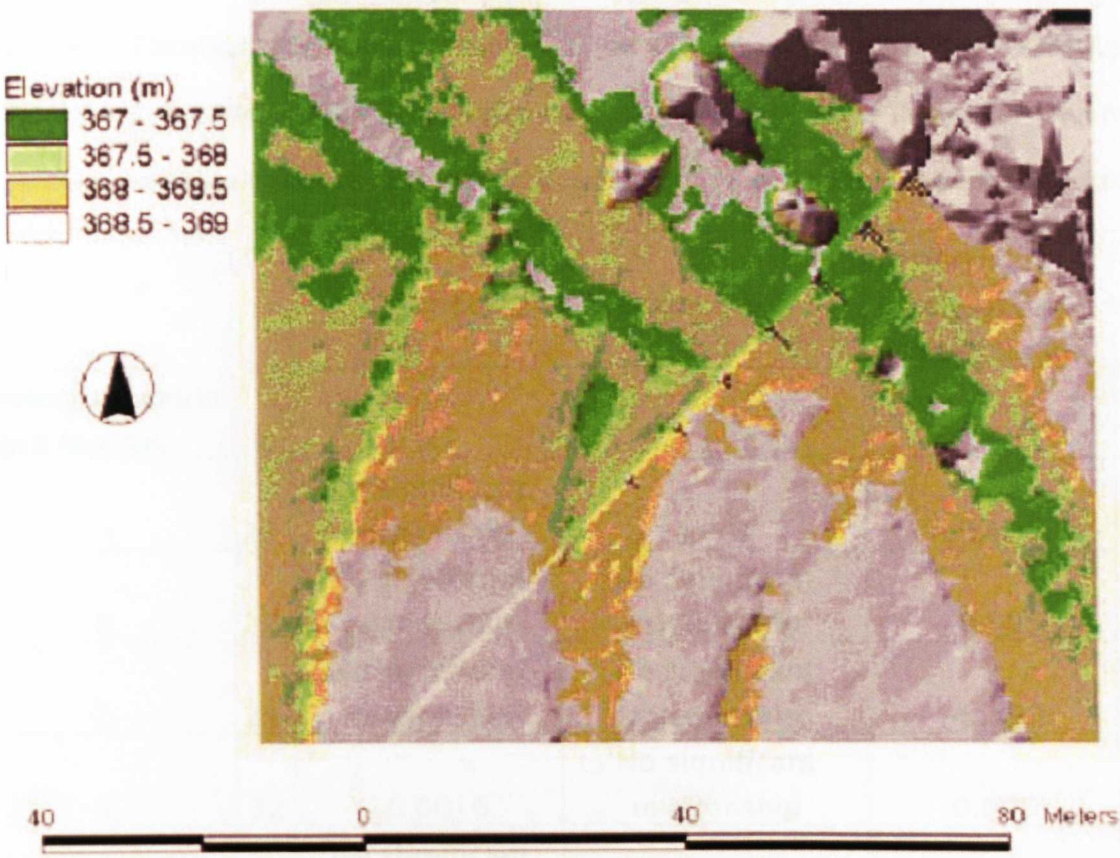

Figure 4.15. Elevation steps at the edge of DEM overlap areas

The extent of these systematic errors on each DEM surface were quantified using the GCP and Check data set 1, excluding points that were included in the final triangulation accepted for DEM generation. This is not an ideal data set for this task because the data are not fully independent. These were points discarded from the block formation process. However these data were the only ones of sufficient quality and with suitable spatial distribution available at the time of error quantification and modeling.

The error correction procedure developed corrects initially for DEM surface tilt and then for systematic error in elevation. Linear trend lines were fitted to the error values derived from Check data set 1. The quality of the derived relationship was tested by comparison of the R^2 value against a 95% (0.05) significance value. Significant relationships were applied to the data and the residual elevation correction value was calculated. The results of this process can be seen in **Table 4.6.**

		Surface tilt correction (m)		Residual elevation correction (m)
Photogrammetric Block Number	N	x	y	z
-1	26	No significant relationship	0.002	-0.007
0	27	No significant relationship	No significant relationship	-0.095
1	24	No significant relationship	No significant relationship	-0.199
2	32	-0.0016	No significant relationship	0.005
3	10	No significant relationship	0.0027	-0.001
4	16	0.0008	-0.0017	-0.001
5	17	No significant relationship	No significant relationship	0.083
6	10	0.0029	No significant relationship	0
All relationships applied were significant at the 95% confidence level.				

Table 4.6 Correction of systematic errors for individual DEM surfaces

Some of these errors are substantial in particular the 0.19m systematic elevation error in block number 1 (a result also confirmed by comparison with Experimental Reach 1) and the 0.0029m tilt in block 6, a tilt that equates to 0.29 metres over 100m. The origin of these errors is unlikely to be the result of the block triangulation process because **Table 4.2 (Section 5.6)** shows the block triangulation unit weight scores all approach unity and the GCP residuals all average at under 0.01m with standard deviations at 0.15m or below. The likely causes of these errors is the data inputted into the photogrammetric procedure in particular the poor quality GCPs. Due to logistical reasons the GCPs used in the photogrammetry were collected after the flights had successfully taken place and used features visible on the photographs, predominantly vegetation. This is far from optimal for three reasons: 1) the distribution of recognizable vegetation was not even, leaving some areas with few points. 2) the determination of exact points on the ground from the photographs was inaccurate in X and Y. 3) determining Z was inaccurate because of differing heights of vegetation and ambiguity as to which surface the photographs are 'seeing'.

4.5.14 Removal of poorly represented terrain in DEM overlap areas

Close examination of DEM surfaces before mosaicking showed that terrain representation was rarely equal between surfaces because the number and distribution of stereo matched points varies between DEMs. This means that mosaicking of these surfaces will result in reduction of overall data quality because well defined areas and interpolated areas are averaged during the mosaicking process. This is unacceptable given that one of the aims of the post processing is to increase or in this case maintain data quality.

The disparity in data quality between DEM surfaces is best examined through the use of the .stat files, which show all matched points (**Figure 3.16**). The upstream DEM (**Figure 3.16a**) has a low point density in the overlap zone but the same terrain covered by the downstream DEM (**Figure 16b**) has a greater point density making it a better representation of the surface being measured.

To correct this problem and optimize terrain quality the following procedure was used:

1) Point density was calculated using a 10m filter for all zones.

2) All 10m filter areas with less than 20 matched points were marked for each DEM

3) For any given overlap zone the terrain surface with the least marked DEM was accepted in its entirety and mosaicked with the other DEM with marked areas filtered out.

This process has the advantage of ensuring that the whole overlap zone includes elevation values whilst filtering out the terrain that is most interpolated. Filtering out of all terrain on the grounds of point density would have been insufficient because flat bar top areas are typically poorly matched but this does not represent a problem because only low point densities are necessary to represent flat terrain.

Following application of both correction methods the DEMs were mosaicked using the feathering mosaicking function in Erdas Imagine.

4.5.15 Stage 4 Final Correction surface

By the end of stage three each individual DEM had been fully corrected and all constituent parts had been joined to form a reach scale DEM. However a comparison of the DEM with a larger quantity of checkpoint data showed that large systematic errors were still present. These errors were not too excessive to inhibit basic geomorphological enquiry but large enough to inhibit more sophisticated analysis such as sediment budgeting. Testing of a final correction surface showed significant improvements in elevation. This surface was developed using 50% of Check Data set 2 and applied to the mosaicked DEM.

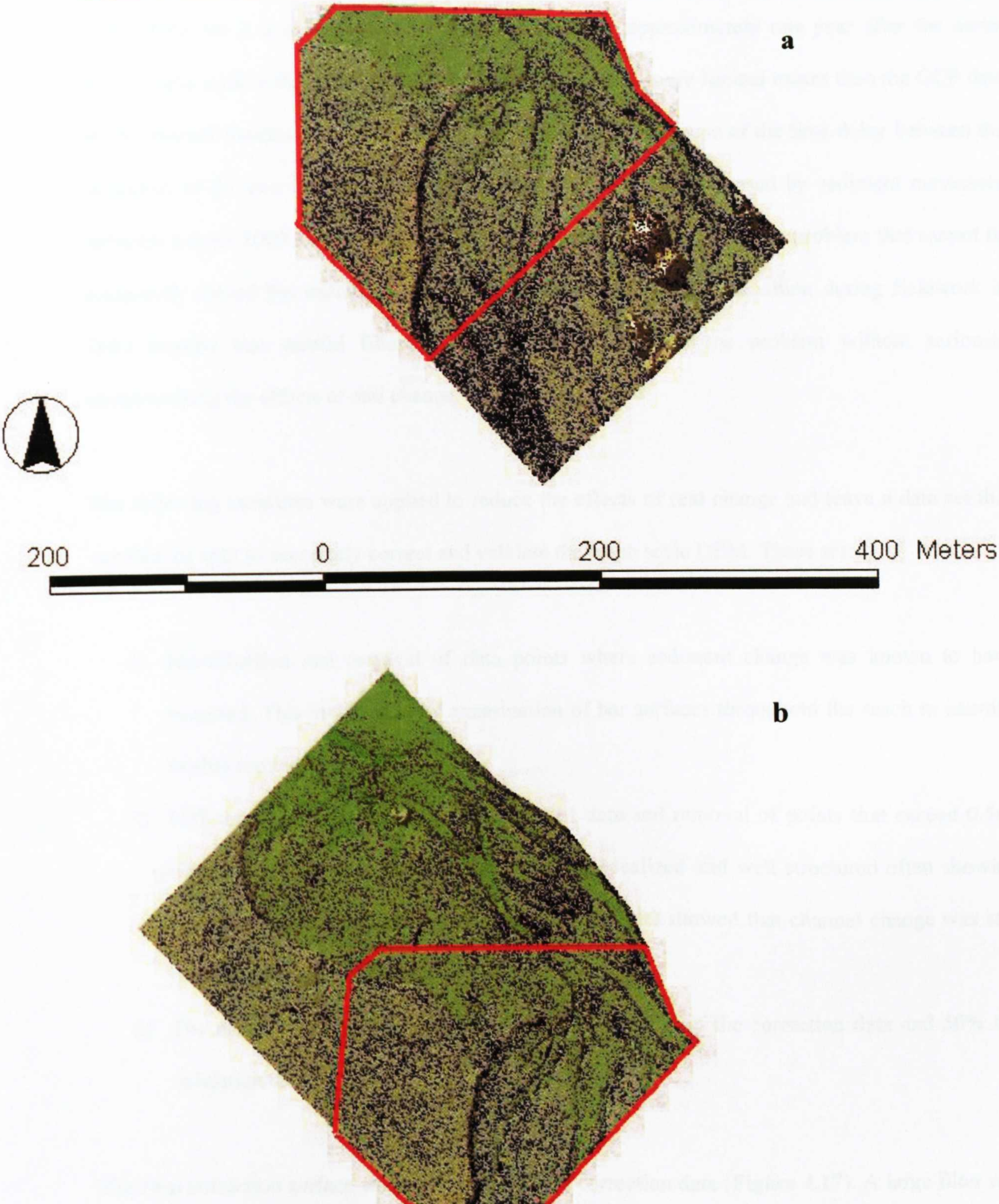

Figure 3.16. Density and distribution of matched points

Check Data set 2 is a large data set collected in 2001, approximately one year after the aerial photographs used in the photogrammetry. The data set has a more limited extent than the GCP data set but instead focuses 7515 points in the active floodplain. Because of the time delay between the collection of the two data sets there is a danger that real change caused by sediment movement between August 2000 and June 2001 could be attributed as error. This is a problem that cannot be completely solved but examination of bars, zones of erosion and deposition during fieldwork in 2002 implied that careful filtering of data could minimize the problem without seriously compromising the effects of real change.

The following measures were applied to reduce the effects of real change and leave a data set that can then be split to accurately correct and validate the reach scale DEM. These are:

1) Identification and removal of data points where sediment change was known to have occurred. This involved close examination of bar surfaces throughout the reach to identify freshly moved material.
2) Differencing of checkpoint data with DEM data and removal of points that exceed 0.5m. Changes of this magnitude tend to be highly localized and well structured often showing channel change. Examination of these areas in 2002 showed that channel change was still occurring at many of the sites.
3) The data set was split with 50% of the data making up the correction data and 50% the validation data.

The final correction surface was modeled using the correction data (**Figure 4.17**). A large filter was used in the modeling of the correction surface to ensure that systematic error was well represented. Each cell on the correction surface averaged all cells within a search radius of 30m. This large filter size was very important for three reasons; it ensured that one error measurement or a small cluster of measurements could not dominate the cell error values. It also ensured that random error was well smoothed. Finally it ensured that real changes that had not been filtered out by previous treatments of the data set were smoothed over an area considerably larger than the spatial extent of the changes themselves.

The complete photogrammetric DEM is shown in **Figure 4.18**

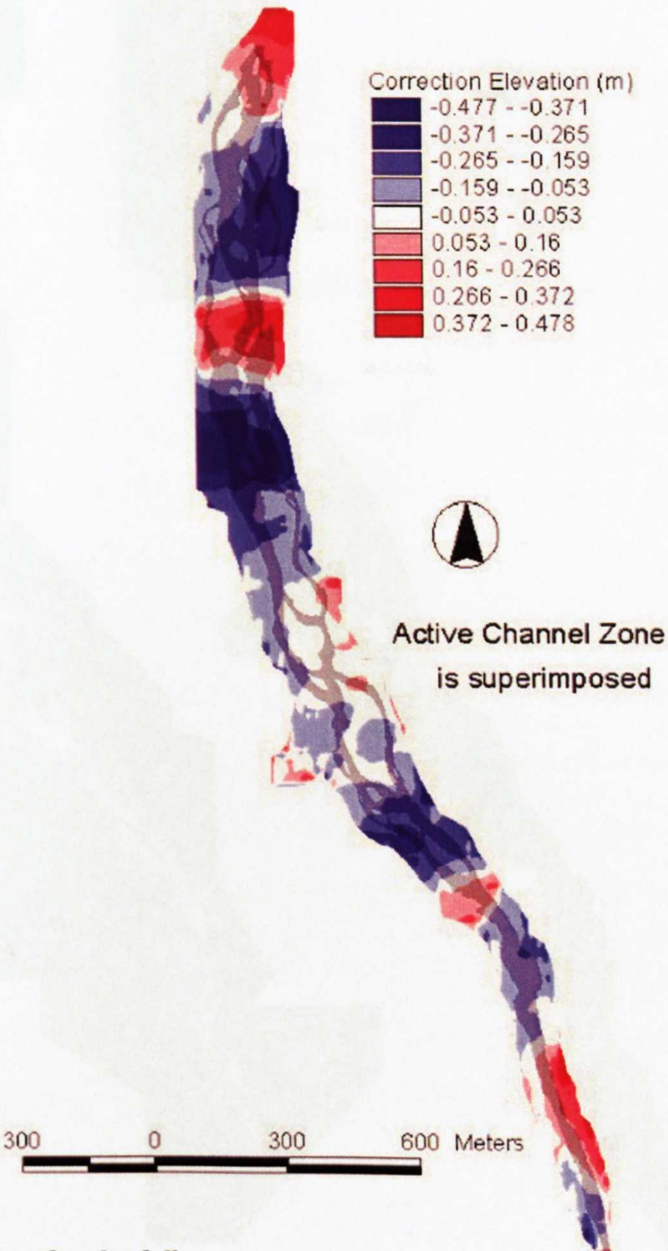

Figure 4. 17. Correction surface for the full photogrammetric DEM

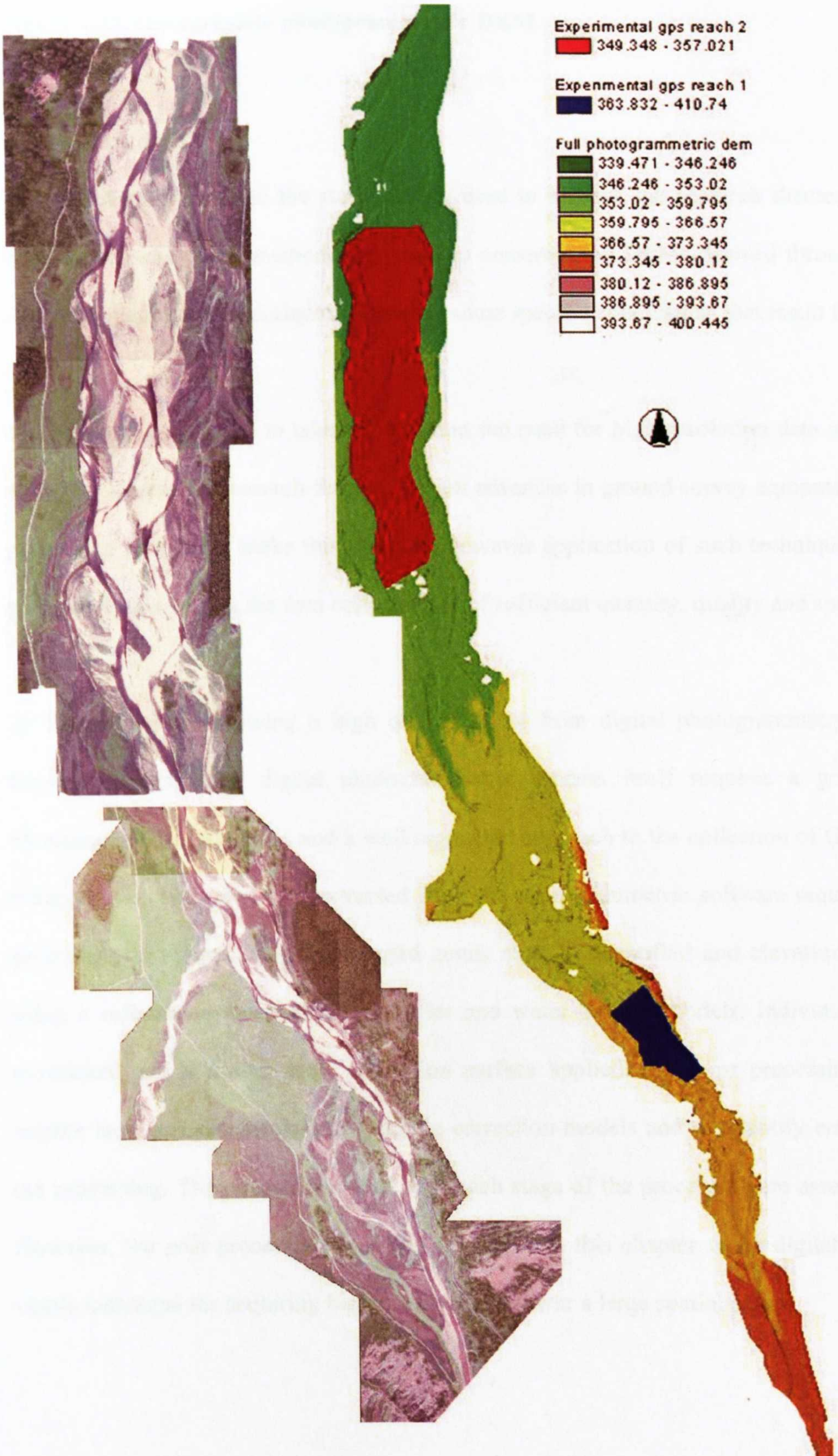
Experimental gps reach 2
349.348 - 357.021
Expenmental gps reach 1
363.832 - 410.74
Full photogrammetric dem
339.471 - 346.246
346.246 - 353.02
353.02 - 359.795
359.795 - 366.57
366.57 - 373.345
373.345 - 380.12
380.12 - 386.895
386.895 - 393.67
393.67 - 400.445

Figure 4.18.The complete photogrammetric DEM

4.6.0 Conclusions

This chapter has outlined the study design used to address the research themes and has given a detailed account of the methodology used to construct the DEMs derived through ground survey and photogrammetric techniques. There are some specific conclusions that result from this chapter.

1) The study design had to take into account the need for high resolution data over a large spatial extent to address the research themes. Recent advances in ground survey equipment and digital data processing techniques make this possible, however application of such techniques requires careful planning to ensure that the data collected are of sufficient quantity, quality and spatial distribution.

2) The process of deriving a high quality DEM from digital photogrammetry is not a straight forward process. The digital photogrammetric process itself requires a good knowledge of photogrammetric principles and a well organized approach to the collection of GCP data and block triangulation. The raw DEM extracted from the photogrammetric software requires extensive post processing to reduce error. Submerged zones must be identified and elevation values re-defined using a reflectance based depth classifier and water surface models. Individual DEMs must be mosaicked and a further error correction surface applied. The post processing procedures also require large amounts of data to generate correction models and to quantify error at each stage of the processing. The errors associated with each stage of the processing are assessed in **Chapter 5**. However, the post processing solutions presented in this chapter make digital photogrammetry a viable technique for acquiring high quality DEMs over a large spatial extent.

3) The development of a reflectance based sub-aqueous depth classifier was inhibited by the quantity and spatial distribution of data. The derived relationship between DN and water depth poorly described water depths in many of the orthophotographs with estimated ME of up to 0.1m.

CHAPTER 5. DEM QUALITY RESULTS AND ANALYSIS TECHNIQUES

Abstract

Initially, this chapter defines the overall quality of DEMs derived using GPS and remote sensing survey techniques. A high resolution GPS derived DEM (Experimental Reach 1) is shown to be of very high quality using standard measures of DEM quality: Mean Error (ME), Standard Deviation of Error (SDE) and Root Mean Square Error (RMSE) **(Section 5.2)**. This surface is then used as a 'true surface' with which to test improvements to the quality of a photogrammetric surface resulting from the post processing procedures described in **Chapter 4 (Section 5.3)**. The grid-to-grid analysis allows a full statistical description of error along with more qualitative descriptions of the spatial structure of error. The detailed analysis of the grid-to-grid approach is supported by the results of a spatially extensive survey point comparison. The last DEM quality statistics to be defined are for a low resolution GPS derived DEM (Experimental Reach 2) **(Section 5.4)**. These statistical indicators of DEM quality are used in the second half of the chapter, which aims to assess if the DEMs can reliably be used to derive geomorphologically significant variables. The Level of Detection (LOD) thresholds for each DEM are defined to show their value in describing sediment movement **(Section 5.7)**. Finally, the Mean Bed Level (MBL) of the photogrammetrically derived DEM is compared with the MBL of the high resolution GPS derived DEM to show if fluctuations in MBL can be reliably identified **(Section 5.8)**.

5.1.0. Introduction: DEM Quality

The focus on data quality that has been emphasised in previous chapters is continued here. Accurate assessments of data quality are the key to effectively addressing the research themes. The first research theme in particular is addressed in this chapter. The theoretical characteristics of data acquisition techniques used for deriving DEMs were discussed in **Chapter 3**, these were incorporated into a study design in **Chapter 4**. This chapter aims to assess the quality of the resultant DEMs initially through conventional measures of DEM quality but then also the effects of these errors on specific geomorphologically significant morphometrics. Conventional measures of photogrammetric quality are described in **Chapter 3 Section 2**, these are ME (a measure of accuracy) SDE (a measure of precision) and RMSE. A combination of ME and SDE is considered a more reliable indictor of DEM quality than RMSE because this fails to measure systematic error effectively (Lane, 2000). The conventional method for deriving these statistics is to compare the modelled surface with a number of surveyed points. However much of the analysis in the chapter will compare the modelled surface against a 'true surface' defined using higher quality survey points. Using a true surface in this manner gives several advantages over comparing survey points against a modelled surface. Every part of the modelled surface is compared against every part of the 'true surface' so all parts of the surface are equally well represented in the error statistics. When survey points are compared against the modelled surface inconsistencies in the survey point distribution mean some areas of terrain are over-represented in the analysis. The 'true surface' also allows the comparison of derived variables such as slope and volumetric comparisons.

The quality of 3 DEMs will be defined (**Figure 5.1**). These are: Experimental Reach 1: A high resolution GPS derived DEM of limited spatial extent (300m × 60m), the Full Photogrammetric DEM: a photogrammetrically derived DEM of the entire braided river system (3000m × 1000m) and Experimental Reach 2: a low resolution GPS derived DEM covering a larger spatial extent than Experimental Reach 1 (800m× 100m). These are the 3 DEM's that will be used in subsequent analysis in later chapters of this thesis.

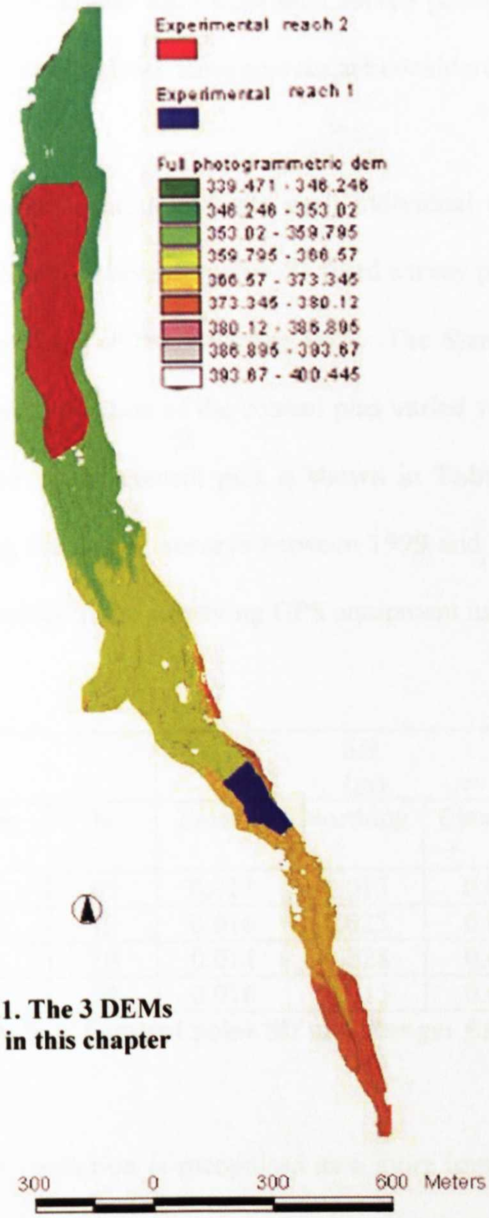

Figure 5.1. The 3 DEMs analysed in this chapter

5.2.0 Defining the overall quality of a high resolution GPS derived DEM.

Experimental Reach 1 **(Figure 5.1)** was surveyed annually from 1998-2000 using high resolution ground survey, predominantly GPS although a limited number of points were surveyed using EDM in deep water areas and close to the valley wall. A full description of the two surveys undertaken between 1998 and 1999 can be found in Brasington *et al.* (1999). This section highlights the more important aspects of the surveys and defines their quality using independent data.

The ground survey data, like any measured data, incorporate error. This results from the finite number of points used to construct the DEM surface, the point resolution, and error in x, y and z incorporated into each individual survey point through the inaccuracies and imprecision of the survey device. Both these sources are considered briefly here.

The error incorporated into each individual survey point was assessed using a control grid consisting of surveying pins. 21 fixed survey points were surveyed 19 times in 1998 to establish the precision of the surveying GPS. The Standard Deviation (SD) and Maximum range of the measured position of the control pins varied very little between points. The results of re-survey of four of the control pins is shown in **Table 5. 1.** Re-survey of the same control network during the annual surveys between 1999 and 2002, showed similar results. This demonstrates the quality of the surveying GPS equipment used in the ground survey.

		SD (m)				Maximum Range (m)		
Point	N	Easting	Northing	Elevation		Easting	Northing	Elevation
1	19	0.017	0.015	0.026		0.068	0.086	0.075
11	19	0.016	0.023	0.031		0.050	0.075	0.1
12	19	0.014	0.028	0.028		0.050	0.092	0.102
21	19	0.016	0.015	0.027		0.059	0.086	0.097

Table 5. 1. Control point SD and Range: Experimental Reach 1

Point resolution is recognised as a more important control on DEM quality (Brasington *et al.*, 1999). Point resolution controls how well roughness elements of different sizes are represented by the derived DEM. The effect of point resolution on DEM representation of morphology was investigated in a series of numerical experiments by Brasington *et al.* (1999). The Experimental Reach 1 data from 1999 were thinned progressively, randomly removing 10% of the survey points and the quality of the DEMs was assessed in two ways. The DEM representation of detail was assessed by comparing the surface area of the DEM with the 2-dimensional planimetric area (**Figure 5.2**). This shows that the SA:PA ratio increases rapidly for point densities between 0.1 and 0.3 pts/m^2. It levels off between 0.3 and 0.75 pts/m^2 and then rises again between 0.75 and 1.2pts/m^2. Brasington *et al.* (1999) urges caution when pursuing a physical explanation for the break of slope at approximately 0.3 pts/m^2 although it is suggested that this reflects the boundary between micro and macro scale roughness units.

The second experiment examined the errors incorporated into DEMs due to the elimination of survey points. The thinned DEMs were differenced from the original high-resolution DEM surface and the change in information content was assessed by volumetric change per unit area (**Figure 5.3**). There is a rapid increase in information as point density increases from 0.1pts/m^2 to 0.3 pts/m^2, there is also an imbalance as cut exceeds fill. The rate of information gain between 0.3 and 1 pts/m^2 continues to increase systematically at a lower rate. These results are consistent with the first experiment by Brasington *et al.* (1999). The break in slope at 0.3pts/m^2 is interpreted as the result of loss of micro-scale information. Both these experiments demonstrate the need to match the information content of the survey with the fundamental length scales of the subject. The content of both experiments is of direct relevance to the quality of both the ground survey derived DEMs used in this project because Brasington *et al.* (1999) was based on Experimental Reach 1.

The three surveys of Experimental Reach 1 between 1998 and 2000 (**Table 5.2**) show a high overall point density of between 0.69pts/m^2 and 1.42 points/m^2. The mean moving window density is a different approach for deriving a measure of point density. It shows similar results to the overall density statistic.

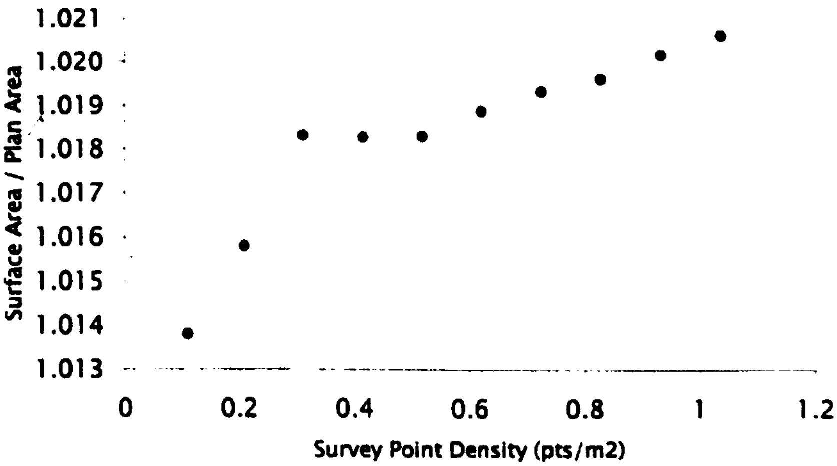

Figure 5.2 The effect of point density on representations of morphology measured using the ratio of surface area to plan area. Taken from Brasington *et al.*, 1999.

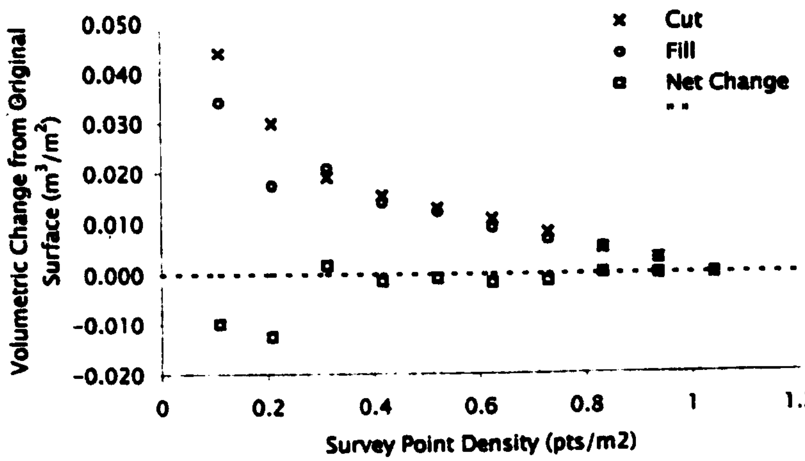

Figure 5.3. The effect of point density on volumetric change. Taken from Brasington *et al.*, 1999.

Survey	Survey area(m^2)	Overall Density (pts/m^2)	Mean Moving Window Density (pts/m^2)
1998	13,401	0.69	0.64
1999	13,401	1.10	0.98
2000	22,836	1.42	1.35

[1] Overall density = ∑pts/area

[2] Moving window densities calculated for a moving 3m radius circular window

Table 5.2 Survey point density: Experimental Reach 1

The high quality and high density of survey points suggests that the DEMs derived from the 1998-2000 surveys of Experimental Reach 1 (**Figure 5.4**) will be of very high quality when compared to independent check data. **Table 5.3** shows that conventional statistics of DEM quality, derived by comparison of the 2000 DEM of Experimental Reach 1 with independent GPS check data, are encouraging. ME (a measure of accuracy) is below 0.02m in both submerged and exposed areas of the DEM. SDE (a measure of precision) is below 0.05m for both submerged and exposed areas of the DEM. The difference between the submerged and exposed zone can be accounted for by the lower point resolution in the submerged zone. The accuracy and precision of the 2000 DEM suggest that it is a very good representation of the morphology of Experimental Reach 1.

	n	ME (m)	SDE (m)	RMSE (m)
Submerged topography	127	0.019	0.049	0.052
Exposed topography	312	-0.008	0.021	0.023

Table 5.3 Conventional statistics of DEM quality: Experimental Reach 1, 2000

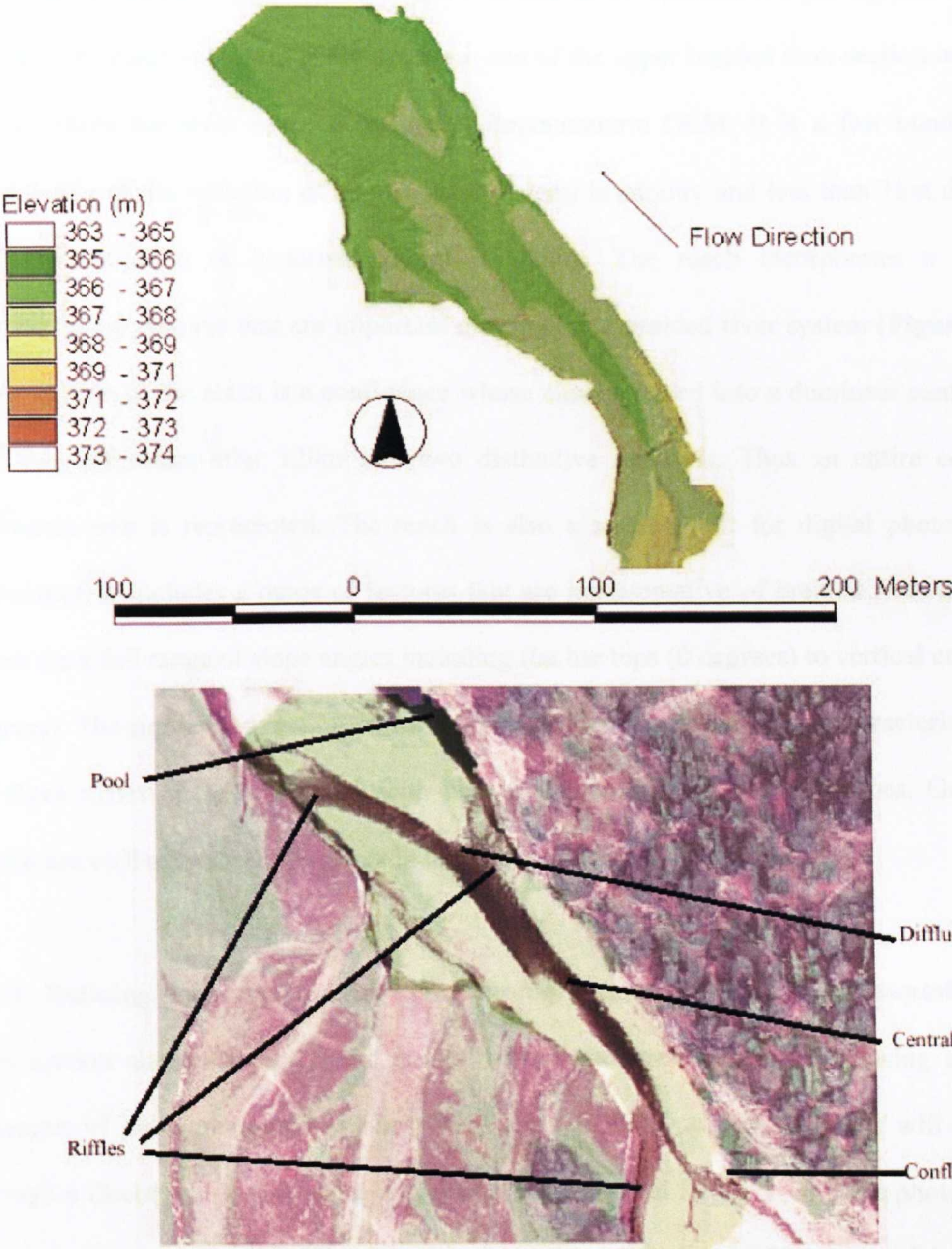

Figure 5.4 DEM and Orthophoto of Experimental Reach 1

5.2.1 The Experimental Reach 1 DEM as a 'true surface'

The errors in the Experimental Reach 1 surface are very small which suggests that it could be used as a suitable indicator of surface quality for less precise survey methods such as digital photogrammetry. If it is assumed that the GPS derived surface is a 'true surface' then it can be compared with a photogrammetrically derived surface to give a very detailed quantitive description of the errors within the photogrammetric survey. The location and morphology of

Experimental Reach 1 also make it a good choice as an indicator of photogrammetric DEM quality. The reach is located at the upstream end of the upper braided river section on the River Feshie within the areas covered by the photogrammetric DEM. It is a few hundred metres downstream of the initiation of contemporary lateral instability and less than 1km downstream from the initiation of historical lateral instability. The reach incorporates a number of morphological features that are important elements in a braided river system (**Figure 5.4**). The upper section of the reach is a confluence whose channels feed into a dominant central channel that then bifurcates after 120m into two distinctive channels. Thus an entire confluence - diffluence unit is represented. The reach is also a suitable test for digital photogrammetric techniques. It includes a range of features that are representative of braided river morphology. There are a full range of slope angles including flat bar tops (0 degrees) to vertical cut banks (90 degrees). The submerged sections show a broad range of depths and flow characteristics. There are three riffles in the reach each with different water surface and bed slopes. Greater water depths are well represented by pools in the lower right hand channel (>2m)

5.3.0. Defining the overall quality of the photogrammetric DEM: Experimental Reach 1

This section aims to establish the quality of the photogrammetric DEM using conventional measures of photogrammetric quality, these are ME, SDE and RMSE. This will be achieved through a direct grid-to-grid comparison of a Experimental Reach 1 with the photogrammetric DEM. Grid to grid differencing means each grid cell value within the grid is differenced (removed from) the corresponding grid cell in a second grid. This analysis is similar to the grid–to-grid comparison used by Brasington *et al* (2003) except a breakdown of DEM quality at every stage of post processing will be provided here so that the quality of the post processing procedures described in **Chapter 4** can be demonstrated. The grid-to-grid comparison is an unconventional approach for deriving statistics. The conventional approach would be to directly compare the surveyed points with the photogrammetric DEM. The grid to grid comparison was used because it ensures that every part of the DEM is equally represented in the error statistics despite localised differences in point resolution and it highlights discrepancies in x and y in the photogrammetric block triangulation model. The grid to grid comparison was carried out using Arcview GIS

The grid comparison was conducted with a clipped version of Experimental Reach 1 (a spatial reduction). The reduction was necessary because Experimental Reach 1 was not covered by a single, unmosaicked, photogrammetric DEM. Even with this reduced grid extent the comparison still provided a very large statistical sample (200,000+) of observations. The grid-to-grid method has the added advantage of offering excellent visualisation of errors (**Figure 5. 6**). The errors that can be seen in **Figure 5. 6** are residual errors that could not be eliminated by the DEM post processing procedures described in detail in **Chapter 4**. The effectiveness of these procedures can be seen in **Figure 5. 5**.

Figure 5.5 shows that the errors associated with the raw DEM (**Stage 1**) are of the same magnitude as those described by comparative studies. Westaway (2001) had research objectives specifically focused on the acquisition of braided river morphology using digital photogrammetry. The errors in the raw DEMs derived by Westaway (2001)(Dry ME= 0.225m-0.105m Wet ME 0.794m-0.342m, Dry SDE 0.228m-0.124m, Wet SDE 0.707m-0.282m) are comparable with the raw DEM errors shown in **Figure 5.5**. These errors are considerably greater than the maximum theoretical precision of the survey, which is defined by the object space pixel resolution (**Equation 3.5**). There are a number of factors that explain the discrepancy between theoretical and actual error associated with the raw DEM. The GPS and EDM equipment used to generate the 'true surface' and measure the location of GCPs incorporates a different set of errors (described in **Chapter 3** and in **Section 5.2.0** above) that affect the triangulation of the photogrammetric block and the assessment of error. The necessity of using natural features as GCPs is likely to have increased error. During the photogrammetric process manual identification of the GCP on the digital imagery is required. The natural features used for GCPs made this process more difficult leading to increased error in x, y and z. This effect was compensated for by increasing the number of GCPs gathered, producing redundancy in the photogrammetric process however the final effect on the quality of the photogrammetric triangulation model cannot be quantified.

After re-interpolation **(Stage 2)** the Photogrammetric DEM has improved little. This process was conducted for correctness, to ensure that both the GPS DEM and photogrammetric DEM were interpolated using the same algorithm (TIN). The re-interpolation has resulted in minor improvements in all three parameters.

The subaqueous zone processing **(Stage 3)** only affected the submerged areas of the DEM. The elevation of the subaqueous points is reduced substantially by the processing procedure resulting in a change in the wet ME from 0.117m to –0.368m. This means the submerged elevation values change from being too high to being too low. The change is the result of the application of a reflectance based depth classifier (discussed in **Chapter 4 Section 5.9**). This underestimation of submerged elevation appears initially to increase error but it brings the ME of the submerged part of the DEM closer to that of the dry areas (-0.175m) allowing systematic correction of the entire surface in the next processing stage. The SDE of the subaqueous zone is substantially reduced by the processing due to the increased uniformity of water depths derived by the subaqueous classifier.

The nature of the systematic error correction procedure **(Stage 4)** means that each DEM extracted from Orthomax is corrected by different amounts for surface tilts and systematic error. The photogrammetric DEM covering Experimental Reach 1 was analysed according to the procedure in **Chapter 4 Section 5.12**. No statistically significant tilt was found but the analysis showed that the DEM was systematically too low. The addition of 0.198m to the elevation of the photogrammetric DEM substantially reduced ME and RMSE.

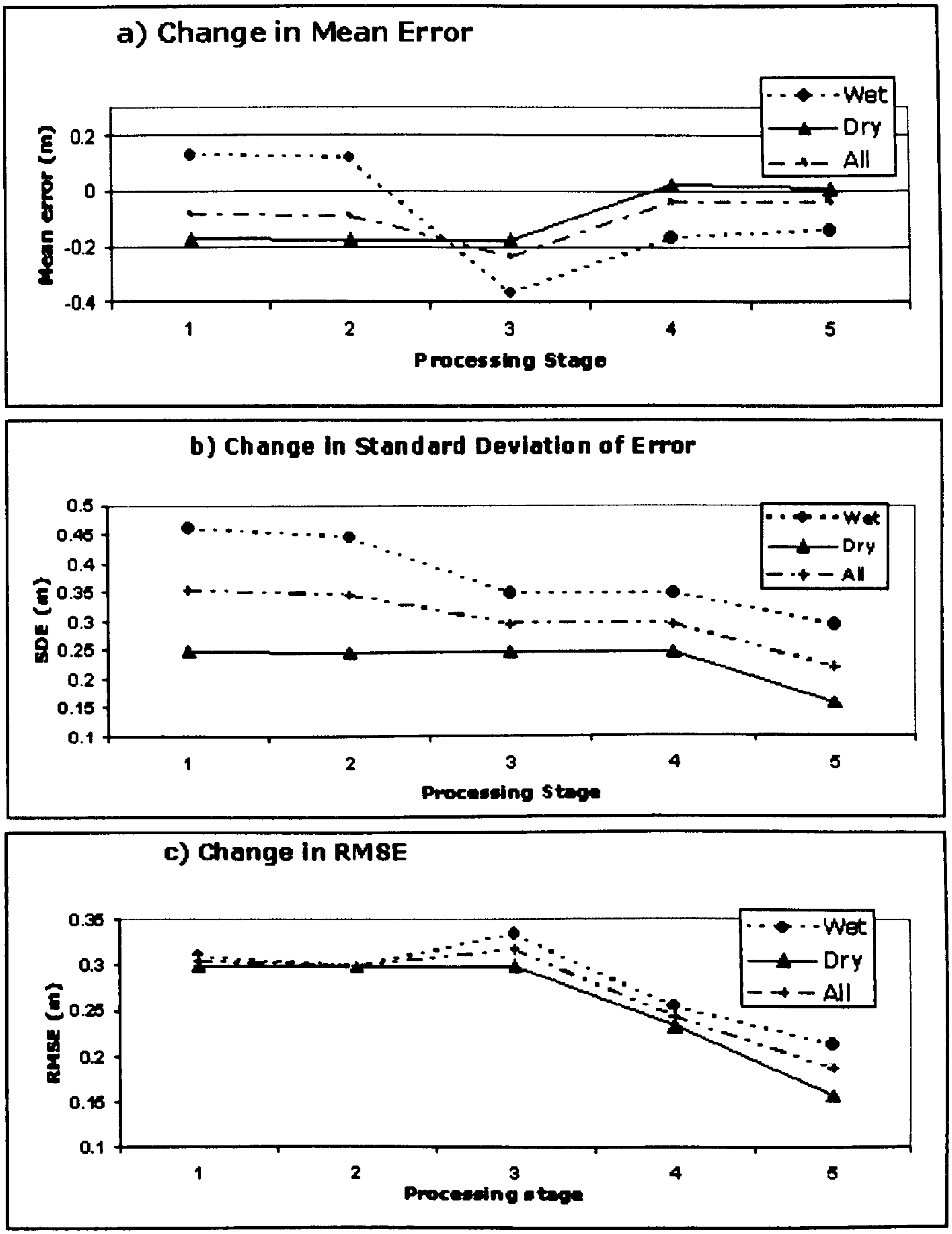

Number	Description	Corresponding processing stage number (Chapter 4 Figure 4.6)
1	Raw DEM extracted from Orthomax	1
2	After Re-interpolation using TIN	2
3	After Subaqueous zone processing	2
4	After Systematic error correction	3
5	After application of error correction surface The complete DEM	4

Figure 5. 5. Changes in DEM quality statistics due to post-processing procedures.

The application of the final correction surface (**Stage 5 Chapter 5 Section 5.14**) resulted in substantial reductions to SDE (0.294m – 0.219m) and RMSE (0.244m – 0.188m). ME was also marginally reduced. The combined effects of the post processing procedures were to reduce ME from –0.083m to –0.036, SDE from 0.354m to 0.219m and RMSE from 0.304m to 0.187m. These represent important improvements to the quality of the DEM that greatly increase its value. They compare well with the only analogous previous research (Westaway 2001) where SDE of 0.26m (exposed) and 0.32m (submerged) were reported. Westaway (2001) employed many similar correction techniques including a depth classifier mosaicking and a final correction surface. Westaway (2001) also employed a method for automatically finding photogrammetric pixel matching blunders, which could then be removed improving precision by reducing SDE. The method involved reducing the resolution of the DEM surface and comparing this with the high resolution surface. Points that exceeded a given elevation difference were removed, the threshold value was set at 1m.

The errors that remain are well represented visually by the grid-to-grid differencing approach (**Figure 5.6**). This visualisation shows the extra value of the grid-to-grid comparative approach over more conventional approaches involving low-resolution spatially extensive data sets. The spatial distribution of error can be analysed qualitatively to show weaknesses in the digital photogrammetric system and post processing procedures.

Negative errors (blue) show photogrammetrically derived elevations below those of the GPS derived elevations. The most visually striking errors are those of the submerged zone topography. The main channel is predominantly underestimated except in the deep pool (**Figure 5.6**) where elevations are overestimated. These errors predominantly reflect the limitations of the depth classifier (**Chapter 4 Section 5.7**), which is not effective at representing water depth above 0.8m The inadequacies of the method for determining the water surface are illustrated by Riffle A, a steeply sloping riffle at right angles to the main channel. The 5m×5m minimum, smoothing filter (**Section 4.5.9**), artificially lowers elevations at the top of the riffle producing a negative elevation error. The filter has this effect because it replaces the value at the water's edge with the lowest value within a 5m×5m area. The lowered elevations are then interpolated to derive the water surface. Removal of the water depth from the interpolated water surface means the resultant bed elevations are too low. This effect can also be seen at Riffle B.

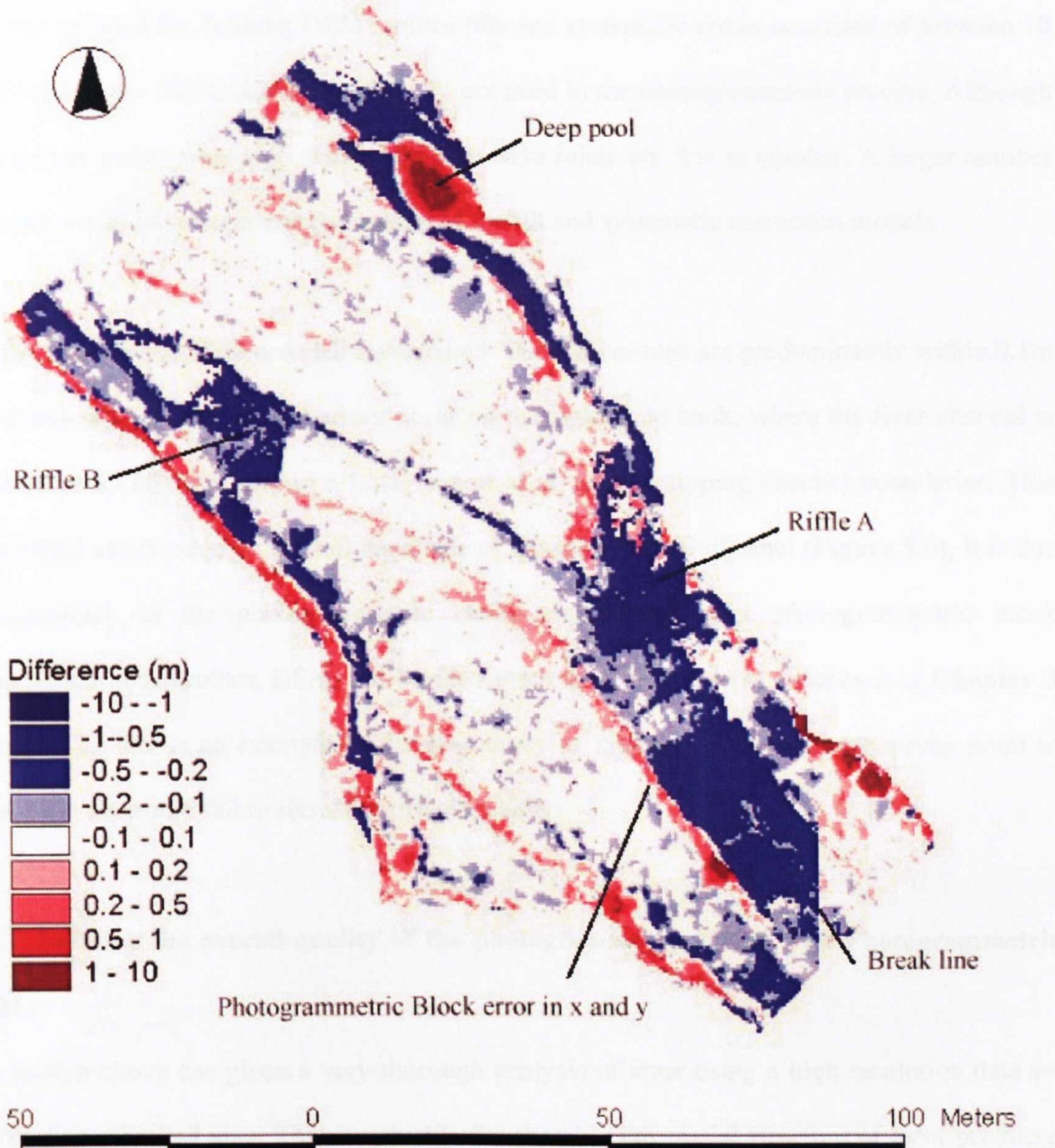

Figure 5. 6 Errors remaining in the photogrammetric DEM after post-processing shown by a DEM of difference (Photogrammetrically derived DEM – GPS derived DEM). Blue values represent areas where the photogrammetrically derived DEM is lower than the GPS derived DEM.

The distinctive break line in the lower right of **Figure 5. 6** is a result of the mosaicking process where an upstream photogrammetric DEM intersects with the downstream photogrammetric

DEM. Although a feathering function is used in the mosaicking process this is not always sufficient to remove all discontinuities from the DEM. In this case the discontinuity is visible on the photogrammetric DEM itself (**Figure 5.4**). This and other discontinuities represent the partial failure of the systematic error and tilt correction part of the post processing (**Chapter 4 Section 5.12**). This is due to the limited size of the data set that was available for this process. The data set used for defining DEM surface tilts and systematic errors consisted of between 10 and 27 points per DEM, consisting of GCPs not used in the photogrammetric process. Although these survey points were well distributed they were relatively few in number. A larger number of points would have improved the quality of the tilt and systematic correction models.

The dry areas of the DEM are well represented. The flat bar tops are predominantly within 0.1m of the true surface. The largest errors occur on the right hand bank, where the river channel is constrained by bedrock, and to a lesser extent at all steeply sloping channel boundaries. This latter effect can be seen on the left hand side of the main central channel (**Figure 5.6**), it is due to inaccuracy in the photogrammetric block triangulation. The photogrammetric block triangulation and resultant DEM can be inaccurate in x, y and z (as described in **Chapter 3 Section 3.2**), this is an example of the inaccuracy in x and y. Conventional survey point to DEM analysis would fail to show this effect visually.

5.3.1. Defining the overall quality of the photogrammetric DEM: Full Photogrammetric DEM

The section above has given a very thorough analysis of error using a high-resolution data set confined to a limited area. This is valuable for showing the spatial structure of error produced by digital photogrammetry and post processing but it does not show the quality of the entire photogrammetric DEM. The Experimental Reach 1 analysis is based almost exclusively on a single photogrammetrically derived DEM based on a single photogrammetric block triangulation (the exception being Stage 5 which involves the mosaicking of two DEM surfaces). This spatially limited sample means the results (particularly ME) cannot be taken as an indication of DEM quality for the entire photogrammetric DEM. In order to establish error for the entire photogrammetric DEM a second approach was used. The Full Photogrammetric DEM was compared with a sample of survey points taken from Check data set 2 using a conventional differencing survey point to grid approach. **(Table5.4).** Check data set 2 consists of 7515 survey points derived from GPS survey in 2001.

	n	ME (m)	SDE(m)	RMSE(m)
Full Photogrammetric DEM	1186	-0.006	0.163	0.163
GPS Reach 1 (dry)	<200,000	0.010	0.157	0.157

Table 5.4 DEM quality statistics for the Full Photogrammetric DEM (check points – photogrammetric DEM) and the equivalent statistics for Experimental Reach 1. The value n is the number of values used in the calculation.

The statistics for the entire photogrammetric DEM show that it is of comparable quality to the section assessed in detail using Experimental Reach 1. Two factors need to be considered when assessing the differences between the spatially limited, Experimental Reach 1 approach and the lower resolution assessment of the Full Photogrammetric DEM. Firstly the ground survey data used comparatively with the Full Photogrammetric DEM were collected a year later (2001) than the photographs used for constructing the model (2000). These data points were closely scrutinised at the time of collection to ensure that real channel changes occurring in the intervening year had minimal impact. In practice this meant survey of the more stable elevated channels and bar surfaces. The analysis using Experimental Reach 1 **(Figure 5.6)** shows that these bar top areas have the lowest errors and this means that the error statistics in **Table 5.4** are likely to marginally underestimate error. Second; the points collected for comparison with the Full Photogrammetric DEM (Check data set 2) are all dry points. The comparison of values given in **Table 5.4** gives the equivalent dry points for Experimental Reach 1.

Examination of the spatial structure of error **(Figure 5.7)** is also encouraging. The majority of errors are localised affecting just single points suggesting that these are the result of random error or photogrammetric pixel matching blunders rather than systematic errors. This demonstrates the effectiveness of the post processing procedures developed in **Chapter 4.**

Figure 5.4 also raises a further issue about the quality of the checkpoint data set. Given that the photogrammetric DEM covers a large area (1877007 cells over 469251.5m^2) the check data set is not very large (1186 points). The small number of points is compounded by their poor spatial distribution, which is characterised by clustering on stable bar top and bank line features. This means that errors in the DEM surface are differentially represented based on the proximity of check points and this could lead to mis-representation of error in **Table 5. 4**. Areas with a lower point density are less well represented than areas with a higher point density. This problem does not occur with the grid-to-grid system used for Experimental Reach 1 because areas with a lower point density are as equally well represented as areas with a higher point density but the influence of interpolation is increased.

5.4.0 Defining the error of Experimental Reach 2

This chapter has so far defined the quality of two DEMs. A high resolution GPS derived DEM described in Brasington *et al.* (1999) and a spatially extensive high resolution photogrammetrically derived DEM. One final DEM needs to be defined before the 'fit for purpose' analysis of **Sections 5.6-5.8** can take place. Experimental Reach 2 is a GPS derived DEM but with a lower resolution than Experimental Reach 1 **(Figure 5.8).** It was surveyed to provide high quality data to address the dynamic scaling properties within research theme 3.

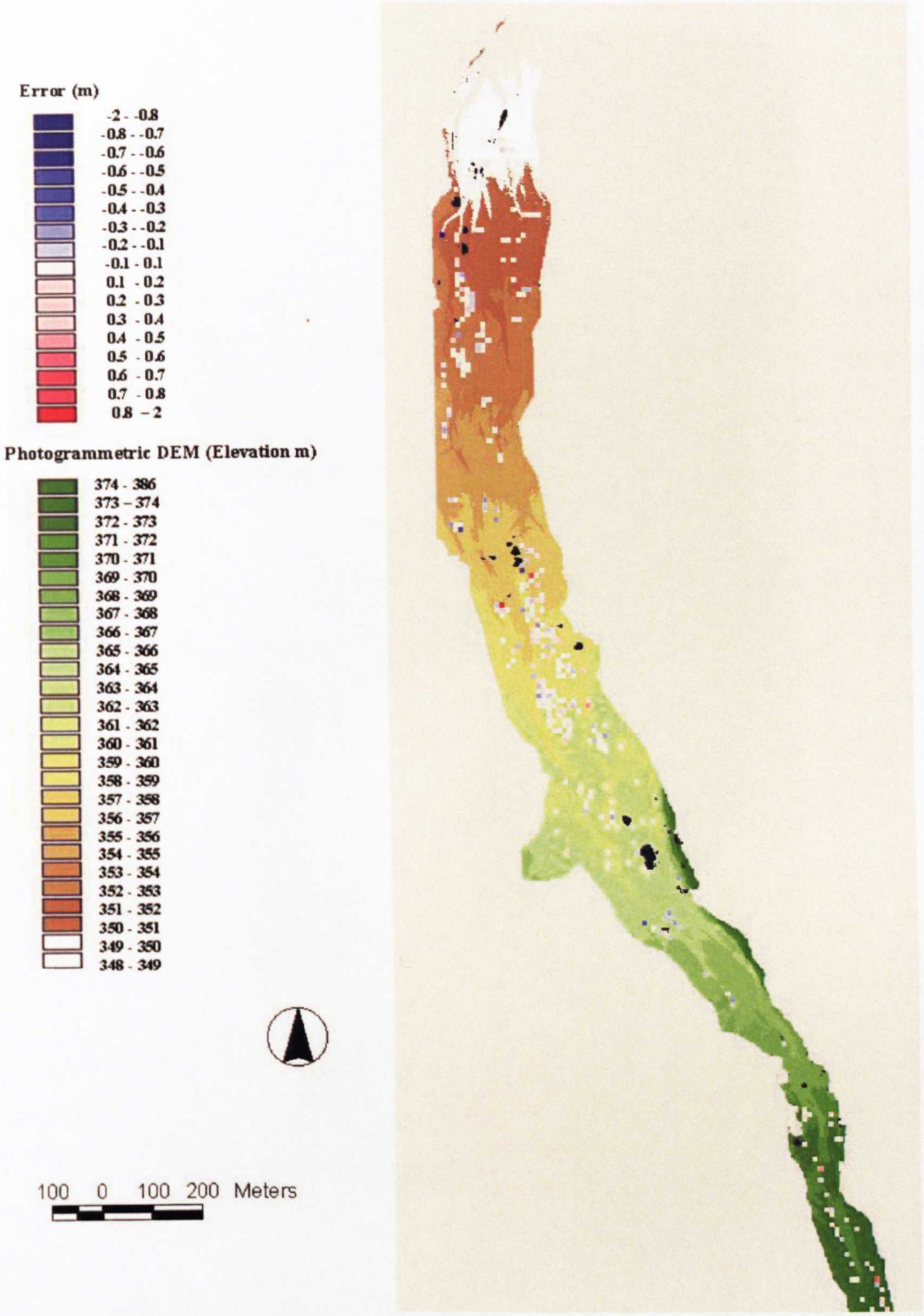

Figure 5.7 Spatial structure of error for the Full Photogrammetric DEM. The error values are derived from 1186 independent check points differenced against the photogrammetric DEM (Photogrammetric DEM – check points). Blue cells represent photogrammetric values below check point values.

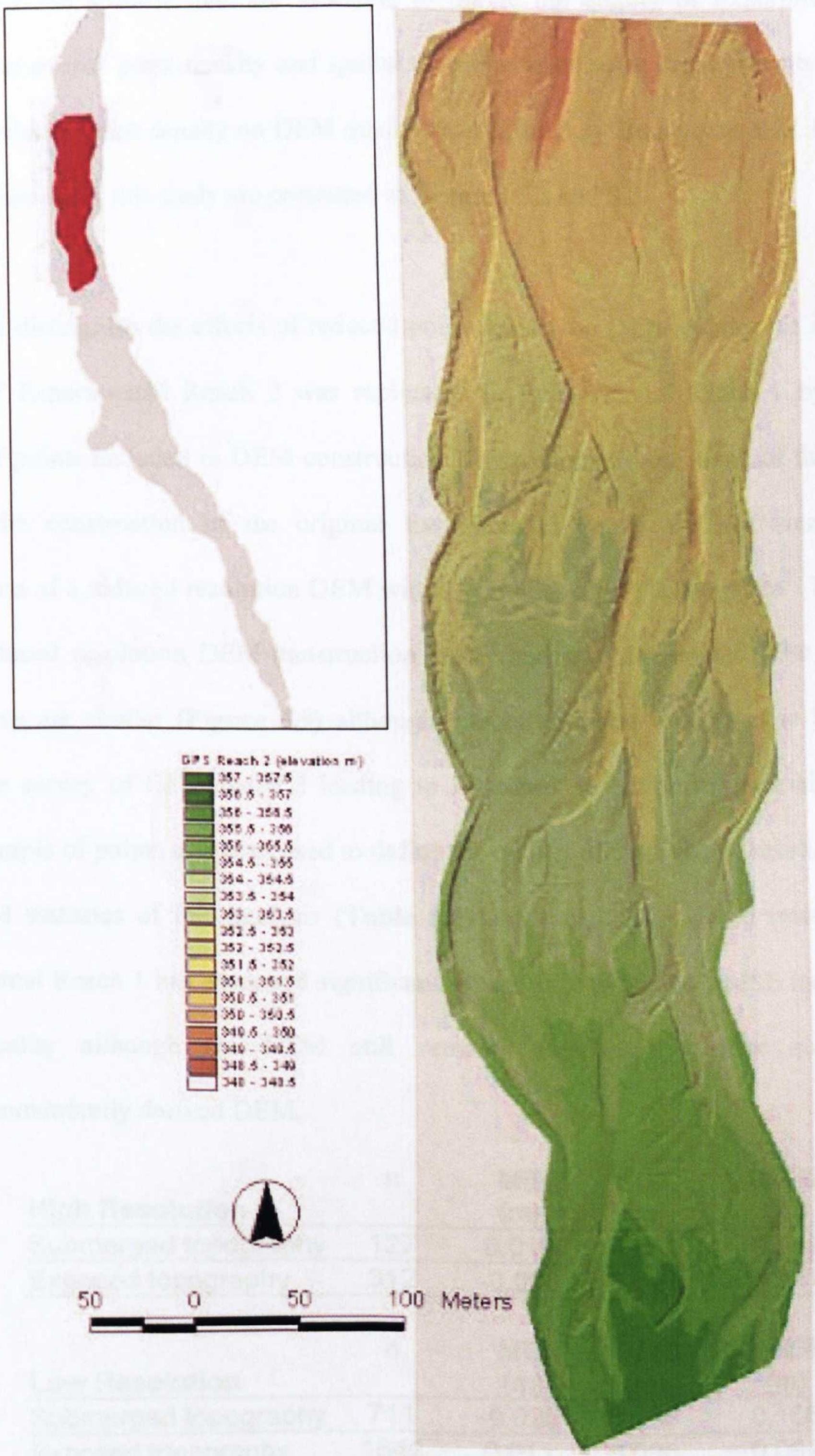

Figure 5.8 GPS derived DEM of Experimental Reach 2

The quality of Experimental Reach 2 DEM is lower than that of the Experimental Reach 1 DEM not because the individual measurements are of a lower quality, the same equipment and measurement techniques are used for both surveys, but because the point resolution is lower

(0.19pts/m^2). No specific data are available to define the quality of Experimental Reach 2 however the overall point density and spatial distribution of point density can be defined. The effect of reduced point density on DEM quality was defined by Brasington *et al.* (1999) and the important results of this study are presented in **Figures 5.2** and **5.3.**

In order to distinguish the effects of reduced point density on DEM quality the measured point density of Experimental Reach 2 was replicated in Experimental Reach 1 by reducing the number of points included in DEM construction. Approximately one tenth of the 29686 points used in the construction of the original Experimental Reach 1 DEM were used in the construction of a reduced resolution DEM with a point density of 0.190 pts/m^2. The points used in the reduced resolution DEM construction were randomly determined. The distribution of these points are similar **(Figure 5.9)** although greater attention was given to breaks in slope during the survey of GPS Reach 2 leading to increased definition of channel boundaries. A further sample of points was then used to define the quality of the reduced resolution DEM. The formalised statistics of this analysis **(Table 5.5)** show that the reduced resolution DEM of Experimental Reach 1 has produced significant increases in SDE and RMSE indicating a lower DEM quality although the DEM still remains significantly better quality than the photogrammetrically derived DEM.

High Resolution	n	ME (m)	SDE (m)	RMSE (m)
Submerged topography	127	0.019	0.052	0.049
Exposed topography	312	-0.008	0.023	0.021

Low Resolution	n	ME (m)	SDE (m)	RMSE (m)
Submerged topography	711	-0.025	0.106	0.108
Exposed topography	1542	0.011	0.096	0.097

Table 5. 5 High and low resolution DEM quality statistics: Experimental Reach 1. The value of n differs between the high and low resolution analysis because more redundant survey points were available to test the low resolution DEM.

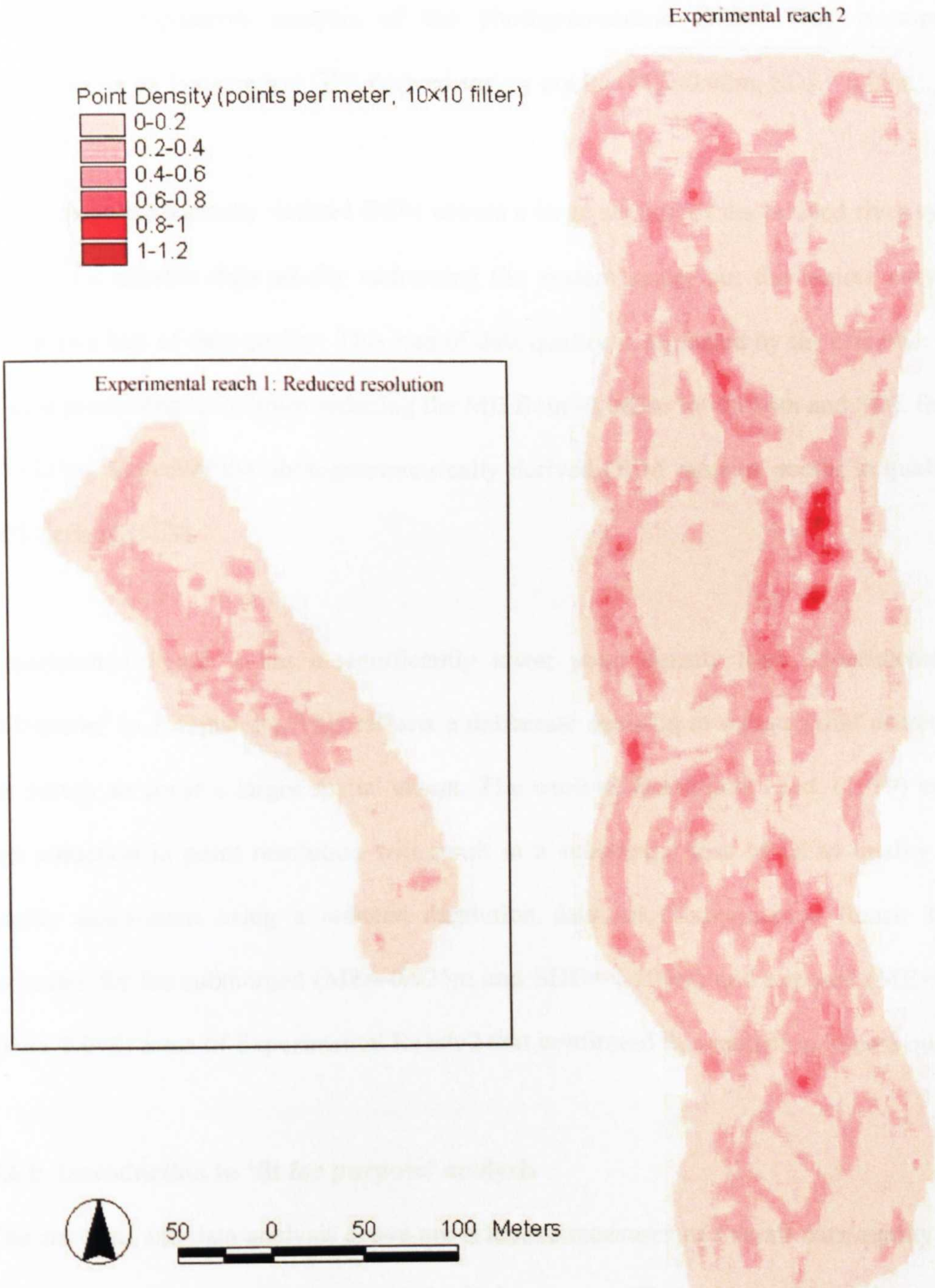

Figure 5.9 Point densities for the reduced resolution Experimental Reach 1 DEM (left) and Experimental Reach 2). Calculated using a 10×10m filter.

5.5.0 Conclusions on overall DEM quality

The data quality analysis above has re-enforced the attributes of the 3 DEMs. The high resolution GPS derived DEM (Experimental Reach 1) is very high quality suggesting it is the best possible representation of the reach. The high quality of individual points (SD<0.02m) coupled with the high point density (1.42pts/m^2) suggests that the DEM is suitable for an evenly distributed comparative analysis of the photogrammetric DEM. This is supported by comparison with independent GPS derived survey points (ME<0.02m, SDE< 0.05m).

The photogrammetrically derived DEM covers a large section of the braided river system. This makes it a suitable data set for addressing the system scale, but the remote survey method results in a loss of data quality. This loss of data quality is remedied by the effective application of post processing techniques reducing the ME from -0.083m to -0.036m and SDE from 0.354m to 0.219m. However the photogrammetrically derived DEM remains poorer in quality than the GPS derived DEM.

Experimental Reach 2 has a significantly lower point density than Experimental Reach 1 (0.19pts/m^2 to 1.42pts/m^2). This reflects a deliberate decision to reduce point density to enable the survey to cover a larger spatial extent. The work of Brasington *et al.* (1999) suggests that this reduction in point resolution will result in a substantial loss of DEM quality. The DEM quality assessment using a reduced resolution data set (Experimental Reach 1) produced estimates for the submerged (ME=-0.025m and SDE= 0.106m) and exposed (ME=0.011m and SDE= 0.096) areas of Experimental Reach 2 that confirmed this reduction in data quality.

5.6.0. Introduction to 'fit for purpose' analysis

The statistics and data analysis above are effective measures of overall data quality but they do not relate directly to useful geomorphological measures. The sections below aim to address this by defining the robustness of two morphometrics, Level of Detection (LOD) threshold and Mean Bed Level (MBL). These morphometrics were chosen because they can be directly linked to the research themes. LOD threshold (**Section 5.7**) defines the limits of each DEM as an indicator of sedimentary change, this relates to the third research theme, which is concerned with the dynamic scaling properties of the system. MBL defines the average elevation of values for regularly spaced transects across the study system (**Section 5.8**) this enables an analysis of the downstream scaling properties of static form to address research theme 2. The high resolution GPS derived DEM, Experimental Reach 1 is used as a 'true surface' to compare with the photogrammetrically derived surface to determine the magnitude and frequency of error derived MBL fluctuations. The definitions and explanations of the morphometrics, LOD and MBL are kept to a minimum within this chapter. More extensive explanations of LOD are provided in **Chapter 7** and MBL in **Chapter 8,** chapters that also consider the merits of these morphometrics over other morphometrics (e.g. slope).

5.7.0 Defining a LOD Threshold

If the morphological method is to be used for defining sedimentary movement then a LOD threshold must be defined for each data acquisition method. This analysis relates directly to Research theme 3 because it uses measures of data quality to define the threshold below which derived channel and sedimentary changes become unreliable. This analysis replicates and extends the analysis of LOD thresholds presented in Brasington *et al.* (2003).

A volumetric measure of the sedimentary budget using the morphological method is doubly sensitive to DEM quality because it incorporates errors from both surfaces used in differencing. As outlined in Brasington *et al.* (2003), simple error propagation theory can be used to define this provided that both surfaces can be treated as independent. (Taylor, 1982). For a derived Variable U, calculated through addition or subtraction of a derived variables, Z_1 and Z_2, each associated with errors δz_1 and δz_2, the total error in U can be estimated using **Equation 4.1**

$$\delta u = \sqrt{(\delta z_2^1 + \delta z_2^2)}$$ **Equation 4.1**

This error propagation theory gives a formalized method for estimating the level of detection. The standard deviation calculated using independent check data, is used to estimate δ and a term, t, is introduced to specify the threshold LOD for a given confidence interval, so that:

$$Ucrit = t\sqrt{(SDE_1^2 + SDE_2^2)}$$ **Equation 5.2**

Where Ucrit is the critical threshold, SDE_1 and SDE_2 are the standard deviation of error in each surface respectively and t is the critical t-value at the chosen confidence level. A t-value of 1 indicates a confidence level of two SDE or 95%. For the calculations below a t-value of 1 was used.

The pattern of errors in **Figure 5. 6** shows differences in the magnitude of errors between the dry and submerged (termed wet) areas of the DEM. This significant difference in the spatial distribution of error complicates the use of **Equation 5.2**. Without differentiating between wet and dry areas then the derived LOD threshold would not be correct for wet or dry cells. Wet cells would have a LOD threshold too low and the result would be a budget more dominated by error than **Equation 5.2** defines. Dry cells would have a LOD too high and this would mean that correctly measured sedimentary changes would be attributed to error and discounted. With the differentiation of wet and dry cells the correct amount of error can be attributed to each area and areas that change from wet to dry or vice versa can also be attributed a correct LOD threshold. **Table 5.6** shows the LOD threshold with the wet and dry areas of the DEM differentiated.

The processing stages described in **Chapter 4** result in a dramatic improvement to the LOD threshold from 1.277m to 0.723m for wet-wet cells and 0.685m to 0.449m for dry-dry cells. The LOD thresholds for the photogrammetric DEM are still notably higher than for the Experimental Reach 1. The low resolution ground survey DEM, Experimental Reach 2 results in a LOD threshold that is four times higher than the high resolution GPS DEM but this is still half that of the photogrammetric DEM. The final LOD thresholds defined in **Table 5.6** are for a combined approach using both GPS and photogrammetrically derived DEMs.

Photogrammetrically derived DEM - (Experimental Reach 1 **Figure 5.3**)			
	Wet – Wet (m)	Wet - Dry/Dry – Wet (m)	Dry – Dry (m
Stage 1	1.277	1.025	0.685
Stage 2	1.234	0.996	0.679
Stage 3	0.960	0.832	0.679
Stage 4	0.960	0.832	0.679
Stage 5	0.806	0.648	0.436
Extended Reach (**Figure 5.1**) Stage 5	0.723	0.602	0.449
GPS derived DEM - (Experimental Reach 1 Figure 5. 4)			
	Wet – Wet (m)	Wet - Dry/Dry – Wet (m)	Dry – Dry (m
High resolution	0.136	0.104	0.058
Low resolution	0.468	0.370	0.234
GPS DEM (low resolution) and Photogrammetric DEM (stage 5)			
	Wet – Wet (m)	Wet - Dry/Dry – Wet (m)	Dry – Dry (m
	0.659	0.453 - 0.594	0.350
LOD at 95% confidence interval			

Table 5. 6 LOD Thresholds for the photogrammetric DEM (through post-processing stages 1-5), GPS DEMs (high and low resolution) and a combined low resolution GPS DEM and photogrammetric DEM.

5.7.1 Sensitivity analysis

Although the LOD thresholds give a level for masking out error they cannot differentiate between error and real change. This means that real changes that fall below the LOD threshold are also masked out. Sensitivity analysis is one method for assessing how much real change is being masked out by the LOD threshold approach. Experimental Reach 1 gives the opportunity for this analysis because high quality DEMs of the same area were constructed for 3 different epochs (annual intervals 1998-2000). A DEM of difference was constructed for the 1999-2000 surveys and this was progressively thresholded at coarser levels of detection from 0.1m to 1.0m. The dramatic loss in information can be seen in **Figure 5. 10**. There is a rapid drop off in information away from the 0.1 LOD threshold. This is most pronounced for deposition where the amount of sediment falls by half with a LOD threshold of 0.3m.

This pattern is indicative of the structure of erosion and deposition within the braided river environment. Erosion typically occurs in discrete areas where large amounts of sediment are scoured (e.g. cut banks). Deposition tends to be spread over larger areas with bar top trapping of individual clasts an important mechanism (Ashmore, 1991; Bluck, 1979). These different patterns of sedimentary change will fundamentally affect the ability of low precision survey methods to produce an unbiased sedimentary budget. Any analysis of Experimental Reach 1 carried out with a 0.5m threshold would conclude that the Reach was in sedimentary equilibrium over the year (1999-2000). Lowering the LOD threshold to 0.1m would show that deposition in the reach is significantly larger than erosion. Lowering the LOD substantially below 0.1m is unsound due to the precision of the GPS derived DEM, but the quantity of deposition might continue to grow exponentially until the LOD reaches the median grain size (0.05m). At this point the majority of veneer deposits equal to or above the median clast size would be correctly detected, only fine grained deposits would be undetected.

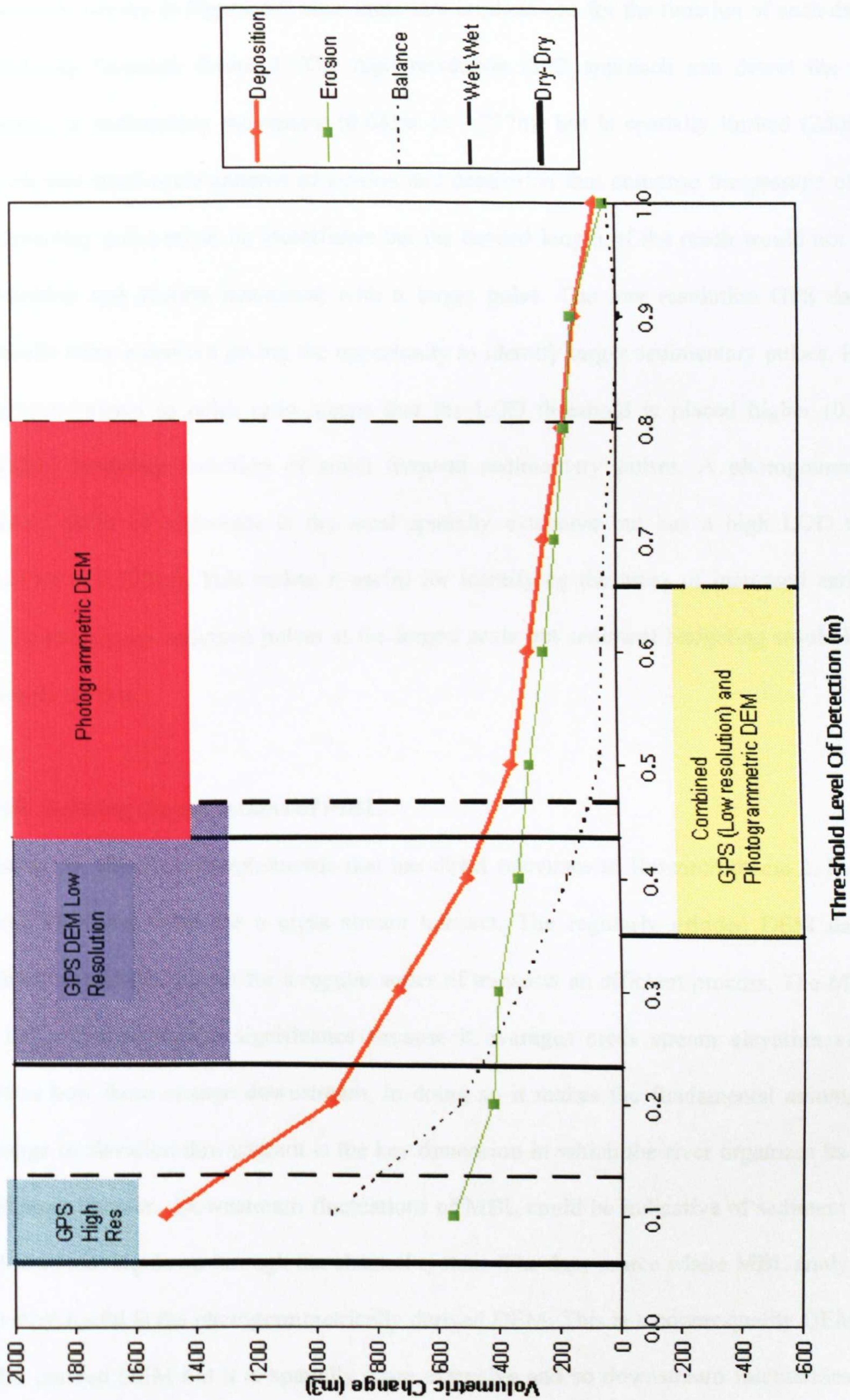

Figure 5. 10. Sediment volume changes at different LOD thresholds with survey method LOD thresholds superimposed.

The results shown in **Figure 5.7** have important implications for the function of each data set in addressing Research theme 3. The high resolution GPS approach can detect the smallest changes in sedimentary movement (0.685m to 1.277m) but is spatially limited (250m). This means that small-scale patterns of erosion and deposition that compose the passage of a small sedimentary pulse might be identifiable but the limited length of the reach would not span the deposition and erosion associated with a larger pulse. The low resolution GPS data set is spatially more extensive giving the opportunity to identify larger sedimentary pulses. However, the lower signal to noise ratio means that the LOD threshold is placed higher (0.234m to 0.468m) hindering detection of small frequent sedimentary pulses. A photogrammetrically derived DEM of difference is the most spatially extensive but has a high LOD threshold (0.449m to 0.723m). This makes it useful for identifying the areas of increased activity that might accompany sediment pulses at the largest scale but sediment budgeting would be biased towards erosion.

5.8.0 Defining the robustness of MBL.

Change in MBL is a morphometric that has direct relevance to Research theme 2. MBL is the mean elevation value for a cross stream transect. The regularly gridded DEM data makes extraction of MBL values for a regular series of transects an efficient process. The MBL series is of geomorphological significance because it averages cross stream elevation values and shows how these change downstream, in doing so it makes the fundamental assumption that change in elevation downstream is the key dimension in which the river organizes its form and sediment transfer. Downstream fluctuations of MBL could be indicative of sediment pulses of all sizes moving down through the channel system. The data source where MBL analysis would be most useful is the photogrammetrically derived DEM. This is a poorer quality DEM than the GPS derived DEM but it is spatially more extensive and so downstream fluctuations of MBL can be defined over a greater distance. Although the overall quality of this DEM is defined above in **Section 5.3** the suitability of applying the Photogrammetric DEM to show changes in

MBL is not. This section aims to characterize the magnitude and pattern of error in MBL so that detailed analyses of waveform magnitudes and frequencies in **Chapter 6** can be better assessed.

The justification for using MBL to measure downstream periodicities is described in full in **Chapter 6** but is summarized here. The passage of sediment pulses of different magnitudes and frequencies through the river channel system will inevitably result in the differential elevation of some areas of channel over others. The sediment pulses are likely to progress down the channel using complex assemblages of deposition and erosion to produce a net effect of increased MBL as each passes. The detection of these pulses is reliant on finding a method that is robust enough to enable the magnitude and frequency of specific pulses to be identified. This raises two main issues. Firstly, the data used to define MBL must be high quality but also the magnitude and types of error must be well established. In particular systematic fluctuations in error must be minimal relative to the magnitude of the waveform to be identified. Secondly, the lateral extent of each cross section must be identified. This is problematic because unlike differencing of DEMs where the lateral extent is defined by the channel changes themselves, the extent of the active channel is often poorly defined. The lateral impact of a sediment pulse is also likely to depend on its magnitude. Very small magnitude pulses could just affect the main active channel whereas large magnitude pulses are likely to not only increase the elevation of a wider cross section but also increase lateral instability. This problem is tackled in more detail in **Chapter 6** where the channel is classified into zones of stability. The following analysis of Experimental Reach 1 will use a section of this classification **(Figure 5. 11)** to define the cross sectional extents for analysis and give an indication of how MBL differs between classifications. The classifications used in **Figure 5.11** are (i) submerged (defined by the water classification used in the DEM processing, (ii) classification 1 (a very active area close to the submerged zone defined by it's lack of vegetation) and (iii) classification 2 (a less active area in which some vegetation has colonized the channels and bars).

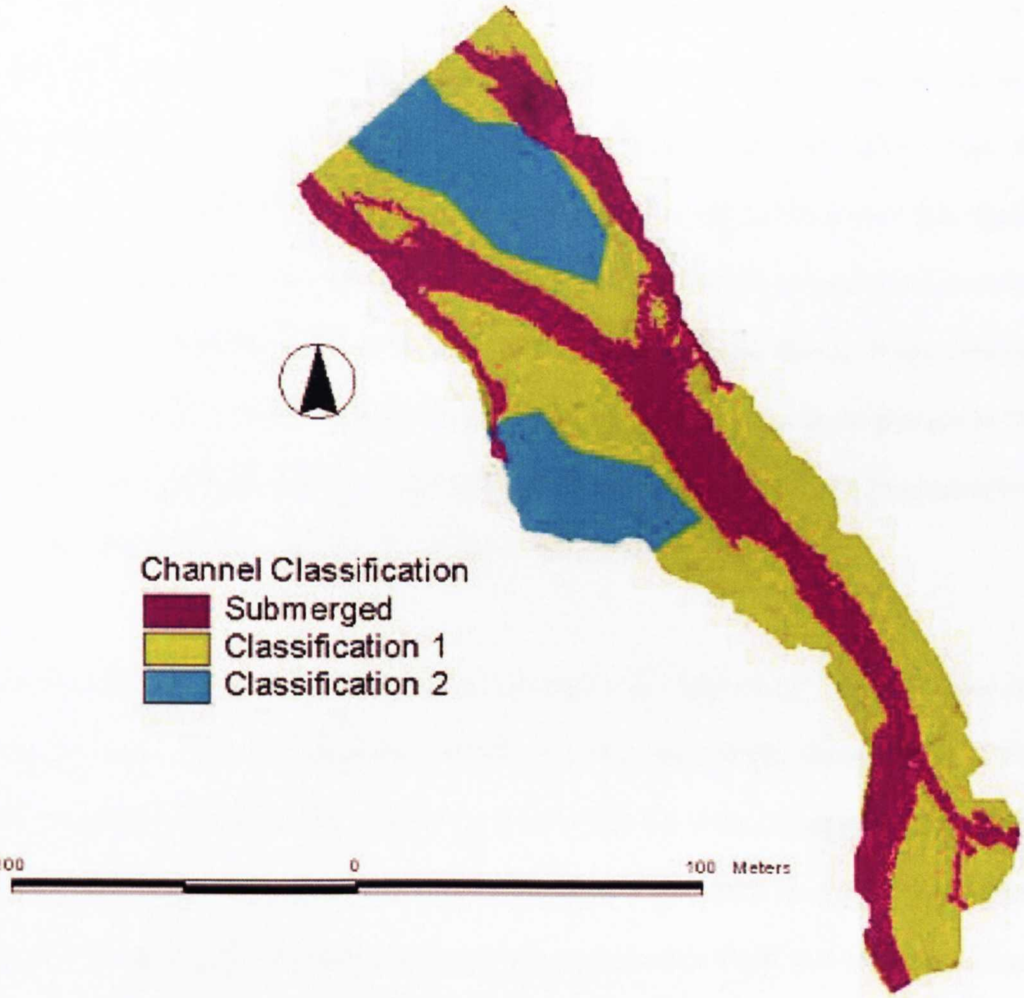

Figure 5.11 Channel classification for Experimental Reach 1

5.8.1. Comparison of MBL for Experimental Reach 1

The MBL series were extracted from the photogrammetric DEM and the GPS derived 'true surface' covering Experimental Reach 1. The mean average for cross sections was calculated using the channel classification shown in **Figure 5.11** to define the width of each transect. The highest possible downstream resolution was used, this was dictated by the resolution of the DEMs (0.5m). The derived MBL series were de-trended using a linear relationship to define average bed slope. This relationship, derived through least squares regression, had an R^2 of 0.953 and defined the bed slope as y =0.0115x (Approx 1%). The MBL series extracted for both the photogrammetric DEM and the GPS derived 'true surface' are shown in **Figure 5.12**.

These demonstrate that MBL is well represented by the photogrammetric DEM. The Submerged classification (A) replicates the negative bias found in the analysis of the photogrammetric DEM in **Figure 5.6**. The deep pool at 250m downstream is the exception where MBL is elevated. The inclusion of very active areas via the inclusion of Classification 1 (**B**) significantly reduces this bias and the averaging effect reduces the impact of the overestimation of deep pool elevations. The inclusion of Classification 2 (**C**) increases these effects. Wave structures (or periodicities) can be seen in all three classifications but they decrease in magnitude as the cross sectional width increases due to the smoothing effect of averaging. The Photogrammetric DEM tends to produce the same periodic structures as the GPS derived DEM.

The errors between the two survey methods are shown in **Figure 5.13**. The GPS derived DEM, the 'true surface', has been differenced with the photogrammetrically derived DEM (GPS DEM – photogrammetric DEM). The error bars on the left show the magnitude and downstream distribution of errors incorporated into cross sections. These error bars show the difference in elevation between MBL calculated using the photogrammetric DEM and MBL calculated using the GPS derived 'true surface'. These error bars are included because it is important to establish the quality of the photogrammetrically derived MBL series by defining the error present in each cross section, this gives an indication of how much error propagates from the DEM to the cross section and how much is random error that is cancelled out over the cross section.

A Classification Submerged

B Classification 1

C Classification 2

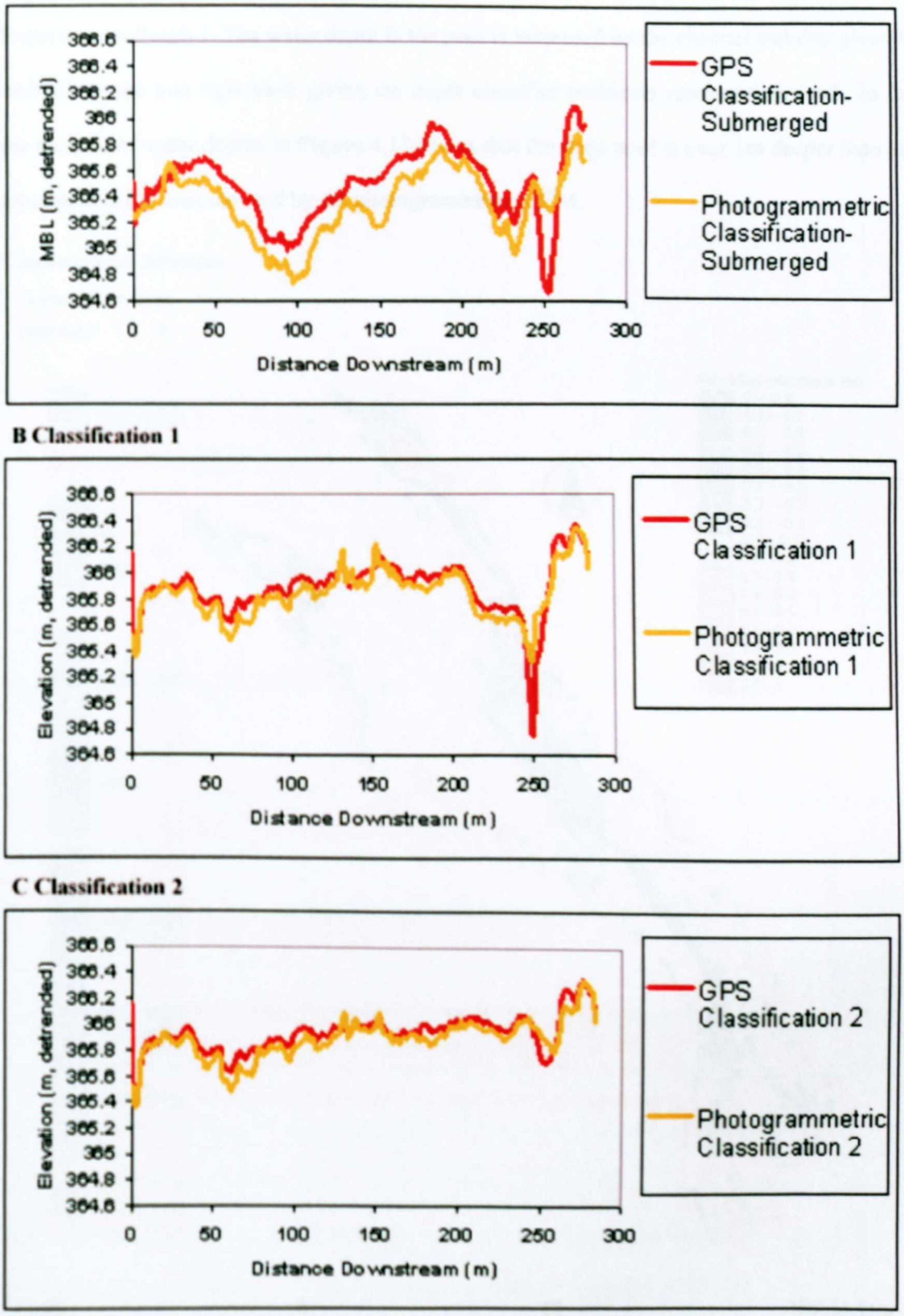

Figure 5. 12 GPS and photogrammetric extractions of MBL from Experimental Reach 1 for three channel classifications.

The area of positive error produced by the deep pool is out of character with the rest of the Experimental Reach 1. The water depth in the pool is increased by the channel stability given by bedrock on the true right bank giving the depth classifier problems representing depth. In fact the analysis of water depths in **Figure 4.13** shows that the deep pool is over 1m deeper than any other pool in the area covered by the photogrammetric DEM.

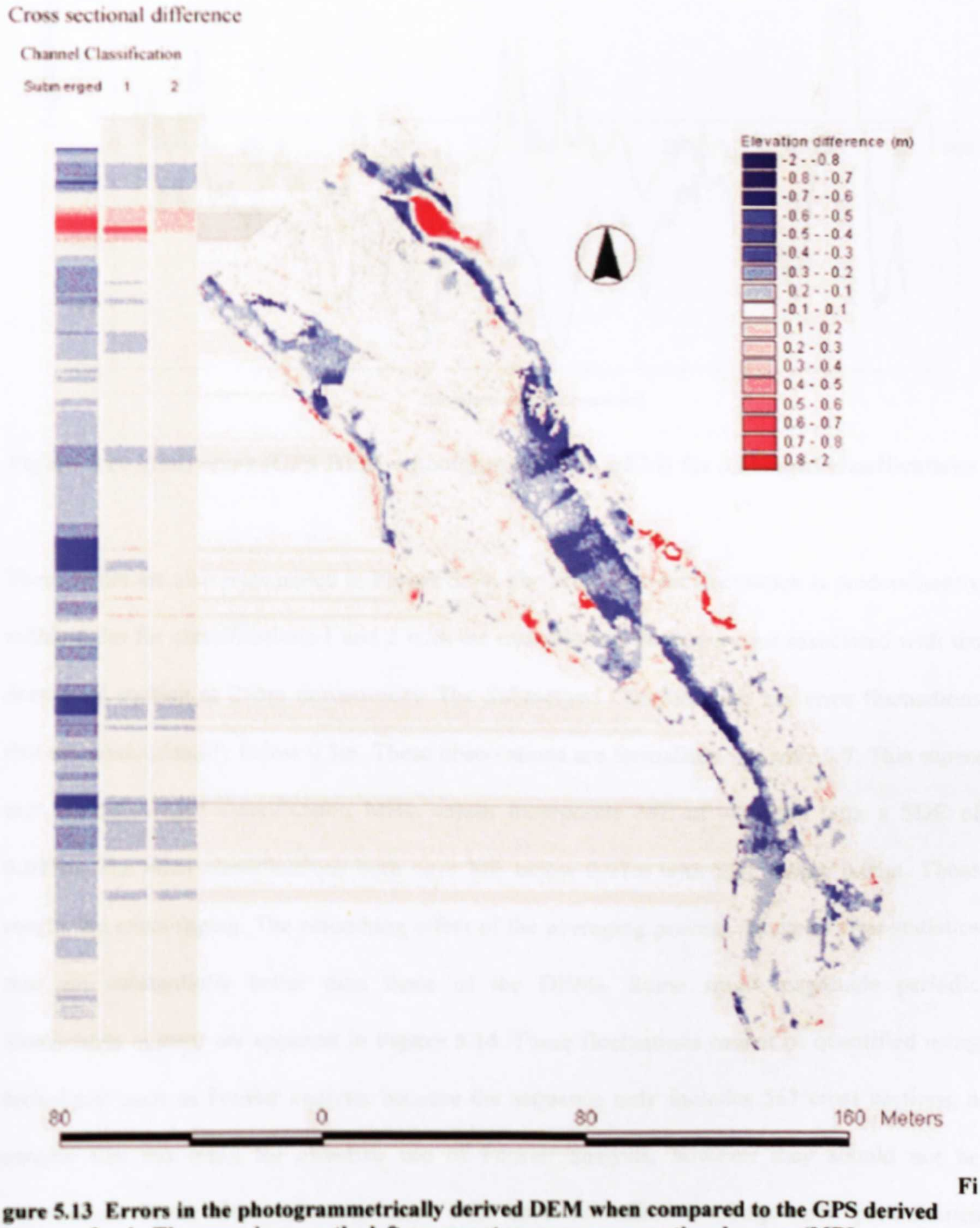

Figure 5.13 Errors in the photogrammetrically derived DEM when compared to the GPS derived 'true surface'. The error bars on the left represent average cross sectional errors (MBL error). Red represents areas of the photogrammetric DEM that are too high. Blue represents areas of the photogrammetric DEM that are too low

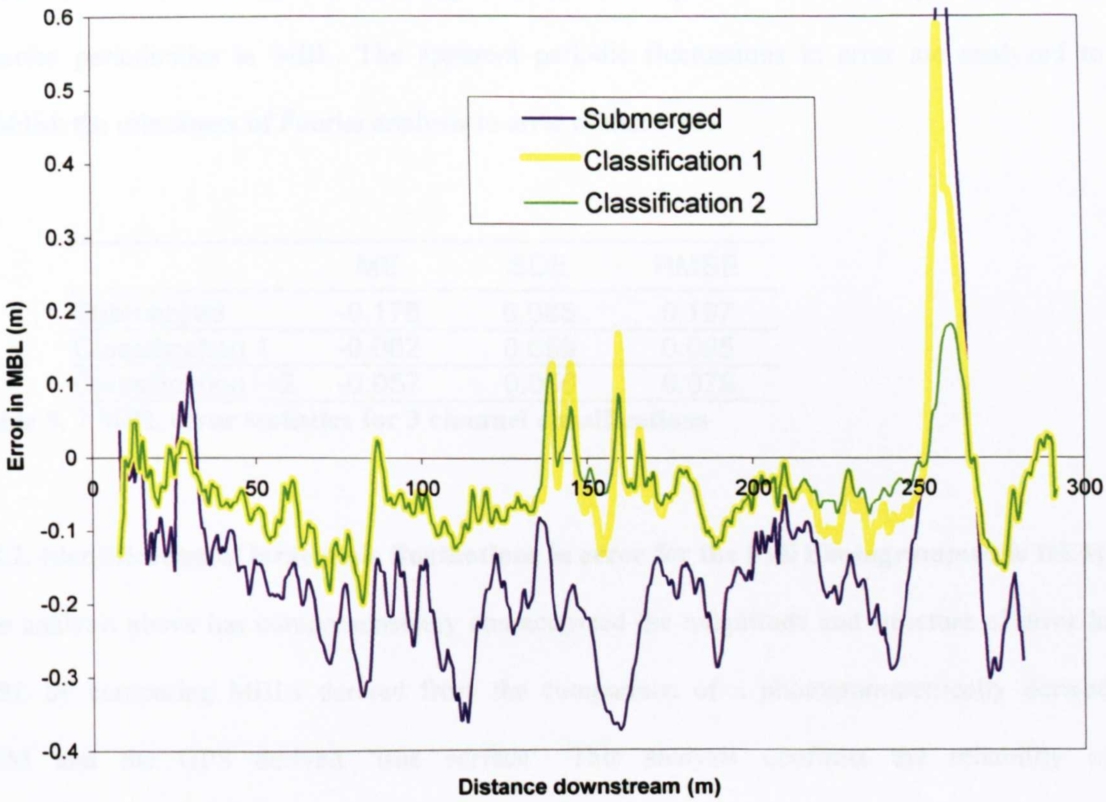

Figure 5.14 MBL error (GPS DEM – photogrammetric DEM) for 3 channel classifications

These errors are also represented in **Figure 5.14**. The scale of error fluctuation is predominantly within 0.2m for classifications 1 and 2 with the exception of the large error associated with the deep pool starting at 250m downstream. The Submerged Classification has error fluctuations the that are predominantly below 0.3m. These observations are formalised in **Table 5.7**. This shows that the submerged classification MBL values incorporate ME of –0.178m with a SDE of 0.085m. The other classifications both have ME below 0.07m with SDE below 0.06m. These results are encouraging. The smoothing effect of the averaging process results in error statistics that are substantially better than those of the DEMs. Some small magnitude periodic fluctuations in error are apparent in **Figure 5.14**. These fluctuations cannot be quantified using techniques such as Fourier analysis because the sequence only includes 567 cross sections, a sample size too small for effective use of Fourier analysis, however they should not be overlooked. These fluctuations in error will have no effect on large-scale periodicities associated with the passage of large sediment pulses but they could generate sufficient noise to render small MBL fluctuations indistinguishable. In **Chapter 6** Fourier analysis is used to describe periodicities in MBL. The apparent periodic fluctuations in error are analyzed to establish the robustness of Fourier analysis to error of that type.

	ME	SDE	RMSE
Submerged	-0.178	0.085	0.197
Classification 1	-0.062	0.059	0.085
Classification1+2	-0.057	0.056	0.079

Table 5. 7 MBL error statistics for 3 channel classifications

5.8.2. Identification of large scale fluctuations in error for the Full Photogrammetric DEM

The analysis above has comprehensively characterized the magnitude and structure of error in MBL by comparing MBLs derived from the comparison of a photogrammetrically derived DEM and the GPS derived 'true surface'. This analysis confirms the reliability of photogrammetric DEMs for defining MBL at small scales but it is not spatially extensive enough to confirm that fluctuations in error do not occur at larger scales. Systematic errors in individual photogrammetrically derived DEMs could be a cause of periodic fluctuations in the mosaicked photogrammetric DEM. **Figure 5.15** demonstrates this effect. The figure shows a series of DEM surfaces tilted to represent systematic errors. When these are mosaicked, using a feathering function similar to that used to mosaic the photogrammetrically derived DEMs, the result is a surface incorporating the systematic errors. The post processing procedures developed in **Chapter 4** were aimed specifically at reducing this effect. This section aims to assess how effective this process has been.

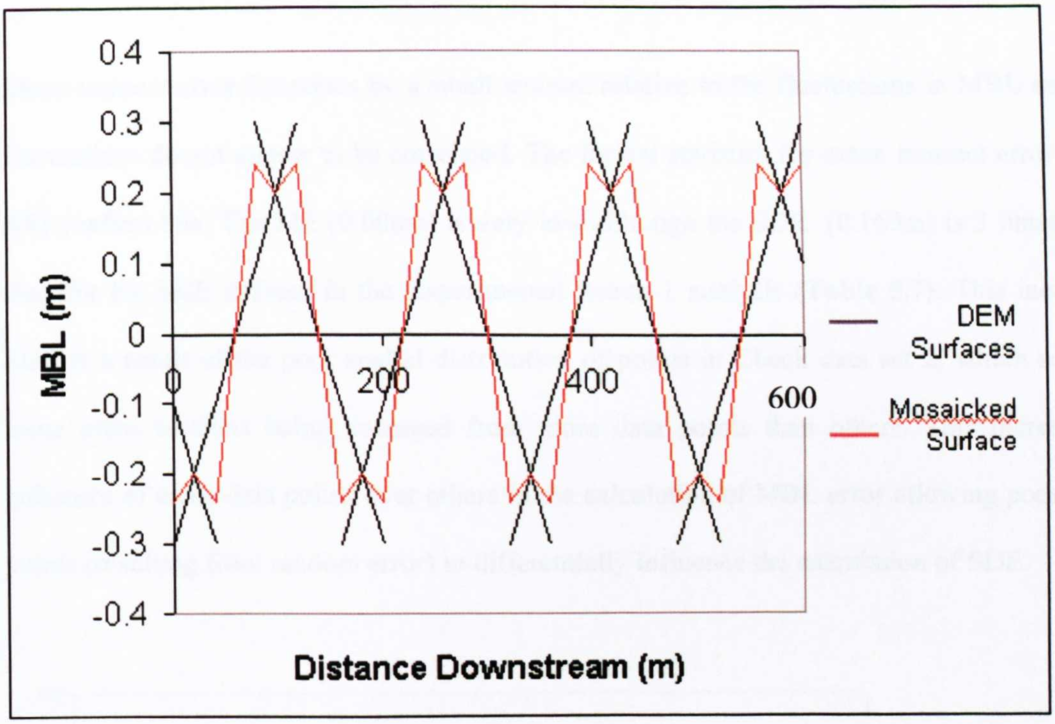

Figure 5. 15 Theoretical periodicities in mosaicked photogrammetric DEMs.

The magnitude and structure of fluctuations in error in MBL were quantified using 1186 independent survey points from Check Data set 2. The survey points were collected over the entire photogrammetric reach using GPS. These were differenced with the photogrammetric DEM (Survey points – photogrammetric DEM) to determine the photogrammetric DEM error at the survey points. Individually these error values are not a good indicator of large scale systematic fluctuations in photogrammetric DEM error because each value incorporates random errors (discussed in **Chapter 3**). To make the error values representative of large scale systematic fluctuations they were averaged over transects with a 30m downstream resolution. This means that within any given transect a distribution of error values is represented and the average value should better represent the ME in that transect. This averaging technique is appropriate because any large scale systematic fluctuations in error resulting from systematic errors in individual DEM surfaces will have a wavelength in excess of 200m because each individual photogrammetrically derived surface covers approximately 300m downstream. The results of this process are shown in **Figure 5.16**, the mean transect error is compared to MBL (detrended for bed slope) to show the different magnitudes of the signal fluctuations.

Mean transect error fluctuates by a small amount relative to the fluctuations in MBL and these fluctuations do not appear to be correlated. The formal statistics for mean transect error **(Table 5.8)** confirm this. The ME (0.006m) is very low although the SDE (0.163m) is 3 times higher than for the SDE defined in the Experimental Reach 1 analysis **(Table 5.7)**. This increase in SDE is a result of the poor spatial distribution of points in Check data set 2, which results in some cross sections being averaged from more data points than others. This increases the influence of some data points over others in the calculation of MBL error allowing poor quality points (resulting from random error) to differentially influence the calculation of SDE.

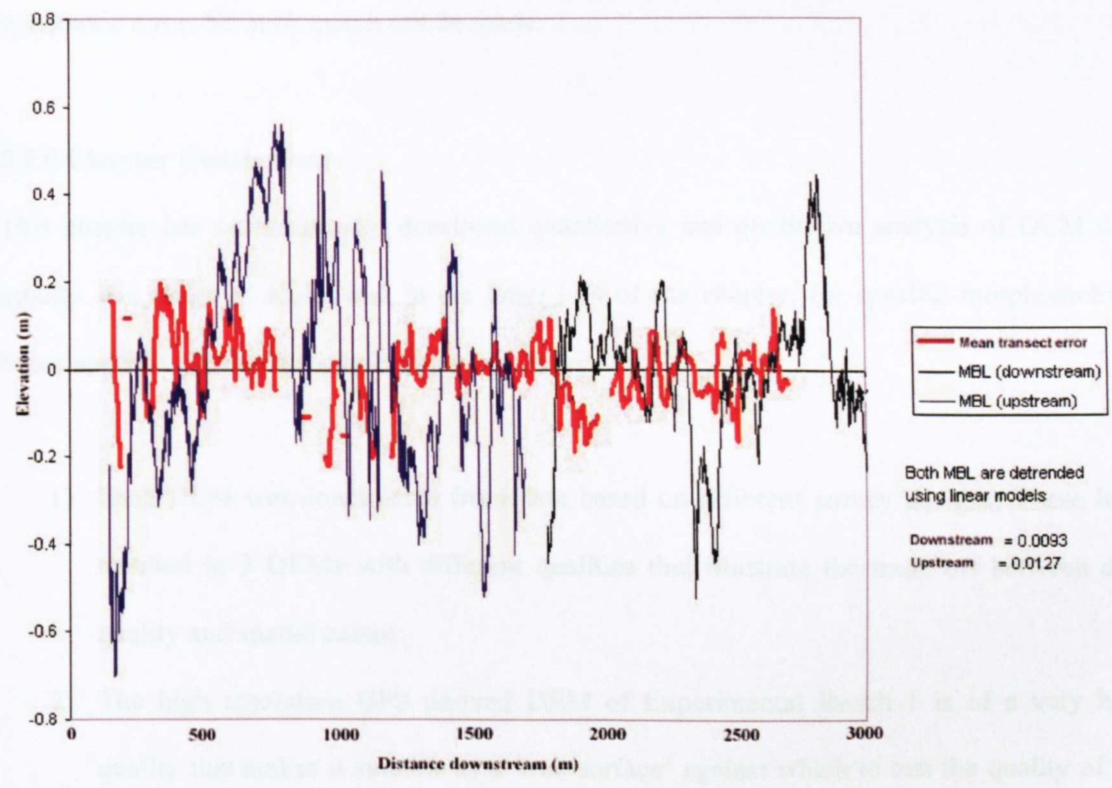

Figure 5.16. Mean transect error (check points –photogrammetric DEM) and fluctuation in MBL. MBL is extracted for two subsystems, upstream and downstream. This was done because a break in slope was identified halfway down the photogrammetric DEM (Chapter 6). Each subsystem was independently detrended for slope.

	n	ME (m)	SDE(m)	RMSE(m)
MBL error	705	-0.006	0.163	0.163

Table 5.8 Mean transect error statistics. Derived from the photogrammetric DEM and Check Data Set 2

The analysis in this section has been inhibited by the size of the check data set. The small number of survey points spread over the large area covered by the photogrammetric DEM has hindered the analysis because random error associated with each individual point has reduced the reliability of the Mean transect error. A larger sample would reduce the impact of random error allowing a more accurate estimation of Mean transect error and a better determination of large scale, downstream fluctuations in error. However, the limited survey data available have been sufficient to demonstrate that systematic errors in individual DEMs, incorporated into the mosaicked DEM surface do not have an identifiable impact on derived MBL. If, for instance, systematic fluctuations in Mean transect error could be matched up with similar fluctuations in MBL in **Figure 5.16** this would demonstrate the effect of photogrammetrically induced systematic error. No such match can be made.

5.9.0 Chapter Conclusions

This chapter has systematically developed quantitative and qualitative analysis of DEM data quality at a range of scales and in the latter half of the chapter, for specific morphometrics. Some specific conclusions can be drawn from this:

1) Each DEM was constructed from data based on different survey designs. These have resulted in 3 DEMs with different qualities that illustrate the trade off between data quality and spatial extent.
2) The high resolution GPS derived DEM of Experimental Reach 1 is of a very high quality this makes it suitable as a 'true surface' against which to test the quality of the photogrammetrically derived DEM.
3) When the quality of the photogrammetric DEM was assessed the effectiveness of the post processing procedures, developed in **Chapter 4**, at reducing ME and SDE was demonstrated. These data quality improvements make the photogrammetric DEM a more useful model with which to test the research themes 2 and 3.

4) The quality of the low resolution GPS derived DEM, Experimental Reach 2, was estimated using a reduced resolution DEM of Experimental Reach 1. It was found to be of significantly poorer quality than the high resolution GPS derived DEM (supporting the findings of Brasington *et al.*, 1999) but significantly better quality than the photogrammetric DEM.

5) The LOD analysis shows that DEM differencing using two photogrammetric DEM's has a high LOD threshold. The LOD threshold is substantially lower for a low resolution GPS derived DEM and lower again for a high resolution GPS derived DEM.

6) The rate of information loss as LOD thresholds increase is not equal between erosion and deposition. Deposition tends to take the form of thin bar top veneers, which cannot be detected by imprecise survey methods such as photogrammetric methods. Erosion tends to be deep and more easily detectable.

7) Determination of MBL is a technique less reliant on very high quality DEM data because the random errors associated with imprecise methods such as photogrammetric techniques cancel each other out over the width of a transect. However systematic errors within DEMs will adversely effect derived MBL.

8) Analysis of derived MBL by comparing a GPS derived 'true surface' against the photogrammetrically derived surface showed fluctuations in error below 0.2m (Classifications 1 and 2), this is supported by statistical analysis which showed ME< 0.065m and SDE< 0.06m.

9) The effect of systematic errors, resulting from the photogrammetric process, on the derivation of MBL was tested using a spatially extensive check data set. No match was found between the fluctuations of mean transect error and MBL. The size and distribution of the checkpoint data set inhibited more sophisticated treatment of the error fluctuations.

Overall the analysis in this chapter has addressed research theme 1 which is concerned with the acquisition, correction and testing of high quality morphological data. In particular this chapter has demonstrated the use of photogrammetric and ground survey data to meet the requirements of multiscale, spatially extensive data to address the scaling characteristics of static morphology and sediment movement. The errors associated with these data sources have been defined using conventional techniques and using fit for purpose analysis to assess the impact of error on specific morphometrics.

CHAPTER 6. DEFINING PERIODICITIES IN STATIC MORPHOLOGY

Abstract

Analysing the static morphology of a river system is one way of determining the influential organisational properties of the system. However, this is reliant on defining a method that accurately represents the behaviour of the river system at a variety of scales and for a number of channel orientations **(Section 6.2.0)**. Initially the rationale for linking self-organisation to static form is discussed. This is followed by a justification of the use of Mean Bed Level (MBL) as a means of quantifying organisation within braided river channels. In particular MBL is a morphometric that can determine self-organisation in the downstream direction. MBL is extracted for an upstream and downstream sub-system using a number of classifications to define transect width **(Section 6.3.0)**. The problem of analysing the MBL sequences to relate them to self-organisation is addressed. The fundamental problem is how to demonstrate that braided river form, as defined by MBL, can be analysed to show scaling characteristics. The Fast Fourier Transform (FFT) is adopted as a method for deconstructing the MBL signal into its constituent periodicities **(Section 6.4.0)**, a technique that identifies dominant scales within the data series. A number of problems and limitations of the FFT are addressed. The qualities of the FFT are further demonstrated by reconstructing the MBL sequence using the results of the FFT. The impact of MBL error on FFT results is assessed using information collected in **Chapter 5** **(Section 6.5.0)**. The extent of the MBL classifications are shown to influence the derived periodicities with narrow classifications showing high frequency waves and wider classifications low frequency waves **(Section 6.6.0)** The periodicities derived from the FFT suggest a link between low frequencies and large topographic features although smaller morphological units are shown to have little relation to medium scale bed level frequencies. The periodicities are also shown to be scale invariant suggesting that the study system could be self-organised **(Section 6.7.0)**

6.1.0 Introduction

Chapter 5 established the overall quality of the three DEMs used in this project and then went on to define the effects on two specific morphometrics, LOD threshold (applicable when differencing DEMs) and MBL. The MBL analysis demonstrated that the photogrammetric DEM could be reliably used for defining MBL because errors tend to cancel each other out over the width of each transect resulting in low error statistics. This chapter aims to use the high quality spatially extensive photogrammetric DEM to address some of the important themes introduced in **Chapter 2** in particular the imprint of self organisation on static morphology. There are some important questions concerning the organisational properties of braided rivers that can only be answered using three-dimensional morphological data collected over a large area. In particular what periodic structures are present in channel form associated with the storage of sediment as it is conveyed through the system, and how these sediment waves correspond to other forms of channel organisation such as confluence diffluence units. High quality morphological data means the structure of periodicities can be analysed to show the scaling characteristics of the system. If the periodicities can be shown to be scale invariant (fractal) then this offers evidence that the system could be self organised.

This chapter is built around a number of concepts that have not been widely applied within geomorphology before now and certainly break from reductionist forms of geomorphological analysis. The rationale behind these concepts is presented below along with the assumptions that underlie their use.

6.2.0 Static morphology as an indicator of river processes and self-organisation

The idea of using static morphology as an indicator of self organisation is reliant on the concept that a set of organisational processes at work in the river system will interact with river channel form in such a way as to leave an imprint of that organisation on river channel morphology. This concept is well established in fluvial geomorphology with theories such as hydraulic geometry (Leopold *et al.*, 1964, also termed regime theory) directly linking morphological form with flow magnitude and channel processes. The development of hydraulic geometry theory in the 1950's and 1960's by geomorphologists from the United States Geological Society (especially Leopold, Wolman and Miller) represented a quantitive revolution in geomorphology because static morphological form was linked to formative discharge using logarithmic plots to describe a functional explanation between width, depth, slope and changing discharge.

The use of form to describe channel organisation has also been investigated using planimetric data. Planimetric analysis of braided rivers has produced braiding indices (Brice, 1964) and more sophisticated morphometrics such as those suggested by Rust (1978) and Howard *et al.* (1970) (see discussion in **Chapter 2**). More recently the fractal analysis of Sapozhnikov and Foufoula-Georgiou (1996) has determined some of the scaling relationships associated with the planimetric form of braided rivers. Within most of these studies the concept of the form being studied is questioned, however a majority then go on to accept that the area of inundation is the most appropriate form to be used even if this is a low flow form, not representative of the floods that actively produce channel form. An exception to this is of Sapozhnikov and Foufoula-Georgiou (1997) who showed apparently stationary fractal scaling parameters for braided river forms defined by different levels of inundation. The three dimensional topographic data in this thesis is ideally suited to challenging and testing the boundaries of the form being studied. With DEM data the extent of inundation need not define the extent of the system being studied because real elevation values are used. This represents a real improvement in theoretical terms because, instead of measuring residual flow down a channel, real patterns of channel configurations can be measured and these are likely to better represent self organisation within the system over a number of timescales.

There are theoretical and observational reasons why channel form can be used as an indication of the self-organisation of a braided river system such as the River Feshie. Observations of river channels and in particular braided river channels show a degree of organisation and these lead to simple system scale models describing the organisation of planimetric channel form (Brice, 1964; Rust, 1978) and defining the spatial relations between morphological units (Howard *et al.*, 1970). More detailed studies have defined form process interactions operating in specific morphological units such as chute and lobe structures (Ferguson *et al.*, 1992) and confluence diffluence units (Ashmore *et al.*, 1992)

These studies are predominantly concerned with morphological structures that can be observed and identified with the human eye. Confluence-diffluence units and chute and lobe units are studied because they are the obvious organisational structure that can be identified when braided rivers are observed, particularly at low or moderate flows. However, the organisational structures within a river system may not always be detectable using crude observations. For instance small changes in elevation over large distances can account for large volumes of sediment and yet these would not be apparent when observing braided rivers in the field, using planimetric sources or conventional ground survey techniques. Similarly temporal changes in morphology might show patterns of sediment erosion or deposition that are under or over estimated by planimetric or observational studies. In particular the migration of a small lobe of sediment during a moderate flood event might block an active channel causing it to become inactive or unblock an existing inactive channel causing a major channel avulsion. Alternatively large numbers of small sedimentary movement events might go unnoticed by observers because their net effect on channel change is spread over a wide area. The three dimensional data developed in this thesis give the opportunity for identifying forms of self organisation that could not be identified using planimetric means or by close observations in the field.

Theoretical reasoning from physics based theories of self-organisation also suggests channel form could be a suitable indicator of self-organisation. Studies that have been designed to directly investigate SOC in the laboratory environment have made links between the static morphological form and the SOC state. Frette *et al.*, (1996) monitored one of the first systems to show SOC, a rice pile. The SOC was demonstrated by the power law distribution of rice avalanches. The static morphology of the rice pile was also studied and found to be fractal because it exhibited elevation fluctuations of all sizes. The link between SOC and static form has been suggested by other researchers in particular Rinaldo, (1996) who showed that the fractal form of a drainage basin channel network could be replicated by a computational model based on self organised critical principles.

The discussion above has given a generic rationale for using static morphology as an indicator of self-organisation but clearly the validity of any approach will be dependent on its exact implementation. Most importantly how can an approach quantify the self-organisation imprinted onto static morphology, and what spatial and temporal scales of system operation are incorporated into any approach.

6.2.1 Morphometrics

The term morphometric is used in this thesis to refer to a derived parameter that measures morphology. The term morphometric and the development of morphometrics for describing landforms are discussed in Evans (1987, 1997). This section considers some of the possible approaches for defining a morphometric that can capture some of the characteristics of self-organisation imprinted on static morphology. To do this successfully the morphometric will need to simplify the information in the three dimensional topographic data into a form that clarifies the signal produced by self-organisation. There are inevitable assumptions necessary in any data analysis of this kind. Some morphometrics and associated assumptions are considered below.

There are numerous possibilities for devising morphometrics for three-dimensional topographic data because DEMs can be interrogated efficiently using GIS packages such as ArcView (now ARCGIS) or Erdas IMAGINE. One starting point for defining a morphometric that can adequately define self-organisation is to consider some of the characteristics of braided river morphology. If morphology were considered as a spatial distribution of angles then clearly much of the organisation imprinted on the static morphology would be well represented.

Braided river morphology is predominantly composed of low angle surfaces on bar tops although these are incised with channels with high angles. Very high angled cut banks tend to be common features and reflect the lateral instability of the system. Confluences and diffluences are morphologically distinctive and could be characterised in relation to patterns of elevation changes and bed slope angles. A morphometric based around angles derived from braided river morphology could aim to define the spatial distribution and frequency of specific patterns of angle (**Figure 6.1**). This could be achieved by adapting existing pattern recognition software to define specific morphological types.

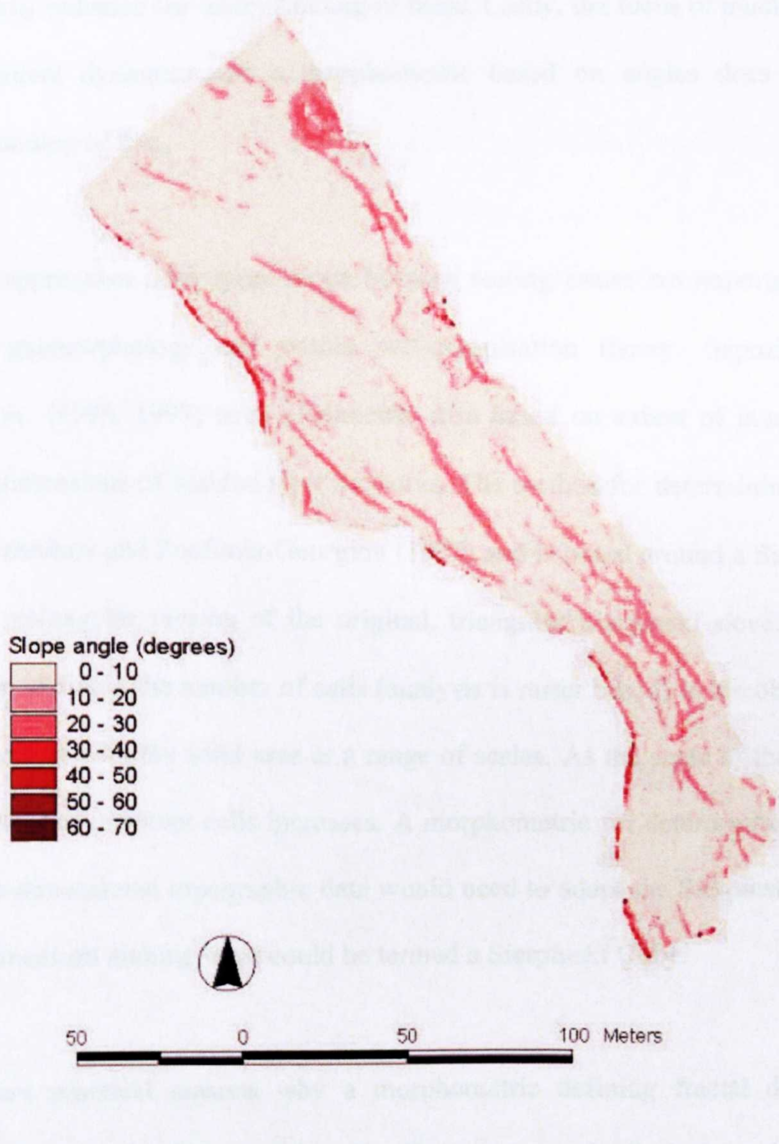

Figure 6.1. Slope angles derived for Experimental Reach 1. Slope angle is dependent on grid cell size and survey point density as well as terrain characteristics.

This morphometric is not appropriate to this study for three reasons. It could not be used to show the scaling characteristics of the topography because grid cell size in part determines angle (Lane, 2000) and so the same feature would produce different angle signatures at different scales. The second reason is that the output from the morphometric could not be interpreted in relation to existing theories on self-organisation because a causal relationship between slope angle, form and self-organisation has not been defined. The only theoretical frameworks that the results would fit into would be conventional geomorphological ones such as braiding indices and confluence-diffluence spacing and the angle based recognition approach would not necessarily enhance our understanding of these. Lastly, the focus of much of this thesis has been on sediment dynamics and a morphometric based on angles does little to advance our understanding of this.

Fractal approaches offer more scope because scaling issues are important within conventional fluvial geomorphology and within self-organisation theory. Sapozhnikov and Foufoula-Georgiou (1996, 1997) used planimetric data based on extent of inundation to establish the fractal dimensions of braided river networks. The method for determining the fractals is defined in Sapozhnikov and Foufoula-Georgiou (1995) and is based around a Sierpinski Carpet (**Figure 6.2**), a rectangular version of the original, triangular Sierpinski sieve. The Sierpinski Carpet works by defining the number of cells (analysis is raster based) in the object under investigation that intercept with the solid area at a range of scales. As the scale of the carpet is reduced then the number of intercept cells increases. A morphometric for determining the fractal dimensions of three-dimensional topographic data would need to adapt the Sierpinsky carpet to analyse the third dimension making what could be termed a Sierpinski Cube.

There are practical reasons why a morphometric defining fractal dimensions from three-dimensional data would be problematic. These concern the limited number of scales that can be effectively represented by the three-dimensional fractal approach. The grid cell size of the DEM in this study is 0.5 metres and this would be the finest scale defined by the Sierpinski cube. The largest morphological features occurring on the Feshie are tens of metres in dimension and this would represent the effective largest scale defined by the Sierpinski cube. The difference between the smallest and largest cube is, in scaling terms, very small incorporating at most two orders of magnitude. The planimetric approach employed by Sapozhnikov and Foufoula-Georgiou (1996,1997) can cover a greater range of magnitudes because two dimensional raster data can be accurately defined at very small scales and this is not then subject to the aggregation necessarily involved in photogrammetric techniques. There are also practical problems surrounding the implementation of three dimension fractal analysis and these mean any new fractal method would need to undergo extensive, well documented testing before it is deemed reliable. Sapozhnikov and Foufoula-Georgiou (1995) used exactly this approach focusing large amounts of research time on overcoming the complexities of defining a valid method for defining planimetric fractal dimensions but offering very little discussion of the techniques for acquiring the planimetric data or the validity for using inundated area as the parameter to be analysed.

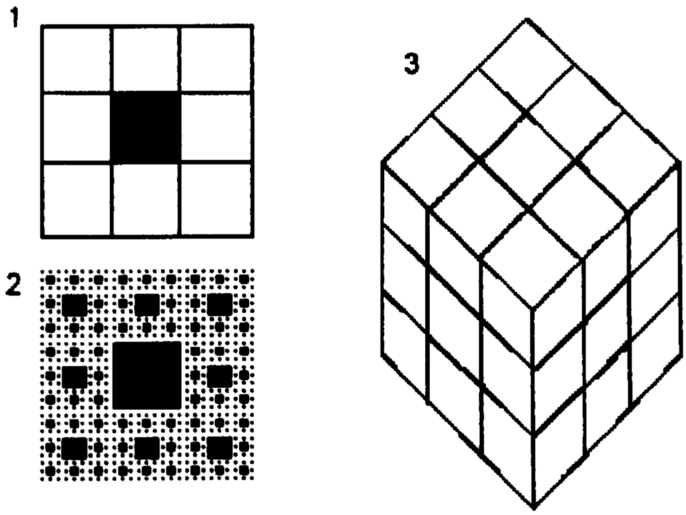

Figure 6.2. 1) the generator of a 3×3 Sierpinsky carpet with one square taken out (solid area) and (2) the Sierpinsky carpet used for defining the fractal dimension of 2 dimensional raster data. Taken from Sapozhnikov and Foufoula-Georgiou (1997). 3) The generator of a Sierpinsky Cube, a hypothetical structure for defining the fractal dimension of 3 dimensional data such as DEMs. The cube taken out (solid volume) is the single cube in the centre.

The morphometric that is implemented in this chapter is Mean Bed Level (MBL) derived from cross sectional transects of the DEM (**Equation 6.1**). MBL equals the mean average elevation value calculated using all the values in a cross stream transect. A series of MBL values gives an indication of downstream fluctuations in elevation. There are compelling reasons why a series of derived MBLs is a useful morphometric for quantifying the self-organisation imprinted on static form. These are detailed more fully below. The MBL morphometric is based on the assumption that the river organises itself from upstream to downstream . This assumption has been made by other researchers adopting a systems based approach (Paola and Foufoula-Georgiou, 2001) The lateral instability, that is characteristic of braided rivers, is accounted for by a number of channel classifications that determine the width of each transect. The exact nature of the channel classifications is discussed in **Section 2.3.0.**

$$MBL(y) = \frac{1}{n} \sum_{X=1,n}^{n} (z(x))$$ **Equation 6.1**

Where

MBL(y)= MBL for a given transect

Z = elevation

n= the width sample index. Its values are $n=0, 1, 2....,N-1$.

There are two conventional geomorphological justifications that support the use of MBL as a morphometric. The first is to consider MBL in relation to the conveyance of sediment from upstream to downstream. **Chapter 2** describes many of the issues surrounding bedload transport. Experimental studies have been particularly effective at showing the temporal fluctuation of sediment transfer by measuring sediment output from physical models (Ashmore, 1991). One conceptualisation is that temporal fluctuations will be represented by similar spatial fluctuations as the sediment is conveyed through the physical model. Indeed it is this morphological form resulting from sediment transfer on which the morphological method of quantifying sediment budgets (Neill 1969, McLean and Church, 1999) is based. There are many uncertainties associated with this conceptualisation not least because no data have been collected to directly link spatial fluctuations in MBL with temporal fluctuations in sediment volume. It is by no means certain that spatial fluctuations in MBL propagate downstream, although studies of sediment waves show that this does occur in the case of singular increases in bed level caused by the passage of single waves (Lisle *et al.*, 2001). The second geomorphological justification is to use MBL as a (more) accurate method for defining specific length scales over which the system operates. These may correspond to specific morphological units such as confluence –diffluence units or chute –pool units. These units have been extensively studied as individual units as part of the reductionist approaches adopted within fluvial geomorphology (Ashworth *et al.*, 1992; Davoren, 1986; Ferguson *et al.*, 1992) but they have also been characterised by system scale planimetric studies using concepts like braiding indices (Brice, 1964) or quantitive indices (Rust, 1978; Howard *et al.*, 1970). Deconstruction of the MBL series could define specific wavelengths associated with morphological units and in doing so provide evidence for the scale specific operation of certain processes in the system.

Studies investigating SOC have also produced theoretical arguments and evidence that support the use of MBL as a morphometric. The most notable of these is Frette *et al.* (1996) investigation of the SOC of rice piles. The rice pile systems were formed between 2 glass plates with an aperture that varied between model runs. The magnitude and frequency of avalanches within the rice pile were found to conform to an inverse power law suggesting that the system was SOC. Crucially the cross sectional forms of the rice pile were also analysed and these were shown to be scale invariant and fractal. This finding is important because it establishes a link between the fractal static form of SOC systems, defined using cross sectional elevation, and the dynamic behaviour of SOC systems, defined using avalanche magnitude and frequency. The cross sectional measurements of the rice pile experiment are a useful analogy to the MBL morphometric. MBL sequences represent a single static form, which, if shown to be fractal, could be indicative of a system that tends toward SOC. However, fractal scaling in a small number of MBL sequences cannot be taken as proof of SOC because SOC is a dynamic state requiring large numbers of sequential sediment movement events to prove its existence.

There are a number of potential problems in application of the MBL morphometric. Firstly, the cross sectional averaging results in the loss of a lot of elevation information that describes the lateral processes that are at work in the braided river system. There is a question as to how MBL can represent the self-organisation of the system. Braided river systems have a number of low flow diffluences where there is a large angle (120 to 150 degrees) between the diffluence channels. These channels often lose elevation rapidly after the diffluence but because most of this elevation is lost quasi parallel to the MBL transect this strong lateral effect is not evident in the resultant MBL. This strong lateral component is not present in established SOC systems such as rice piles. This question is best answered by considering the background to this thesis. The MBL morphometric is not an attempt to illuminate the workings of process form interactions at the small scale, it is designed to show large scale self organisation of the entire system. This means that many of the visually striking elevation changes visible in the field are cancelled out over the width of the transect but elevation changes over several hundred metres resulting from self organisation of channel form and bed level might be identified. Lateral scaling properties can never be addressed by MBL, this would take a three dimensional fractal approach.

The second problematic issue relates to anabranching channels. There are anabranching channels on the field site that become detached from the main channel for large distances (>200m) and in some cases develop very different localised bed slopes to the main channel. Should these be considered part of the system given that once developed they only interact with the main channel at the confluence and the diffluence? The answer is that clearly anabranching side channels are part of the system because they were not formed in a void but resulted from the operation of the system. This holistic approach is in keeping with systems analysis approaches, which do not attempt to explain and analyse small sections of the morphological makeup of the system but accept each small section to be the result of the functioning of the wider system.

6.2.2 Deriving transect width

Defining the cross sectional width from which MBL should be derived is an issue that needs careful consideration. If the patterns of fluctuations of MBL are to be used as indications of real self organisation it is important that the cross sectional widths (from which MBL is derived) enclose the full area of the active system. The extent of the active system is itself a point of debate that is largely dependent on the research paradigm adopted. A narrow definition of the active system would classify areas in which sedimentary movement occurred over a small timescale (annual). Over longer timescales sedimentary movement occurs over a larger area classifying a larger part of the channel and floodplain as the active system. This definition is good if sedimentary budgeting is the aim of research.

This study however is approaching the problem of defining the active width from a systems scale background that emphasises the apparent self-organisation demonstrated by complex systems. A suitable definition for the active system is: the area over which the system is organising itself. The area over which the system is organising itself is dependent on what timescale is being considered because over very long timescales the entire braid plain is active whilst at the shortest of timescale only areas where clasts are moving are active. If this second definition of the active system is adopted then the classification problem has changed in character. If it is accepted that the extent of the active system is dependent on the temporal scale of enquiry then a range of practical problems are encountered defining the active system for any given temporal scale. These practical problems arise because it is difficult to determine when specific bars or channels were last active parts of the system.

6.2.3 Defining 'active system' classifications

The River Feshie contains very little evidence from which to determine when specific channels or bars were last active. Most of the evidence available comes from the succession of vegetation on bar tops, which is spatially inconsistent. Vegetation succession is not only reliant on the topographic stability (length of time since reworking) but also the quality of the substrate, moisture availability and seed dispersal. These factors inevitably reduce the reliability of vegetation as a dating method for topographic activity. Despite these inconsistencies in colonisation rates vegetation remains the best measure of activity over a spatially extensive area partly because it can be determined accurately using remote sensing methods. Rumsby *et al.* (2002) successfully classified the River Feshie braidplain at the fieldsite into six classifications using maps and APs defining the channel, exposed sediments, vegetated gravel and palaeochannels.

This thesis used digital image analysis of orthophotographs (RGB images produced as part of the photogrammetric process (**Chapter 4**) to define four 'active system' classifications (**Figure 6.3**). These classifications suffered from many of the problems associated with the Submerged Classification (described in **Chapter 4 Section 5.5**) in particular differences in the photograph exposures. The classifications were extensively manually edited using observations and photographs collected in the field to improve their contiguity and remove erroneous sections not linked in to the main channel distributary system. The narrowest classification is the Submerged classification. This is the same classification used to define the submerged zone during the photogrammetric post processing procedures (**Chapter 4 Section 5.5**). Classification 1 is a very active zone adjacent to the Submerged classification, it is defined by areas of exposed gravel and sediment that have no vegetation and where the gravel is bright in colour. Classification 2 is a less active zone where small amounts of vegetation are established and the gravel is more weathered indicating less recent activity. Classification 3 incorporates areas that are more vegetated than Classification 2. It is also fundamentally different to the other classifications because all island areas (areas surrounded by the other classifications) are included even if they are fully vegetated. This means that Classification 3 is the best representation of the wider floodplain and the longest temporal scales of activity.

6.2.4. Division of the system

Before MBL was extracted a further processing step was required- division into two sub systems- to ensure the reliability of the MBL derivations. There are two reasons why this division was useful. Firstly the valley scale meander bend in the reach means that different parts of the channel are oriented differently according to where they are situated on that bend. This causes problems because the MBL extractions must be taken approximately perpendicular to flow so any extraction method that attempts to deal with the reach as a whole must incorporate this by straightening out the bend in the DEM by either stretching the inside of the bend or compressing the outside of the bend. Such an adaptation to the data is highly questionable and would fundamentally alter its character. Alternative sampling methods based on twisting of the MBL extraction cross sections would have a similar effect. A more appropriate solution is to divide the system into two sub-systems and then rotate and analyse these independently.

Study of the planimetric structure of the system (**Figure 6.3**) reveals no obvious breakpoint where a division would be appropriate. The system starts off as a single channel, after 400m limited channel bifurcations occur with increasing width. After a further 800m the system has evolved into what might traditionally be termed an anastomosing channel pattern. Finally after a further 800m evolution the channel could be termed braided. None of these planform changes are associated with a specific obvious breakpoint.

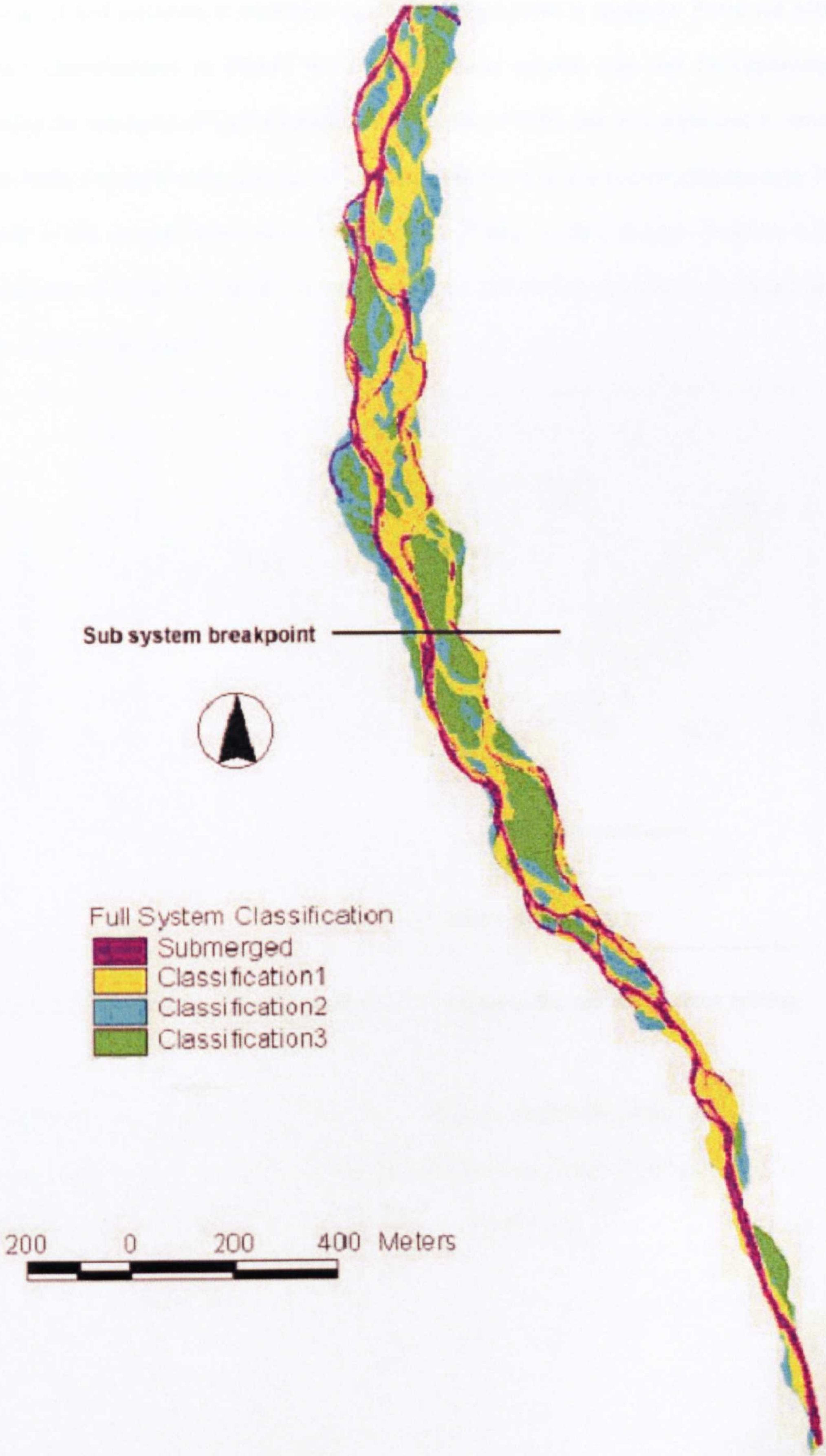

Figure 6.3 Classification of the study site river system

However, if bed elevation is examined an obvious breakpoint is apparent. Extracted MBL for the four classifications in **Figure 6.3** over the entire system may not be appropriate for analysing the subtleties of high frequency fluctuations of MBL but it is sufficient to reveal one system scale fluctuation that presents an obvious breakpoint in the system **(Figure 6.4)**. Further analysis of the system scale wave structure occurs later in this chapter **(Section 6.7)**. The discontinuity of slope that occurs at approximately 1500m downstream is a suitable point at which to divide the system.

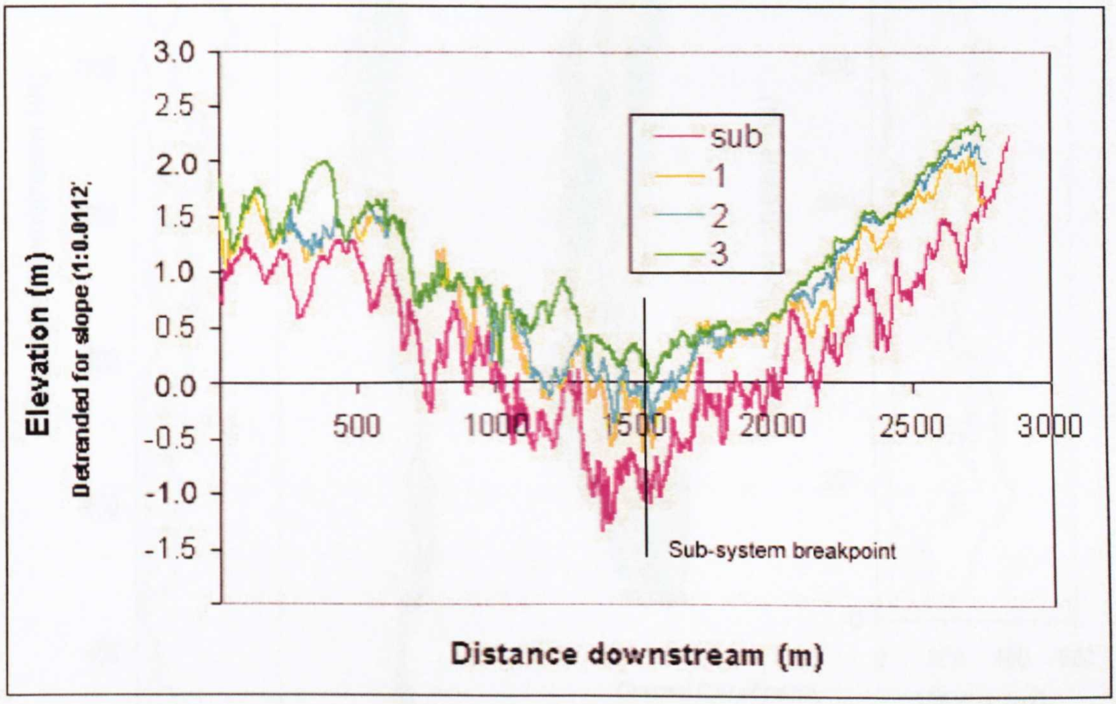

Figure 6.4 MBL derived for each of the 4 classifications for the study river system

The upstream subsystem was rotated by 25 degrees clockwise, using a nearest neighbour sampling method, to make the east to west sampling transect approximately perpendicular to the direction of flow. The resultant DEMs are shown in **Figure 6.3**.

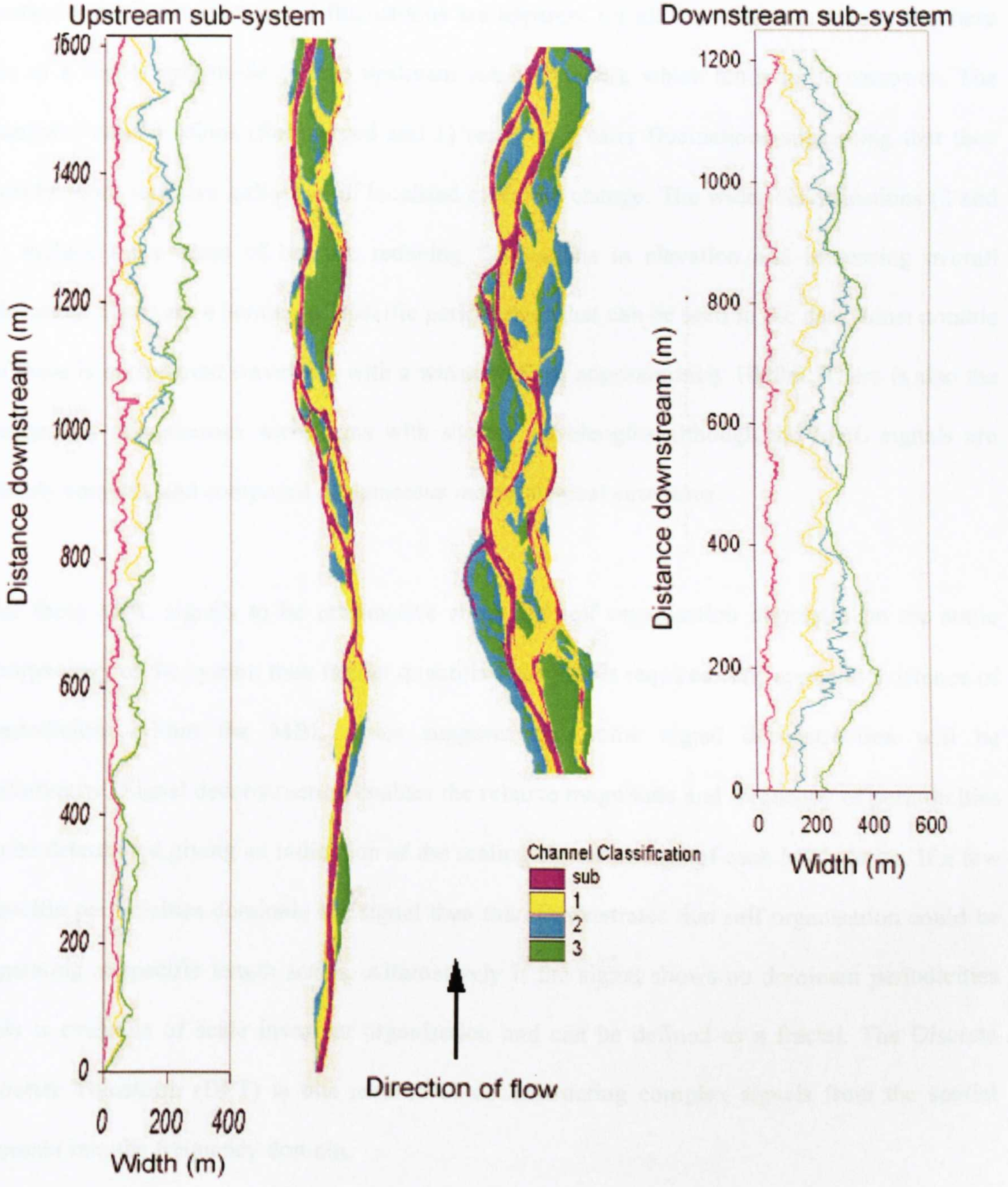

Figure 6.5 Division of the study river system into two sub-systems. The upstream sub-system (left) widens in the downstream direction. There is no trend in the width of the downstream system (right).

6.3.0 Extracted MBL data

MBL was extracted from the photogrammetric DEM using the four classifications and a downstream cross section spacing of 0.5m **(Figures 6.6 and 6.7)** the extracted MBL data show particular attributes. Structured fluctuations are apparent for all the MBL extractions but these are of a higher magnitude for the upstream sub-system (a), which tends to be narrower. The narrower classifications (Submerged and 1) result in greater fluctuations suggesting that they will be more sensitive indicators of localised elevation change. The wider classifications (2 and 3) include more areas of bar top reducing fluctuations in elevation and increasing overall elevation. There are a number of specific periodicities that can be seen in the data. Most notable of these is an apparent waveform with a wavelength of approximately 1000m. There is also the suggestion of numerous waveforms with shorter wavelengths although the MBL signals are clearly complex and composed of numerous morphological structures.

For these MBL signals to be informative about the self organisation imprinted on the static morphology of the system then further quantitive analysis is required. The apparent existence of periodicities within the MBL series suggests that some signal deconstruction will be informative. Signal deconstruction enables the relative magnitude and frequency of periodicities to be determined giving an indication of the scaling characteristics of each MBL series. If a few specific periodicities dominate the signal then this demonstrates that self organisation could be operating at specific length scales. Alternatively if the signal shows no dominant periodicities this is evidence of scale invariant organisation and can be defined as a fractal. The Discrete Fourier Transform (DFT) is one method of deconstructing complex signals from the spatial domain into the frequency domain.

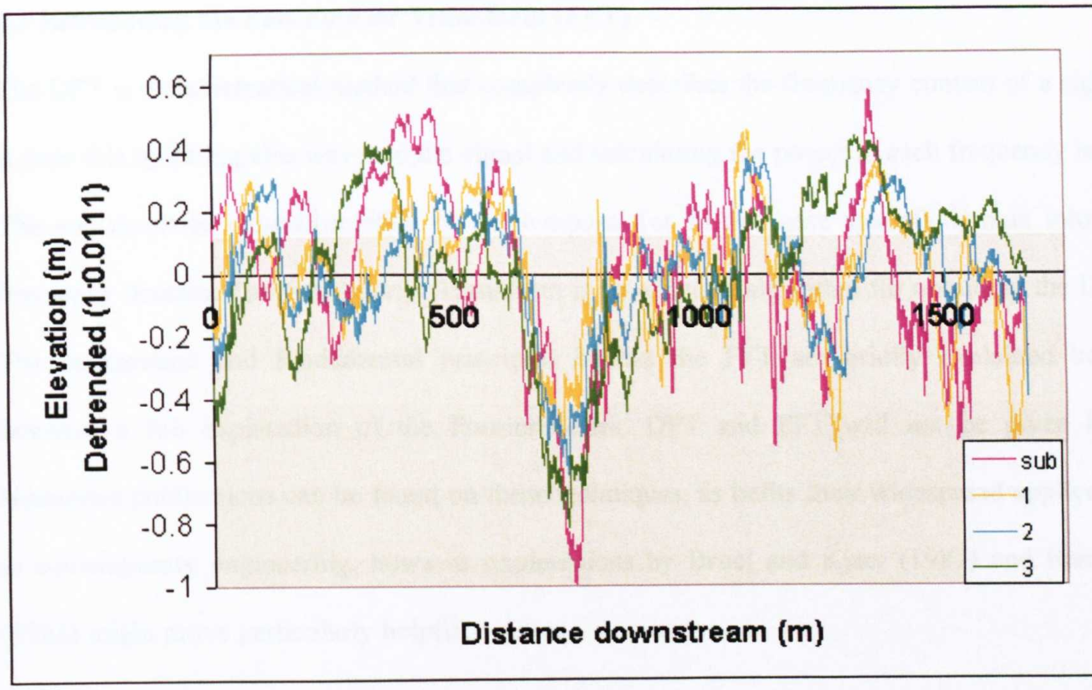

Figure 6.6 MBL extracted from the upstream sub-system

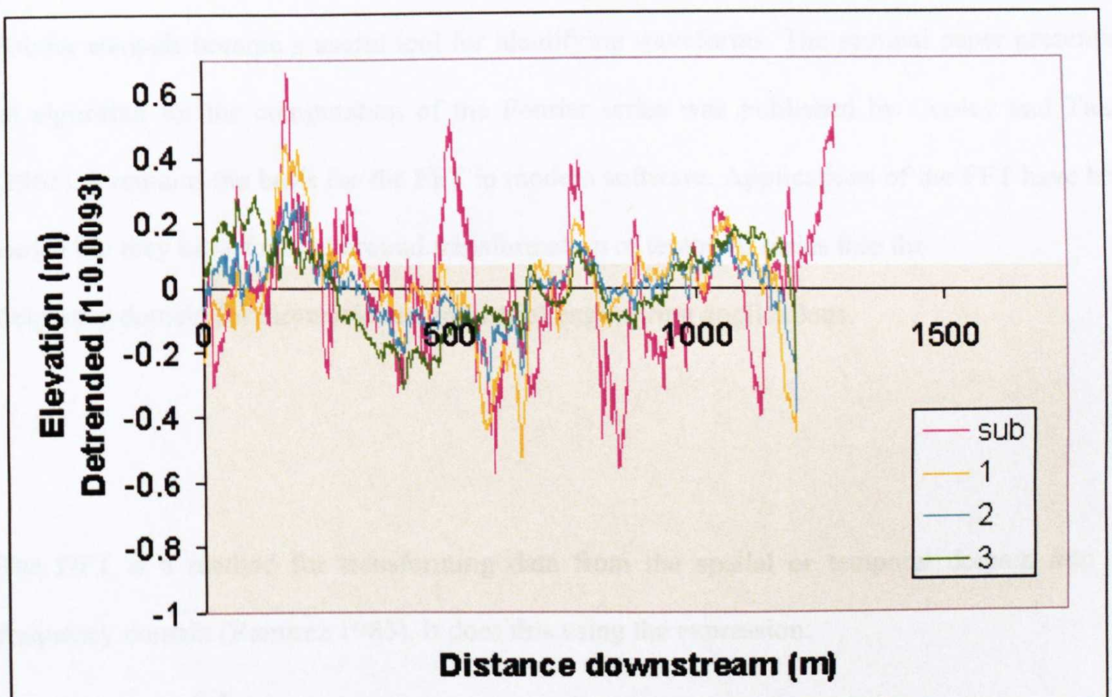

Fi

gure 6.7 MBL extracted from the downstream sub-system

6.4 Introducing the Fast Fourier Transform (FFT)

The DFT is a mathematical method that completely describes the frequency content of a signal. It does this by fitting sine waves to the signal and calculating the power in each frequency band. The end result is a transformation of the temporal (or in this case spatial) domain into the frequency domain. The Fast Fourier Transform is an efficient algorithm for obtaining the DFT. The background and fundamental principles behind the FFT are briefly explained below however a full explanation of the Fourier series, DFT and FFT will not be given here. Numerous publications can be found on these techniques, as befits their widespread application in contemporary engineering, however explanations by Bruel and Kjaer (1987) and Ramirez (1985) might prove particularly helpful.

Fourier analysis is a mature subject. The initial concepts and theory were introduced by J.B.J. Fourier in the 1800s although it was not until the 1960s, when computers became available, that Fourier analysis became a useful tool for identifying waveforms. The seminal paper presenting an algorithm for the computation of the Fourier series was published by Cooley and Tukey (1965), it remains the basis for the FFT in modern software. Applications of the FFT have been varied but they have focused around transformation of temporal series into the frequency domain for electronic and industrial engineering applications.

The DFT is a method for transforming data from the spatial or temporal domain into the frequency domain (Ramirez 1985). It does this using the expression:

$$X_d(k\Delta f) = \Delta t \sum_{n=0}^{N-1} x(n\Delta t) e^{-j2\pi k\Delta f n\Delta t}$$ **Equation 6.1**

Where:

N= number of samples being considered

Δt= the time between samples, referred to as the *sampling interval.* From this, NΔt gives the window length, often referred to as the *time record length.*

Δf= the sample interval in the frequency domain and is equal to $1/N\Delta t$.

n= the time sample index. Its values are $n=0, 1, 2....,N-1$.

k= the index for the computed set of discrete frequency components. Its values are $k= 0,1,2,....N-1$

$x(n\Delta t)$= the discrete set of time samples that defines the waveform to be transformed.

$X(K\Delta f)$= the set of Fourier coefficient obtained by the DFT of $x(n\Delta t)$

e = the base of the natural logarithm

j= the symbol of complex notation, indicating the imaginary part of a complex quantity $(j=\sqrt{-1})$.

With the substitutions, letting $\Delta t = 1$so that $\Delta f = 1/N$, allows the derivation of the more common form of the DFT:

$$DFT : X_d = \sum_{n=0}^{N-1} x(n)e^{-j2\pi kn/N}$$ **Equation 6.2**

The complex exponential is then changed using *Euler's identity* ($e^{\mp j\theta}=\cos\theta \mp j\sin\theta$) to give the DFT as:

$$X_d(k) = \frac{1}{N}\sum_{n=0}^{N-1} x(n)\frac{\cos 2\pi kn}{N} + jx(n)\frac{\sin 2\pi kn}{N}$$ **Equation 6.3**

It is now possible to compute the DFT for any string of waveform samples.

The FFT is a method for calculating the DFT using a greatly reduced number of arithmetic operations. The increased efficiency of the FFT is achieved in a number of ways but the most important of these is the factorization of the matrix version of **Equation 6.3.** into a number (log_2

N) of individual matrices (Ramirez, 1985). The organization of the FFT for a 16 point FFT is shown in **Figure 6.8.**

The data are gathered into successively smaller groups at each stage. This transformation continues until there is one datum per group. This is referred to as the decimation in frequency (Ramirez, 1985).

6.4.1 Testing of the FFT

The FFT was applied to the project data using the FFT function in Matlab (Version 6.5). The software was extensively tested to ensure that the output in the frequency domain was correct. In particular combinations of sine waves with known amplitude, wavelength and phase were processed and the outputs assessed. **Figure 6.9 (a)** shows a data series that is composed of 3 wave forms with identical wave amplitudes but different wavelengths. When this is processed using the FFT the amplitudes and wavelengths are correctly identified **(b).** The shortest wavelength is at (1), this appears as a spike because adjacent wavelengths correctly have an amplitude of zero. The middle wavelength is at (2), this appears with a slope down to the adjacent shorter wavelength because this has an amplitude of zero. However the larger adjacent wavelength (3) has an identical amplitude and so (2) and (3) are joined with a horizontal line.

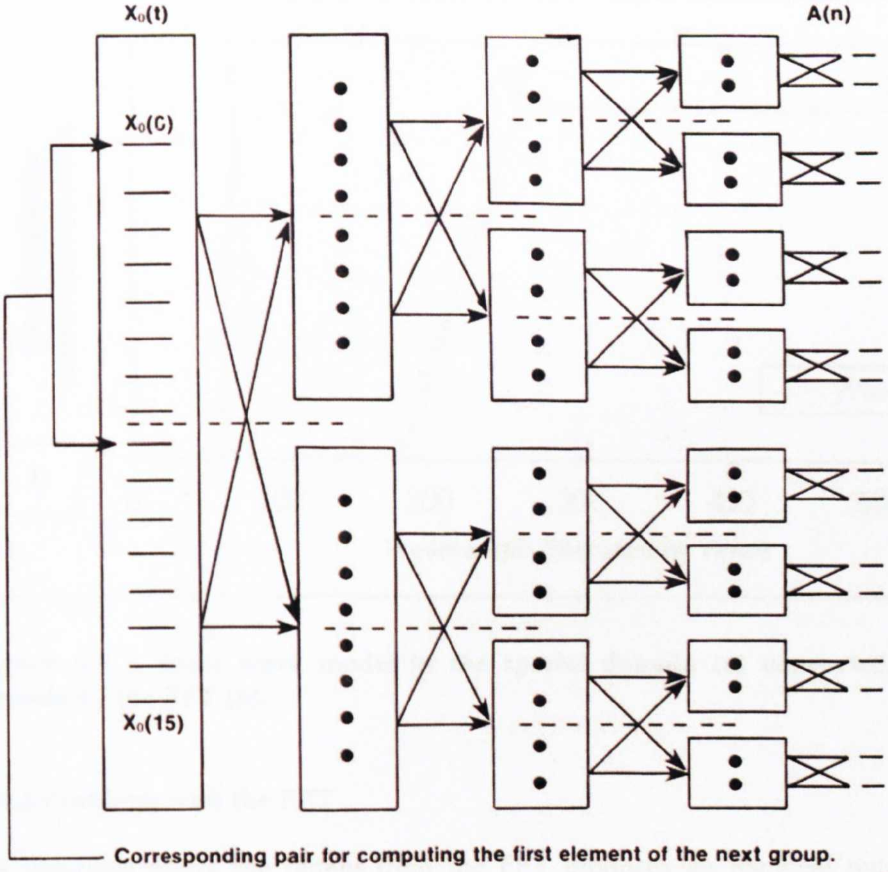

Figure 6.8. The general organization of a decimation in frequency algorithm taken from Ramirez 1985). $X_0(t)$ = the time domain data and A(n) = the frequency domain data. This structure illustrates why input data must be an even power of 2. Software such as Matlab overcomes this problem by padding the input sequence to the nearest even power of 2.

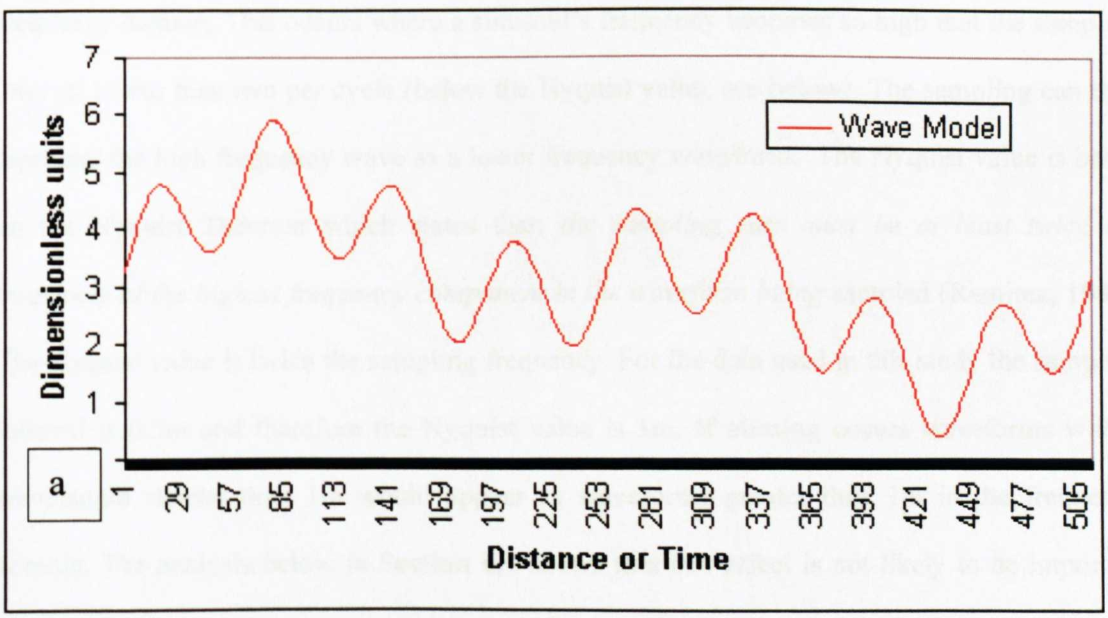

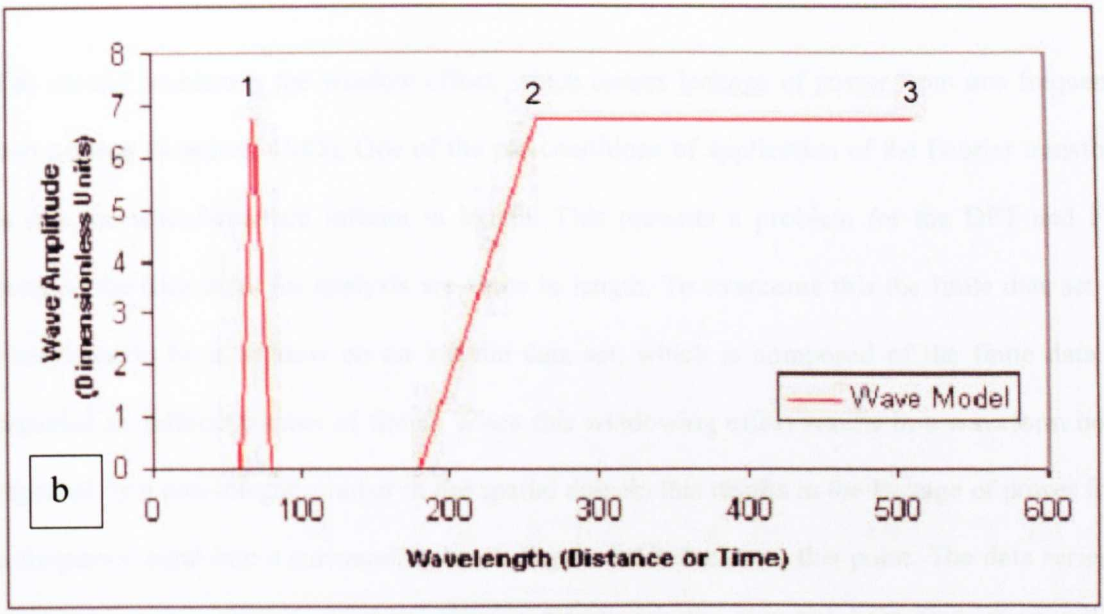

Figure 6.9 A three wave model in the spatial domain (a) converted to the frequency domain by the FFT (b).

6.4.2 Problems with the FFT

As described above the output from the FFT produces an identical outcome as the direct application of the DFT. Therefore the problems with the FFT are also those of the DFT. There are three distinctive problems with the DFT. The first problem is aliasing (Ramirez, 1985) where a very high frequency component is represented by a lower frequency component in the frequency domain. This occurs where a sinusoid's frequency becomes so high that the sampling interval is less than two per cycle (below the Nyquist value, see below). The sampling can then represent the high frequency wave as a lower frequency waveform. The Nyquist value is based on the Nyquist Theorem which states that: *the sampling rate must be at least twice the frequency of the highest frequency component in the waveform being* sampled (Ramirez, 1985). The Nyquist value is twice the sampling frequency. For the data used in this study the sampling interval is 0.5m and therefore the Nyquist value is 1m. If aliasing occurs waveforms with a wavelength shorter than 1m would appear as waveforms greater than 1m in the frequency domain. The analysis below in **Section 6.5** shows that this effect is not likely to be important because the high frequencies where aliasing effects are likely to occur contain very little power in the frequency domain and are dominated by error, so they are deemed insignificant waveforms.

The second problem is the window effect, which causes leakage of power from one frequency into another (Ramirez, 1985). One of the pre-conditions of application of the Fourier transform is that the waveforms are infinite in length. This presents a problem for the DFT and FFT because the data input for analysis are finite in length. To overcome this the finite data set are considered to be a window on an infinite data set, which is composed of the finite data set repeated an infinite number of times. When this windowing effect results in a waveform being repeated by a non-integer number in the spatial domain this results in the leakage of power from a frequency band into a surrounding band. **Figure 6.10** illustrates this point. The data series in **(a)** is identical to that processed in **Figure 6.9** except that it is extended to include a none-integer number of cycles. When this is processed the result is leakage of power (in this case amplitude) from wavelength (2) into the two adjacent wavelengths **(Figure 6.10 b).**

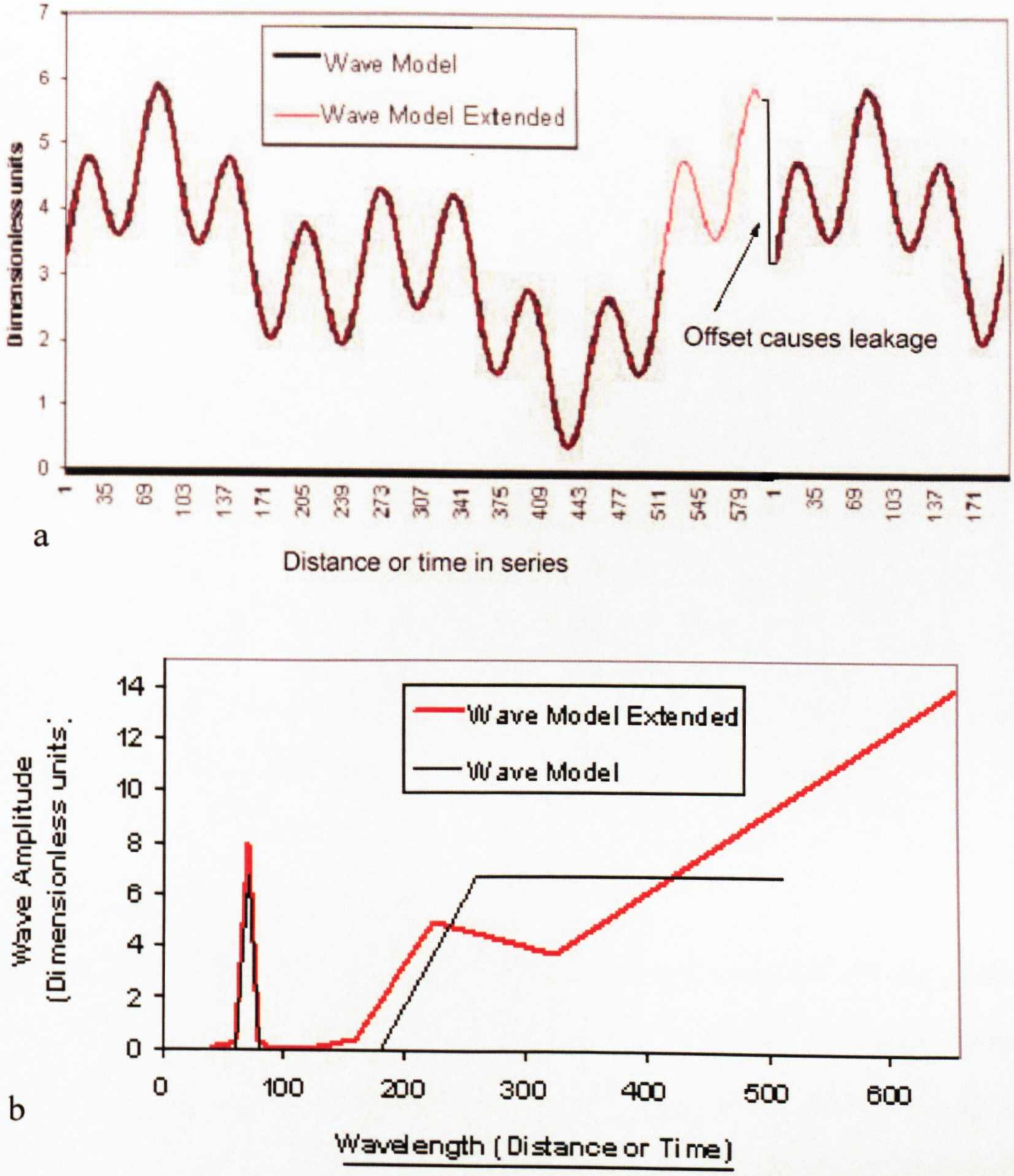

Figure 6.10 The extended three wave model in the spatial domain (a) results in leakage and a poor quality frequency domain model (b)

There are various methods that have been developed for reducing leakage (Ramirez, 1985). The simplest of these is to reduce the size of sampled data so that the start and end of the sampled data are approximately the same value **(Figure 6.10)**. More sophisticated methods involve changing the shape of the sampling window. The window used for the FFT in this thesis is a rectangular window. Windows of different shapes (Triangle, Half Cycle Sine) can be used to reduce leakage (Ramirez, 1985). These were not used in this study because they adversely affect amplitude output.

The final problem with the DFT and FFT is that the frequency components are dictated by the length of the data set that is input into the transform process. This is most evident when the results are displayed in the wavelength and amplitude form as they are in **Figure 6.10**. The longest wavelength derived is equal to the length of the data sequence input into the FFT and the second longest wavelength equal to half that. The amplitude of wavelengths between these two are not determined and this means that a very distinctive powerful waveform could be poorly defined with power from the wave spread between the upper and lower wavelengths. One way of solving this problem is to systematically change the length of the input sequence so that a range of larger wavelengths are derived. But this in turn would cause leakage problems because the start and finish of the data sequences would fall at different elevations. The length of the data input sequence was not altered in this thesis because this in turn would increase leakage because the start and finish of the data series would fail to match up.

6.4.3 Signal reconstruction using the FFT

To ensure that the FFT had been applied correctly and to demonstrate the effectiveness of the FFT process, the MBL signal for Classification 1 (truncated to reduce leakage) was reconstructed using the wavelength, amplitude and phase data output from the FFT **(Figure 6.11)**. The seven most powerful (biggest amplitude) waveforms were used in the reconstruction. **Figure 6.12** shows the first three waves separately. Addition of all seven of the waves produces a good reconstruction of the Classification 1 MBL data **(Figure 6.13)**.

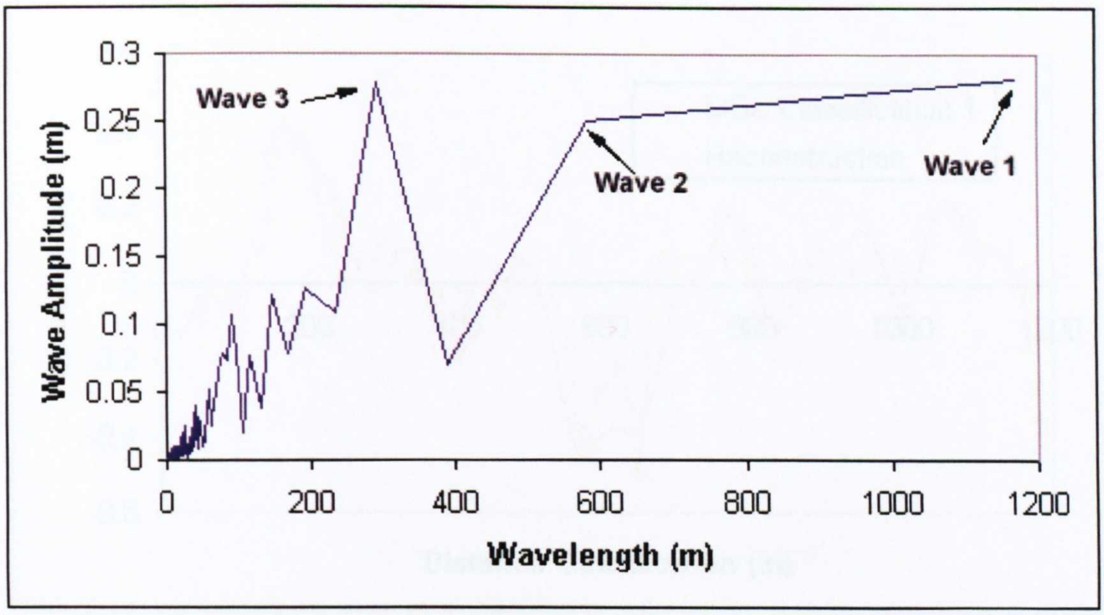

Figure 6.11 Frequency domain information for the upstream sub-system, Classification 1. The three waves with the highest amplitude are identified

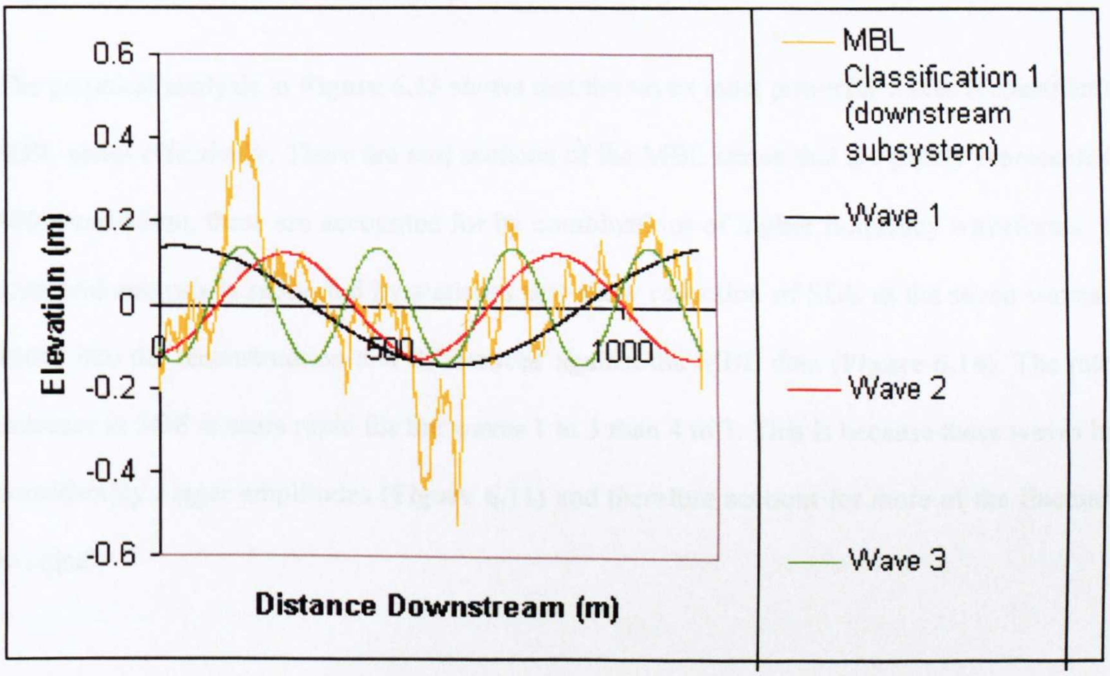

Figure 6.12 The three high amplitude waves are reconstructed using the amplitude, wavelength and phase data derived from the FFT.

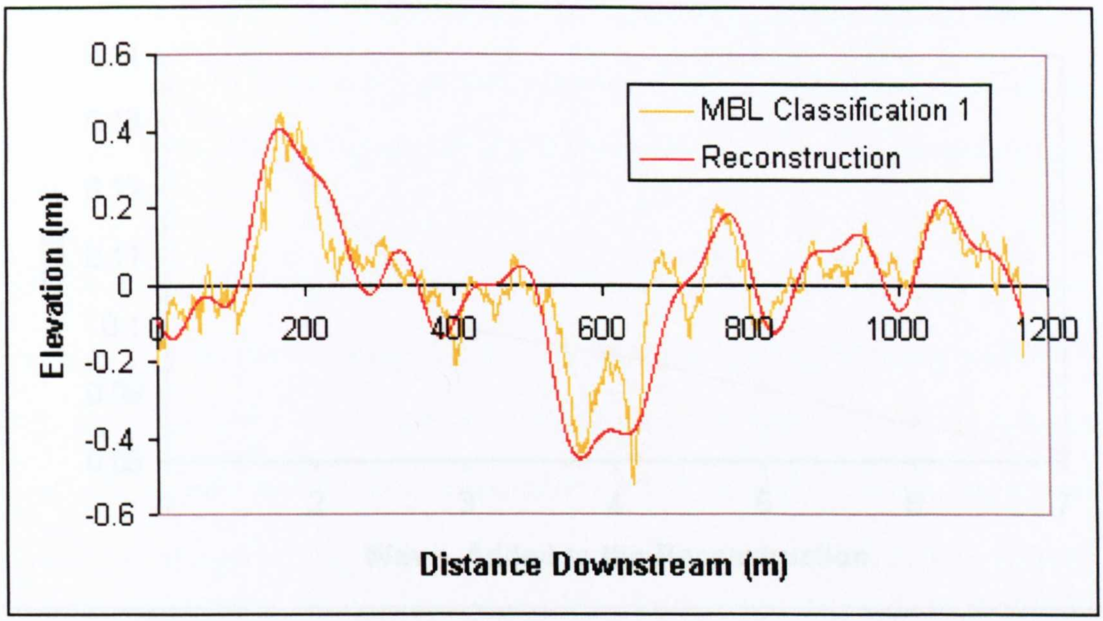

Figure 6.13 The reconstruction and MBL data. The reconstruction is the sum of the seven highest amplitude waves.

The graphical analysis in **Figure 6.13** shows that the seven most powerful waves reconstruct the MBL series effectively. There are still sections of the MBL series that are poorly represented at 600m and 680m, these are accounted for by combinations of higher frequency waveforms. The graphical analysis is supported by statistics that show reduction of SDE as the seven waves are added into the reconstruction and differenced against the MBL data **(Figure 6.14)**. The rate of decrease in SDE is more rapid for the waves 1 to 3 than 4 to 7. This is because these waves have considerably bigger amplitudes **(Figure 6.11)** and therefore account for more of the fluctuation in signal.

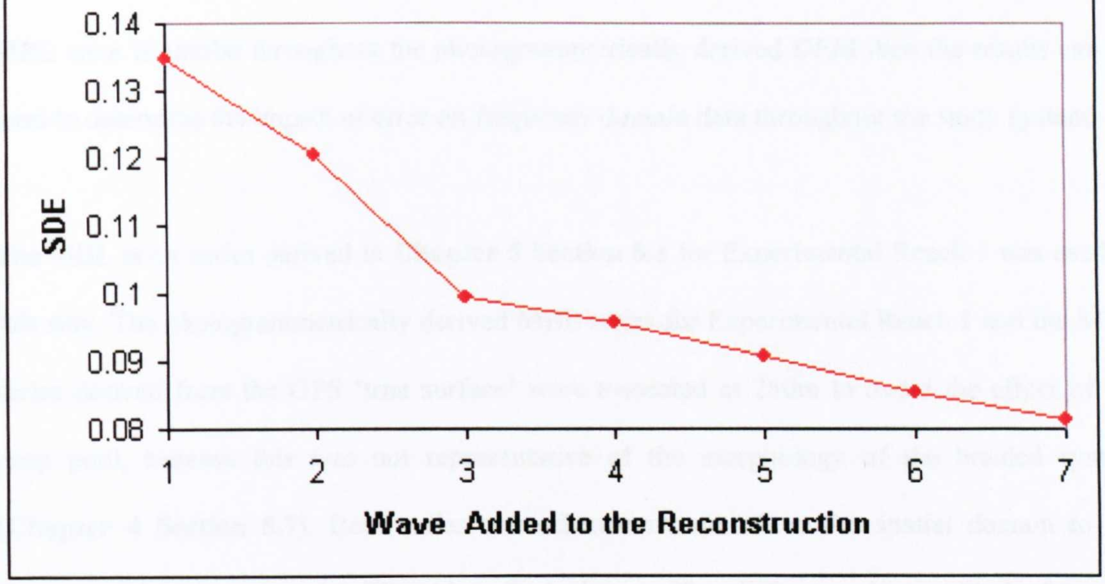

Figure 6.14 The reconstruction compared to the MBL as waveforms are added. The addition of waves results in a reduced SDE.

6.5.0. Error analysis

There are important issues that concern the introduction of uncertainty into derived amplitudes due to errors in the photogrammetric model. Error within the photogrammetric DEM will inevitably be incorporated into derived MBL but at a lesser level (as demonstrated in **Chapter 5 Section 8.1**). However there may be periodicities associated with error within photogrammetrically constructed DEMs resulting from systematic DEM tilts (partially corrected for in **Chapter 4 Section 5.12**). This idea was examined in **Chapter 5** using a spatially extensive check data set that defined the structure of error over the entire photogrammetric DEM. There was no apparent correspondence between fluctuations in error and MBL series although the limit size of the check data set inhibited formal statistical analysis.

The other error analysis of MBL in **Chapter 5** provides a more reliable method for defining the impact of photogrammetrically induced errors. The use of the GPS derived DEM as a 'true surface' against which to test the photogrammetrically derived DEM gave a good indication of the structure and magnitude of error incorporated into MBL when derived from the photogrammetric DEM (**Chapter 5 Section 8.2**). If this structure and magnitude of error is analysed using the FFT it gives an indication of the significance of error in a photogrammetrically derived MBL series. If it is assumed that the structure and magnitude of MBL error is similar throughout the photogrammetrically derived DEM then the results can be used to determine the impact of error on frequency domain data throughout the study system.

The MBL error series derived in **Chapter 5 Section 8.1** for Experimental Reach 1 was used in this way. The photogrammetrically derived MBL series for Experimental Reach 1 and the MBL series derived from the GPS 'true surface' were truncated at 250m to avoid the effect of the deep pool, because this was not representative of the morphology of the braided system (**Chapter 4 Section 5.7**). Both series were then converted from the spatial domain to the frequency domain using the FFT (described above). The difference in amplitude for each derived frequency was calculated by subtracting the 'true surface' amplitudes from the photogrammetric surface amplitudes (**Figure 6.15**). **Figure 6.15** is a measure of the amplitude of periodicities introduced into the frequency domain by the errors associated with photogrammetrically derived MBL. This demonstrates that the magnitude of error in MBL changes very little over a number of orders of magnitude.

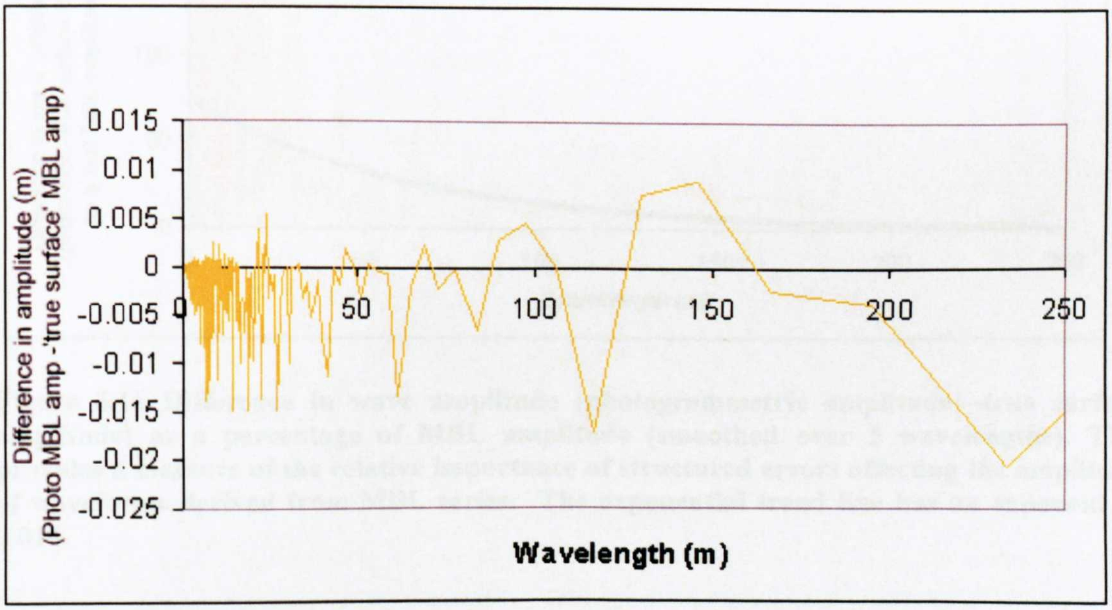

Figure 6.15 Difference in wave amplitude (Photogrammetrically derived MBL amplitudes – 'true surface' derived MBL amplitudes). The result shows the impact of photogrammetrically induced error on derived periodicities.

Figure 6.15 is not a comprehensive way of viewing the change in amplitude resulting from photogrammetrically induced error because it fails to take into account the magnitude of difference in amplitude relative to total amplitude. As wavelengths decline then amplitudes also tend to decline **(Figure 6.11)** and so the errors in amplitude need to be put in relative terms. **Figure 6.16** achieves this by putting the difference in amplitude relative to total amplitude (smoothed over 5 wavelengths). **Figure 6.16** shows that in general the importance of error on the amplitude of derived wavelengths decreases as wavelengths increase. The exponential trend line describes this trend. Less than 5% of the amplitude of wavelengths over 200m is attributable to error, approximately 40% of amplitude is attributable to error for 50m wavelengths and in excess of 70% for wavelengths less than 10m. There are some exceptions to this pattern, the spike in error for the 130m wavelength accounts for 50% of the magnitude of the derived MBL waveform. For wavelengths shorter than 65m there are increasing numbers of error spikes suggesting that the derived MBL amplitudes are less reliable. This is interpreted as a cut-off wavelength below which amplitudes are dominated by error.

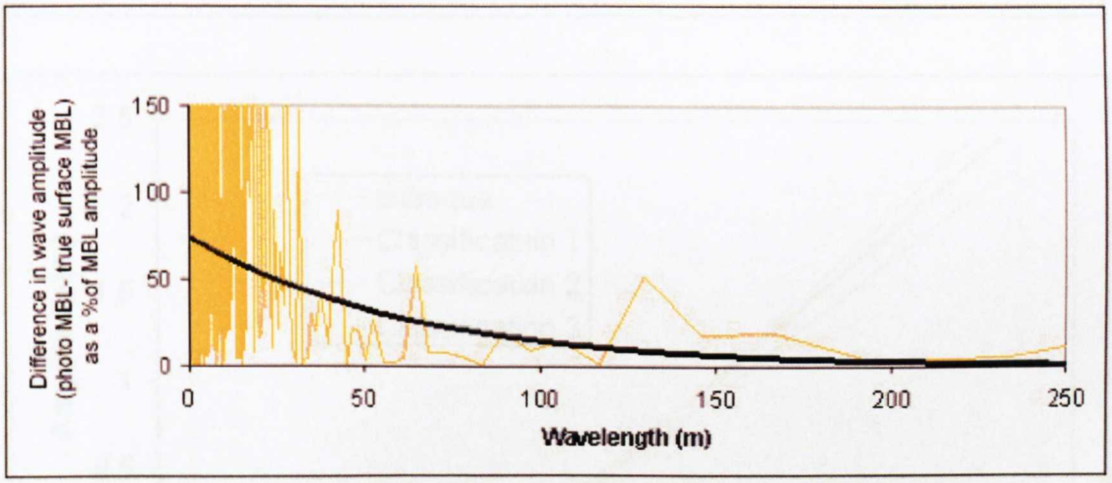

Figure 6.16 Difference in wave amplitude (photogrammetric amplitude –true surface amplitude) as a percentage of MBL amplitude (smoothed over 5 wavelengths). This provides a measure of the relative importance of structured errors affecting the amplitude of waveforms derived from MBL series. The exponential trend line has an exponent of 0.016.

6.6.0 Application of the FFT

The FFT was initially applied to the MBL derived from the full braided system. These data show a single distinctive wave structure that dominates the MBL **(Figure 6.16 a)**. The results from the FFT show this very clearly (**Figure 6.16b**). All classifications show that the longest wavelength (approximately 2700m) has significantly larger amplitude than any of the other wavelengths. The shorter wavelengths were investigated via division into two subsystems (upstream and downstream) for the reasons described in **Section 6.2.2**

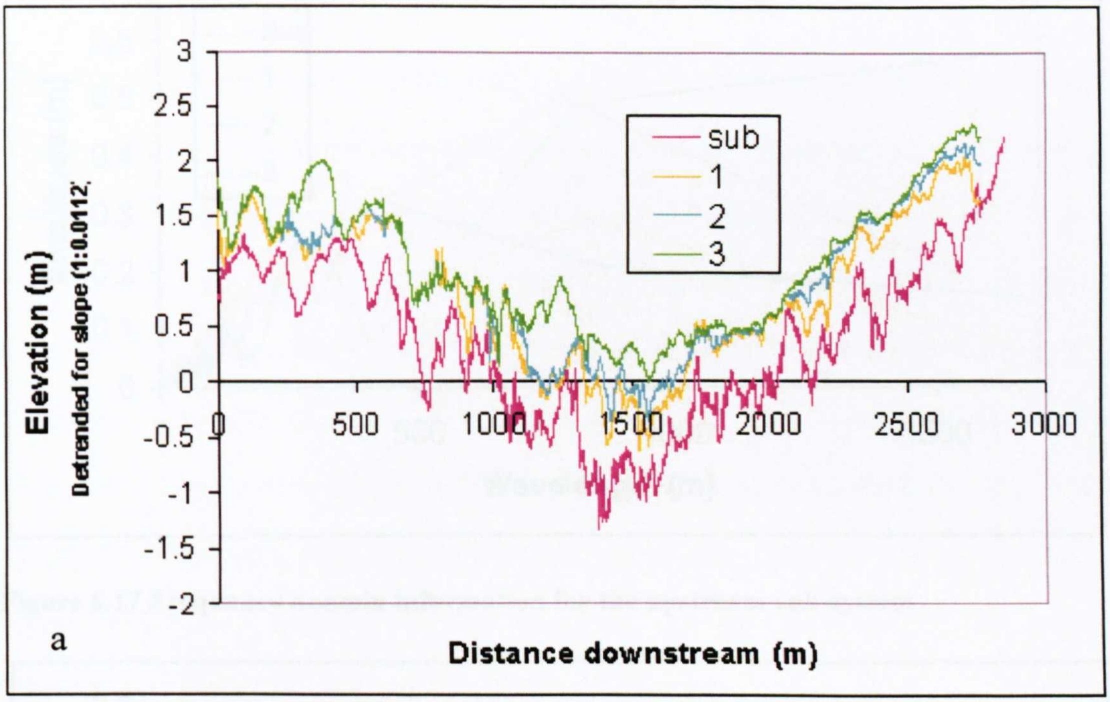

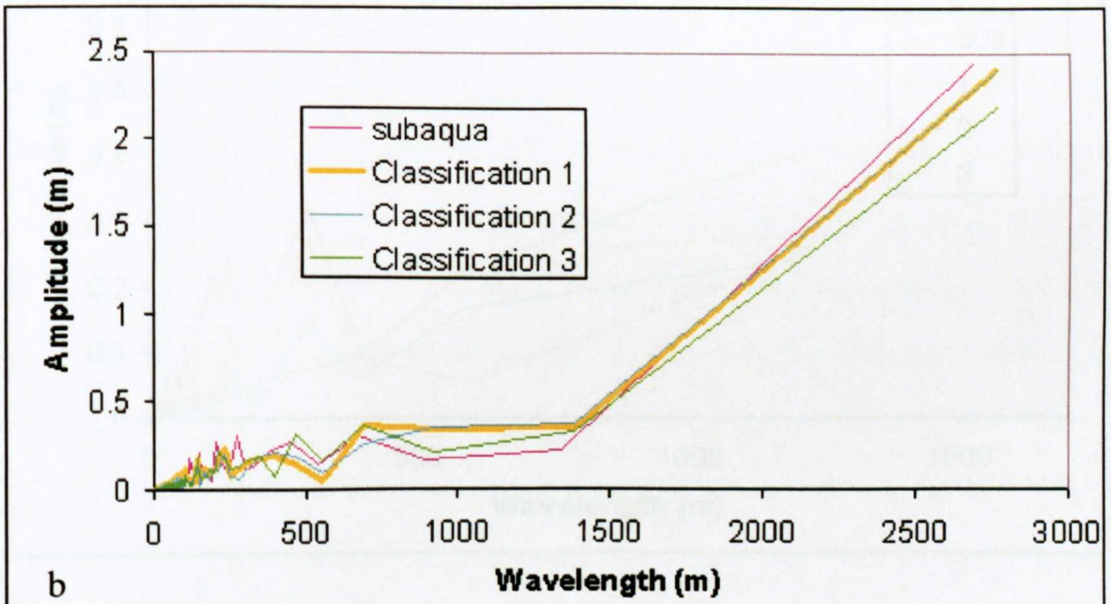

Figure 6.16 MBL series for the full study system (a) and the derived frequency domain (b). The 2700m wavelength is the dominant periodicity.

The FFT analysis of the sub-systems gives a better indication of the shorter wavelengths that are present in the MBL data. Each MBL series was truncated as suggested in **Section 6.4.2** so that the start and finish were approximately the same elevation value because this reduces leakage and increases the quality of the FFT results.

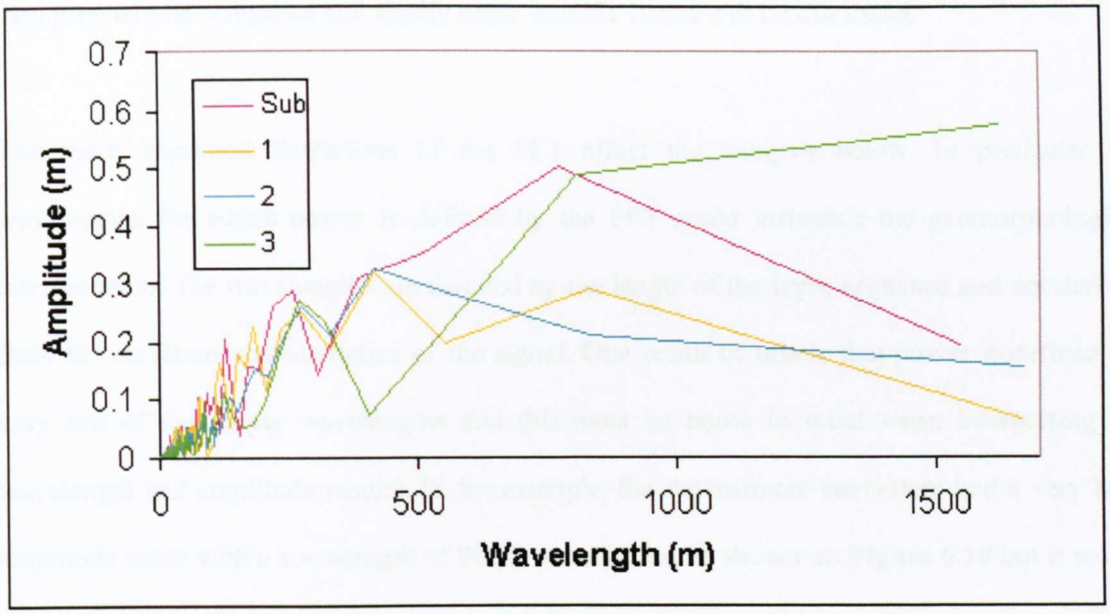

Figure 6.17 Frequency domain information for the upstream sub-system

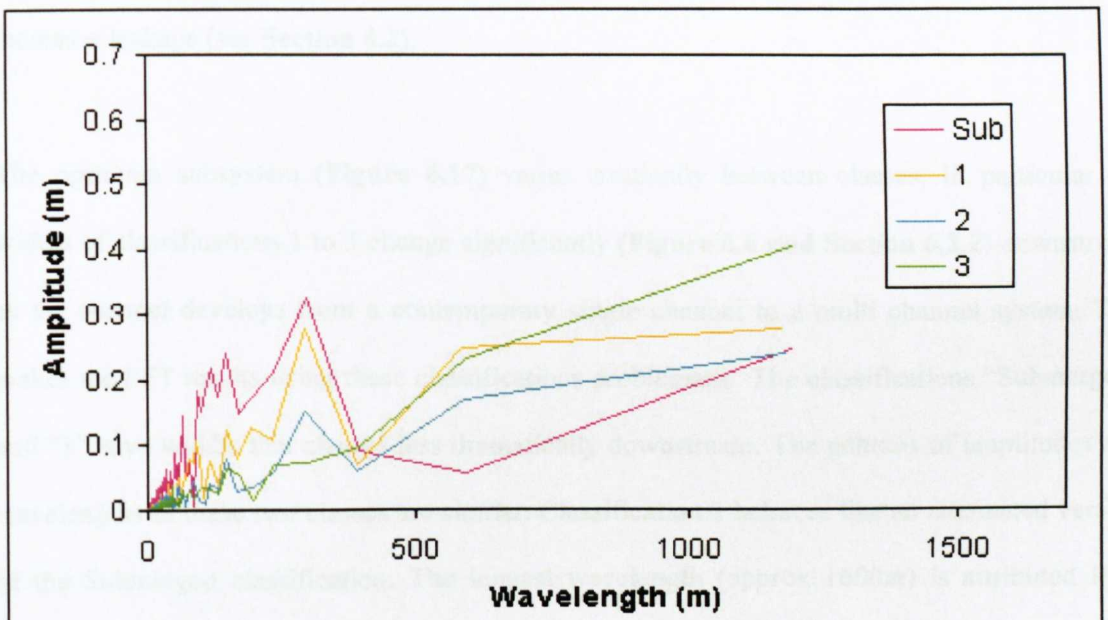

Figure 6.18 Frequency domain information for the downstream sub-system

6.6.1 FFT results

The results of the FFT process are shown in **Figures 6.17 and 6.18.** In this section the frequency domain results for the upstream and downstream system will be described separately then they will be compared and finally some specific issues will be discussed.

The more important limitations of the FFT affect the analysis below. In particular the wavelengths for which power is defined by the FFT could influence the geomorphological interpretation. The wavelengths are dictated by the length of the input sequence and not derived from the elevation characteristics of the signal. One result of this is that power is defined for very few of the longer wavelengths and this must be borne in mind when interpreting the wavelength and amplitude results. If, for example, the downstream subsystem had a very high amplitude wave with a wavelength of 900m it would not be shown on **Figure 6.18** but it would increase the amplitude of the 1200m and 600m wavelengths. This problem cannot be solved unless the length of the input sequence is altered, however this is not possible because it increases leakage (see **Section 4.2**).

The upstream subsystem **(Figure 6.17)** varies erratically between classes. In particular the widths of classifications 1 to 3 change significantly **(Figure 6.6 and Section 6.2.2)** downstream as the channel develops from a contemporary single channel to a multi channel system. This makes the FFT results using these classifications problematic. The classifications "Submerged" and "1" have widths that change less dramatically downstream. The patterns of amplitudes and wavelengths of these two classes are similar. Classification 1 behaves like an attenuated version of the Submerged classification. The longest wavelength (approx 1600m) is attributed little amplitude but the next wavelength down (approximately 750m) is a dominant wavelength attributed an amplitude of 0.5m (submerged) and 0.3m (Classification 1). A second dominant wavelength is at approximately 450m which is attributed an amplitude of 0.35m for both classifications. The last dominant wavelength is common to all four classifications and is at approximately 300m where amplitude is raised to over 0.25m. There are a number of lesser amplitude spikes at shorter wavelengths predominantly in the Submerged classification.

The downstream subsystem **(Figure 6.18)** has a pattern of wavelength and amplitude that is more coherent than the upstream subsystem. The widest "Classification 3" has higher amplitudes for the longer wavelengths but at the 400m wavelength this reverses and the narrower "submerged classification" has systematically higher amplitudes. This reversal of dominant wavelengths is to be expected. It shows that the short wavelengths described by the Submerged classification are limited in lateral extent because they are only present at a reduced level in the wider classifications. The narrowest, Submerged Classification, is dominated by high amplitudes at shorter wavelengths, which drown out the signal produced by longer wavelengths reducing their amplitude. Classification 1 is the best overall classification because it incorporates many of the high amplitude spikes at both long and short wavelengths. Similar to the upstream subsystem there is a pronounced spike at 300m for all classifications except "Classification 3".

The differences in the structure of the wavelength and amplitude between the upstream and downstream subsystems are best explained by considering the structure of the classifications for each **(Figure 6.6)**. In the upper section of the upstream sub-system the active channel is narrow. As the channel begins to braid, Classifications 1 to 3 begin to increase as the active channel widens, changing the nature of elevation fluctuations included in the MBL classification. This makes the use of the FFT problematic because the FFT generates a set of waves with fixed amplitude and frequency that describe the power present in the whole data set input into the process. If the nature of the fluctuations in MBL is changing within the data set input into the process then the FFT will not account for this. The result is that the changing nature of the morphology of the upstream subsystem produces an erratic FFT output in which it is difficult to determine patterns of wave structures that dominate each classification. In contrast the downstream subsystem exhibits multi channel behaviour throughout and the widths of each classification change little (**Figure 6.6**). The output of the FFT is better structured with larger wavelengths dominated by wider classifications and shorter wavelengths dominated by narrower classifications. One interpretation of this is that the FFT is more suited to describing the statistically more stationary morphology of the downstream subsystem. An alternative interpretation is that the better organisation of the downstream subsystem is more appropriate for the classification system to define and this means that the patterns in the wave structures produced by that organisation are better defined.

The distinctive increase in amplitude at the 300m wavelength is apparent in both the up and downstream subsystems and for a number of the classifications. It is better defined in the downstream subsystem where it is best represented on the narrower classifications (Submerged and 1) although it does not occur for Classification 3. One possible cause of this distinctive increase in amplitude is the photogrammetric method of deriving the DEM from which the MBL is extracted. This is possible because each of the DEMs input into the DEM mosaicking process was approximately 300m in length and systematic errors in these surfaces could cause a false periodicity to occur when the data is transformed using the FFT. This explanation is unlikely for two reasons. Firstly, DEMs from which the MBL data were derived were corrected using a number of procedures (**Chapter 4**) including systematic correction of individual DEMs and a final correction surface. The quality of the finished DEM was shown to be very high (**Chapter 5**) and the analysis against independent check data at the system scale (**Chapter 5**) showed no 300m periodicity of error. Secondly, there are differences between the sizes of the amplitude spike between classifications for the downstream subsystem. This would not occur with a periodicity caused by systematic errors in the photogrammetrically derived surface because this would effect all elevation values and all classifications equally.

None of the amplitudes of the waveforms are very large (<0.5m), this reflects the observation that braided systems have little relief. The width of the transects used to define MBL also has the effect of reducing the amplitude of the waveforms. To fully understand the small amplitudes it is important that they are viewed as representations of mean elevation over the entire width of the transect. The small amplitudes represent average changes in elevation amounting to thousands of square metres of sediment. A quantity that takes significant amounts of energy to organise into its form. The exact amounts of sediment incorporated into each wave structure are calculated below.

6.7.0 Analysis

The error analysis presented in **Section 5** of this chapter demonstrates that periodicities derived from photogrammetrically acquired MBL data are reliable for wavelengths above 65m. Wavelengths shorter than 65m are likely to become dominated by error because these typically have lower amplitudes. The MBL series for both the upstream and downstream system has been deconstructed using the FFT to convert the spatial series into the frequency domain. The derived periodicities can be analysed in two separate contexts. The first is a conventional geomorphological approach, which seeks to interpret the results in the context of large topographic controls and small-scale morphological units. The second is a systems level approach that considers what scaling properties the waveforms show and whether these can be taken as evidence of a self-organised system

6.7.1. Conventional geomorphological interpretation

A conventional geomorphological interpretation links the larger wavelengths to large-scale topography such as hill slopes and inputs from tributaries. Smaller scale periodicities could be linked to pool- riffle sequences or meander wavelength patterns or other organisational forms that are apparent from ground observations or planimetric analysis. This section attempts to interpret the waveform data in this context.

The longest wavelength is the system scale wavelength (approximately 2700m) described in **Figure 6.13.** This is the highest amplitude wavelength (2.0m-2.4m) in the system and can be interpreted as the dominant control on bed elevation other than the mean valley floor slope (approx 1%). There are some specific large-scale topographic features that operate outside the study system that could have a direct impact on this dominant wave. They occur predominantly in the upstream sub-system and are illustrated in **Figure 6.19**.

The Allt Lorgaidh – the tributary that joins the subsystem halfway down is associated with a large alluvial fan, believed to be of late glacial age (Robertson-Rintoul 1986). This appears to have a major impact on elevation **(Figure 6.19 A)**. Shortly after the tributary junction the rate of decline in MBL reduces causing the increasing MBL in the detrended MBL series **(Figure 6.16)**. The tributary bed and fan surface are very steep (in excess of 3%) and this ensures that bed load is active within the tributary. No measurements of tributary morphology or bed load were possible but changes to the poorly consolidated clastic bed and banks were noted between 1998 and 2002. The tributary and alluvial fan affects the system in two ways. It forces the study system eastwards towards its valley wall and thereby increasing restraint on the system. This is not a hard immovable channel constraint as would be imposed by bedrock and there is evidence of the study system eroding the Holocene terraces, as indicated by a palaeochannel and terrace edge **(Figure 6.19 B)**. It also adds sediment to the study system at the halfway point and this could be influential in triggering lateral instability and braiding.

The upstream sub-system is more obviously affected by the constraint of the alluvial fan and valley walls. One of the high amplitude wavelengths is 800m and this can also be linked to topographic features **(Figure 6.19). Figure 6.19** compares the 800m wavelength with the 2000 orthophotograph and the most detailed geomorphological map of the area (taken from Rumsby *et al.*, 2002). The geomorphological map gives an alternative classification scheme that includes demarcation of palaeochannels and the edges of the valley floor. The map emphasises the complex structure of the valley floor, composed of contemporary and palaeochannels constrained by valley walls and Holocene terraces. The upstream end of the reach is emerging from valley wall constraint **(C)**. Further downstream the river channel is tight up against the eastern bank **(D)** where a debris slip adds coarse clastic material. The channel is inhibited from meandering westwards by the reworked later Holocene terraces **(E)**. These topographic effects can be linked to the 800m waveform. When the active channel meanders westwards towards the alluvial fan then elevations are greater than when it meanders eastwards and is hard up against the valley wall. The valley wall inhibits the channel from adjusting laterally and instead the channel deepens. A localised example of this effect can be seen in Experimental Reach 1 where the deep pool is over 2m deep (**Figure 5.6**). This analysis implies that valley scale topography could have a controlling effect on the larger wavelength periodicities present in the study system. If this is accepted then any self-organisation of form by the river system itself would be moderated by external topographic constraints.

Conventional geomorphology recognises a number of periodicities (more typically referred to as length scales) that are present in alluvial channels including braided channels. Pool –riffle sequences and meander bend wave structures have been measured for single channel systems with considerable success (Ferguson, 1975). Similar organisational structures have been identified for braided river systems although the complexity of the system has inhibited research, restricting studies to those that only address single confluence -diffluence units, chute –pool units (Ferguson *et al.,* 1992) or address system wide organisation planimetically (Rust, 1978; Howard *et al.,* 1970).

A number of theoretical models of river braiding have been suggested based on the planimetric organisation of confluence diffluence units (Williams and Rust, 1969; Rust, 1978). One simple model is used by Rust (1978) to define a braiding parameter using the ratio of braid length and meander wavelength. This model is overly simplistic and in no way represents the complex assemblages of bars and channels that form most braided rivers. This complexity is acknowledged by Rust (1978) however the model offers a simplified braiding form with which to consider the effects of the MBL morphometric (**Figure 6.20**).

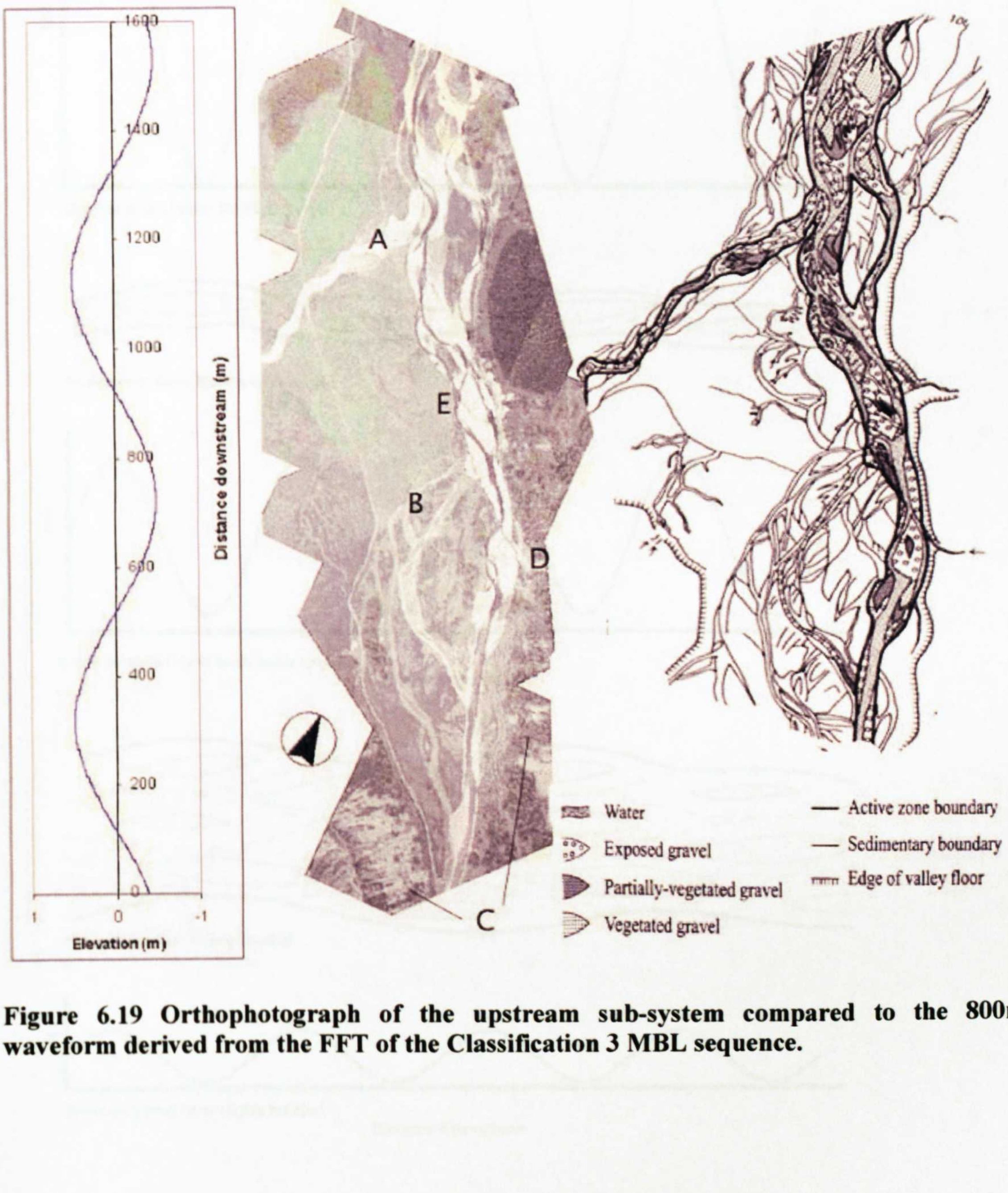

Figure 6.19 Orthophotograph of the upstream sub-system compared to the 800m waveform derived from the FFT of the Classification 3 MBL sequence.

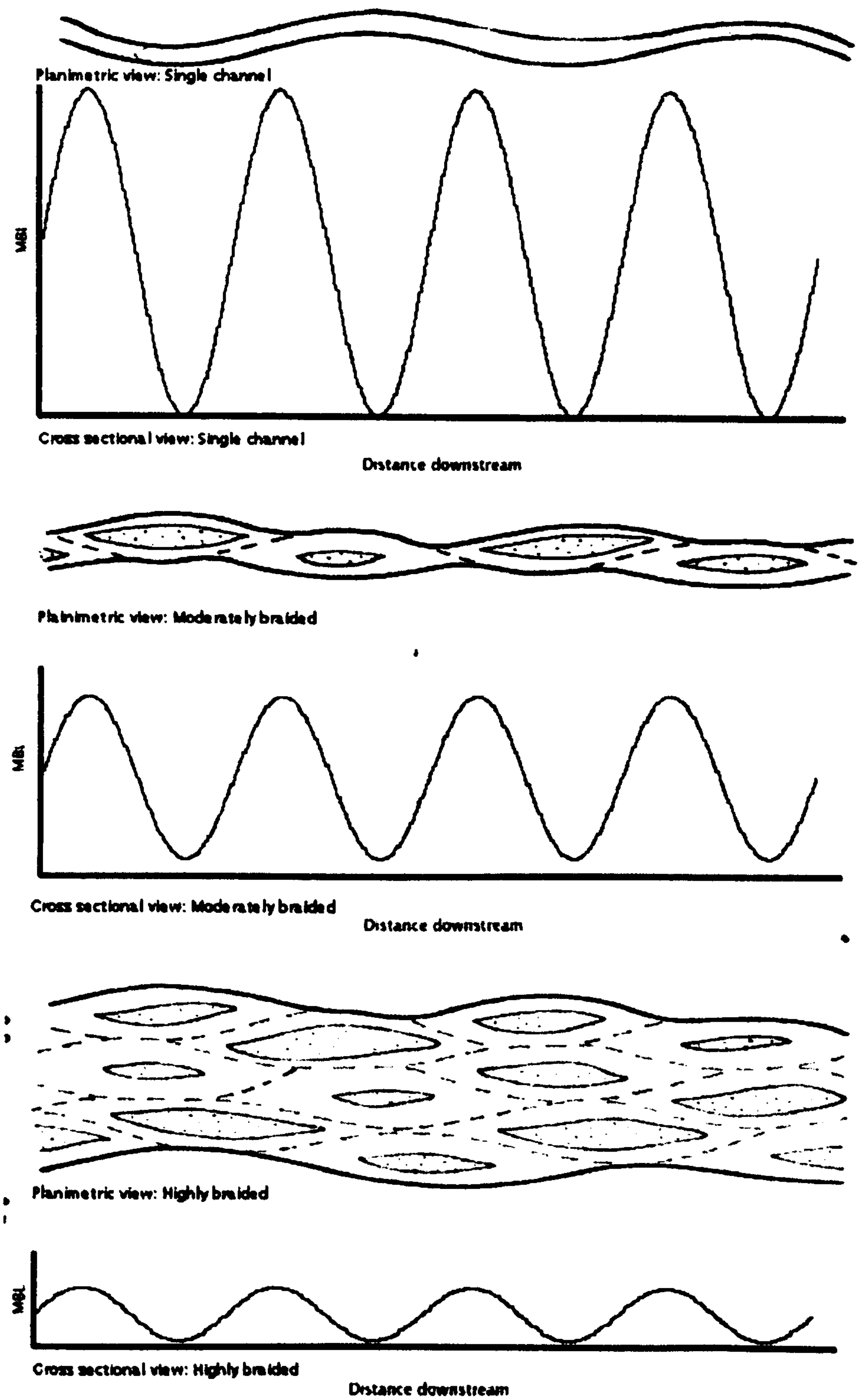

Figure 6.20. A conceptual model showing three simplified channel forms (taken from Rust 1978) and their impact on MBL. As the channel widens the magnitude of the derived MBL is reduced because deeper areas in one channel are offset against raised medial bars and shallower areas of other channels.

This highly idealised model of braiding links meandering to periodic fluctuations in MBL. When active system width increases, then the periodic fluctuation in MBL remains but with a reduced wave amplitude because the deviation in elevation is divided by more cells due to the averaging process.

Although observations of braided rivers show that real systems are more complex than the model in **Figure 6.20** suggests, there could still be periodicities in MBL that are linked to channel structures such as confluence-diffluence units. This is supported by some of the results from the FFT. Two of the medium frequencies, 150m and 300m are dominant (attributed high amplitudes) which could indicate periodicities generated by conventional channel structures. This interpretation is not supported by a comparison of the 150m and 300m wavelengths with the downstream subsystem orthophotograph **(Figure 6.21).** Neither of the waveforms reliably links up to the repetitive morphological forms such as confluence- diffluence units or pools and riffles identifiable on the orthophotograph. For example the 300m waveform has a low value at 600m downstream that corresponds to a deep pool but this does not occur at 300m where the low value corresponds to a riffle. The 150m waveform also fails to reliably correspond to channel form.

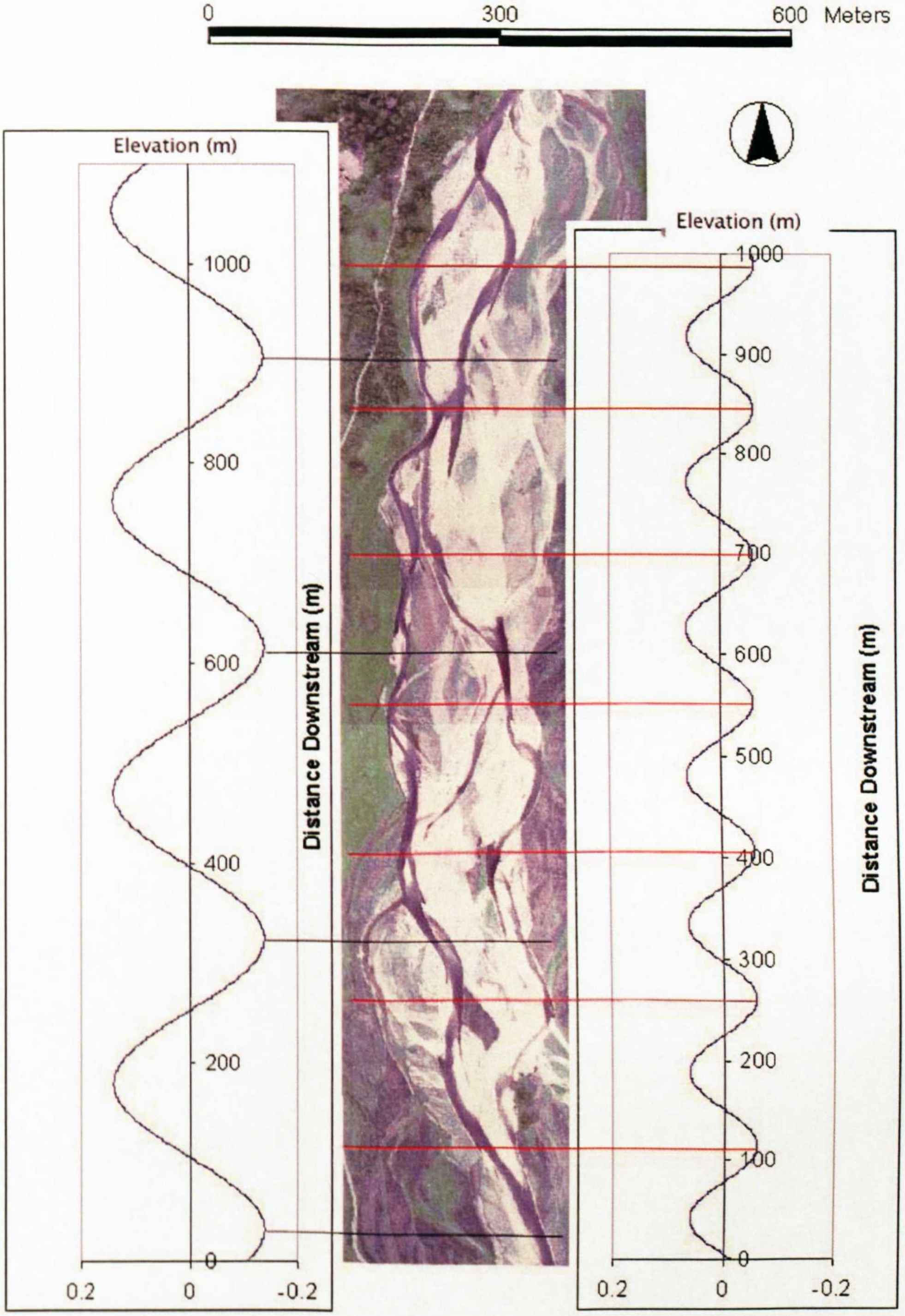

Figure 6.21 Orthophotograph of the downstream sub-system compared to the 300m and 150m wavelengths derived form the FFT of the Classification 1 MBL sequence.

This lack of correspondence between the two data sources can be explained. The periodicity data show organisation of sediment storage and channel topography that cannot be identified using planimetric analysis or field observations because the periodicities represent subtle changes in elevation over hundreds of metres. However the conventional forms of organisation that are recognised both planimetrically and in the field, are those defined by patterns of high slope angles and (normally) inundation, including confluences, pools and cut banks. These are not identified using FFT deconstruction of MBL series suggesting that their influence on system wide sediment storage is limited. This point implies that self organisation within the system might be operating on a level not detectable by conventional techniques and forms of analysis.

An alternative and arguably more appropriate method for interpreting the MBL series is a systems level approach that attempts to determine self organisation in the MBL series by considering the relative magnitudes and frequencies of the waveforms that compose the signal.

6.7.2 Systems level interpretation

The data analysis above shows that certain periodicities can be reliably identified within the static morphology of the riverbed although these do not appear to correspond to conventional morphological units. The dominant research themes in this thesis have focused on a systems level approach that is concerned with identifying scaling or scale invariance within the river channel system and assessing evidence of SOC. The amplitude and frequency data are now therefore analysed in relation to SOC theory.

6.7.3 MBL as an indicator of SOC

This section suggests ways in which the periodicities can be related to a specific self-organisation theory, SOC, to test if they are indicative of SOC within the Feshie (braided) river system. Implicit within this is the idea of how SOC theory is related to the braided river system. It is for this reason that a rationale that links static morphology to sediment dynamics and SOC is presented in **Figure 6.22**

SOC can be established by analysing patterns of sedimentary movement

↓

Sedimentary movement and static morphology are directly related i.e. as sediment moves it changes the morphological form of the river channel.

↓

Therefore the SOC signal will be imprinted on a series of static forms

Figure 6.22 Rationale for identifying SOC in river system morphology

There are some contentious issues with this rationale. The original physical and computational models that lead to the development of SOC theory (Bak *et al.*, 1987) dealt with avalanches down sand or rice piles. It was the power law distribution defined by the magnitude and frequency of these avalanches that was taken as being indicative of SOC. However many theorists have postulated a link between fractal structures in static morphology and the SOC state (Bak, 1996). This postulated link is supported by the findings of Frette *et al.* (1996) who showed a rice pile to be SOC and the resultant static morphologies fractal.

If the link between SOC and scale invariant static morphology is accepted then establishing the scaling properties of the periodicities derived from the MBL series could be the first step in determining the SOC properties of the field site. The periodicities described in **Figures 6.17 and 6.18** can be used in this way if the wave amplitudes are converted into wave volumes. This conversion is necessary because sediment volume or mass was used to determine SOC in rice and sand piles (Bak, 1996) because it is a good indicator of self-organisation. This was achieved using the following equation.

$$Volume(m^3) = \frac{Amplitude \times Frequency}{2}$$ **Equation 6.4**

Where Frequency = 1/ wavelength

The wave volume can then be compared with wave frequency to determine if a power law scaling relationship exists. This means that when the wave magnitude and frequency are plotted on a log-log-plot the fractal dimension of the data can be defined using a linear model (Tate, 1998). The application of FFT techniques for defining fractals in this way is a standard tool in the analysis of time series data (Chatfield, 1984). The FFT has been used within geoscience to define the fractal dimensions for ocean floor topography (Gilbert and Malinverno, 1989) and rock surface roughness and land surface topography (Mulla, 1988). The application of a linear model to a log-log plot is a straightforward technique to use however it does suffer from a number of limitations highlighted by Tate (1998). The FFT samples the data at discrete points, this means that the length of the input sequence dictates the derived frequencies. This means that the FFT computations do not determine the actual wavelengths within the signal but calculates the magnitude of a series of predetermined frequencies. Tate (1998) recommends the use of the Maximum Entropy Method (MEM) to overcome this problem. The MEM is a method for estimating the power spectral density (magnitude and frequency) which is consistent with the principles of entropy and information gain (Tate, 1998). The MEM technique was not used in this thesis because it is a more complex technique to apply successfully and many of the benefits of MEM such as smoother and higher resolution estimates (Fougere, 1985) can be achieved through appropriate detrending and windowing procedures. Appropriate detrending and data windowing have been applied to each MBL series (**Section 6.4.2**) used in this thesis.

The quality of the fractal relationship has been assessed using estimates of R^2 value to show how well the linear model fits the magnitude frequency data plotted on a log-log plot. The current problem with using this technique is that there is little advice and no consensus as to what R^2 value constitutes a fractal. Andrle (1996) argues that an R^2 value of 0.99 may contain significant non-linearity however Klinkenberg and Goodchild (1992) arbitrarily selected 0.90 as the cut-off value. The alternative to arbitrarily selecting an R^2 cutoff value is to place confidence limits around the estimated regression line that determines fractal dimension (Gardner and Altman, 1989). In this thesis no arbitrary cut-off value for R^2 will be defined. Instead R^2 values are taken as indicators of how fractal (or scale invariant) the MBL series are. This allows a comparison of the scale invariance of the MBL series classifications. The lowest R^2 values are the most scale specific classifications and the highest R^2 values are the most fractal (scale invariant) classifications.

When the FFT derived MBL periodicities are plotted on logarithmic scales to show their scaling properties (**Figure 6.23**) the results are initially very encouraging. There is an apparent scaling relationship between wave volume and wave frequency. However most of the data points on **Figure 6.23** are for wavelengths below 65m (frequency of 0.015), but the analysis is **Section 6.5** shows that only wavelengths above 65m can be reliably determined. All data points for wavelengths below 65m will be ignored in the following analysis.

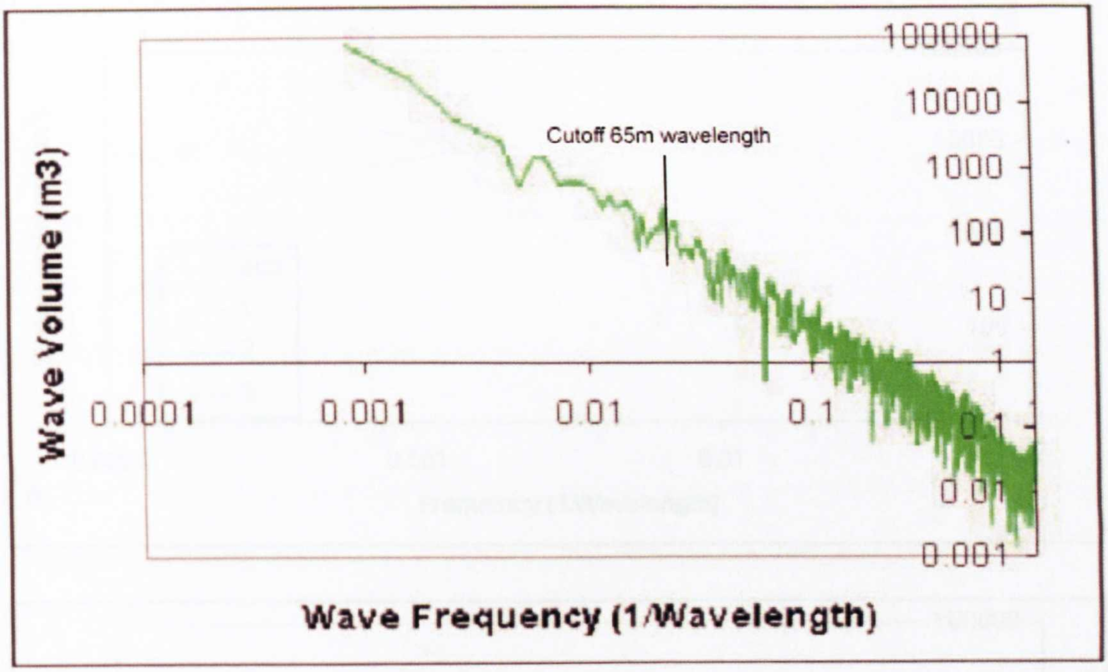

Figure 6.23 Frequency and Magnitude of the waveforms derived from the FFT of downstream sub-system, Classification 3, MBL sequence

Only wavelengths above 65m are shown in **Figure 6.24** and **Table 6.1**. The downstream sub-system shows fractal scaling that increases in quality from the narrowest to the broadest classification. The upstream subsystem also shows strong fractal scaling relationships but these do not increase systematically with increasing width of classification. This inconsistency is in line with that shown in **Figure 6.17**.

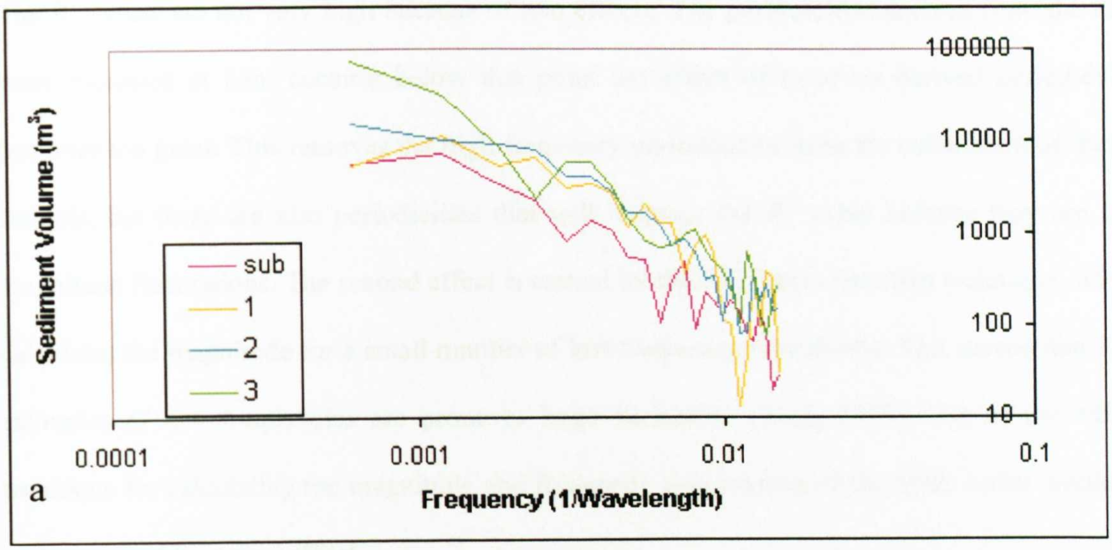

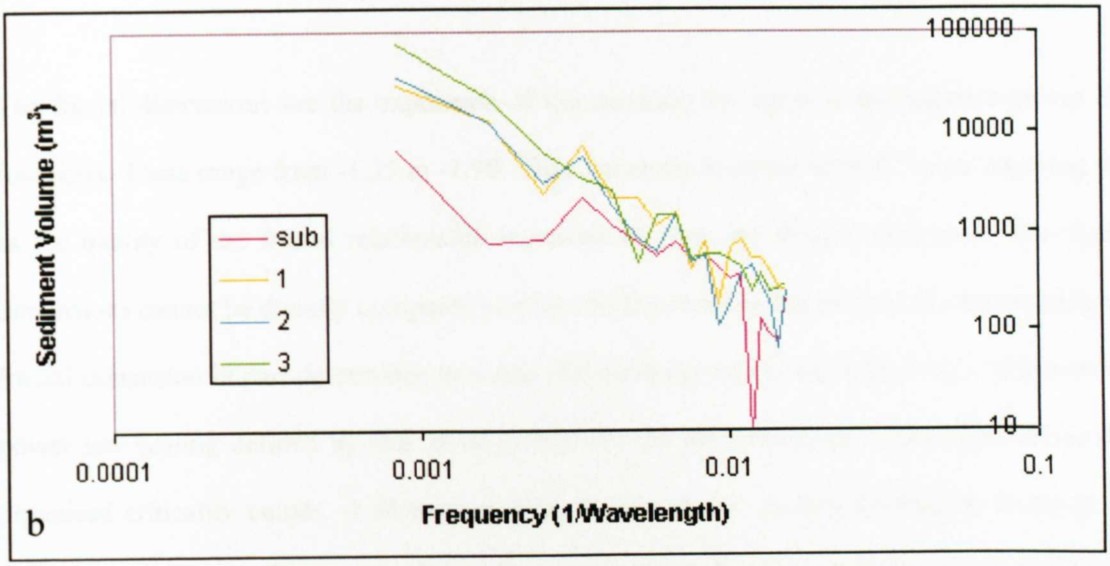

Figure 6.24 Magnitude and Frequency data for the upstream (a) and downstream (b) sub-systems

Upstream Sub-system

	Equation	R^2 value
Sub	$0.038x^{-1.76}$	0.86
1	$0.079x^{-1.76}$	0.65
2	$0.079x^{-1.76}$	0.86
3	$0.040x^{-1.98}$	0.91

Downstream Subsystem

	Equation	R^2 value
Sub	$0.427x^{-1.35}$	0.58
1	$0.334x^{-1.61}$	0.87
2	$0.043x^{-1.93}$	0.89
3	$0.054x^{-1.96}$	0.94

Table 6.1 Equations and R^2 values for power law functions fitted to the magnitude and frequency data in Figure 6.21

The R^2 values are not very high because of two effects. The periodicities derived from the FFT were truncated at 65m because below this point the effect of error on derived periodicities becomes too great. This removes the high frequency periodicities from the calculation of the R^2 statistic, but these are also periodicities that will increase the R^2 value because they are low magnitude fluctuations. The second effect is caused by the FFT deconstruction technique, which calculates the magnitude for a small number of low frequency waveforms. This means that FFT estimates of low frequencies are prone to large variability (Tate, 1998). Use of the MEM technique for calculating the magnitude and frequency components of the MBL series would in part remedy this second effect.

The fractal dimensions are the exponents of the equation for each of the negative power law functions. These range from -1.35 to -1.98. They generally increase with R^2 value implying that as the quality of the fractal relationship increases so does the fractal dimension. The fractal dimensions cannot be directly compared to other studies because the method for determining the fractal dimension in part determines its value (Klinkenberg and Goodchild, 1992). However the power law scaling defined by Bak *et al.*,(1987) for the computational model that defines self organised criticality equals –1.58 and the rice pile power law scaling defined by Frette *et al.*, (1996) equals –1.54. The fractal dimensions determined for three braided river systems by Sapozhnikov and Foufoula-Georgiou (1996) using two dimensional fractal analyses were between 1.50 and 1.55.

The results presented in **Figure 6.24** and **Table 6.1** show a wide variability in the quality of fractal relationships (R^2) and fractal dimension (equation exponent). To better understand these results some theoretical points need further consideration. The analysis in **Section 6.7.0** makes clear that the upstream subsystem is likely to be less self organised, or exhibit a weaker self organised signal, than the downstream subsystem. The upstream subsystem is influenced by valley walls and inputs from a tributary as well as going through large morphological changes from the upstream end where it is a single channel to the downstream end where it is wider, multi channel system. Despite all these inconsistencies, which imply disruption to self-organised behaviour (or the imprint of self organised behaviour onto static morphology) the upstream subsystem exhibits greater scale invariance than the downstream system as defined by R^2 values (**Table 6.1**). There are three possible explanations for this result.

The first explanation is that each of the subsystems is equally self organised and imprints this equally on its morphology. This is possible because despite the disruption of lateral sediment inputs, bedrock and tributaries, the self-organisation of the upstream system is robust enough to dominate these factors. Despite the obvious morphological differences between the subsystems they both have predominantly alluvial bed and banks and are predominantly poorly constrained laterally.

The second explanation is that the periodicities produced by the FFT from the MBL sequences are an insensitive technique with which to measure SOC. Fundamental to this are the classifications, which need to offer a sensitive indicator of the magnitude of a range of frequencies. At the centre of delimitation of each classification is the notion of timescale. The classifications represent a range of timescales, the narrowest (Submerged) is partially re-worked with each competent flood event. Wider classifications such as Classification 2 might only be re-worked over decadal timescales. This suggests that the sensitivity of each classification to self-organisation is dependent on timescale. The narrowest classification is sensitive to self-organisation at the shortest timescale and the widest is sensitive to re-working at longer timescales. The classification with the highest R^2 value is the classification that best represents change over a range of timescales. It is possible that the classifications in the upstream sub-system better represent the broad range of timescales that are instrumental in organising sediment structure.

Thirdly, the rationale presented in **Figure 6.22** may be incorrect because the SOC signal may not be imprinted on static morphology. The waveforms derived from the FFT could be dominated by other factors. The organisation in river form could include an element of self-organisation but this may not be indicative of SOC, which is a specific form of self-organisation.

The impact of classification width on the quality of the fractal relationship needs clarifying. Assuming that channel relief reduces with channel width then the derived periodicities for wide 'active systems' have a reduced amplitude. If this is taken to its logical conclusion then very wide 'active systems' will tend towards deviations in MBL of zero after linear detrending.

Some of the results in this chapter support the idealised model presented in **Figure 6.16**. The upstream subsystem is narrower than the downstream subsystem in every classification and this is reflected in the variability of MBL for both sub-systems **(Figure 6.7 and 6.8)**. The upstream periodicities resulting from this also have larger amplitudes than their downstream sub-system equivalents. The periodicities derived for the downstream sub-system classifications **(Figure 6.24)** also support part of the idealised model. The wider classifications (2 and 3) show a reduction in medium frequency amplitudes, such as wavelengths that might be associated with confluence-diffluence units (150m-300m), but critically they also show an increase in the amplitude of lower frequencies. This is important because it implies that wider classifications are better indicators of self-organised structures with long wavelengths. In terms of fractal scaling properties the recognition of periodicities with long wavelengths is significant because it means that the fractal relationship is improved. The low frequency periodicities are statistically identical to medium and high frequency periodicities indicating scale invariance.

The scale invariance shown by these results is supported by other studies. The channel and bar ordering developed by Williams and Rust (1969) (Rust, 1978) implicitly supports the concept of identical structures of different scales within braided channels. This is supported by the more rigorous techniques employed by Sapozhnikov and Foufoula–Georgio (1998) which shows planimetric fractal scaling is robust to the effects of discharge, so as stage increases and channels widen then there is still the same scaling relationship between large and small channels.

Collectively these studies show that scale invariance is an integral part of braided river form, which should not be overlooked when developing conceptual models of form or process.

6.7.4 Periodicities as actual sediment waves.

This section attempts a more speculative analysis of the periodicities derived from MBL. It is largely conceptual but provides a means of drawing together conventional geomorphological analysis with a systems level approach.

If the spatial MBL series is considered analogous to a temporal sediment transport series then the periodicities can be conceptualised as actual sediment waves migrating down and conveying sediment through the system. The waves migrate downstream via complex assemblages of erosion and deposition. The narrower channel classifications show the high frequency, low magnitude waves most effectively and these are likely to migrate rapidly downstream due to their position in very active areas of the channel. The wider classifications show the longer, higher magnitude waveforms that migrate more slowly down the active system.

The idea of multiple sediment waves operating simultaneously in the same system is not an idea that is prevalent in research into sediment dynamics or sediment pulses. A majority of studies measuring the migration of sediment pulses tend to track the form and rate of specific sediment inputs (Nichols, 1995) and assume that the sediment pulse is the only important sediment transfer event active in the channel. Similarly studies measuring sediment transport rates are not designed to establish the scaling characteristics of sediment discharge (Ashmore, 1991) and so any wave structures operating over a large range of scales will not be identified.

If the periodicities are considered to be real sediment waves migrating through the system then their scale invariant magnitude and frequency can be taken as direct evidence of SOC.

The implication is that self-organisation in braided river systems should be measured not only by quantifying sediment movement itself but also by measuring the larger scale composite forms. The waveforms described in **Section 6.7.0** are examples of those composite forms. They are clearly too large to be the result of singular sediment movement events but they are composed of numerous sediment movement events which reflect the organisational properties of the system. The longer wavelength high amplitude periodicities are the equivalent of the very infrequent high magnitude avalanches that occurred within the rice pile, whereas a single sediment movement which is typically very small in size is the equivalent of a single sand grain moving on the sand pile, the smallest most frequent avalanche.

6.8.0 Conclusions

The above analysis shows some success using conventional geomorphological analysis in linking the periodicities defined by the FFT with specific features. The larger wavelengths are linked to large-scale topographic features particularly for the upstream subsystem. However the medium wavelengths were not considered to be the result of elevation fluctuations controlled by conventional morphological units such as confluence-diffluence and pool-riffle units because the periodicities failed to match up to specific observable features on orthophotographs.

SOC offers a more structured framework in which to analyse the magnitude and frequency data. In particular the derived periodicities occur over a large range of scales suggesting that the active system morphology is scale invariant and could be SOC. The use of the FFT for deconstructing MBL series raises important issues about the way sediment movement is organised throughout the system. In particular the concept of waveforms of multiple magnitudes and frequencies operating in the same system links the static morphological structures with dynamic scaling and SOC.

If the derived periodicities are conceptualised as actual sediment waves migrating downstream then the potential theoretical significance of the derived periodicities is substantial. It means that braided river channels should be considered not as static forms through which sediment pulses pass but forms that are integral to the structure of sediment movement. There is no published sediment transport data for braided rivers with which to support this conceptualisation. The practical problems of gathering data in the field prohibit time series of sufficient length and resolution to make a detailed multi-scale signal deconstruction such as the FFT possible. However there are qualitative descriptions of how sediment moves in braided rivers backed up by cross sectional and planimetric measurements (Ferguson and Werritty, 1983; Ashmore, 1991) and these broadly support the concept of sediment waves progressing downstream changing channel elevations.

There are some important questions that arise from this final analysis. Are the periodicities durable and capable of withstanding sedimentary movement without significant changes in wavelength or amplitude? Or will sedimentary movement and channel changes result in the emergence of new wavelengths with a similar, scale invariant, magnitude and frequency structure. To answer these questions MBL series collected over decadal timescales is required. The MBL series would need to be derived from high quality DEMs with high spatial resolution (<1m) and an annual temporal resolution. These DEMs could be used to determine the magnitude and frequency of actual sediment movement using the morphological method (see next chapter) and compare these with periodicities derived from MBL analysis.

CHAPTER 7. THE SCALING PROPERTIES OF SEDIMENT MOVEMENT

Abstract

This chapter attempts to identify characteristics of sediment dynamics in the system to determine if these are consistent with a SOC system. Initially a reduced reach is identified and described (7.2). Channel changes and sediment movement are identified by differencing of the 2000 photogrammetric DEM with a 2002 GPS derived DEM (7.3). The implications of the changes are analysed in relation to the methods used in **Chapter 6**, the morphological method and SOC (7.4). The morphological changes between 2000 and 2002 are quantified using a FFT deconstruction of a cross sectional sediment balance (7.5). The wave structures and scaling characteristics of this deconstruction are considered (7.6). This dynamic component is then compared to MBL changes over the same period (7.7). Finally the implications of static scaling (**Chapter 6**) and dynamic scaling (this chapter) are discussed to determine to what extent they are indicative of SOC (7.8).

7.1.0 Introduction

Chapter 6 established the scale invariant credentials of the waveforms derived from MBL. The scaling relationship was shown to improve for the wider classifications, which better represented the larger wave structures operating in the 'active system'. The fractal form has links to SOC systems but cannot be taken as direct evidence because SOC is a dynamic state, defined by the magnitude and frequency of specific events. An alternative approach to the problem of system scale organisational behaviour is dynamic scaling, the scaling characteristics of measured or derived sediment movement. The third research theme (**Chapter 2 Section 8.3**) specifically addresses this. The key questions attached to the theme concern whether sediment movement occurs according to specific length scales or is it scale invariant and how do the scaling characteristics compare to the scaling characteristics of static morphology.

The flux of sediment through a river channel can be measured by differencing of DEMs, a technique that gives spatially distributed information about scour and fill. The volume and pattern of these changes is direct evidence of how the river system organises itself. To address this more directly the magnitude and frequency of specific movement events must be considered. However in the braided river environment actual measurements of sediment movement events are hard to achieve. Measurement of sediment movement over a number of events is a more realistic goal, made possible using the morphometric technique. This raises further questions though, as the derived sediment movement is the amalgamation of a multitude of smaller events with differing magnitudes and frequencies and for it to be interpreted appropriately it must first be deconstructed into its constituent parts.

The data presented in this chapter allow the testing of the resilience of the fractal structures defined in **Chapter 6** when morphological changes occur. This is important because it is concerned with how the scale invariance demonstrated for the upstream and downstream subsystems can be replicated after a number of sediment movements and channel changes. If static morphology has scale invariant wave structures for more than one MBL series then this provides evidence that the system is organising itself according to a structure that is robust to sediment movement and channel changes, a robustness that may be indicative of SOC.

The fourth research theme introduced in **Chapter 2 Section 8.4** will also be discussed in this chapter. This is a broader research theme considering the implications of the scaling properties of both the static and dynamic morphology. In particular it attempts to describe the importance of the scaling characteristics in relation to self organisation and in particular SOC. Evidence from other studies describing braided river form and bedload dynamics will be included in a broader discussion of self organisation within river channels and drainage basins.

7.2.0 The reduced reach: Experimental Reach 2

A 650m long reach of the lower sub-system was chosen as a suitable extended reach with which to consider the dynamic properties of the braided system (**Figure 7.1**). This section was chosen for GPS resurvey in 2002 because significant observable channel changes had occurred since the 2000 survey. The reach was situated at the most braided section of the study system. It included a wide active area of exposed sediment including multiple channels and confluence diffluence units.

The spatial extent of the 2002 survey was dictated by the spatio temporal factors associated with ground survey. Photogrammetrically derived DEMs of the full system were not possible because aerial surveys were not undertaken in 2001 or 2002. Although the lack of photogrammetric data in 2001 or 2002 limited the spatial extent of analysis, the higher accuracy and precision of the GPS survey reduced the LOD threshold (described in **Chapter 5 Section 7.0**).

The two DEMs used for analysis in this chapter are shown in **Figure 7.2.** The first DEM is a section of the photogrammetric DEM used in the previous chapter. The photogrammetric DEM was constructed from aerial photographs taken in 2000. Generic issues surrounding the quality of photogrammetrically derived DEMs can be found in **Chapter 3** and a quality assessment specific to the 2000 DEM can be found in **Chapter 5**. The second DEM is constructed from a medium resolution GPS survey of the same area undertaken in 2002. Theory relating to the quality of GPS survey can be found in **Chapter 3** with data quality estimates for the DEM given in **Chapter 5**.

The important characteristics of the data sets are summarised in **Table 7.1**. The photogrammetric DEM has a SDE of 0.163m and ME of –0.006m. This is a poorer quality than the GPS data set, which has a SDE of 0.096m and ME of –0.011m. The analysis in **Chapter 5 Section 5.7.0** shows that when differenced the DEMs have a LOD threshold of between 0.350m (dry to dry) to 0.659m (wet to wet). This is substantially lower than analyses that uses two photogrammetric DEMs (0.449-0.806m). This highlights one of the advantages of combining survey methods. However there are also disadvantages. Close examination of the two DEM surfaces shows textural differences. The photogrammetrically derived DEM incorporates small-scale roughness resulting from the higher point resolution but also small pixel matching anomalies, no such roughness is present in the GPS derived survey.

Figure 7.1 Orthophotograph of the reduced reach section (Experimental Reach 2) of the downstream sub-system

	SDE (m)	ME (m)
Photogrammetric DEM (2000)	0.163	-0.006
GPS derived DEM (2002)	0.096	-0.110

Table 7.1. The data quality statistics for the photogrammetric and GPS derived DEMs.

Figure 7.2 DEMs of Experimental Reach 2. On the left the 2000, photogrammetrically derived DEM. On the right the 2002 GPS derived DEM

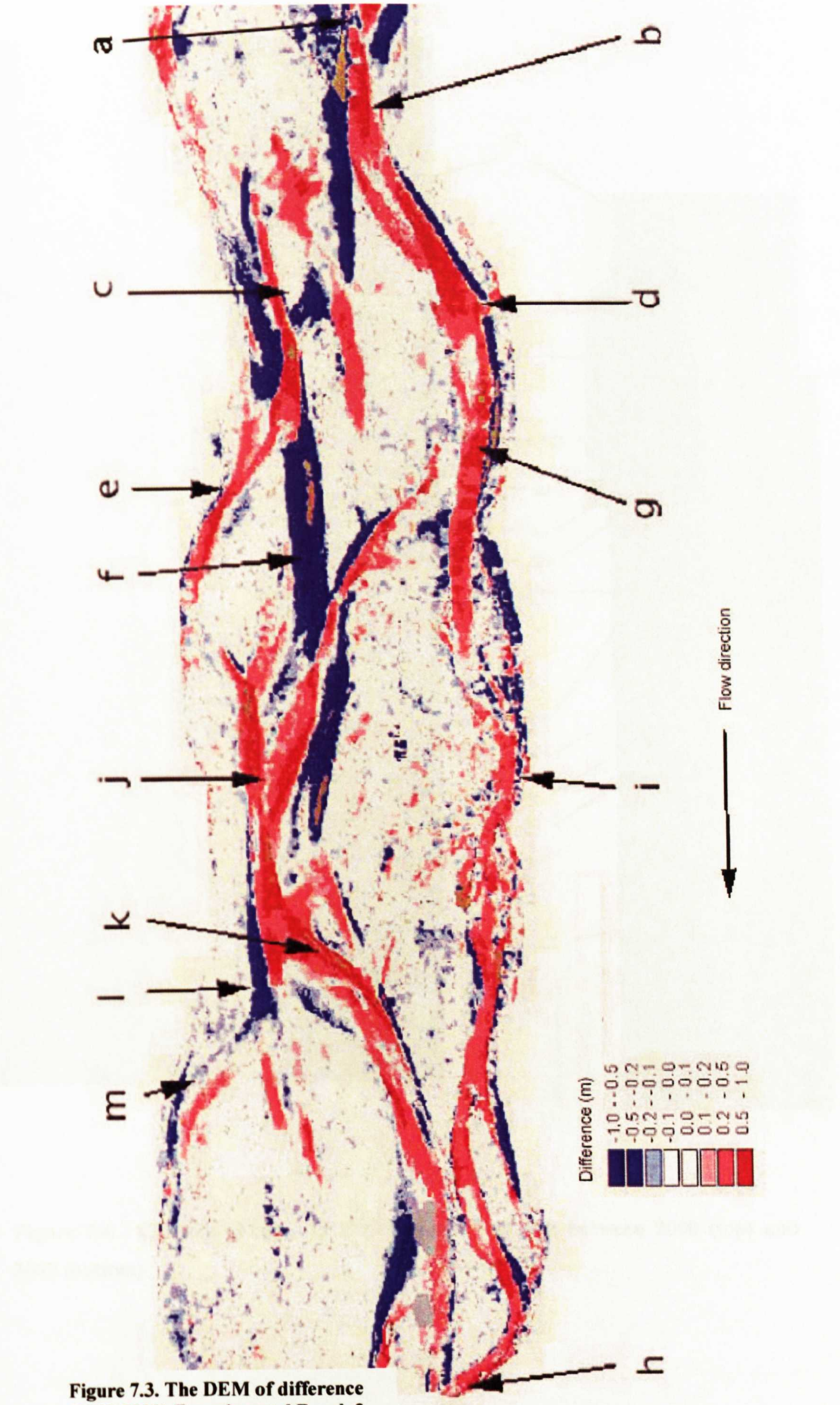

Figure 7.3. The DEM of difference (2002-2000) Experimental Reach 2

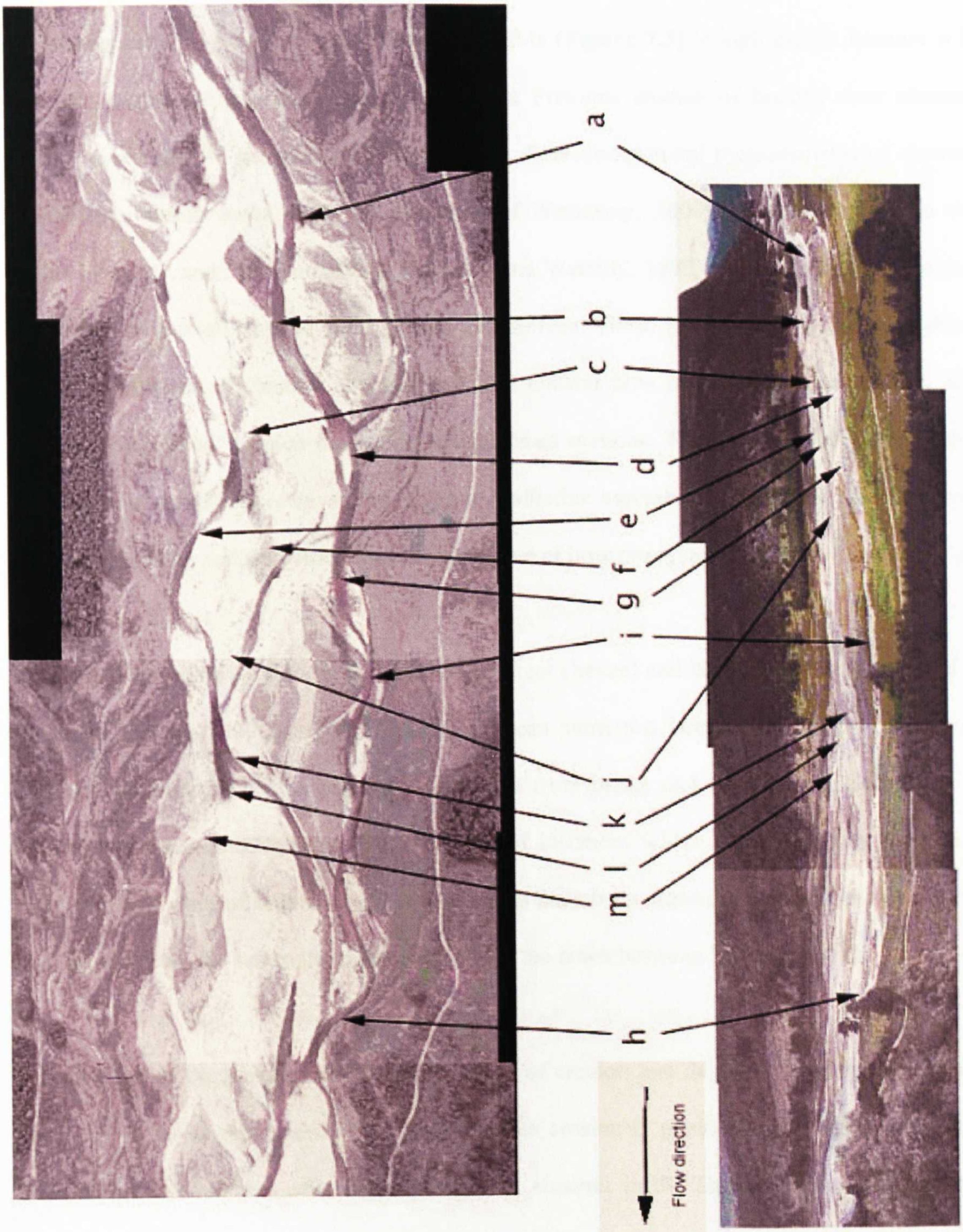

Figure 7.4 . Channel changes in Experimental Reach 2 between 2000 (top) and 2002 (bottom)

7.3.0 Channel changes 2000-2002

The channel change data from the differenced DEMs (**Figure 7.3**) is high quality because it is based on high-resolution three dimensional data. Previous studies of braided river channel change have failed to generate such high quality three dimensional measurements of channel change over similar areas (with the exception of Westaway, 2000). Previous studies on the Feshie (Werritty and Ferguson, 1980; Ferguson and Werritty, 1983) used planimetric mapping augmented by a small number of cross sectional profiles. These gave limited information about the exact structure of channel changes and it is unclear how much submerged erosion and deposition is missed between the widely spaced cross sections. The DEM of difference in this study is considerably more revealing. Even a qualitative assessment of **Figure 7.3** can reveal patterns of erosion and deposition that are indicative of how the system organises itself.

Figure 7.3 and **Figure 7.4** show that some significant channel and bar changes have occurred in the reach between 2000 and 2002. There have been numerous lateral shifts in the position of channels associated with the cutting of sediment from banks and bars and the deposition of sediment in channel. There are also a number of instances where entire channels have been blocked off by slugs of sediment and new channels have been created. Overall there is a general shift in flow from the left to the right hand side of the reach between 2000 and 2002.

At the head of the reach there are two couplets of erosion and deposition **(a)** these represent lateral shifts in the movement of the channel. The erosion is predominantly bank cutting and lowering of bar surfaces whereas deposition is channel infill. These couplets are just two examples of compensating channel activity that will result in a negligible change in cross sectional MBL. At **(b)** there is a significant channel change. The 2000 channel is aggraded and erosion of a right hand bar has generated a new channel that directs flow to the right hand side of the system, breaching a vegetated bar at **(c)**. The main left hand channel **(d)** has cut some of the left hand edge of the system but the loss of flow resulting from the new channel at **(b)** and **(c)** means there has been substantial within channel deposition. At **(e)** the deposition is of a similar depth but very different in character. The right hand side channel has been blocked by a poorly consolidated gravel lobe with a distinctive avalanche face at the downstream end. The blocked right hand channel is compensated for by a completely new channel (f). Again (e) and (f) represent a lateral change in channels used to convey flow which represents a major re-organisation of flow in the right hand side of the system. The new channel (f) is straighter than (e) and has a more direct route to the confluence at (j).

Midway down the reach a left hand side channel separates itself from the rest of the system at (g) and remains split off from the rest of the system until rejoining at (h). This side channel took a large amount of low stage flow in 2000 but deposition at (g) reduced this to a very small amount of through gravel infiltration by 2002. Deposition has predominated in the left hand channel although localised areas of bank cutting and channel erosion are also present (i). The confluence-diffluence at (j) is a very active section of the reach. The confluence moved upstream between 2000 and 2002 as a result of the new channel at (e) which produced bar erosion on the left hand side of the confluence and coupled deposition on the right hand side. At the diffluence this is reversed with deposition on the left hand side (k) and erosion on the right hand side. Erosion of an existing channel at (m) is coupled with bar top deposition.

It is difficult to relate these changes to morphological changes reported in other studies because the morphology of the Feshie is very different to that described in a study such as Luce's (1994) measurement of confluence zone dynamics in the Sunwapta River, Canada or the channel and bar structures described by Bluck (1964, 1979). The descriptions of change in these papers are based on survey methods such as planimetric mapping and cross sections and detailed definitions of different types of bar. This makes it very difficult to compare the channel changes in this thesis with those of previous research. The acquisition of DEMs leads to a method of describing topography not as complex combinations of bars defined by a researcher, but as a single morphological form defined by the DEM. The channel changes are also better defined by the DEM differencing process than is possible through lengthy written descriptions.

The most applicable study of bar and channel changes is Ferguson and Werritty (1983), which describes channel changes at the study site from 1977 to 1981. The most detailed descriptions of channel changes provided by Ferguson and Werritty (1983) are of diagonal bar evolution where diagonal flow over the longitudinally aligned edge of an elongated gravel sheet leads to the evolution of extensive compound features. Patterns of channel change and flow distribution described by Ferguson and Werritty (1983) are similar in character to those that occurred between 2000 and 2002 for instance, between June 1977 and August 1978 flow switched from a channel on the true right bank and became more evenly distributed with a true right bank channel. Between 2000 and 2002 the new distributary channel cut at (c) re-distributes low flow from the true left bank over to a channel close to the true right bank. It is not possible to compare specific patterns of erosion and deposition because channel change was only defined by a few cross sections by Ferguson and Werritty (1983) however the cross sections that were re-surveyed annually showed scour and fill of up to 1m an amount greater than measured between 2000 and 2002.

The channel changes shown in **Figure 7.3** are the result of flood events occurring over a two year period (**Figure 7.5**) The discharge information in **Figure 7.5** was derived from stage readings at Feshiebridge gauging station, located approximately 15km downstream from the fieldsite. The catchment area for the Feshiebridge gauge is 232km^2, which is approximately 3 times larger than the catchment area above the fieldsite (80km^2). The area contributing to the Feshiebridge catchment downstream of the fieldsite has similar topography and flood generating conditions. It is assumed that all areas of the catchment contribute similar relative quantities of flow at the Feshiebridge gauge. Discharge at the fieldsite is assumed to be 1/3 of that measured at Feshiebridge. There are clear problems with downscaling by area but this approach is consistent with records from a gauge maintained by St Andrews University in the late 1970's situated 1km downstream from the study site.

Figure 7.5 shows Feshiebridge discharge from January 2000 to July 2002. During the 23 months between surveys, there were 21 flows over 30m^3 s^{-1}, equating to 10m^3 s^{-1} at the field site. The level of flow competence has not been measured at the fieldsite but channel changes resulting from flows of approximately 10m^3 s^{-1} have been observed. The large number of competent flows (>21) means that sediment could have been mobilised on a number of occasions. There were 5 events over 60 m^3 s^{-1} (equating to 20m^3 s^{-1} at the fieldwork site) in the winter of 2002. The largest flow recorded was over 110m^3 s^{-1} in February 2002 and the mean flow 9.4m^3 s^{-1} over the whole period.

These flow conditions are broadly consistent with those described by Werritty and Ferguson (1980). The mean flow at Feshiebridge between 1951 and 1974 was 8.1m^3 s^{-1} and the largest flood on record was 200m^{3}s^{-1} in September 1961, a flow significantly larger than any of the floods between 2000 and 2002, but also a flood that had significant impact on channel morphology (Werritty and Ferguson, 1980). Flood records from the University of St Andrews gauge reported by Ferguson and Werritty (1983) show 51 floods exceeding 20m^3 s^{-1} in the first 3 years (1978-1981) of the operation of the gauge. If these results are upscaled to the Feshiebridge gauge then this equates to 17 floods per year with a discharge of 60m^{3}s^{-1} a significantly larger number than was recorded between 2000 and 2002 (5) equating to 2.5 60m^3 s^{-1} floods per year. This suggests that the period when Werritty and Ferguson were working at the field site was a time of greater flood frequency and it is likely that this was also a time of increased sedimentary activity.

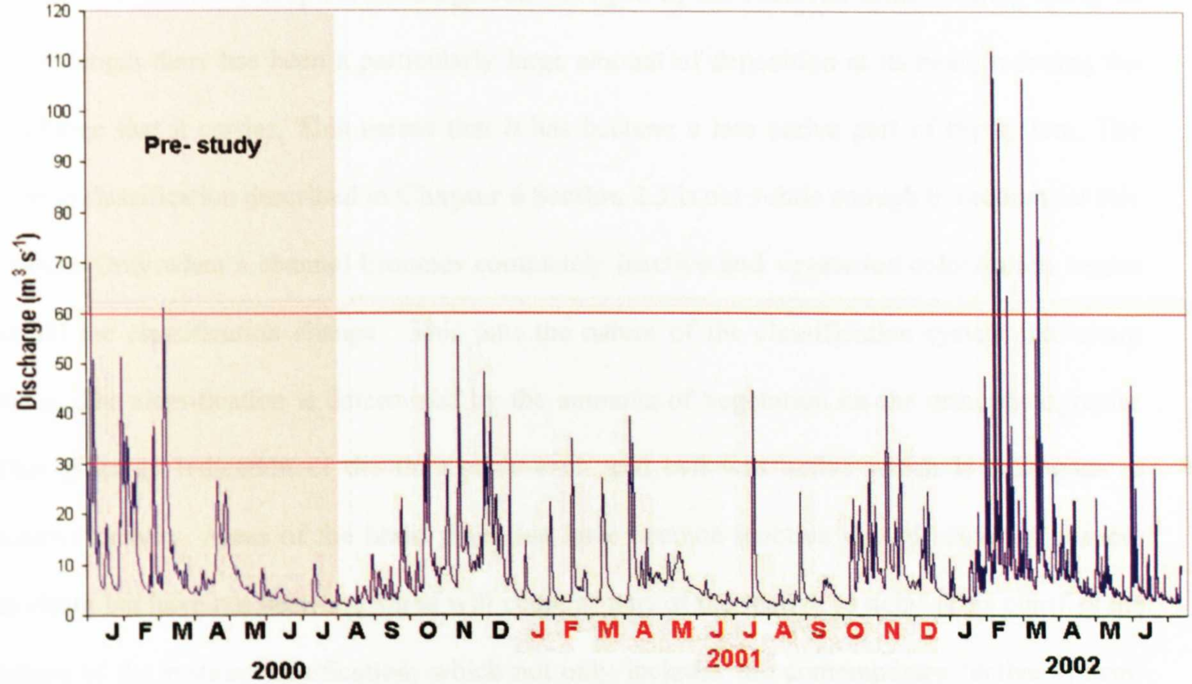

Figure 7.5 Feshie Bridge discharge record (January 2000 to July 2002). Data from SEPA

7.4.0 Analysis: Implications for the active system classifications and MBL morphometric

The channel change analysis above illustrates some of the strengths and weaknesses of the techniques used in this thesis. A feature of the analysis above is that many changes are lateral. The left hand channel shows a reduced dominance between 2000 and 2002 and many of the channels shift laterally resulting in a couplet of erosion and deposition. This is encouraging because it shows the interconnectivity of the system and supports the systems level approach adopted in this thesis. In particular lateral interconnectivity is indicated by the location of zones of erosion and deposition. This strong lateral interconnectivity is not identifiable using the cross-sectional MBL morphometric because this reduces all cross sectional variability and morphological changes into a single average elevation. Many of the couplets shown in **Figure 7.3** such as **(a-b)** and **(e-f)** will cancel each other out leaving MBL unchanged. This highlights the limitations of the MBL morphometric which is only suited to determining patterns in downstream elevation change.

The channel change analysis also provides additional insight into the implications of the 'active system' classification adopted. Although channel (**g** to **h**) has received some infilling along its entire length there has been a particularly large amount of deposition at its head, reducing the discharge that it carries. This means that it has become a less active part of the system. The system classification described in **Chapter 6 Section 2.3** is not subtle enough to account for this change. Only when a channel becomes completely inactive and vegetation colonisation begins would the classification change. This puts the nature of the classification system into sharp focus. The classification is determined by the amounts of vegetation on the orthophotographs. This gives an indication of the time since each grid cell was active which is analogous to relative activity. Areas of the braid plain that have become inactive due to upstream channel avulsion but have not been vegetated will count as part of the 'active system'. This clarifies the nature of the system classification, which not only includes the contemporary 'active system' but also the lag effect produced by vegetation colonisation times. The classification issue is further complicated by the magnitude and frequency of flood flows. A relatively low magnitude event might be large enough to move sediment but may not inundate all the exposed areas of gravel. An infrequent high magnitude event may result in the inundation and potential morphological adjustment of vegetated areas. Werritty and Ferguson (1980) reported a similar effect. The analysis of APs and flood records for the study site between 1946 and 1977 showed fluctuations in the planimetric form of the channels that Werritty and Ferguson (1980) linked to high magnitude flood events. In particular a large flood in 1961 remained the dominant element in channel changes up to 1978.The importance of the 1961 flood in dominating channel form for a few decades does not make the classifications ineffective as a means of defining self organisation. In fact the opposite is true, the classifications must incorporate the impacts of high magnitude events on morphology in order to represent the significance of high magnitude events. However, it is not clear how the 'active system' classifications relate to different flood magnitudes and frequencies except that the classifications represent a balance between the channel widening capabilities of the system and the channel narrowing resulting from vegetation colonisation

7.4.1 Implications for sediment budgeting

One of the most compelling reasons for acquiring high quality DEMs of braided river morphology is its potential utility in sediment budgeting. The morphological method developed by Neill (1987) estimates the bedload transport rate from morphological change. Two methods have been developed. The step length method (Neill, 1971; Church *et al.*, 1987) identifies a step length distance of travel between sediment source and sediment sink and this is used to calculate a transport rate. Neill (1971) applied this approach to a meandering channel, estimating that the typical transport length was from the outer edge of one meander bend to the inner edge of the next. It was assumed that the volume eroded equalled the volume deposited. The step length approach has also been applied to braided rivers (Ferguson and Ashworth, 1992; Goff and Ashmore, 1994) where the spatially complex patterns of erosion and deposition must be identified using morphological survey. The identification of distinctive zones of erosion and deposition is then used as the transport distance. This approach is problematic because spatially complex patterns of erosion and deposition make it difficult to identify the step length and poor estimation of step length. The second method uses survey data (typically cross sections) to identify volumes of erosion and deposition. This relationship is expressed using the sediment continuity equation:

$$Q_{bi} - Q_{bo} = (1 - \eta)dV_b / dt$$

Equation 7.1

Where Q_{bi} and Q_{bo} are volumetric rates of transport of bed material into and out of the reach of interest. η is bed sediment porosity and V_b is the volume of bed material stored in the reach; $dV_b/dt>0$ indicates aggradation. The fundamental problem with this approach is that an estimation or measurement of either the volume of sediment into the reach (Q_{bi}) or volume of sediment leaving the reach (Q_{bo}) is required. This second requirement was met by McLean and Church (1999) who identified a point of zero transport at the end of a reach of the lower Fraser River, Canada, allowing the calculation of the sediment budget for a number of subreaches or cells. The accuracy of the approach is based on the spacing of cross sections relative to the scale of channel investigated and the assumed or estimated sediment throughput at either end. The second method has been used by Ferguson and Ashworth (1992), Goff and Ashmore (1994) and Luce (1994) but all these studies were hindered by the coarse spatial resolution of transects relative to the scale of the channel under investigation. Lane (1995) payed more attention to the quantification of the river channel form using oblique photogrammetric techniques and ground survey of the proglacial stream of the Haut Glacier d'Arolla, Switzerland. The sediment supply conditions were determined using Helley Smith bedload sampling at the upstream and downstream end of the reach.

Neither of these methods will be adopted below because both have limitations, which inhibit their effectiveness at addressing the research themes outlined in **Chapter 2**. The pattern of erosion and deposition with **Figure 7.3** is spatially complex, inhibiting the identification of step lengths. The second method is reliant on estimation of sediment entering or leaving the reach, a precondition possible on a proglacial stream such as that used by Lane (1995) where sediment is active on a daily basis and competent flows are not too large to inhibit the use of a Helley-Smith sampler. The Feshie fieldsite prohibits the estimation of sediment entering or leaving the reach because the timing of flood events cannot be predicted and no viable sampling method is available. However, this thesis is not primarily concerned with sediment budgeting but more the structure of bedload flux, its scaling characteristics and what this says about self organisation within the system. The DEM of difference can be used in this context because it allows for the calculation of sediment volumes for a large number of sub-reaches or cells at high resolutions (0.5m).

7.4.2 Implications for self organisation

Whilst the DEM of difference (**Figure 7.3**) does not allow the effective application of sediment budgeting techniques, it is of sufficient quality to allow the identification of sediment flux. In this section the scaling characteristics of downstream sediment flux will be deconstructed using the FFT to identify the dominant wavelengths that compose the morphological changes in the two years between surveys. This will provide evidence of the dynamic self organised properties of the system, in particular the scaling characteristics of change.

The large number of flood events in the two years between surveys means that it would be misleading to conceptualise the channel changes as the result of a single sediment movement event. The evidence of channel change presented in the DEM of difference is very different to the single avalanche events recorded by Held (1990) or Frette *et al*, (1996). Held (1990) measured the change in mass of a sandpile constructed on circular disks as sand was added one grain at a time and Frette *et al.*, (1996) recorded the size of rice pile avalanches by differencing side profiles of rice piles constructed between glass plates. Both approaches measured the response of the system after each grain input. In contrast the DEM of difference is the result of numerous sediment movement events and channel changes and as such it must be viewed as an amalgamated or compound form.

One method for determining the downstream self organised properties of the system is to quantify changes by aggregating cross stream erosion and deposition to produce a cross sectional sediment balance. Each cross section has a downstream width of 0.5m and this was used to calculate the volume of erosion and deposition per cross section (**Equation 7.2**)

$$d_l + e_l = V_{chan} \qquad \textbf{Equation 7.2}$$

d_l = volume of deposition (m^3)

e_l= Volume of erosion (m^3) a negative quantity

V_{chan}= change in volume (m^3)

The V_{chan} morphometric shares many of the characteristics of the MBL morphometric. A series of V_{chan} values shows downstream changes in sediment volume giving an indication of the length scales over which sedimentary change occurs downstream. V_{chan} avoids one of the weaknesses of the MBL morphometric because it does not require cross sectional widths to be defined using a classification. Instead the volumetric changes in sediment within the cross section define the V_{chan} statistic. Areas of the channel that are inactive between surveys will not have changed and will not affect the V_{chan} statistic. This gives a very accurate indication of the 'active system' over the 2 year period between surveys in contrast to the classifications used for MBL transects which are approximations of the 'active system' over longer timescales.

However the V_{chan} statistic is a cross sectional metric and does not take into account any of the lateral variability in erosion and deposition. Summation of volumetric changes in cells within a cross section means that any lateral organisation cannot be determined. This is problematic because lateral instability has been recognised as an important characteristic of braided river behaviour (Paola, 2001). The DEM of difference (**Figure 7.3**) also shows the importance of cross stream changes. The couplets of erosion and deposition that accompany a lateral shift in channel position or channel dominance show that cross stream organisation is important in the reach. An indication of how important lateral organisation is can be achieved by calculating the amount of sediment compensated for in any given cross section. This is defined as:

$$V_{comp} = Min(d_1, e_1) \qquad \textbf{Equation 7.3}$$

V_{comp} is the amount of sedimentary change in a cross section that is compensated for. This means that if a cross section has deposition of $10m^3$ and erosion of $11m^3$ then V_{comp} will equal $10m^3$ and V_{chan} will equal $1m^3$. V_{comp} is always equal to the lowest value whether this is erosion or deposition. Both V_{comp} and V_{chan} in Experimental Reach 2 are shown in **Figure 7.6** , derived from the DEM of difference.

These data show that V_{comp} fluctuates less than V_{chan} over all levels of detection. With no LOD threshold **Figure 7.6 a)** V_{comp} has a Mean of $19.15m^3$ and SD of $5.76m^3$ compared with V_{chan} with a mean of $2.87m^3$ and a SD of $14.85m^3$ When the LOD threshold is increased to 0.5m **(b)** the SD values are reduced for both morphometrics to 5.35 for V_{comp} and 10.13 for V_{chan}. The 1m

LOD threshold excludes large amounts of information and sections of the reach show apparent inactivity. Of the 3 LOD thresholds shown in **Figure 7.6** the 0.5m threshold is likely to be the most realistic estimate of change because of the LOD thresholds defined in **Chapter 5**.

The V_{comp} and V_{chan} morphometrics have signals with very different structures. V_{comp} has few large scale fluctuations. This confirms that a significant level of lateral organisation is occurring consistently throughout the reach. The V_{chan} signal includes powerful large scale fluctuations and these increase the SD significantly. This suggests that dynamic organisation in a downstream direction includes powerful low frequency waveforms. The differences in the structure of the two signals confirms the systems scale approach used throughout this study. Lateral organisation (V_{comp}) is occurring within the reach but its magnitude fluctuates less than that of downstream organisation (V_{chan}), which shows larger scale fluctuations. In order to better describe these differences in signals they were deconstructed using the FFT.

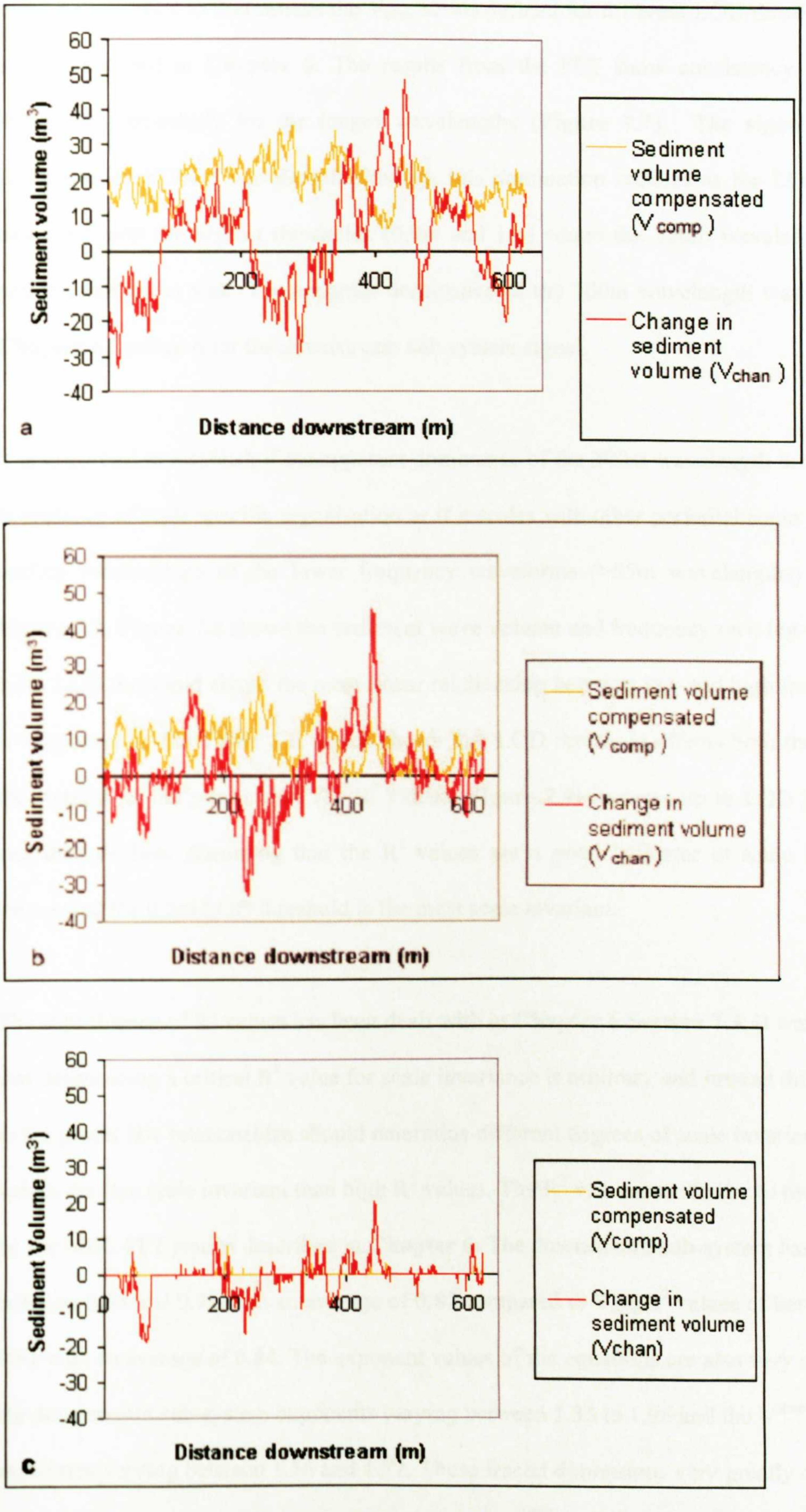

Figure 7.6. Downstream Changes in V_{chan} and V_{comp} for no LOD threshold (a), 0.5m LOD threshold (b) and 1m LOD threshold (c)

The FFT was used to deconstruct the V_{chan} series defined for different LOD thresholds using the method outlined in **Chapter 6**. The results from the FFT show consistency between LOD thresholds particularly for the longer wavelengths (**Figure 7.7**). The signal is apparently dominated by a 300m wavelength although this domination reduces as the LOD threshold is increased until the highest thresholds (0.9m and 1m) where the 300m wavelength becomes a power (amplitude) sink. The apparent dominance of the 300m wavelength was also shown in **Chapter 6 Section 6** for the downstream sub-system signal.

It is important to establish if the apparent dominance of the 300m wavelength in the V_{chan} series is evidence of scale specific organisation or if it scales with other periodicities in the series. The scaling relationships of the lower frequency waveforms (>55m wavelengths) are shown in **Figure 7.8. Figure 7.8** shows the sediment wave volume and frequency on a log-log graph. The 0.5m LOD threshold shows the most linear relationship between low and high frequencies. This is supported by the **Table 7.1,** which shows that LOD threshold effects both the equation and the strength of the power law. The R^2 values (**Figure 7.9**) increase up to LOD threshold 0.5m and then decline. Assuming that the R^2 values are a good indicator of scale invariance this means that the 0.5m LOD threshold is the most scale invariant.

The significance of R^2 values has been dealt with in **Chapter 6 Section 7.3**. It was concluded that determining a critical R^2 value for scale invariance is arbitrary and instead the fit of the data to the power law relationships should determine different degrees of scale invariance. Low R^2 values are less scale invariant than high R^2 values. The R^2 values are similar to those exhibited by the MBL FFT results described in **Chapter 6**. The downstream sub-system has R^2 values of between 0.58 and 0.94 with an average of 0.82 compared to V_{chan} R^2 values of between 0.65 and 0.93 with an average of 0.84. The exponent values of the equations are also very similar with the downstream sub-system exponents varying between 1.35 to 1.96 and the V^{chan} derived exponents varying between 1.56 and 1.72. These fractal dimensions vary greatly compared to those described by Sapozhnikov and Foufoula-Georgiou (1996) who used a planimetric approach to define fractal dimensions for 3 braided rivers. Their fractal values ranged from 1.50 to 1.58.

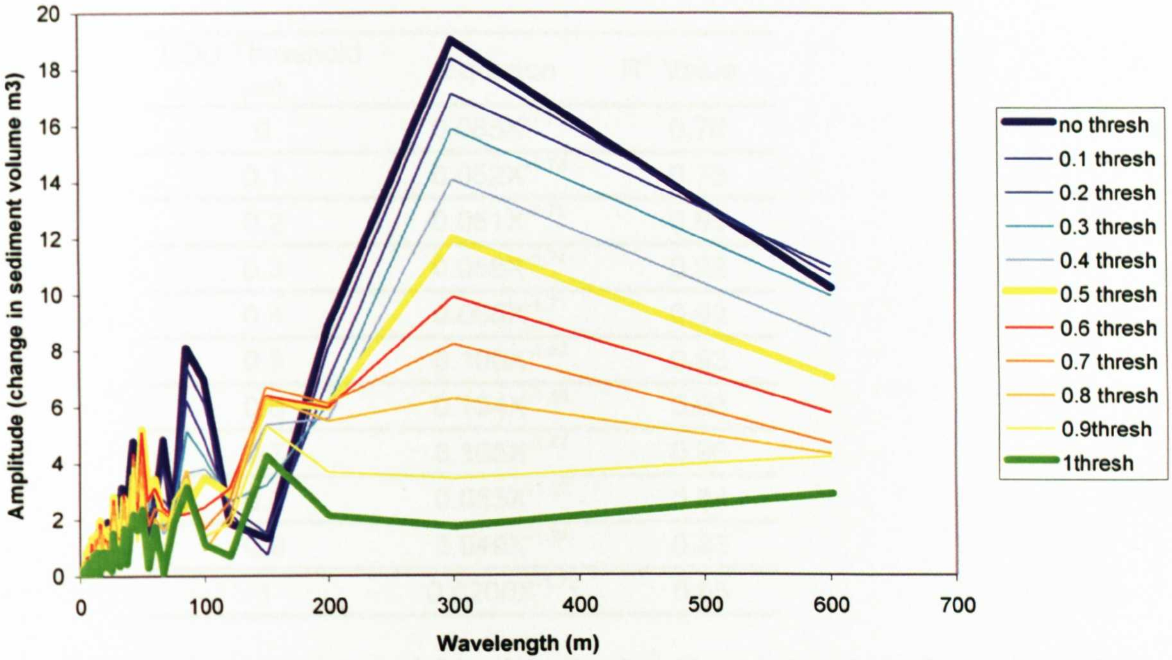

Figure 7.7. The deconstructed V_{chan} series. The high magnitude 300m wavelength attenuates rapidly as the threshold is increased

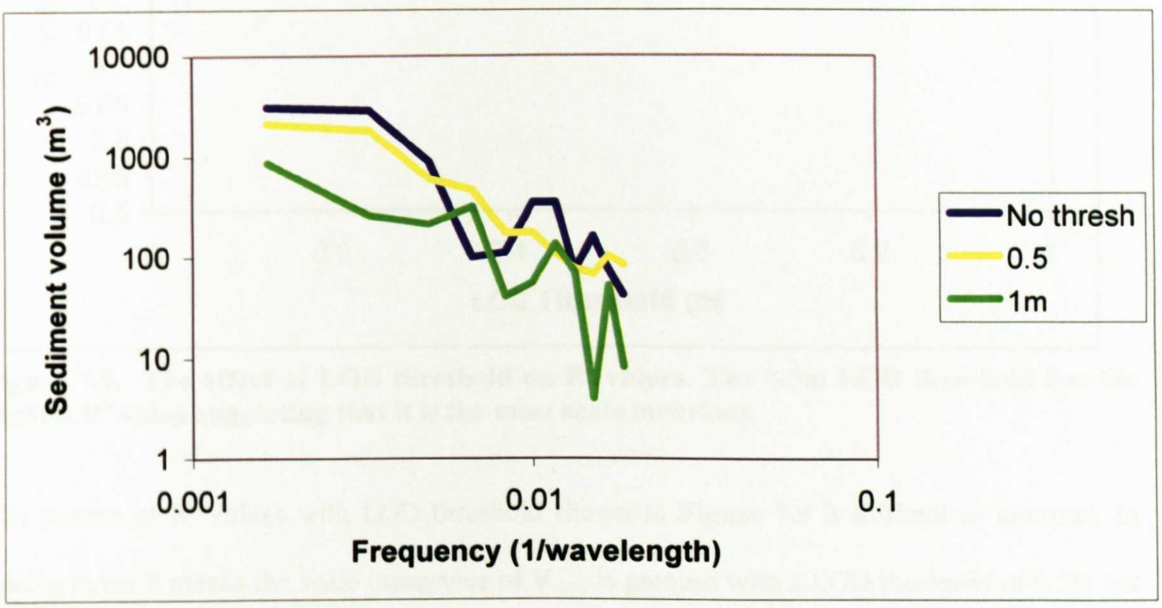

Figure 7.8. Frequency domain data for the V_{chan} series

LOD Threshold (m)	Equation	R^2 Value
0	$0.065X^{-1.73}$	0.76
0.1	$0.052X^{-1.75}$	0.73
0.2	$0.051X^{-1.76}$	0.85
0.3	$0.058X^{-1.74}$	0.92
0.4	$0.065X^{-1.71}$	0.93
0.5	$0.100X^{-1.62}$	0.93
0.6	$0.124X^{-1.56}$	0.93
0.7	$0.105X^{-1.57}$	0.90
0.8	$0.053X^{-1.67}$	0.84
0.9	$0.049X^{-1.64}$	0.83
1	$0.0200X^{-1.72}$	0.65

Table 7.1 Power law equations and R^2 values fitted to V_{chan} derived waveforms shown in Figure 7.8.

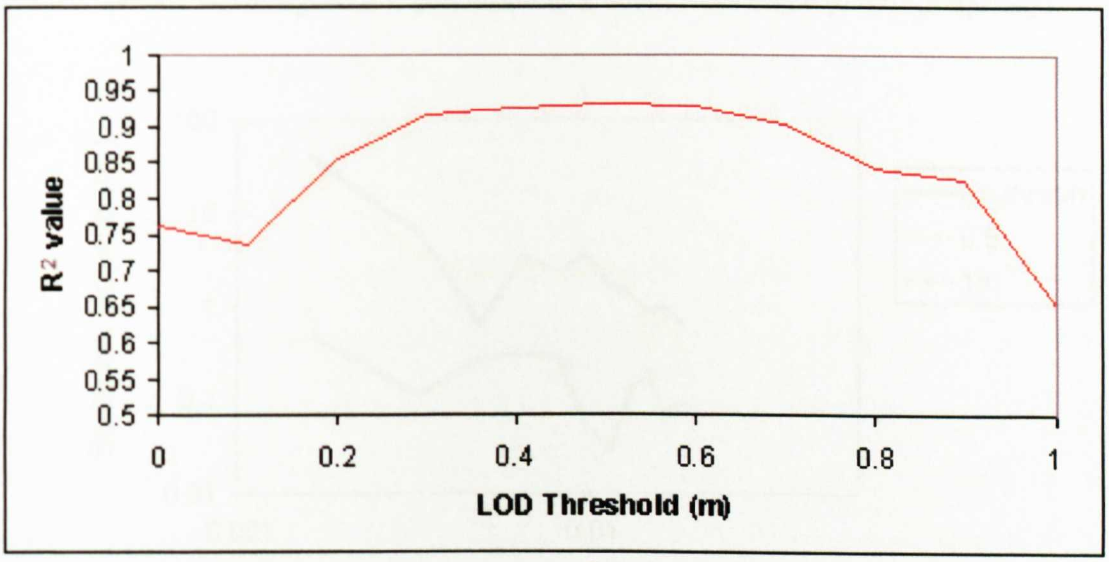

Figure 7.9. The effect of LOD threshold on R^2 values. The 0.5m LOD threshold has the highest R^2 value suggesting that it is the most scale invariant.

The pattern of R^2 values with LOD threshold shown in **Figure 7.9** is difficult to interpret. In simple terms it means the scale invariance of V_{chan} is greatest with a LOD threshold of 0.5m but what this says about the way channel changes are detected is less clear. One interpretation is that photogrammetrically produced error has a periodicity of 300m and this enhances the 300m wavelength within the DEM of difference. The data quality analysis in **Chapter 5** was unable to closely define the magnitude of low frequency waveforms although the analysis in **Chapter 5 Section 7.0** showed that the full photogrammetric DEM had a SDE of 0.163m. As the LOD threshold is increased the dominance of the error in the 300m wavelength is reduced allowing the scale invariance of the V_{chan} signal to dominate. As the LOD threshold increases the scale invariance is reduced because the amount of data to compose the signal is reduced.

The quality of the scale invariance of V_{chan} is demonstrated when it is compared to a FFT deconstruction of V_{comp} **(Figure 7.10)**. The V_{comp} series shows few large scale fluctuations and this is reflected in the deconstructed signal. The equation values for V_{comp} **(Table 7.2)** show that the negative exponents of the power laws are lower (>-1.33) than for V_{chan} (<-1.55). A similar situation exists with the R^2 values, which are all below 0.76 indicating a poor relationship between the data and the power law. These data demonstrate that the V_{comp} series between 2000 and 2002 is not scale invariant. Lateral organisation in the reach changes downstream according to a few specific wavelengths. It is dominated by a 600m wavelength (0.0016 frequency)

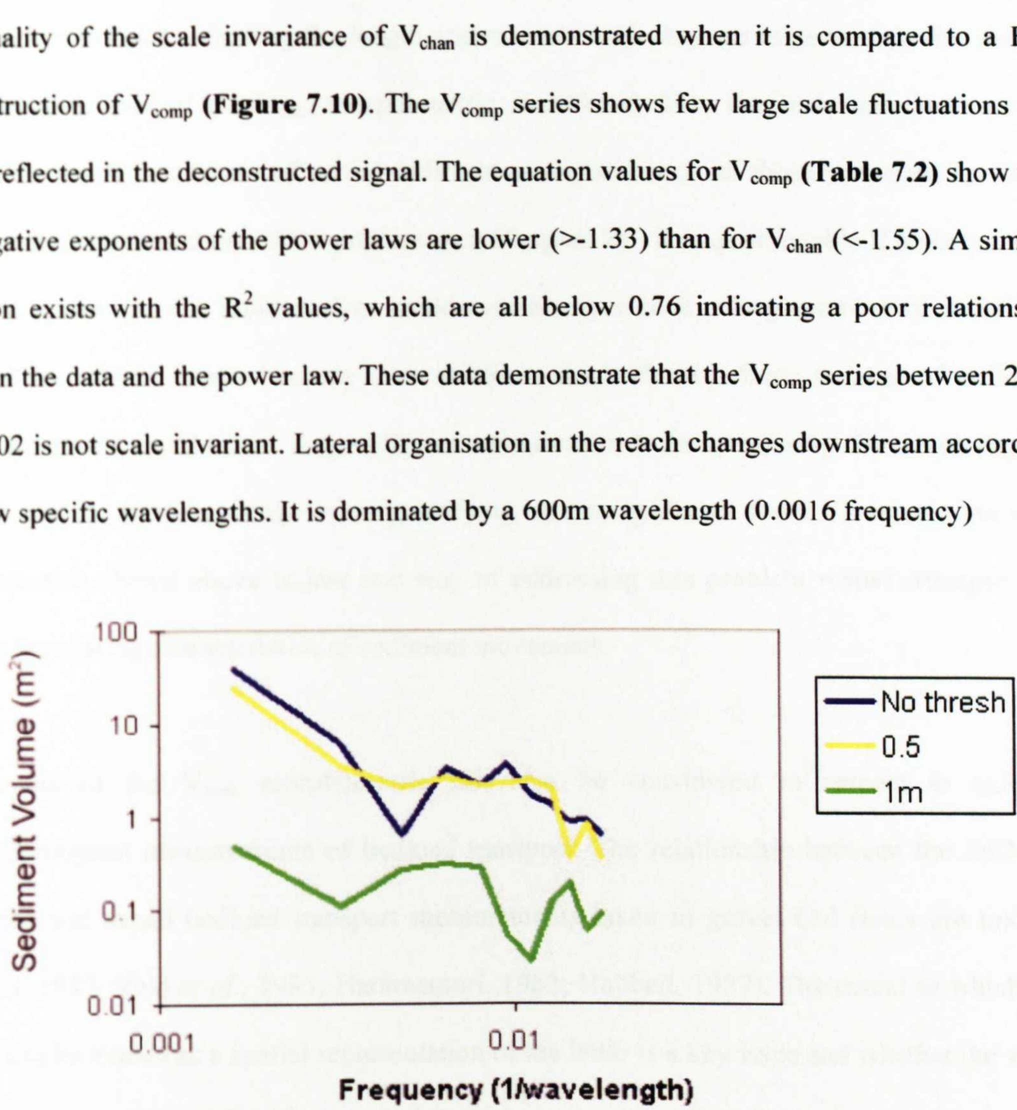

Figure 7.10 Frequency domain data for the V_{comp} series

LOD threshold (m)	Equation	R^2
0,0	$0.003x^{-1.33}$	0.67
0.5	$0.003x^{-1.35}$	0.76
1,0	$0.005x^{-0.68}$	0.34

Table 7.2. Power law equations and R^2 for the V_{comp} series. The R^2 values are low suggesting that the power laws are not good representations of the data

7.6.0 Analysis of V_{chan}

The V_{chan} results cannot be interpreted in the same way as a large number of individual sediment movement events because the V_{chan} morphometric is an amalgamated form, composed of many individual events and indicating the length scales over which they are organised. In this respect the scale invariance of the V_{chan} morphometric is different from the scale invariance of the probability density functions of actual sediment movement such as those presented by Frette (1996), which are based on 10000 profiles (see **Chapter 2**). It is questionable if a study of the sediment dynamics of a braided river could ever measure such a large number of individual sediment movement events because even within a single flood a large number of sediment movement events could occur. Any sediment measurement techniques using the morphological method will be prone to only ever quantifying an amalgamated form. However, the FFT deconstruction shown above is just one way of addressing this problem whilst attempting to identify the scaling characteristics of sediment movement.

The results of the V_{chan} morphometric can also be considered in respect to existing geomorphological measurements of bedload transport. The relationship between the DEM of difference and actual bedload transport measurements taken in gravel bed rivers are unclear (Tacconi, 1987; Reid *et al.*, 1985; Hammamori ,1962; Hubbell, 1987). The extent to which the former can be treated as a spatial representation of the latter is a key issue and whether the wave structures derived from the V_{chan} statistic can be treated as directly analogous of temporal sequences of bedload movement is unclear. For instance the way in which the temporally 'pulsing' bedload sequences described by Tacconi (1987) or Reid *et al.* (1985) would be represented spatially in a system like the Feshie is unknown. The assumption made by some authors is that these temporal pulses correspond to the migration of gravel dunes (Tacconi, 1987), is in keeping with the morphological method, but the question remains as to whether a pulsing temporal sequence in the Feshie field site would necessarily lead to a corresponding spatial wavelength. The answer is almost certainly no. The reach where the DEM of difference was derived is more complex than those monitored by Tacconni (1987) or Reid *et al.*, (1985), it underwent substantial channel changes over the two years between surveys suggesting wholesale changes to the interaction of fluid flow and morphological form. Any regular pulsing linked to specific bedforms would likely have been changed by such wholesale reorientation of flow.

The relative complexity of the fieldsite as a braided river rather than a single thread channel is important. The temporal pulses measured by (Tacconi (1987) and Reid *et al.,* (1985) are some of the best quality bedload measurements recorded to date but they were made using fixed apparatus on single channel rivers which were more constrained and stable than the Feshie fieldsite. These examples are supported by numerous other studies of bedload measurements taken using Helley-Smith type samplers (Hammamori, 1962; Hubbell, 1987) which have shown similar pulsing behaviour and bed load transport rates varying between zero and four times the mean rate (Hubbell, 1987). However braided systems have been shown to be substantially more complex than single channel systems with larger, more complex fluctuations in bedload (Ashmore, 1991). The experimental braided rivers studied by Ashmore (1991) show great variability in channel geometry and morphology over time and space even at a constant discharge and these are tied to highly non-uniform bed load transport. Short term fluctuations are attributed to local changes on the scale of individual unit bars (Ashmore, 1988). It is this complexity of form and bedload dynamics together with lateral instability that suggests that braided rivers could be SOC. The lateral instability is important because it means the system can respond rapidly to changes in volumes of sediment and flow, an essential feature of SOC systems (Paola and Foufoula-Georgio, 2001). A laterally constrained single thread system is less three dimensional, the channel cannot adapt rapidly to changing flow and sediment volumes.

A more conclusive interpretation of the dynamic morphology is not possible without a number of iterations of sediment movement allowing the comparison of a number of FFT deconstructions. This would enable some important questions to be answered. To what extent does the 300m wavelength consistently emerge, or are other sediment movements dominated by change at different wavelengths and does the overall relationship between the waveforms significantly differ after an alternative number of flood events? These questions suggest that a great deal more information is needed before the implications of the FFT deconstructions can be interpreted fully allowing direct linkage with SOC theory.

7.7.0 Comparison of MBL 2000-2002

Chapter 6 discussed the link between the scale invariance of static morphology and the SOC of sediment dynamics. The acquisition of the 2002 GPS DEM allows this link to be investigated in more detail because it gives a second static surface from which to generate the MBL statistics. The differences between the structure of 2000 and 2002 FFT deconstructions can then be compared and considered in relation to the V_{chan} periodicities giving a more comprehensive view of the relationship between static morphology and channel change. The MBL series for 2000 measures the composition of waveforms before change, the V_{chan} statistic shows the waveforms derived by measuring sediment movement and the 2002 MBL series shows the composition of waveforms after change.

To make the comparison between the 2000 and 2002 static morphologies valid then the FFT must cover the same extent of the system. To do this the 2000 downstream subsystem DEM was reduced in size to cover the same extent as the 2002 GPS derived DEM. The FFT was then applied to the reduced MBL series (**Figure 7.11**). The comparison of FFT results re-enforces the importance of defining waveforms using data extending over the entire system. The reduced system has similar amplitudes for the smaller wavelengths (particularly 80m) but the longer wavelengths are less well defined. In particular the 300m wavelength which is very well defined for the downstream sub-system is poorly represented in Experimental Reach 2 with the nearest amplitude spike at 200m. Experimental Reach 2 is also too short to identify the longest wavelengths, which means there is the potential for distortion of the scaling relationship. However the overall relationship defined by the Experimental Reach 2 is in line with that produced by the full downstream sub-system.

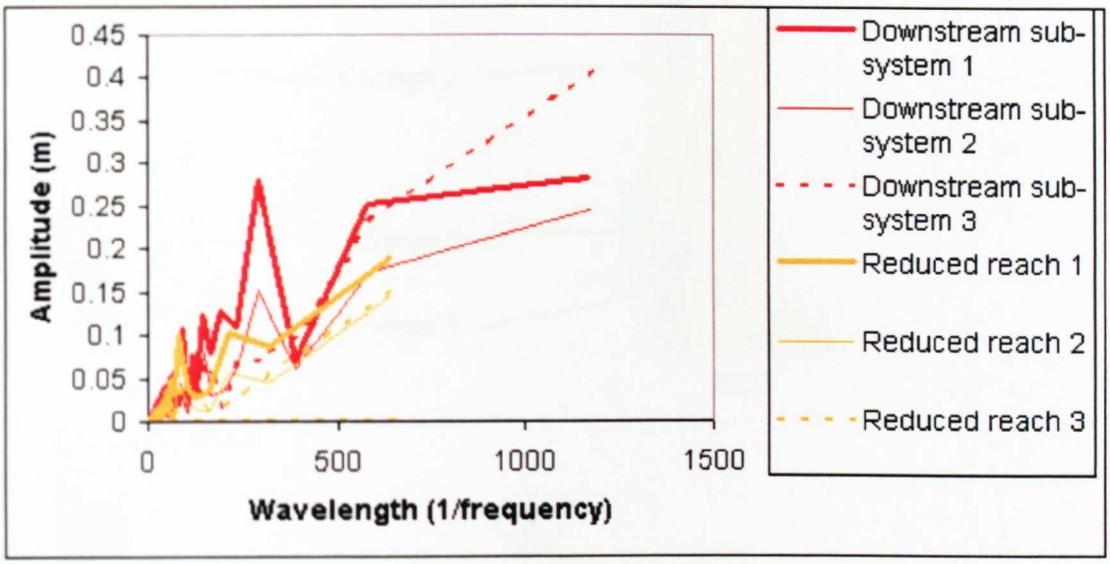

Figure 7.11 The 2000 MBL series deconstructed for the downstream subsystem and Experimental Reach 2 (classifications 1-3). The Experimental Reach 2 data is a truncated form of the downstream subsystem data hence the low frequencies are not represented.

Before the comparison between the 2000 and 2002 static morphologies could be made the active system classification had to be applied to the 2002 channel form. Because no aerial photographs were available with which to do this, the classification was based on oblique photographs and survey point data collected in the field during 2002 (**Figure 7.12**). The main difference between the 2000 and 2002 classifications is that classification 1 is expanded because of some cutting of channel banks and newly deposited/re-worked mid channel islands.

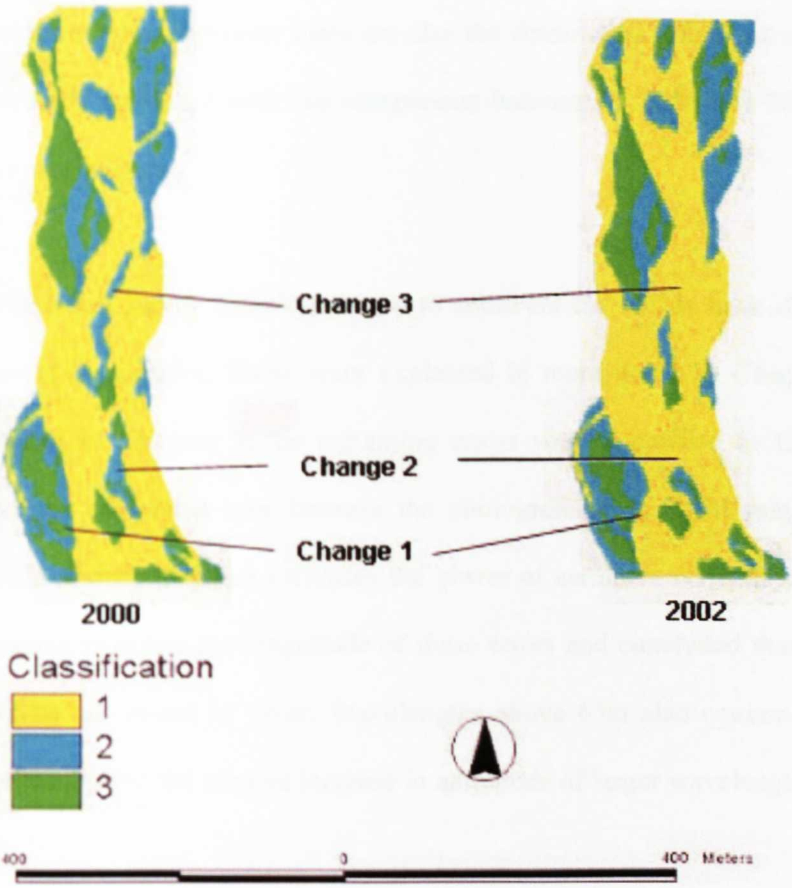

Figure 7.12 The Experimental Reach 2 'active system' classifications for 2000 (left) and 2002 (right). The three major planform changes are shown.

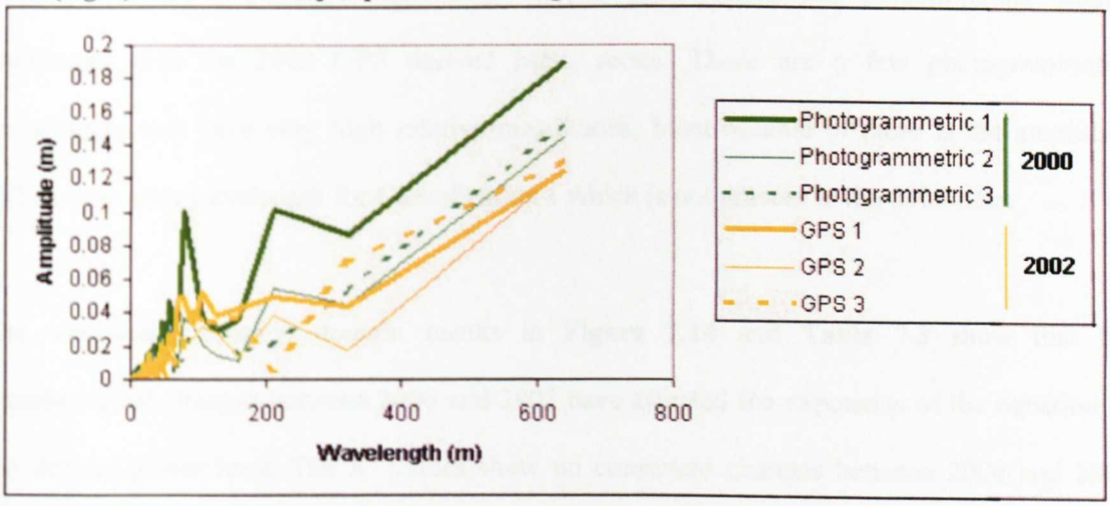

Figure 7.13 Deconstructed MBL series for the Experimental Reach 2. The 2000, photogrammetrically derived DEM is shown in green and the 2002, GPS derived DEM is shown in yellow.

When comparing the results of the 2000 and 2002 FFT deconstructions there are two effects that need to be taken into account. Firstly, there are differences caused by changes in morphology between 2000 and 2002. This is the element of the deconstruction that is useful and are considered below, however there are also the detrimental affects of error on the signal. This is particularly important with this comparison because the 2000 and 2002 surveys used different survey techniques.

The different survey techniques used to construct the DEMs have different types of errors at different magnitudes. These were explained in more detail in **Chapter 3** and were partially corrected in **Chapter 5,** the remaining errors were quantified in **Chapter 6**. The important errors are re-iterated here because the photogrammetric DEM may have error operating at specific periodicities that increases the power of certain wavelengths. **Chapter 5 Section .8.0** attempted to define the magnitude of these errors and concluded that wavelengths below 65m could be dominated by error. Wavelengths above 65m also contain error but these are less significant given the relative increase in amplitude of larger wavelengths.

The FFT deconstructions of the MBL series (**Figure 7.13**) show that the structure of waveforms is similar between the two dates. The longer wavelengths in particular have similar structures although the 2000 photogrammetrically derived MBL series has predominantly higher amplitudes than the 2002 GPS derived MBL series. There are a few photogrammetric wavelengths that have very high relative magnitudes. Most notable of these is the amplitude spike of the 80m wavelength for Classification 1 which is not present in the 2002 data.

The truncated frequency domain results in **Figure 7.14** and **Table 7.3** show that the morphological changes between 2000 and 2002 have affected the exponents of the equation of the derived power laws. The R^2 values show no consistent changes between 2000 and 2002 suggesting that the sediment movement that had occurred in the intervening period had very little impact on the scaling characteristics of the static morphology. This is the expected result because the V_{chan} statistic has a well defined linear power law (R^2 of >0.9) suggesting sediment movement is also scale invariant. The changes over the two year period are not greater than the difference between the full downstream subsystem and Experimental Reach 2 which implies that Experimental Reach 2 is of sufficient length to quantify the downstream scaling present in the system but cannot reliably be used to indicate subtle changes in scaling.

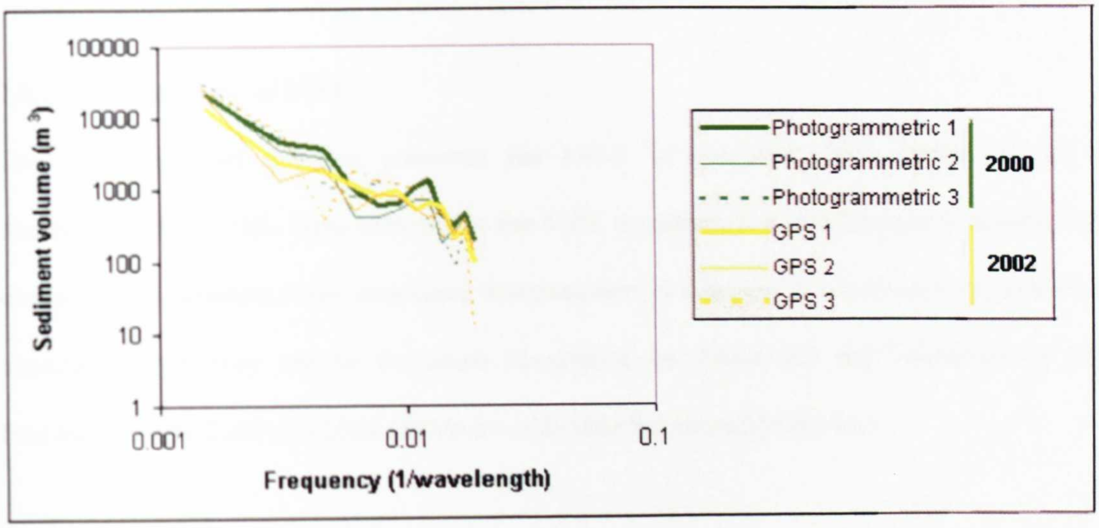

Figure 7.14 Frequency domain results for the 2000 and 2002 MBL series

	Classification 1		Classification 2		Classification 3	
	Equation	R^2 value	Equation	R^2 value	Equation	R^2 value
Photogrammetric Downstream Sub-system	$0.334x^{-1.61}$	0.87	$0.043x^{-1.93}$	0.89	$0.054x^{-1.96}$	0.94
Photogrammetric Experimental Reach 2	$0.005^{-0.1.62}$	0.88	$0.257x^{-1.67}$	0.83	$0.065x^{-1.97}$	0.89
GPS Experimental Reach 2	$0.375x^{-1.59}$	0.91	$0.510x^{-1.52}$	0.84	$0.234x^{-2.15}$	0.72

Table 7.3. Power law equations and R^2 values for the MBL series

7.8.0 Discussion

The data presented in this chapter address a number of the questions raised in **Chapter 6** by helping to clarify the specific role of MBL morphometric and linking static form to actual sediment dynamics. The discussion below considers the reliability of the results, and goes on to consider the evidence for and against the SOC of braided rivers. The implications of SOC to the study and management of braided rivers are assessed. Finally these results are contextualised to show the impact of the systems level approach as opposed to reductionist research paradigms.

7.8.1 The sensitivity of MBL

The first important question concerns the effect of morphological change on the FFT deconstruction of MBL. How sensitive is the MBL morphometric and frequency domain data to change. If the apparent scale invariance demonstrated in **Chapter 6** is a chance occurrence then channel change may reduce the scale invariance by increasing the amplitude of higher frequencies. The 2000 and 2002 DEMs provide data for investigating this.

The DEM of difference shows some significant morphological changes over the two year period. Many of these are accounted for by the V_{comp} morphometric, which shows lateral changes resulting from channels shifting position and erosion of one channel boundary being compensated for by deposition at the other channel boundary. However there are still some net changes in cross sectional volume, measured by V_{chan}, that show downstream sediment movement is scale invariant. Despite these significant morphological changes the deconstructed MBL signals for 2000 and 2002 are very similar which indicates the insensitivity of the MBL morphometric to channel change over bi-annual timescales. When the method for defining MBL is considered, this insensitivity might be expected. The channel classification which defines the active width over which the MBL is calculated is an approximation of the 'active system' over decadal timescales and the changes that occurred between 2000 and 2002 were small in comparison. MBL is also unable to distinguish morphological change that is lateral, and the 2000 to 2002 DEM of difference includes considerable amounts of lateral change. The robustness of the power law associated with the MBL is encouraging because it shows that relatively small morphological changes, whilst having an effect on the amplitude of specific wavelengths, do not affect the overall scale invariance of the MBL series.

This highlights a fundamental question concerning the sensitivity of MBL- can the scale invariance of the deconstructed MBL be used as evidence of SOC given that it is insensitive to two years of morphological change incorporating multiple change events. This question is important because the relationship between static fractals and SOC is unclear. If the fractal is a static signature of SOC then the insensitivity of MBL is unimportant. Studies such as Rinaldo's fractal drainage network (1996) suggest this linkage. The fractal drainage basin is the result of scale invariant processes sediment movement processes operating over long periods of time or over many iterations of the model. A single high magnitude sediment movement event occurring in a single iteration of the model will have very little impact on the fractal form. In contrast the rice pile produced by Frette (1996) shows that the static fractal form can undergo wholesale changes in response to a single avalanche event implying small scale interactions between fractal form and SOC avalanches.

Ultimately both fractal form and SOC dynamism are scale invariant so a postulated link between the sensitive rice pile of Frette (1996) and the insensitive river structure of Rinaldo (1996) could begin with scaling. In Frette's work SOC is indicated by the inverse power law of the magnitude and frequency of avalanches events. In a very large system very large avalanches can occur affecting the static form of a large part of the system but these occur infrequently. Small avalanches will also occur affecting the static form of small parts of the system but these changes will not be identified unless the measurement techniques employed can determine small changes. By implication changes at all magnitudes and frequencies could be occurring in Rinaldo's computational drainage network causing high frequency changes to the smallest fractal form. Alternatively, if Frette had constructed a rice pile of sufficient size (and had sufficient equipment to measure it) then the fractal structure would show apparent insensitivity with rapid changes only occurring as a result of the largest magnitude events. Put in these terms the sensitivity of fractal form is a function of scale of enquiry. Using this rationale the MBL morphometric shows insensitivity because it will only show system changes as a result of very high magnitude events or large scale fluctuations. The highest volume V_{chan} sediment wave is an order of magnitude smaller than that of the highest volume MBL wave and as such it only has a minor effect. Therefore MBL is a good measure of the scale invariance of braided river systems over decadal timescales but an insensitive measure of change over shorter timescales.

7.8.2 Self- organisation of braided river systems

This chapter supports many of the findings of **Chapter 6**. The scale invariance of the 2000 upstream and downstream sub-systems corresponds well with the scale invariance of the 2002 GPS survey of Experimental Reach 2. More importantly the structure of actual sediment change between 2000 and 2002 has also been shown to be scale invariant and although this is not as conclusive as measurements of the magnitude and frequency of individual sediment movement events it is a useful alternative method of deconstructing the large number of individual events that comprise channel change.

The fundamental theory that has underlain much of the methodology of this thesis is SOC, a theory that is directly linked to the scale invariance of process and form. The evidence of scale invariance presented in this thesis is suggestive but not sufficient to fully establish the SOC credentials of the system because the power law relationships cannot be considered as direct indicators of SOC in the same way that probability density functions of multiple avalanches can. The MBL data represents a single static form and the V_{chan} data just a single iteration of change. If these morphometrics could be derived annually over decades then change of different magnitudes could be established. Numerous FFT deconstructions could show if the same wave structures dominate every iteration (showing scale specific behaviour) or if the dominant wavelengths fluctuate over time. This would allow a better understanding of the attributes of the morphometrics and the operation of the system.

The results of this thesis should not be considered in isolation. There are other studies within geomorphology that have also analysed the structure of braided river morphology and found scaling relationships. The channel ordering approach adopted by Rust (1969) as a method for quantifying the structure of channels implicitly accepts that braided systems self organise into a channel hierarchy (**Chapter 2**). Sapozhnikov and Foufoula-Georgio (1996, 1997, 1998) quantify this scale invariance using fractal scaling methods to show that the planform properties of braided rivers exhibit self affine geometrical scaling (**Chapter 2**).

Much of the dynamic behaviour of braided river systems is similar to that of SOC systems. Bedload movement shows apparent stochasticism including wide fluctuations even at constant flow conditions (Ashmore, 1988; Hubbell, 1987; Hoey, 1992) and braided channels appear to behave as a system showing upstream and downstream connectivity. The patterns of compensating erosion and deposition as quantified by the V_{com} morphometric is indicative of this connectivity. The dynamic behaviour of braided rivers has also been demonstrated by Sapozhnikov and Foufoula-Georgio (1996) who showed that experimental flume models scale dynamically.

Whilst this combined collection of evidence is persuasive and consistent with how a SOC braided system might behave there are a number of counter arguments. Firstly many researchers have found that SOC is not necessarily a robust state. Even experimental studies using slowly driven granular systems have not shown SOC to be a universal phenomenon. Although Frette (1996) describes a rice pile system in which the dynamics exhibit SOC behaviour this is dependent on the large aspect ratio of the grains. Other rice pile systems studied by Frette (1996, 1997) showed that a characteristic avalanche appeared which is inconsistent with the ideas of SOC. Similarly studies of actual sand piles (Held *et al.*, 1990) have failed to reproduce the clear SOC shown by numerical models of sand pile dynamics with behaviour consistent with SOC for smaller sand piles replaced with that of a 'relaxational oscillator' for larger sand piles, scale invariance is replaced by scale specific behaviour.

Secondly, it is unclear how the SOC of slowly driven granular systems should be related to braided river systems. The SOC behaviour of granular systems is seen as a method of dissipating the potential energy of the granules, however potential energy in a braided river is supplied by both the water and sediment moving through the system. Which of these sources of potential energy dominates the self organisation of the system is unclear because both morphological form and fluid flow interact. Although both sediment movement and fluid flow are closely coupled they operate over very different timescales (Paola and Foufoula Georgio, 2001). This study has focused on sediment movement and the imprint of SOC onto static morphology whereas Sapozhnikov and Foufoula-Georgiou (1996, 1997) studied fluctuations in the distribution of water and how it interacts with morphology.

Lastly, whilst the evidence presented in **Chapter 6** and this chapter is conducive to a system that is SOC it is also consistent to a system that is organised according to many other states. The MBL series in **Chapter 6** could be the result of sediment movement occurring over a specific length scale in specific channels within the system, but due to the multi-channel morphology of the braided system and the averaging of MBL this manifests itself as sediment waves over a range of frequencies. Numerous DEM iterations could prove this by establishing the dominance of specific length scales over decades. Similar criticisms are possible of the V_{chan} statistic, which could also be indicative of a dominant length scale.

If the evidence that the fieldsite is SOC is accepted then the critical theoretical question becomes; at what point does the system become SOC. At the top end of the fieldsite the river is a single channel and so sediment movement might be scale specific 'pulsing' as suggested by Reid *et al.* (1985) and it could be fluctuating over four times the average as described by Hammamori (1962). For it to change to a SOC system, bedload fluctuations of all scales must develop. This change could occur through increased lateral instability, which increases the amount of sediment that could be mobilised in any single flood event. A key issue is how quickly the system changes from being 'pulsing' to being SOC. This same question has been asked by SOC theorists that have established that SOC is not necessarily a robust state (Held *et al.*, 1990). Held *et al.*, (1990) established that sand piles built on a 1.5 in diameter plate were

SOC but those on a 3.0 in diameter plate were not. The threshold between the two states has not yet been determined.

7.8.3 Implications of SOC to the study of braided rivers

If the behaviour of braided rivers could be demonstrated to be SOC then this could have profound implications for the way in which they are studied and managed. At the broadest scales it could affect the conceptual model that river scientists use to contextualise research. This is the model upon which scientific assumptions are often implicitly founded and as such it could have far reaching implications for the design, implementation and interpretation of research.

One traditional model of channel development is based on the concept of hydraulic geometry (also termed regime theory), the quantitive description of how river width, depth, velocity and related properties very with changing discharge over time at one site 'at a point hydraulic geometry' or along and between rivers (Ferguson, 1986). Hydraulic Geometry was developed in the 1950s and 1960s by engineers and geomorphologists of the United States Geological Society (especially Leopold, Wolman and Miller), as a method for providing a functional explanation of river channel form. River properties such as width, depth and velocity were compared to discharge using logarithmic plots (Leopold and Maddock, 1953). These relationships form the basis of understanding the relationships between river channel form and discharge. A simple model based on these principles is presented in Hey (1987). Periods of channel erosion are considered the result of a decline in sediment input or increased sediment transport capability at a certain point. Conversely, periods of deposition are considered to be the result of sediment increased input or localised reductions in sediment transport capacity. A state of static equilibrium is considered the idealised final state in which shear stress is dissipated evenly throughout the channel resulting in low sediment transport. A system that has maximised entropy so that water is conveyed through channels is doing the least amount of work and the only fluctuations present in the system are externally generated sediment and flow fluctuations

(Hey, 1987). A steady state conceptualisation of the way sediment dynamics work is clearly not applicable to a SOC braided river system. SOC systems are not steady state and can generate fluctuations of all magnitudes based on the operation of the system alone without the need for fluctuations of external inputs.

The discussion by Pitlick of Hey's model (Hey, 1987) raises the question of at what scale the model would be a useful engineering or geomorphic tool, suggesting that a characteristic scale of channel response exists. This scale specific approach would not be appropriate for a SOC system because of the scale invariance of its bedload dynamics and morphology. The only scale specific consideration with a SOC system is the scale at which the system operates, whether this be the drainage basin scale, the river channel scale or the reach scale. This chapter has adopted a reach scale, and the previous chapter a braided system scale, in an attempt to identify the dominant forms of organisation within the system, however forms of organisation operating at much larger temporal and spatial scales are inevitably controlling the magnitude and frequency of sediment flux and flow flux. The braided river system analysed in this thesis organises its sediment flux and channel morphology with these predetermined inputs

The evidence presented in this thesis whilst inadequate to demonstrate the existence of SOC in braided river channels is sufficient to challenge the conceptualisation of river channels in equilibrium tending towards a steady state. The relative downstream uniformity of lateral organisation in the DEM of difference is strongly outweighed by the periodicities of actual morphological change (V_{chan}), which indicate large downstream fluctuations in sediment movement not consistent with the even dissipation of shear stress. The large fluctuations in MBL are testament to a system that is not tending towards a steady drop in elevation but one that incorporates large scale MBL fluctuations.

The concepts involved with landscape and system evolution have been considered at length by Schumm (1979). Schumm stressed the concept of geomorphic thresholds as a way of explaining why systems behave in different ways. Extrinsic geomorphic threshold explain why systems affected by similar external forces (for instance climatic change) behave in different ways. A system that is close to a geomorphic threshold could undergo wholesale changes when the external force was applied whereas another similar system could show very little effect. Perhaps more important than this is the concept of intrinsic geomorphic thresholds (Schumm, 1979). This is the idea that landforms change without a change in external controls but as a result of the operation of the system. Schumm (1979) points out that erosional and depositional changes can be an inherent part of the normal development of landscape and do not require a change in an external variable. The concept of intrinsic thresholds is consistent with SOC theory, an important part of both concepts is that the system can generate large scale fluctuations in form and behaviour as a result of the internal operation of the system. Schumm (1979) considered the fluctuations in erosion and deposition as a dynamic equilibrium, part of the hunt for a new equilibrium.

If intrinsic thresholds are applied to a braided system that is self organised critical then it is possible to speculate a link between MBL and channel pattern. **Figure 7.15** shows a speculative link between a MBL series composed of seven waveforms and a geomorphic threshold. This series is applicable to MBL fluctuations over time 'at a point' or as downstream MBL fluctuations. As MBL series changes the rise in bedlevel triggers a change in planform when the threshold is reached. In braided rivers such as the Feshie the rise in bedlevel could be the cause of channel widening, channel avulsion and channel pattern instability such as that described by Werritty and Ferguson (1980). The study of the South Tyne at Lambley, UK by Passmore and Macklin (2000) described localised channel instability propagating downstream. The model shown in **Figure 7.15** offers a viable explanation for this. A rise in bed level resulting from the downstream migration of a particularly large waveform causes lateral instability only when a threshold is crossed. In hydraulic terms this threshold could be the point at which channel capacity is reduced sufficiently to allow flood flows to erode channel banks, widening the channel. In fact if SOC theory is fully applied then **Figure 7.15** is an oversimplification. A system with scale invariant sediment dynamics has numerous sediment waves of different magnitudes and frequencies propagating through the channel at any one time. The MBL at any one point is determined by the magnitude, frequency and phase of all the waves.

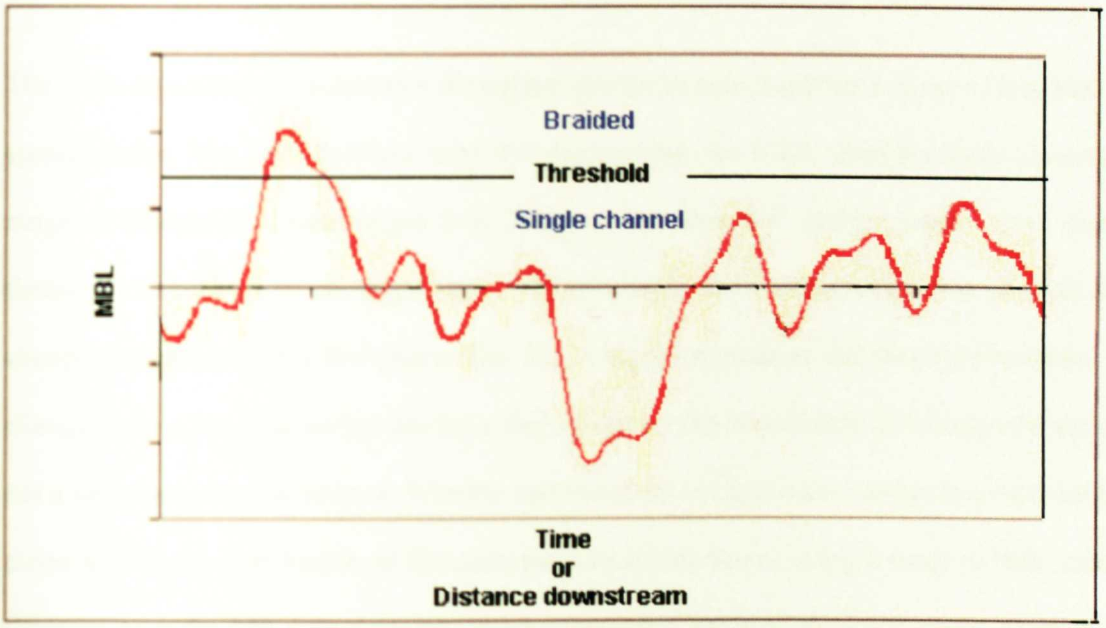

Figure 7.15. A conceptual model showing the relationship between MBL and distance downstream or time, constructed using 7 sine waves. The threshold is crossed only when several wave forms combine to raise MBL. This model is designed to be analogous of the South Tyne at Lambley where the channel is predominantly a single channel but lateral instability is migrating downstream.

There are numerous factors that have not been considered in the analysis of this thesis but have been shown by previous geomorphological research to have impacts on the form and function of gravel bed rivers. In particular the makeup of the river bed and banks including the size and shape of particles, channel armouring and packing. Conventional geomorphological ideas suggest that these could be integral parts of form–process interactions and this suggests that they could also be integral to the operation of the system. It is not possible to offer insight into the effects of these factors on the organisation of the system using the systems level methodology adopted in this thesis. The systems level approach does not attempt to break down the system into its constituent parts but aims to determine the operation of the system as a whole. If this thesis had attempted to assess the impact of specific factors on the operation of the system then this would have been ineffective. As well as the practical problems with producing spatially consistent measurements of factors such as sediment size or packing over a range of scales there are also theoretical problems of determining the influence of individual factors in a system with multiple degrees of freedom. The numerous problems of reductionism (**Chapter 2**) would severely impede such an approach.

The focus on scaling characteristics throughout this thesis links together a range of temporal and spatial scales. The classifications used for determining the MBL morphometric represent a range of timescales. Classification 3 is likely to represent the 'active system' over decadal timescales in contrast to Classification 1, which is likely to be more responsive of small scale changes occurring over a few years. The V_{chan} statistic represents the shortest timescale, real changes over a two year period but for a limited reach. The importance of linking timescales is not a new theme in river science. Werritty and Ferguson (1980) linked change over a number of timescales on the river Feshie, at the same fieldsite as this thesis, using a range of data sources. Changes over the 200 year timescale were determined through historical maps, changes that occurred at a 30 year timescale were determined from aerial photographs and changes at the one year timescale were determined through field survey. Each of these timescales was used to show different characteristics of channel change. The 200 year timescale showed that distinctive channel patterns that could be explained by spatial variations in valley topography were virtually fixed at that 'graded' timescale. The 30 year timescale showed a relationship between channel patterns and incidence of high-magnitude events. The 1 year timescale suggested that some of the channel changes could be understood in terms of hydraulic processes.

A limiting factor to linking together timescales is the quality of the data sources available. Longer timescales tend to have poorer quality data sources (mapping) allowing planimetric analysis whereas short timescales allow topographic survey and three dimensional analysis. This generates a large disparity in the types of analysis possible at different timescales. One of the strengths of the approaches employed in this thesis is that they attempt to link a number of timescales by measuring channel form, indicative of sediment organisation at decadal timescales with actual sediment movement (organisation) at bi-annual timescales. This means the structure of channel organisation and its behaviour have been more closely linked over a range of timescales than was possible in the work of Werritty and Ferguson (1980).

7.8.4 Implications of SOC to the management of rivers

SOC could have significant implications for the management of braided rivers because in principle knowledge of the frequency of a range of small magnitude events could be used to predict the frequency of large magnitude events. A similar technique has been suggested for earthquake management by Carlson and Langer (1989). Understanding the frequency of large magnitude events in braided rivers will enable managers to implement management strategies based on the probability of large events occurring. Establishing magnitude frequency relations of sediment flux enables the identification of episodes of channel instability or reduced channel capacity. Similar information defining the magnitude and frequency of flow flux is already a key tool for river managers.

However the management implications of a SOC braided river system should not be overstressed. The river should not be taken out of context because the drainage basin in which the river is situated and overriding climatic changes have been conclusively established as important controls on sediment movement behaviour (Rumsby, 1991). In particular the wider catchment (land use, slope channel coupling) controls the overall sediment balance of the braided river, whether it is aggrading or in equilibrium. Moreover SOC is a state that describes the workings of the system when it is in dynamic equilibrium. There is of course some evidence that drainage basins themselves could be SOC (Rinaldo *et al.*, 1996) a finding that could have more far reaching implications for river channel and hillslope management because it suggests that the drainage basin is the most important unit to be managed and all management should stem from considerations at the drainage basin scale.

7.9.0 Conclusion

This chapter has demonstrated that sediment movement in Experimental Reach 2 at the fieldsite was scale invariant over a two year period between 2000 and 2002. These changes have had little effect on the scaling characteristics of the static morphology of the reach as measured by MBL deconstructions. These findings address the third research theme (**Chapter 2 Section 8.3**), the dynamic scaling properties of the field site. Although both sediment movement and static morphology have been shown to be scale invariant this does not demonstrate that the system is SOC. There are a number of theoretical links between fractal (scale invariant) form and scale invariant processes which must be more closely defined. There is also doubt how SOC should be tested in a braided river system because both sediment and flow flux are present and the system does not work in isolation from the rest of the drainage basin. These findings are of relevance to research theme four which is an attempt to interpret the scaling characteristics of both dynamic and static data sources.

Demonstrating that braided rivers are SOC systems may never be possible, due in part to problems recording the magnitude and frequency of sediment movement events. The best approach to understanding SOC in braided river systems may be an experimental one. A flume allows extra control over variables such as discharge, sediment input and temporal sequences giving the opportunity to more closely define the nature of sediment movement events and morphology. However real braided rivers do not work in isolation but are a specific form of river channel system working within other larger systems such as the drainage basin system. These larger systems dictate many of the inputs to the braided system, which will undoubtedly have an influence on the functioning of the system. In the case of the River Feshie fieldsite the discharge and sediment load entering the top of the system is not steady state but is controlled by fluctuations in the upstream drainage basin system.

CHAPTER 8 CONCLUSIONS

Abstract

This chapter concludes this thesis by summarising the most important findings. The importance of the systems level approach and SOC are re-iterated in **8.1.0** along with an explanation of where this places the thesis in relation to reductionist research paradigms. Each of the research themes is taken in turn in **8.2.0** to outline the main findings and answer the key questions raised in **Chapter 2**. A specific focus is put on defining problems with the research area that need remedying before further progress can be made. Section **8.3.0.** concludes the thesis by suggesting some approaches and questions for future research.

8.1.0. Introduction

'Ultimately, the strength of a science depends upon the development, consistency and synergism of empirical and theoretical approaches. At any one time, the mismatch between facts and ideas can seem extreme: unexplained observations and untested and unrealistic theories may abound. But it is this mismatch which is the main driving force behind scientific progress.' (Cox and Evans, 1987)

Many of the ideas presented in this thesis may initially seem at odds with convention, for example, the systems level approach fails to respect reductionist approaches because it does not attempt to explain the organisation of the braided river system in terms of traditional parameters such as shear stress or bed roughness. The theory (SOC) that has driven this research thesis is a mismatch to contemporary approaches for defining braided river behaviour because it has scale at its core and it fundamentally looks for similarities between scales rather than breaking down each scale into a set of causative processes. This 'black box' approach may well be considered regressive by contemporary process driven theorists however because it challenges the accepted norms and is well supported by a small but influential number of studies (Sapozhnikov and

Foufoula) it could profoundly change the way braided river dynamics are investigated or modelled in the future

This study tested the applicability of SOC by looking for evidence of scale invariance in existing literature and employed new data acquisition and processing techniques to provide new evidence about the self-organisation of the River Feshie, Scotland.

8.2.0 Research themes revisited

Each of the research aims described in **Section 2.8.0** are now revisited and assessed in light of the evidence and presented in **Chapters 3-7**.

Research Theme 1: Acquisition, correction and testing of high quality morphological data

Collection of high quality morphological data was one of the most important aspects of this research. Research themes 2, 3 and 4 required the morphological data to be high resolution but also spatially extensive. In order to achieve this, the specific qualities of each data collection method were identified. Ground survey techniques proved very successful at acquiring very high accuracy, high precision data over a limited spatial extent, although this required significant field resources. Photogrammetry proved a better survey technique over larger spatial areas allowing the survey of the entire braided system, although the acquired data were of a poorer quality and required significant laboratory processing.

In **Chapter 2**, some specific questions were asked; what techniques for acquiring morphological data are most appropriate for addressing the multi-scale, spatially extensive data required for scaling analysis at the system scale? And what magnitude and structure of error is incorporated into DEMs using ground and remote survey techniques and how does this effect the application of those DEMs to problems of scaling and self organisation? These will be answered below.

The analysis in **Chapter 3** examines the strengths and weaknesses of different survey techniques and established that ground survey techniques particularly surveying GPS were effective at acquiring very high accuracy, high precision DEMs of a section of braided river but airborne techniques should be employed over larger areas. **Chapter 4** implemented these techniques. Some specific lessons can be learned particularly from the application of digital photogrammetric techniques. Photogrammetric project work must be meticulously planned from the start. In particular, the reliability of the aerial survey platform and overhead weather conditions are integral to success along with having large amounts of ground truth data collected as close to the flight date as possible. Modeling water depth using empirical methods requires data collected as the photogrammetric data is acquired or at identical stage readings, such data must be spatially extensive covering all aerial photographs with submerged zones.

In **Chapter 5** photogrammetric DEM error was described by comparison with a 'true surface'. The results were revealing about the structure of error present in digital photogrammetrically derived DEMs. However, if photogrammetry is to be increasingly used to monitor braided river form it is important that not only the magnitude but also the structure of error are more carefully examined using similar comparative techniques. In particular, the weaknesses of the digital photogrammetric approach (subaqueous zones and mosaicking) should be assessed not only as single error statistics but also spatially.

2.8.2 Research Theme 2. Static scaling properties

The second research theme aimed to identify downstream patterns in channel form indicative of system scale organisation. Two specific questions were asked; how can patterns in morphology, indicative of self-organisation be reliably identified? In addition, what scaling characteristics are emergent from analysis at the system scale?

This thesis has measured static morphology based on the assumption that static morphology is imprinted with the signal of self-organisation and it is therefore an outcome of the system.

However, it is possible to view static morphology as just one of the processes working within the black box and the system outcome is the actual magnitude and frequency of the sediment movements. No such measurements were possible in this thesis although the DEM of difference provides some insight into the periodicities associated with sediment movement over a 2-year period.

The development of the MBL morphometric was an attempt to define a measure of static morphology. The MBL morphometric makes use of the three dimensional data acquired using photogrammetric and ground survey techniques but it is still fundamentally constrained by the need to define the extent of the classification two dimensionally. In this respect, the morphometric is little advanced on the work of Rust (1978) who also developed a range of classifications for the same channel system. There can be little doubt that the classification based on perceived activity (mainly vegetation cover) is a weakness of the morphometric. There are a few possible improvements that could be made to address this issue. The improvement of models that simulate fluid flow such as McArdell and Faeh (2001) could allow the simulation of flood events of a range of magnitudes, classifications could then be based on simple measures such as extent of inundation or more sophisticated measures such as estimated shear stress.

The application of the FFT to deconstruct the MBL series was intended to provide a method for defining the scaling characteristics at the system scale. This analysis was complicated by problems inherent to the FFT technique such as leakage of power and frequencies defined by the length of the data series. The most significant problem came from the use of the frequency domain data for defining the scaling characteristics of the signal using linear regression. The fitting of linear trend lines to the frequency domain data produced fractal dimensions based on the exponent but existing literature was unclear what R^2 value constituted scale invariance. Further research into the use of the FFT and linear regression for defining fractals is essential if the derived fractal dimensions are to be used over a number of iterations with a single river system or comparatively between river systems.

Research Theme 3: Dynamic scaling properties

The third research theme focused on the dynamic properties of system scale organisation as characterised by the flux of sediment through the river channel. The specific questions attached to the theme continued the idea of identifying scaling characteristics: Does sediment movement occur according to specific length scales or is it scale invariant? In addition, how do the dynamic scaling characteristics compare to the static scaling characteristics?

The DEM differencing provided specific evidence of morphological change over the 2-year period between surveys. Sediment flux downstream was quantified using a cross sectional morphometric V_{chan} and this demonstrated that sediment flux was not scale specific. The channel changes over the two-year period had very little influence on the scaling characteristics of MBL showing that it is an insensitive measure of small scale morphological changes.

Research theme 4: The self organised properties of braided rivers

The final research theme is broader because it aimed to take an overview of all the evidence in previous published research and the evidence presented in **chapters 6 and 7** of this thesis. The following question was asked: Do the static and dynamic scaling characteristics determined in this thesis support the idea that braided river systems are self organised critical?

Despite all the problems with defining the scaling characteristics of static and dynamic morphology some specific forms of organisation have been identified. The static form of the study site shows fluctuations in elevation which deviate from the average bed slope and these clearly represent a form of self-organisation. Similarly channel changes between 2000 and 2002 show similar low frequency fluctuations. These demonstrate that sediment movement is not a steady state but fluctuates over many orders of magnitude. Such evidence supports the idea that braided river systems could be self organised critical.

8.3.0 Future research

There are clearly problems with some of the unconventional application of techniques used in this thesis, however the data presented show the importance of new techniques for DEM generation of large areas of braided systems. Such techniques allow river scientists to analyse data for the whole system not just very spatially limited reaches or confluence units where flow and sediment flux are strongly influenced by upstream changes. This thesis represents just one attempt at applying a systems level approach to the problems of river form and process but as other researchers employ new technologies to do likewise then this will inevitably lead to the development of new theory on the operation of the system and the role of sediment flux and scaling within the system. An experimental approach is one way of advancing understanding rapidly because it allows a good amount of control over the input flux of both sediment and fluid. New laser profiling techniques for acquiring morphological data of flume surfaces present the opportunity of rapidly acquiring high resolution DEMs of the flume surface at set time intervals.

Flume experimentation alone will be insufficient to provide answers to the large amount of variability present in the fluvial environment and field studies must attempt to address these. In particular, the distinctive change in channel form between meandering and braiding needs further explanation. Does the change represent a wholesale change in the operation of the system where sediment movement conforms to new rules or does sediment movement stay essentially the same with channel form changing when a threshold is crossed, triggering lateral instability? Either way the results are important for the modeling of river channels and drainage basin dynamics.

Research Theme 3: Dynamic scaling properties

The third research theme focused on the dynamic properties of system scale organisation as characterised by the flux of sediment through the river channel. The specific questions attached to the theme continued the idea of identifying scaling characteristics: Does sediment movement occur according to specific length scales or is it scale invariant? In addition, how do the dynamic scaling characteristics compare to the static scaling characteristics?

The DEM differencing provided specific evidence of morphological change over the 2-year period between surveys. Sediment flux downstream was quantified using a cross sectional morphometric V_{chan} and this demonstrated that sediment flux was not scale specific. The channel changes over the two-year period had very little influence on the scaling characteristics of MBL showing that it is an insensitive measure of small scale morphological changes.

Research theme 4: The self organised properties of braided rivers

The final research theme is broader because it aimed to take an overview of all the evidence in previous published research and the evidence presented in **chapters 6 and** 7 of this thesis. The following question was asked: Do the static and dynamic scaling characteristics determined in this thesis support the idea that braided river systems are self organised critical?

Despite all the problems with defining the scaling characteristics of static and dynamic morphology some specific forms of organisation have been identified. The static form of the study site shows fluctuations in elevation which deviate from the average bed slope and these clearly represent a form of self-organisation. Similarly channel changes between 2000 and 2002 show similar low frequency fluctuations. These demonstrate that sediment movement is not a steady state but fluctuates over many orders of magnitude. Such evidence supports the idea that braided river systems could be self organised critical.

APPENDIX 1. ORTHOMAX DEM COLLECTION PARAMETERS

The parameters which control the OrthoMAX Vision automated stereo-matching algorithm.

Minimum threshold (Default 0.6) and Noise threshold (Default 0.4) The minimum acceptable correlation coefficient used to consider (noise threshold) and consider (minimum threshold) at each point. Lower values mean more points are considered and accepted as successful matches, respectively, which may result in a larger number of false matches. The default value is thought to reflect the average correlation for points matched by the human eye. Decisions over appropriate value should be made with reference to local topography and image quality. Where terrain is rugged or image quality poor, it may be necessary to lower these thresholds.

Maximum parallax (Default 5) The maximum vertical search range (in pixels of xparallax) below and above a predicted elevation for a given point. The predicted elevation is either taken from the previous RRDS, or in the case of the coarsest RRDS, from an average of points used in block triangulation. Higher values of maximum parallax will cause DEM generation to be slower, since a greater elevation range is interrogated at each point. This parameter is directly related to elevation changes in the imagery, and should be increased if these are large.

Minimum template size (Default 7) and Maximum template size (Default 9)
The smallest initial and largest final template size (in pixels) used by the area correlator. A value of *a* represents a 'window' shape of *a* x *a* pixels and means a^2 pixels will be used in the correlation calculation. Matching begins using the minimum template size and continues to larger templates if the matching fails for a given template size. Smaller templates will increase the precision of a given match, but also increase the number of unsuccessful matches. Larger template sizes are usually needed if image content is low, but will generally smooth terrain and dramatically increase processing time.

Minimum precision (Default 0.5) The minimum acceptable estimated precision (in pixels) for a point passing the minimum threshold test. This parameter determines the precision label attached to each successfully matched point. Lower values of precision are more likely to indicate a correct match. All matched points are labelled as good, fair or poor, with precision bandwidths of onethird of the minimum precision value. Reducing the minimum precision value makes the process more selective, although changing this parameter only changes the criterion used to accept points and not the actual precision of the match.

Rejection factor (Default 1.5) A smoothing factor for rejecting anomalous spikes and pits during post-processing. During postprocessing after each RRDS, the correlated elevation is compared against the elevation estimated from neighbouring pixels in an attempt to remove false highs and lows in the dataset. A point is rejected if its elevation value is more than the rejection factor times the standard deviation of neighbouring points different from the average value of surrounding points. Larger values reduce the number of points rejected.

Skip factor (Default 2). The minimum spacing of points used at a given RRDS (apart from the finest resolution RRDS), increased to accelerate the generation of large DEMs.

Edge factor (Default 2.5). A parameter which helps to control ambiguous correlations which may result in false fixes. The edge factor describes the ratio between the major and minor axis of the error ellipsoid, computed using the estimated precision of each correlated pair of image points. A ratio higher than the edge factor suggests an elongated error ellipse and an unreliable correlation. Such points are removed and an interpolated elevation used.

Start RRDS (Default 4) and End RRDS (Default 0). The start and end RRDS values dictate the range of resolutions the Vision algorithm works through in the stereo-matching process. Block triangulation results are used to determine the initial elevation of the model, such that when elevation range is large, the start RRDS should be increased. The end RRDS should be set to zero to obtain the highest precision from the process.

***Y* parallax allowance (Default 0)** The *Y* parallax allowance is designed to enable successful DEM generation when the block triangulation results suggest that perfect collinearity has not been achieved. If this is the case, the epipolar constraint may be less effective at identifying search areas for stereo-matching. Increasing this parameter allows greater variation in search window location. Given a robust bundle adjustment solution, lowering this parameter will allow more precise stereo-matching.

Re-sampling (Default On) Re-sampling governs whether bilinear interpolation (on) or nearest neighbour interpolation (off) is used during orthorectification of image patches.

Post processing (Default On) An option to determine whether post-processing (including both interpolation and blunder editing) is performed after completion of correlation at each RRDS.

(Source Westaway 2001 based on Tateishi and Akutsu, 1992; ERDAS, 1995; Smith, 1997; Gooch *et al.*, 1999;Lane *et al.*, 2000).

APPENDIX 2. GLOSSARY

Chapter 2

1/f noise: Scale invariant dynamic system behaviour. The power of the signals frequency component is inversely proportional to the frequency, f.

SOC: Self Organised Criticality is a theory that describes non-linear, wide ranging fluctuations in a systems behaviour whilst at statistical equilibrium.

Chapter 3

EDM: Electronic Distance Measurer, A surveying device that establishes location in X,Y and Z, relative to a benchmark.

DEM: Digital Elevation Model, a three dimensional computer model showing X, Y and Z.

GPS: Global Positioning System, a system for defining position in X,Y and Z using orbiting satellites.

LiDAR: Light Detection And Range, a method for deriving range. Usually mounted on an aerial platform to derive X, Y, and Z co-ordinates.

Chapter 4

DN: Digital Number, the number given to each pixel on a digital photograph representing its colour or spectral reflectance. For colour imagery this number is between 1 and 256.

Experimental Reach 1: A very high resolution GPS derived DEM of a limited spatial extent (300m × 60m),

Experimental Reach 2: a low resolution GPS derived DEM covering a larger spatial extent than Experimental Reach 1 (800m× 100m).

Full Photogrammetric DEM: A photogrammetrically derived DEM of the entire braided river system (3000m ×1000m)

GCP's: Ground Control Points, used to calculate the photogrammetric block

Chapter 5

LOD threshold: A threshold derived from statistical measures of DEM quality used to determine real changes in sediment volume in a reach. Values under threshold could be the result of measurement error.

MBL: Mean Bed Level, The mean average elevation of a cross section of river channel.

ME: Mean Error, a measure of DEM accuracy

RMSE: Root Mean Square Error, a measure of DEM quality that does not differentiate between accuracy and precision

SDE: Standard Deviation of Error, a measure of DEM precision

TIN: Triangulation Interpolation Network, a method for interpolating X,Y,Z data to define a Digital Elevation Model.

Chapter 6

Classification 1: A very active zone adjacent to the Submerged classification defined by areas of exposed gravel and sediment that have no vegetation and where the gravel is bright in colour.

Classification 2: A less active zone where small amounts of vegetation are established and the gravel is more weathered indicating less recent activity.

Classification 3: This classification incorporates areas that are more vegetated than Classification 2. It is also fundamentally different to the other classifications because all island areas (areas surrounded by the other classifications) are included even if they are fully vegetated. This means that Classification 3 is the best representation of the wider floodplain and the longest temporal scales of activity.

DFT: Discreet Fourier Transform, a mathematical method that completely describes the frequency content of a signal. The computational version of the DFT is termed the Fast Fourier Transform.

FFT: Fast Fourier Transform, a method for deconstructing a signal into its constituent periodicities, a technique that identifies dominant scales within the data series. The FFT is an efficient algorithm for obtaining the DFT.

Submerged classification: A classification defined by the areas of channel submerged at low flow.

Sub-system upstream and downstream: The system was divided into 2 subsystems to aid further analysis. The division was made at breakpoint in MBL.

Chapter 7

V_{chan}: is defined as the change in volume for a given cross section. Subsequent values show downstream changes in sediment volume given an indication of downstream organisation

V_{comp}: is the amount of sedimentary change in a cross section that is compensated for. It is the amount of change in a cross section that is cancelled out by opposing change within the same cross section. It is a measure of lateral activity and reorganisation.

References

Acomley, R. M., Cutler, M. E. J., Milton, E. J. and Sear, D. A. 1995, 'Detection and mapping of salmonid spawning habitat in chalk streams using airborne remote sensing'. In: Remote Sensing in Action, Proceedings of the 21st Annual Conference of the Remote Sensing Society, Southampton, 267-274.

Andrews, E.D and Parker G. 1987. 'Formation of a coarse surface layer as the response to gravel mobility' in: Sediment Transport in Gravel-bed Rivers (Eds) Thorne, C., R., Bathurst, J., C., and Hey, R., D. 131-152.

Andrle, R. 1996. The west coast of Britain and statistical self-similarity in nature, Earth Surface Processes and Landforms, 21, 955-962.

Ashmore, P. E. 1982, Laboratory modelling of gravel braided stream morphology, Earth Surface Processes and Landforms, 7, 201-225.

Ashmore, P. E. 1985, Process and form in gravel braided streams: laboratory modelling and field observations, Unpublished Ph.D. Thesis, University of Alberta. Edmonton.

Ashmore, P. E. 1988, Bed load transport in braided gravel-bed stream models, Earth Surface Processes and Landforms. 13. 677-695.

Ashmore, P. E. 1991, 'How do gravel-bed rivers braid, Canadian Journal of Earth Science, 28,

Ashmore, P. E., and Church, M. A., 1998, 'Sediment transport and river morphology: a paradigm for study'. In: Gravel bed rivers in the environment (Eds) Klingeman, P.C., Beschta, R.L., Komar, P.D. and Bradley, J.B., Water Resources Publications, Highlands Ranch, Colorado, USA, 11-148.

Ashmore, P.E., Ferguson, R. I., Prestegaard, K. L., Ashworth, P. J. and Paola, C. 1992, 'Seoondary flow in anabranch confluences of a braided gravel-bed stream', Earth Surface Processes and Landforms, 17, 299-311.

Bak, P..1987, Self-organised criticality: An explanation of 1/f noise, Physical Review Letters, 59(4), 381-384.

Bak, P. 1996, How nature works, Oxford University Press, Oxford.

Bak, P., and Chen, K. 1991, Self organised criticality. Scientific American 264,46.

Bannister, A., Raymond, S. and Baker, R. 1998, Surveying, 7th edition, Longman, Harlow.

Barker, R., Dixon, L. and Hooke, J. 1997, 'Use of terrestrial photogrammetry for monitoring and measuring bank erosion', Earth Surface Processes and Landforms, 22(13), 1217-1227.

Berge, C., 1962, Theory of Graphs and its applications, John Wiley, New York.

Bluck, B.J., 1964. Sedimentation of an alluvial fan in southern Nevada, Journal of Sedimentary Petrology, v. 34, pp.395-400

Bluck, B.J. 1979, Structure of coarse grained braided stream alluvium, Transactions of the Royal Society of Edinburgh, 70, 181-221.

Bradbrook, K. F., Lane, S. N. and Richards, K. S. 2000, 'Numerical simulation of three-dimensional, time-averaged flow structure at river channel confluences', Water Resources Research, 36(9), 2731-2746.

Brasington, J. and Richards, K.S. 1998. Interactions between model predictions, parameters and DTM scales for TOPMODEL. Computers and Geosciences 24, 299-314.

Brasington, J., Rumsby, B. T. and Mcvey, R. A. 2000, 'Monitoring and modelling morphological change in a braided gravel-bed river using high resolution GPS-based survey', Earth Surface Processes and Landforms, 25, 973-990.

Brazier, V. and Ballantyne, C.K. 1989. Late Holocene debris cone evolution in Glen Feshie, western Cairngorm Mountains, Scotland. Transactions of the Royal Society of Edinburgh:Earth Sciences, 80, 17-24.

Brice, J.C. 1964, Channel patterns and terraces of the Loup Rivers in Nebraska. U.S. Geological Survey Prof. Paper 422-D.

Brown, D.C. and Arbogast, A. F. 1999, 'Digital photogrammetric change analysis as applied to active coastal dunes in Michigan', Photogrammetric Engineering and Remote Sensing, 65(4), 467A74.

Brunsden, D. and Chandler, J. H. 1996, 'Development of an episodic landform change model based upon the Black Ven Mudslide, 1994-1995'. In: Advances in hillslope processes (Eds) Anderson, M. C. and Brooks, S. M., Wiley, Chichester, 88-896.

Bryant, R. C. and Gilvear, D. J. 1999, 'Quantifying geomorphic and riparian land cover changes either side of a large flood event using remote sensing: River Tay, Scotland', Geomorphology, 29(34), 307-321.

Butler, J. B., Lane, S. N. and Chandler, J. H. 1998, 'Assessment of DEM quality characterising surface roughness using close range digital photogrammmetry', Photogrammetric Record, 19(92), 271-291.

Butler, J. B., Lane, S. N., Chandler, J. H. and Porfiri, K. 2001, 'Through-water close-range digital photogrammetry in flume and field environments', Photogrammetric Record.

Carter, C. S. and Shankar, U. 1997, 'Creating rectangular bathymetry grids for environmental numerical modelling of gravel-bed rivers', Applied Mathematical Modelling, 21, 699-708.

Chandler, J. H. 1999, 'Effective application of automated digital photogrammetry for geomorphological research', Earth Surface Processes and Landforms, 24, 51-63.

Chandler, J. H. and Ashmore, P. 2001, 'Detecting braided river channel change using terrestrial oblique digital imagery and automated digital photogrammetry'. In: Geomatics, Earth Observation and the Information Society, Proceedings of the First Annual Conference of the Remote Sensing and Photogrammetric Society, Remote Sensing and Photogrammetric Society, London, 12-14 September 2001.

Chandler, J. H. and Clark, J. 5. 1992, 'The archival photogrammetric technique: Further application and development', Photogrammetric Record, 14(80), 241-247.

Chandler, J. H. and Cooper, M. 1988, 'Monitoring the development of landslides using archival photography and analytical photogrammetry', Land and Minerals Surveying, 6, 57-584.

Chandler, J. H., Shiono, K., Rameshwaren, P. and Lane, S. N. 2001, 'Measuring flume surfaces for hydraulics research using a Kodak DC5460', Photogrammetric Record, 17(97), 38-1.

Charlton, M. E., Fuller, I. C., Large, A. R. C., Passmore, D.C., Newson, M.D. and Heritage, C. L. 2001, 'Airborne LiDAR and ground survey for exploring channel dynamics'. Paper presented to a joint meeting of the Photogrammetric Society and the British Geomorphological Research Group, University of Leeds, 17 January 2001.

Chatfield, C. 1984. The analysis of time series-An introduction, Chapman and Hall, London

Christensen,K.,Fogedby, H.C. and Jensen, H.J. 1991, Dynamical and spatial aspects of sandpile cellular Automata. Journal of Statistical Physics 63, 653.

Church, M. 1983 Pattern of instability in a wandering gravel bed channel. In Modern and ancient fluvial systems, (eds Collinson, J.D. and Lewin, J.) Oxford: Blackwell, Special Publication of the International Association of Sedimentologists 6, 69-80.

Church, M and Hassan M.A. 2001, Introduction to the special issue on sediment transport dynamics. Earth Surface Processes and Landforms, 26 1367-1368.

Church, M., McLean, D. and Wolcott, J. F. 1987, 'River bed gravels: sampling and analysis'. In: Sediment transport in gravel-bed rivers (eds.Thorne, C. R., Bathurst, J. C. and Hey, R. D.), Wiley, Chichester, 43-88.

Coldwell, A. E. 1957, 'Importance of channel erosion as a source of sediment, Transactions of the American Geophysical Union, 38, 908-912.

Cooley, J.W. and Tukey, J.W. 1965, An algorithm for the machine calculation of complex fourier series, Math of Comp, 19 (90), 297-301.

Cooper, M. A. R. 1998, 'Datums, coordinates and differences'. In: Landform monitoring, modelling and analysis (eds. Lane, S. N., Richards, K. S. and Chandler, J. H.), Wiley, Chichester, 23- 36.

Cooper, M. A. R. and Cross, P. A. 1988, 'Statistical concepts and their application in photogrammetry and surveying', Photogrammetric Record, 12(71), 637-663.

Cox, N.J. and Evans, I.S. 1987, Introduction to Earth Surface Processes and Landforms Vol 12, 1-2.

Crickmay, C. H. 1960, 'Lateral activity in a river in North Western Canada', Journal of Geology, 68, 377-391.

Davoren, A. and Mosley, M. P.1986, 'Observations of bedload movement, bar development and sediment supply in the braided Ohau River', Earth Surface Processes and Landforms, 11, 643-652.

Derose, R. C., Gomez, B., Marden, M. and Trustrum, N. A. 1998, 'Gully erosion in Mangatu Forest, New Zealand, estimated from digital elevation models', Earth Surface Processes and Landforms, 23,1045-1053.

Desmet, P. J. J. 1997, 'Effects of interpolation errors on the analysis of DEMs', Earth Surface Processes and Landforms, 22, 563-580.

Dixon, L. F. J., Barker, R., Farres, P., Hooke, J., Inkpen, R., Merel, A., Payne, D. and Shelford, A. 1998, 'Analytical photogrammetry for geomorphological research'. In: Landform monitoring, modelling and analysis (eds. Lane, S. N., Richards, K. S. and Chandler, J. H.), Wiley, Chichester, 63-94.

ERDAS 1995, IMAGINE Version 8.2: OrthoMAX user's Guide, Vision International and Manchester Computing.

Evans, I.S., 1987, A new approach to drumlin morphology. In Drumlin symposium, (eds, J. Menzies and J. Rose. A.A.) Balkema, Rotterdam, 119-130.

Evans, I.S. 1998, What do terrain statistics really mean? In Landform Modelling and Analysis. (Eds, S.N. Lane, K.S. Richards and J.H. Chandler). John Wiley and Sons.

Fahnestock, R. K. and Bradley, W. C. 1973, 'Knik and Matanuska rivers, Alaksa: a contrast in braiding'. In: Fluvial geomorphology (ed Morisawa, M.), Allen and Unwin, London.

Ferguson, R.I. 1986, Hydraulics and hydraulic geometry Progress in Physical Geography 10, 1-31.

Ferguson, R. I., Ashmore, P. E., Ashworth, P. J., Paola, C. and Prestegaard, K. L. 1992, 'Measurements in a braided river chute and lobe 1: flow pattern, sediment transport and channel change', Water Resources Research, 28,1877-1886.

Ferguson, R. I. and Ashworth, P. J. 1992, 'Spatial patterns of bedload transport and channel change in braided and near-braided rivers'. In: Dynamics of gravel-bed rivers (eds. Billi, P., Hey, R. D., Thorne, C. R. and Tacconi, P.), Wiley, New York. 89- 104.

Ferguson, R. I. and Werritty, A. 1983, 'Bar development and channel changes in the gravelly River Feshie, Scotland'. In: Modern and ancient fluvial systems (eds. Collinson, J. and Lewin, J.), Blackwell Scientific Publications, Oxford, 181-194.

Finnegan, D. C., Gomez, B. and Smith, L. C. 2001, 'Using laser altimetry to quantify geomorphic change effected by Large scale flooding'. Paper presented to the 97th Annual Meeting of the American Association of Geographers, New York, USA, 27 February -3 March 2001.

Fiorentino, M. and Claps, P. 1993, An entropy based morphological analysis of river basin networks, Water Resources Research, 29, 4, 1215-1224.

Fougere, P.F. 1985, On the accuracy of spectrum analysis of red noise processes using maximum entropy and periodogram methods: simulation studies and application to geophysical data. Journal of Geophysical Research, 90, 4355-4366.

French, J. R. 2001, 'Airborne LiDAR data in support of hydraulic modelling: Representation of form as the key to simulation of process'. Paper presented to a joint meeting of the Photogrammetric Society and the British Geomorphological Research Group, University of Leeds, 17 January 2001.

Frette, V., Christiansen,K., Malthe-Sorenssen,A., Feder,J., Jossang,T., and Meakin, P. 1996, Avlananche Dynamics in a Pile of Rice. Nature 379, 49-52.

Gardner, M.J. and Altman, D.G. 1989. Statistics with confidence, British Medical Journal, Landon.

Gilbert, L.E. and Malinverno, A. 1989. A characterization of the spectral density of residual ocean floor topography, Geophysical Research Letters 15 (12), 1401-1404.

Gilvear, D. J., Waters, T. M. and Milner, A. M. 1998, 'Image analysis of aerial photography to quantify the effect of gold placer mining on channel morphology, Interior Alaska'. In: Landform monitoring, modelling and analysis (eds. Lane, S. N., Richards, K. S. and Chandler, J.H.), Wiley, Chichester, 195-216.

Gilvear D.J. Bryant, R. and Hardy, T. 1999. Remote sensing of channel morphology and in-stream fluvial processes. Progress in Environmental Science 1,3 257-284.

Gleick, J. 1987, Chaos: Making a new science. New York: Viking.

Goff, J. R. and Ashmore, P.1994, 'Gravel transport and morphological change in braided Sunwapta River, Alberta, Canada', Earth Surface Processes and Landforms, 19, 195-212.

Gomez, B. and Church, M. 1989, An assessment of bed load sediment transport formulae for gravel bed rivers. Water Resources Research, 25(6) 1161-1186.

Gong, J., Li, Z., Zhu, Q., Sui, H. and Zhou, Y. 2000, 'Effects of various factors on the accuracy of DEMs: An intensive experimental investigation', Photogrammetric Engineering and Remote Sensing, 66(9), 1113-1117

Gooch, M. J., Chandler, J. H. and Stojic, M. 1999, 'Accuracy assessment of digital elevation models generated using the ERDAS Imagine OrthoMAX digital photogrammetric system', Photogrammetric Record, 16 (93), 519-531.

Gurnell, A. M., Downward, S. R. and Jones, R. 1994, 'Channel planform change on the River Dee meanders, Regulated Rivers: Research and Management, 9, 187-204.

Ham, D. C. and Church, M. 2000, 'Bed-material transport estimated from channel morphodynamics: Chilliwack River, British Columbia', Earth Surface Processes and Landforms, 25(10), 1123-1142.

Hamamori, A., (1962). 'A theoretical investigation on the fluctuation of bedload transport', Delft Hydraulics Laboratory, Report R4, pp 21.

Hassan, M. and Reid, 1.1990, 'The influence of microform bed roughness elements on flow and sediment transport in gravel-bed rivers', Earth Surface Processes and Landforms, 15,739-750.

Held, G. A., Solina, D. H., Keane, D. T., Haag, W.J.,Horn, P.M., and Grinstein, G., 1990, Experimental Study of Critical Mass Fluctuations in an Evolving Sandpile. Physical Review Letters 65 (1990) 1120.

Helley, E.J. and Smith, W. 1971, Development and calibration of pressure-difference bedload sampler, US Geol Survey Open File Rep.pp18.

Hickman, C. D. and Hogg, J. E. 1969, 'Application of an airborne pulsed laser for near shore bathymetric measurements', Remote Sensing of Environment, 1, 47-58.

Hicks, D. M., Duncan, M. J., Walsh, J., Lane, S. N. and Westaway, R. M. 1999b, Braided River Morphodynamics: Research Plan for 1999-2000 and 1998-1999 Fieldwork, National Institute of Water and Atmosphere, Christchurch. Technical Report 51.

Hoey, T. B., 1992, Temporal variations in bedload transport rates and sediment storage in gravel-bed rivers. Progress in Physical Geography, 16: 319-338.

Horton, R.E. 1945, Erosional developments of streams and their drainage basins; hydrophysical approach to quantitative morphology: Geological Society American Bulletin, V 56 pp275-370

Howard, A.D., Keetch, M.E. and Linwood Vincent, C., 1970, Topological and Geometrical properties of braided streams. Water Resources Research, 6 1674-1688.

Huang, Y. D. 2000, 'Evaluation of information loss in digital elevation models with digital photogrammetric systems', Photogrammetric Record, 16(95), 781-791.

Hubbell, D., W., 1987 'Bed load sampling and analysis' in: Sediment Transport in Gravel-bed Rivers (Eds. by Thorne, C., R., Bathurst, J., C., and Hey, R., D.) John Wiley and Sons.104-118

Kansky, K.J., 1963. Structure of transportation networks, Dep. Geog. Res. Pap. 84, University of Chicago, Chicago, Illinois, 1-55.

Keim, R. F., Skaugset, A. E. and Bateman, D. 8.1999, 'Digital terrain modeling of small stream channels with a total-station theodolite', Advanced Water Resources, 23(1), 4148.

Kersarwani, A., Gomez, B., Jacobsen, R. and Smith, L. 2001, 'Using laser altimetry for rapid assessment of post-flood erosional and depositional changes'. Paper presented to the 97th Annual Meeting of the American Association of Geographers, New York, USA, 27, February - 3 March 2001.

Klinkenberg, B. and Goodchild, M.F. 1992. The fractal properties of topography: a comparison of methods, Earth Surface Processes and Landforms, 17, 217-234.

Komar, P.D., 1988, Sediment transport by floods. In Flood Geomorphology (eds Baker, V.R., Kochel, R.C. and Patton, P.C.). New York:Wiley-Interscience, 97-111.

Kondof, G. M. and Swanson, M. L. 1993, 'Channel adjustments to reservoir construction and gravel extraction along Stony Creek, California', Environmental Geology, 21, 256-269.

Lane, S. N. 2000, 'The measurement of river channel morphology using digital photogrammetry', Photogrammetric Record, 16(96), 937-957.

Lane, S. N. 2001, 'The measurement of river channel morphology'. In: Gravel bed rivers V (ed. Mosely, M. P.), New Zealand Hydrological Society, Wellington, New Zealand.

Lane, S. N., James, T. D. and Crowell, M. D. 2000, 'Application of digital photogrammetry to complex topography for geomorphological research', Photogrammetric Record, 16(95),793-821.

Lane, S. N. and Richards, K.S..1997, 'Linking river channel form and process: time, space and causality revisited', Earth Surface Processes and Landforms, 22, 349-368.

Lane, S. N. and Richards, K. S. 1998, 'High resolution, two-dimensional spatial modelling of flow processes in a multi-thread channel', Hydrological Processes, 12(8), 127-1298.

Lane, S. N., Richards, K. S. and Chandler, J. H. 1993, 'Developments in photogrammetry: the geomorphological potential', Progress in Physical Geography, 17(3), 306-328.

Lane, S. N., Richards, K. S. and Chandler, J. H. 1994, 'Developments in monitoring and terrain modelling of Lane, S. N., Richards, K. S. and Chandler, J. H. 1995b, Within-reach spatial patterns of process and channel adjustment'. In: River Geomorphology (ed. Hickin, E. J.), Wiley, Chichester, 251 pages:105-130.

small-scale riverbed topography', Earth Surface Processes and Landforms,19, 349-368.

Lane, S. N., Richards, K. S. and Chandler, J. H. 1995a, 'Morphological estimation of the time integrated bed-load transport rate', Water Resources Research, 31(3), 761-772.

Lapointe, M. F., Secretan, Y., Driscoll, S., Bergeron, N. and Leclerc, M. 1998, 'Response of the Ha! Ha! river to the flood of July 1996 in the Saguenay region of Quebec: Large-scale avulsion in a glaciated valley', Water Resources Research, 34(9), 238-2392.

Laronne, J. B. and Duncan, M. J. 1992, 'Bedload transport paths and gravel bar formation'. In: Dynamics of Gravel-bed rivers,(eds Billi, P., Hey, R. D., Thorne, C. R. and Tacconi, P.), Wiley, Florence, Italy.673

Lawler, D. M. 1993, 'The measurement of river bank erosion and lateral channel change: a review', Earth Surface Processes and Landforms, 18, 777-821.

Leopold, L. B. and Langbein, W.B. 1962, The concept of entropy in landscape evolution, U.S. Geological Survey Prof Paper 500 A:A1-A20.

Leopold, L. B. and Maddock, T., Jr., 1953, The hydraulic geometry of stream channels and some physio-graphic implications, US Geol Survey Prof. Paper 252, pp57.

Leopold, L.B. and Wolman, M.G. 1957, River channel patterns; braided meandering and straight. U.S Geological Survey Prof Paper 282-B.

Leopold, L.B. and Wolman, M.G. and Miller J.P. 1964, Fluvial Processes in Geomorphology, W.H. Freeman and Company, San Francisco and London.

Lewin, J. 1990, 'River channels'. In: Geomorphological techniques, 2nd edition (ed. Goudie, A. S.), Unwin Hyman, London, 280-301.

Lewin, J. and Hughes, D. 1976, 'Assessing channel change on Welsh rivers', Cambria, 3, 1-10.

Lewin, J. and Manton, M. M. M. 1975, Welsh floodplain studies: the nature of floodplain geometry', Journal of Hydrology, 25, 37-50.

Lewin, J. and Weir, M. J. C. 1977, 'Morphology and recent history of the Lower Spey', Scottish Geographical Magazine, 93, 4-51.

Ley, R. G. 1986, 'Accuracy assessment of digital terrain models'. In: Proceedings AutoCarto London, Autocarto London, London, 455-464.

Li, Z. 1992, 'Variation of the accuracy of digital terrain models with sampling interval', Photogrammetric Record, 14(79), 113-128.

Li, Z. 1994, 'A comparative study of the accuracy of digital terrain models (DTMs) based on various data models', ISPRS Journal of Photogrammetry and Remote Sensing, 49(1), 2-11.

Lindsay, J. B. and Ashmore, P. E. submitted, 'Error in the measurement of gravel-bed topography and topographic change. Part 2: the effects of survey frequency on estimates of scour and fill in a braided river model'.

Lindsay, J. B., Ashmore, P. E. and Smart, C. C. submitted, 'Error in the measurement of gravel-bed topography and topographic change. Part 1: error in elevation measurements caused by bed roughness'.

Linton, D. L. 1952, 'Air photographs as tools of geographical research'. In: Rapporte commission utiliser photographie aériennes études geographie, Congress International Geographique, Washington, Paris, 17-28.

Lisle, T.E., Cui, Y.T., Parker, G. Pizzuto, J.E., Dodd A.M., 2001. The dominance of dispersion in the evolution of bed material waves in gravel-bed rivers. Earth Surface Proceses and Landforms 26, 1409-1420.

Lohman, S. W. and Robinove, C. J. 1964, 'Photographic description and appraisal of water resources', Photogrammetrica, 19(3), 87-103.

Luce J.J.W. 1994, Confluence zone sedimentation processes: Sunwapta river, Alberta. Unpublished Master of Science thesis, The University of Western Ontario, London, Ontario.

Lyon, J. G., Lunetta, R. S. and Williams, D. C. 1992, 'Airborne multispectral scanner data for evaluating bottom sediment types and water depths of the St Marys River, Michigan', Photogrammetric Engineering and Remote Sensing, 58(7), 951-956.

Lyzenga, D. R. 1985, 'Shallow-water bathymetry using combined LiDAR and passive multispectral scanner data', International Journal of Remote Sensing, 6(1), 115-125.

Macklin, M.G. and Lewin, J. 1989, Sediment transfer and transformation of an alluvial valley floor: the River South Tyne, Northumbria, UK. Earth Surface Processes and Landforms, 14, 233-46.

Macklin, M.G. and Lewin, J. 1993, Holocene river alluvation in Britain. Zeitschrift fur Geomorphologie Supplement-Band 88, 109-22.

Mandlebot, B. 1983. The Fractal Geometry of Nature. New York: Freeman.

Martin, Y. and Church, M. 1995, 'Bed-material transport estimated from channel surveys: Vedder River, British Columbia', Earth Surface Processes and Landforms, 20, 347-361.

McLean, D. G. and Church, M. 1999[1]. Sediment transport along lower Fraser River 1.Measurements and hydraulic computations. Water Resources Research, 35 (8), 2533-2548.

McLean, D. G. and Church, M. 1999[2]. Sediment transport along lower Fraser River 2. Estimates based on long-term gravel budget, Water Resources Research, 35 (8), 2549-2559.

McArdell, B., W., and Faeh, R., 2001,'A computational investigation of river braiding', In: Gravel bed rivers V (ed. Mosley, M. P.), New Zealand Hydrological Society, Wellington.73 - 93

Miall, A.D., 1977, A review of the braided river depositional environment. Earth Science Reviews. 13, 1-62.

Mulla, D.J. 1988. Using geostatistics and spectral analysis to study spatial patterns in the topography of southeastern Washington State, U.S.A. Earth Surface Processes and Landforms, 13, 389-405

Murray, A. B. and Paola, C. 1994, 'A cellular model of braided rivers', Nature, 371, 54-57.

Murray, A. B. and Paola, C. 1997, 'Properties of a cellular braided stream model', Earth Surface Processes and Landforms, 22, 1001-1025.

Nagao, M., Mukai, Y., Ayabe, K., Arai, K. and Nakazawa, T. 1988, 'A study of reducing abnormal elevations in automatic computations of elevations from satellite data', Archives of Photogrammetry and Remote Sensing, 27, 280-288.

Neill, C. R. 1969, 'Bed forms in the Lower Red Deer River, Alberta', Journal of Hydrology, 7 58-85.

Neill, C. R. 1971, 'River bed transport related to meander migration rates', ASCE Journal of the Waterways and Harbours Division, 97, 783-786.

Neill, C.R. 1987, Sediment balance considerations linking long-term transport and channel processes, in Sediment Transport in Gravel-Bed Rivers, (eds Thorne, C.R., Bathurst, J.D. and Hey, R.D.), John Wiley and Sons Limited, Chichester 225-240.

Nicholas, A.P., Ashworth, P.J. Kirkby, M.J. Macklin, M.G. and Murray, T. 1995. Sediment slugs: Large-scale fluctuations in fluvial sediment transport rates and storage volumes. Progress in Physical Geography 19, 500-19.

Noever,D. A. 1993. Himalayan sandpiles. Physical Review E47, 724.

Nykanen, D. K., Foufoula-Georgiou, E. and Sapozhnikov, V. B. 1998, 'Study of scaling in braided river patterns using synthetic aperture radar imagery', Water Resources Research, 34(7), 1795-1807.

Oros, C. N. 1952, 'River current data from aerial photography', Photogrammetric Engineering, 18(1), 96-99.

Paola, C. 2001, 'Modelling stream braiding over a range of scales'. In: Gravel bed rivers V (ed. Mosley, M. P.), New Zealand Hydrological Society, Wellington. 11-46

Paola, C. ,and Foufoula-Georgiou, E., 2001, 'Statistical geometry and dynamics of braided rivers'. In: Gravel bed rivers (ed. Mosley, M.P.), New Zealand Hydrological Society, Wellington.47-72

Passmore, D.G., Macklin, M.G., Brewer, P.A., Lewin, J., Rumsby, B.T. and Newson, M.D. 1993, Variability of late Holocene braiding in Britain. In: J.L. Best and C.S. Bristow (ed.) Braided Rivers. London, Geological Society, 205-232.

Passmore, D.G. 1994, River response to Holocene environmental change: the Tyne basin, northern England. Unpublished Ph.D. Thesis, University of Newcastle upon Tyne.

Passmore, D.G. and Macklin, M.G. 2000, Late Holocene channel and floodplain development in a wandering gravel-bed river: The River South Tyne at Lambley northern England. Earth Surface Processes and Landforms, 25:1237-1256.

Putnam, W. C. 1947, 'Aerial photographs in geology', Photogrammetric Engineering, 13(4), 557-565.

Pyle, C. J., Chandler, J. H. and Richards, K.S.1997, 'Digital photogrammetric monitoring of river bank erosion', Photogrammetric Record, 15, 753-764.

Rachocki, A., 1981, Alluvial Fans, Wiley andSons Ltd.

Ramirez, R.W. 1985, The FFT: Fundamentals and concepts, Prentice-Hall International

Reid I. Frostick L.E. and Layman J.T. 1985. The incidence and nature of bed load transport during flood flows in coarse-grained alluvial channels. Earth Surface Processes and Landforms, 10, 33-44.

Rice, S. and Church, M. 1998, Grain size along two gravel-bed rivers: Statistical variation, spatial pattern and sedimentary links. Earth Surface Processes and Landforms, 23, 345-363.

Rigon, R. Rinaldo, A., and Rodriguez-Iturbe, I. 1994 On landscape self-organization. Journal of Geophysical Research 99, 11971.

Rinaldo, A. Maritan, A. Colaiori, F. Flammini, A. Rigon, R. Rogriguez-Iturbe, I. Banavar, J.R. 1996 Thermodynamics of fractal Networks, Physical Review Letters, 76 (18), 3364-3367.

Rinaldo, A., Rodriguez-Iturbe, I. and Rigon, R. 1998, 'Channel networks'. In: Annual review of earth and planetary sciences, 26 (eds. Jeanloz, R., Albee, A. L. and Burke, K. C.), Annual Reviews, Palo Alto, California, 289-327.

Ritchie, J. C. 1996, 'Remote sensing applications to hydrology: airborne laser altimeters', Hydrological Sciences, 41(4), 625-636.

Robertson-Rintoul M.S.E. 1986. A quantitative soil-stratigraphic approach to the correlation and dating of postglacial river terraces in Glen Feshie, south-west Cairngorms. Earth Surface

Processes and Landforms, 11, 605-17.

Rodriguez-Iturbe, I., Ijjasz-Vasquez, E., Bras, R. and Tarboton, D. 1992, 'Power law distributions of discharge mass and energy in river basins', Water Resources Research, 28, 1089-1093.

Rumsby, B.T. and Macklin M.G. 1994, Channel and floodplain response to recent abrupt climatic change: the Tyne basin, northern England. Earth Surface Processes and Landforms 19, 499-515.

Rumsby B. 2000 Vertical accretion rates in Fluvial systems: A comparison of volumetric and depth –based estimates. Earth Surface Processes and Landforms 25 1-15.

Rumsby, B.T., Brasington J. and McVey, R. 2001, The potential for high resolution fluvial archives in braided rivers: Quantifying historic reach-scale channel and floodplain development in the River Feshie, Scotland. In: River Basin Sediment Systems: Archives of Environmental Change (Eds) Maddy, D. Macklin, M.G. Woodward, J.C. 445-467

Rust, B.R. 1978, A Classifcation of alluvial channel systems, in Fluvial Sedimentology, edited by Miall, A.D. 187-198

Salo, J., Kalliola, R., Hakkinen, I., Makinen, Y., Niemela, P., Puhakka, M. and Coley, P.D. 1986, 'River dynamics and the diversity of the Amazon lowland forest', Nature, 322, 254-258.

Sapozhnikov, V. and Foufoula-Georgiou, E. 1996, 'Self-affinity in braided rivers', Water Resources Research, 32(5), 1429-1439.

Sapozhnikov, V. and Foufoula-Georgiou, E. 1997, 'Experimental evidence of dynamic scaling and indications of self-organized criticality in braided rivers', Water Resources Research,33(8), 1983-1991.

Sapozhnikov, V. and Foufoula-Georgiou, E. 1999, 'Horizontal and vertical self-organization of braided rivers toward a critical state', Water Resources Research, 35(3), 843-851.

Sapozhnikov, V. B., Murray, A. B., Paola, C. and Foufoula-Georgiou, E. 1998, Validation of braided-stream models: Spatial state-space plots, self-affine scaling, and island shapes', Water Resources Research, 34(9), 2353-2364.

Schumm, S.A., 1968, Speculations concerning paleohydrologic controls of terrestrial sedimentation. Geological Society Am. Bull., 79, 1573-1588.

Schumm, S.A. 1973. Geomorphic thresholds and complex response of drainage basins. In, Fluvial Geomorphology (ed Morisawa, M.) NY State University Publications in Geomorphology, 299-309.

Schumm, S.A. 1977, The fluvial system. New York, Wiley-Interscience

Schumm, S.A. and Khan, H.R. 1972 Experimental study of channel patterns. Bulletin of the Geological Society of America, 83, 1755-70.

Shaw, S. H. 1953, 'The value of air photographs in the analysis of drainage patterns', Photogrammetric Record, 1(2), 4-15.

Shearer, J. W. 1990, 'The accuracy of digital terrain models'. In: Terrain modelling in surveying and civil engineering (eds. Petrie, G. and Kennie, T. J. M.), Whittles, London, 310-316.

Sherstone, D. A. 1983, 'Sediment removal during an extreme summer storm: Muskwa River, North-eastern British Columbia', Canadian Geotechnical Journal, 20(2), 329-335.

Smith, H. T. U. 1941, 'Aerial photographs in geomorphic studies', Journal of Geomorphology, 4(3), 170-205.

Smith, H. T. U. 1943, Aerial photographs and their applications, D. Appleton-Century, New York.

Smith, M. J., Smith, D. G., Tragheim, D. G. and Holt, M. 1997, 'DEMs and ortho-images from aerial photographs', Photogrammetric Record, 15(90), 945-950.

Speight, J. G. 1965a, 'Meander spectra of the Angabunga River', Journal of Hydrology, 3 (1), 1-15.

Stojic, M., Chandler, J. H., Ashmore, P. and Luce, J. 1998, 'The assessment of sediment transport rates by automated digital photogrammetry', Photogrammetric Engineering and Remote Sensing, 64(5), 387-395.

Sundborg, A. 1956, 'The river Klarälven, a study of fluvial processes', Geografiska Annaler, 38(A), 125-316.

Sutherland A.J. 1987 'Static armour layers by selective erosion' in: Sediment Transport in Gravel-bed Rivers (eds. by Thorne, C., R., Bathurst, J., C., and Hey, R., D.) 241-253

Tacconi, P. and Billi, P. 'Bed Load transport measurement by the vortex-tube trap on Virginio Creek, Italy' in : Sediment Transport in Gravel-bed Rivers (eds. by Thorne, C., R., Bathurst, J., C., and Hey, R., D.)254-268

Tate, N.J. 1998. Maximum entropy spectral analysis for the estimation of fractals in topography. Earth Surface Processes and Landforms. 23, 1197-1217.

Taylor, J. R. 1997, An introduction to error analysis: the study of uncertainties in physical measurements, 2nd edition, University Science Books, Sausalito, California, USA.

Van Sickle, J. 1996, GPS for land surveyors, Ann-Habor Press, Michigan, USA.

Warburton, J., Davies, T. R. H. and Mandl, M. G. 1993, 'A meso-scale investigation of channel change and floodplain characteristics in an upland braided gravel-bed river, New Zealand'. In: Braided rivers (eds. Best, J. L. and Bristow, C. S.), Geological Society, London, 241-255.

Werritty, A. and Ferguson, R. I.1980, 'Pattern changes in a Scottish braided river over 1, 30 and 200 years'. In: Timescales in geomorphology (eds. Cullingford, R. A., Davidson, D. A. and Lewin, J.), Wiley, Chichester, 53-68.

Westaway, R.M., Lane, S.N. and Hicks, D.M. 2000, The development of an automated correction procedure for digital photogrammetry for the study of wide, shallow, gravel-bed rivers, Earth Surface Processes and Landforms, 25, 209-226.

Westaway, R.M. 2001, Development of remote sensing methods for measurement of large, gravel-bed, braided rivers. Unpublished Ph. D. University of Cambridge.

Westaway, R.M., Lane, S.N. and Hicks, D.M. 2003, Remote survey of large-scale braided, gravel-bed rivers using digital photogrammetry and image analysis. Int. J. Remote Sensing, 24, 4, 795-815.

Wilcock, P.R. and McArdell, B.W. 1993, Surface-based fractional transport rates: mobilization thresholds and partial transport of a sand-gravel sediment. Water Resources Research 29, 1297-312.

Williams P.F. and Rust, B.R. 1969, The sedimentology of a braided river: J. Sediment. Petrol., V 39, 649-679.

Winterbottom, S. J. 2000, 'Medium and short-term channel planform changes on the Rivers Tay and Tummel, Scotland', Geomorphology, 34(34), 195-208.

Winterbottom, S. J. and Gilvear, D. J. 1997, 'Quantification of channel bed morphology in gravel-bed rivers using airborne multispectral imagery and aerial photography', Regulated Rivers: Research and Management, 13,489-499.

Wise, S.1998, 'The effect of GIS interpolation errors on the use of DEMs in geomorphology'. In: Landform monitoring, modelling and analysis (eds. Lane, S. N., Richards, K. S. and Chandler, J. H.), Wiley, Chichester, 13-16

Wolf, P.R. 1973, Elements of photogrammetry, 2nd edition, McGraw Hill, New York.

Wolf, P. R. and Dewitt, B. A. 2000, Elements of photogrammetry with applications in GIS, 3rd edition, McGraw-Hill, London.

Wolman, M. G. 1967, 'A cycle of sedimentation and erosion in urban river channels', Geografiska Annaler, 49, 385-395.

Yang, C.T. 1971, Formation of riffles and pools, Water Resources Research, 7 (6) 1567-1574.